HB 9/88

Report to:

.National Radiological Protection Board

Atomic Weapons Establishment

H.M. Inspectorate of Pollution

Health & Safety Executive

on

PREPARATORY STUDIES FOR A COMPLEX DISPERSION MODEL

Executive Summary

by J.C.R. Hunt, R.J. Holroyd & D.J. Carruthers

Cambridge Environmental Research Consultants, Ltd.

November 1988

1. SUMMARY

This is an overview of the results of the ten-month study begun in October 1987 by C.E.R.C., primarily by R.J. Holroyd, J.C.R. Hunt and D.J. Carruthers.

1.1 Critical review of wind-field modelling

We have completed a critical review of current methods of modelling wind fields in the atmospheric boundary layer and dispersion from isolated sources, with a particular emphasis on identifying models suitable for general use in dispersion modelling by regulatory and other bodies using small computers and readily available meteorological data. There is a consensus of expert opinion in the U.K., other European countries and the U.S.A. that the meteorological state of the atmospheric boundary layer for dispersion calculations can be specified with greater certainty by a new parameter than by the present Pasquill (A-G) methods based solely on surface measurements. This new parameter is h/L_{MO}; h is the boundary-layer depth and L_{MO} is the Monin-Obukov length which is derived from measurements of heat flux, wind speed and roughness at or near the ground. The limitations of this approach are pointed out. For flow over hills, changes of roughness and changes of surface temperature, a simple classification of different models has been developed which has led to some conclusions as to which models are practical for small computer systems for use in regulatory decision making and probabilistic risk assessment.

1.2 Critical review of dispersion modelling

Our review of dispersion models suggests that there is no current consensus as to the best dispersion model for regulatory use. However, a number of possibilities emerge as practical propositions.

Our review of theoretical and experimental dispersion research shows that:

* current models even for flat terrain do not account for many meteorological situations and for dispersion from high sources

* large changes can occur in the dispersion process and in ground-level concentrations in air flow over hills and other complex surface conditions.

Proposals are made for modelling dispersion over both flat terrain and complex terrain, though at present there is no single personal computer-based model that can account for all the major effects.

As a baseline for comparison with more advanced boundary-layer and dispersion models, the model described in the report NRPB-R91 (Clarke 1979, hereafter referred to as R91) has been programmed (in FORTRAN) to run on an IBM PC AT. For the same computer system and in conjunction with the CEGB, a code named FLOWSTAR has been developed for predicting air flow over hills and roughness changes.

1.3 Principal recommendations

The following points are made for the general form of an improved regulatory model. It should:

(i) be capable of being mounted on a personal computer system, and have a flexible modular form capable of improvement;

(ii) incorporate an improved parameterisation of the boundary layer, and introduce models for the wind fields over complex terrain;

(iii) allow for the systematic application of the most appropriate dispersion models (including Gaussian ones);

(iv) allow models of important phenomena such as precipitation, anomalous meteo-

rological situations (e.g. see breezes) and temporal variations in boundary-layer structure to be included at some stage.

In this way it would

(i) utilise recent, authoritative and widely-accepted meteorological research;

(ii) make full use of meteorological data that is readily available at present;

(iii) account for some major changes of dispersion and concentration in complex conditions that are not predicted by present models.

We estimate that a practical and validated scheme with software and manuals could be obtained with four man-years' effort and we recommend that there should be a co-ordinated, time-tabled development of such a regulatory model by U.K. groups involved in atmospheric dispersion modelling. It would need validation against field and laboratory data and the best advanced research models.

2. REVIEW OF CURRENT WIND-FIELD MODELS FOR USE IN DISPERSION MODELS

2.1 Boundary-layer models

The essential feature of all current practical dispersion models for dispersion over flat terrain is that they are based on the assumption that over a certain range of meteorological conditions the boundary layer has a similar structure. This assumption was used by Pasquill in the U.K. and the research team at Brookhaven in America to define the state of the boundary layer by a single parameter corresponding to each of these range of conditions, ranging from A for a very unstable boundary layer to G for an extremely stable one. These are known as Pasquill Stability categories, PSC.

In many models widely used at present, typified by R **91,** the average structure, stability state, depth and turbulent diffusion characteristics of the boundary layer are either defined by or derived from meteorological measurements taken at ground level. In R **91,** for example, these are: the mean wind speed U; the surface heat flux H; the surface roughness z_0.

Recent meteorological research has shown that boundary layers typical of unstable (A-C) and neutral (D) conditions do have a similar structure. On the other hand, this is not necessarily true of stable (E-G) boundary layers. The significant point is that the state of the boundary layers cannot be specified accurately by any parameter based on surface measurements alone. Today there is a world-wide consensus of opinion amongst research workers that the boundary layer should be specified by a new parameter h/L_{MO}, where L_{MO} is the Monin-Obukov length derived from the surface data U, H and z_o and h is the depth of the boundary layer which nowadays can be measured. For each value of h/L_{MO} the vertical distribution of turbulence is known. Figure **1** shows how the new parameter corresponds approximately to the variation in the R91 parameters.

- *Our conclusion is that modelling and definition of the boundary-layer structure can be considerably improved by using the results of recent research and using a new parameter such as h/L_{MO}. This conclusion is perfectly practical because the required data are provided on a regular basis by the Meteorological Office, for example in their information package PACRAM. In particular, the package includes the mizing-layer depth, h. Algorithms for estimating h from surface data are given in R91. An algorithm for computing h/L_{MO} is given in the full report. (The key references for guiding our recommendations were Clarke (1979) (R91) and Weil (1985) and the accompanying papers in the same issue of J. Climate & Applied Meteorology.)*

2.2 Wind field over complex terrain

2.2.1 Reasons for considering wind fields over complex terrain

Our review has shown that in the atmosphere changes in surface conditions, such as over hills, or changes in surface roughness and temperature, can have a marked effect on the dispersion of pollutants. In particular:

- the rise of buoyant plumes can be strongly affected;
- average maximum ground-level concentrations can be increased, typically by factors of two to three in neutral conditions and even more in stable conditions:
- the pattern of dispersion can be markedly changed leading to significant changes (more than a factor of two) in the distance x_{mx} of maximum ground-level concentration $C_{g\ell mx}$ from the source.

In Fig.2 we give an example of U.S. field and laboratory experiments which shows the amplification of $C_{g\ell mx}$ for various positions of the source relative to a hill.

2.2.2 Models for wind field

We have reviewed the major changes in air flow over complex terrain as a basis for discussing different models. In the literature, there are four main approaches to the problem of defining the wind field over complex terrain for dispersion modelling.

(i) Plat terrain plus warnings:

Assume that the air flow passes over the terrain as if it was flat and take an average roughness length over the plume path. In some models caveats are given as to when this approach leads to significant errors (e.g. report NRPB-R199, Table 1, Jones 1986).

(ii) Simple deflection/impingement models.

Assume some general form for either the deflection of mean flow streamlines or

their impingement onto the ground for airflow over hilly terrain. These models use no actual contours of the terrain, only the height of the terrain immediately below the centre line of the plume. In addition, they may require information about the stratification and windspeed. These methods are useful for estimating the highest surface concentrations on a hill in very stable conditions. Examples are the U.S. Environmental Protection Agency CRSTER and VALLEY models, and their later developments COMPLEX I, II and RTDM. An in-depth review of these and other models by White et al. (1985) revealed significant deficiencies between their predictions and corresponding field measurements.

(iii) Interpolation of the wind field, using terrain data and stratification.

This method uses wind-field measurements at a number of places in and around the area of interest, and then by assuming a rather simple form for the airflow a wind field is constructed between the measurement points. It takes considerable computing power but has been widely used for dispersion modelling. Examples are the UK WAFT model (ApSimon et al. 1984) and in the US, the MATHEW model, on which the ADPIC dispersion scheme is based (Sherman 1978; Lange 1978). The latter model was severely criticised in a searching review by Lewellen et al.(1982).

(iv) Computations involving terrain data-solving differential equations.

This approach appears to be the most promising and so we devote more space to it both here and in the report. In this method the wind field is computed using the differential equations of fluid motions with initial conditions given by the wind field approaching the terrain. The relevant models in the UK are the Meteorological Office Mesoscale model which currently runs only on the Office's computer, and the smaller-scale model FLOWSTAR, developed by CERC in collaboration with the CEGB, for running on an IBM PC AT. This latter model is based on simpler equations corresponding to airflow over hills with average slopes less than about 1/4,

which permits satisfactory results to be generated for a wide range of regions. (The hills are represented mathematically in terms of wave-like undulations superimposed on each other.) Regions where the code is unreliable can be "flagged". This is similar to models developed by Atmospheric Environment Services in Canada, and in Denmark, but these do not cater for the effects of stratification.

The U.S. Environmental Protection Agency has just completed an 8-year programme on modelling flow and dispersion over hills, with special emphasis on highly stable conditions, the outcome of which is the computer code CTDM (Paine et al.1987). Each major hill near the source is represented as an ellipsoid and allowance is made for both strong stratification and plumes impinging onto the hills, but in other respects it is less general than all the aforementioned models.

- *Our conclusion is that the only practical approach for modelling the wind field over complez terrain in dispersion calculations using small and commonly available computer systems, and easily available data, is either to assume the deflection/impingement plume path, which is adequate for some extreme criteria in certain conditions, or to calculate the airflow using a model based on simplified equations that can be computed quickly. There is some research to be done before these simplified models can be used for practical dispersion problems. It is essential that the boundary-layer structure be correctly modelled, as recommended in 52.1, for correct modelling to be possible for complez surface effects. (The key references here are the reviews by White et al. (1985) and by Carruthers, Hunt & Holroyd (1989).)*

3. ADVANCED DISPERSION MODELS

The approaches to modelling dispersion can be classified as follows.

(i) Specification of standard concentration profiles and plume parameters

The essential simplifying features of the Pasquill-Gifford and R 91 approach to modelling dispersion are:

(a) to assume that the profiles of mean concentration downwind of a source have the same shape in all boundary layers, and that the shape is described by a Gaussian curve, centred on the source height, with image points below the ground and above the inversion height, to cater for reflections at those bounding surfaces;

(b) to assume that the vertical and horizontal widths (σ_z, σ_y) of these profiles could be specified for each position downwind (x) and for each meteorological condition (A-G) of the boundary layer;

(c) to assume that σ_z, σ_y are independent of the source height.

Recent research has shown that these assumptions are unrealistic and inaccurate. For example, the plume width parameters were originally derived from measurements of plumes emanating from ground level, the behaviour of which can be quite different from that of plumes from elevated sources. However, the errors in modelling may be as much from a poor definition of the boundary-layer structure as from a poor dispersion model.

(ii) Improving plume parameters but retaining Gaussian profiles

If the state of the boundary layer is better specified (using boundary-layer

rather than surface-layer meteorology) and the profiles of the mean velocity, temperature and turbulence are known, significant improvements are possible in defining the plume widths σ_z, σ_y and the mean wind speed U in the plume. This leads to measurable improvement in the prediction and ordering of measurements of dispersion from elevated sources (see Fig.3a,b).

Figure 4 shows the change in the values of C_{gl} obtained by using these models as compared with R91. There are clearly some significant differences for elevated sources.

In flow over complex surface conditions, such as hills, roughness or temperature changes, some improved estimates of dispersion can be obtained using models of the complex flow fields in this situations, but still using Gaussian profiles. These methods lead to useful and reliable estimates of extreme conditions of high surface concentrations in complex terrain. This is the basis for the newly-proposed EPA complex terrain model CTDM.

So there can be improvement in near-field (less than 30km) dispersion modelling using better models for the boundary layer and complex wind fields. But also the constraints of using Gaussian profile modelling may partly reduce the benefits of better wind-field models.

(iii) Modelling concentration profiles

In general, the Gaussian profile assumption (i) is not accurate, especially in unstable conditions and in complex terrain. Various modelling methods are available; those used in practice include:

(a) *ad-hoc* corrections to Gaussian profiles (such as used by Moore & Lee (1982) at the CEGB);

(b) puff models using real or simulated meteorological input.

(c) stochastic (e.g. random-walk) models of diffusion (as used in ADPIC for example);

(d) solving the diffusion equation;

These methods require considerably more computing time and resources than assuming the Gaussian profiles as in methods (i) or (ii) but allied to experimental studies, they should lead to more accurate practical dispersion models.

- *Our conclusion is that there can be significant improvements in modelling dispersion by improving the modelling of the boundary-layer structure, and the wind field over complez terrain, even while using current Gaussian plume dispersion models (ii). However, the real benefits of a better boundary-layer and complez wind-field models can only be obtained after developing better dispersion models, using the results of complez dispersion models of type (iii).*

4. BENEFITS AND COSTS OF MORE COMPLEX MODELS

4.1 Improvement in boundary-layer description

A better boundary-layer 'definition' based on the parameter h/L_{MO} should be implemented. The advantages are that:

(i) it would be based on recent and authoritative research and an unusual degree of consensus among researchers. The current U.K. classification is not a world-wide or even European standard as the review of Kretzschmar & Mertens **(1984)** makes very clear. There would be a great advantage in moving to a world standard and in ensuring that the U.K. led the way;

(ii) it would enable better use to be made of local measurements of the boundary layer depth h, and, perhaps, encourage such measurements to be made (in France they are standard at nuclear power stations);

(iii) it would provide a basis for specifying dispersion parameters as a function of the height of the source;

(iv) it is essential for matching boundary-layer models to models for air flow and dispersion over complex terrain, which incorporate variations with time of the boundary layer (of great importance for long-range transport) and the effects of precipitation (both the latter are included in models being developed by groups at Imperial College and the U.K. Meteorological Office);

(v) there would be no significantly greater computational cost than in evaluating the Pasquill/Smith stability category;

(vi) it would put in a standard scientific form the advanced methods (especially (ii) and (iii)) introduced by Moore & Lee (1982) for dispersion from CEGB fossil fuel power stations.

4.2 Improvements in air flow modelling

It is possible to develop general and practical air-flow models over many kinds of complex surface, such as hills, roughness and temperature changes. Models are currently available and under development. The reasons for developing such models and comments on the model are given below:

(i) complex terrain often gives rise to the largest surface concentrations of pollution, or the most anomalous dispersion. Even quite simple models can account for many particular effects as recent field studies in the U.S.A. and U.K. have shown;

(ii) complex terrain effects within 30km of sources also need to be considered in probabilistic risk assessment models. Since in these models, many situations and cases need to be considered, simple and fast wind-flow and dispersion models covering most of the likely cases are needed;

(iii) simple and user-friendly schemes for small computer systems are becoming available to model most of the common air-flow situations, to indicate the situations where the models are inadequate, and to model in an ***ad-hoc*** fashion particular critical situations.

The only disadvantages of using air-flow and dispersion models incorporating real terrain effects is that they are more complex and lengthy to program and operate.

The disadvantage of using *simple* models is that they may not account for all the effects included in large-scale more computer-intensive models, but regions where the use of simple models is uncertain can be "flagged". The U.K. Meteorological Office Mesoscale model (Golding 1987), for example, is not is not suitable for the application considered here because it does not permit a sufficiently detailed description of the terrain over the length scale of interest.

4.3 Improvements in dispersion modelling

With better models for the airflow in the atmospheric boundary layer over complex terrain, the evidence is that, compared with the present methods of R91, the prediction of dispersion and surface concentrations can be improved, even when Gaussian plume modelling of the dispersion process is used.

For air flow over flat uniform terrain, the main improvements would be in modelling the less usual conditions of strongly stable and unstable flows, and the changes caused by elevated sources. There would be some indication of the considerable uncertainty in estimating dispersion in strongly stable boundary layers. For near-neutral conditions there would be little change when the sources are less than 100m high. Better models for the air flow over complex terrain would enable systematic changes to be estimated of the distribution of ground-level concentration, and deposition, as well as extremely high occasional concentrations on sloping terrain in highly stable conditions.

This review and that by White et al. (1985) of the more advanced dispersion models currently available suggest that it would be possible to develop significantly improved models for predicting dispersion in the boundary layer and over flat and complex terrain.

More advanced, but more scientifically-based, air flow models and dispersion models for isolated sources would also help improvements in the modelling of related problems, such as dense gas dispersion, dispersion from area sources, and more complex processes in the atmosphere, such as chemical changes, washout, deposition, etc.

4.4 Effort and costs of developing a more advanced dispersion model

- *The main conclusions of this work are that it is indeed possible to develop a more advanced scheme than that described in R91 for predicting the airflow and dispersion up to about 30km from sources in the U.K. and that such a scheme could be implemented on a personal or micro-computer. It should be borne in mind that, to develop such a system, it is necessary to understand and appreciate thoroughly the underlying relevant research work and attributes and limitations of ezisting models. Progress could best be made through collaboration with the NRPB and other relevant ezpert groups, by making use of current developments in the U.S.A., Japan and other European countries.*

We suggest that it would be both possible and desirable to incorporate as sub-models in this scheme processes such as air flow, dispersion, deposition, etc., at present being studied by other U.K. ezpert groups.

REFERENCES

ApSimon, H.M., Kitson, K., Fawcett, M. & Goddard, A.J.H. (1984) Development of a prototype mesoscale computer model incorporating treatment of topography. Commission of the European Communities, Report EUR 9503 EN.

Carruthers, D.J., Hunt, J.C.R. & Holroyd, R.J. (1989) Airflow and dispersion over complex terrain. Proc. 17th NATO-CCMS Int. Tech. Meeting on Air Pollution Modelling and its Applications. Sept. 1988, Cambridge. Plenum.

Clarke, R.H. (1979) A model for short and medium range dispersion of radionuclides released to the atmosphere. (First report of a working group on atmospheric dispersion.) National Radiological Protection Board Report NRPB-R91.

Golding, B.W. (1987) The U.K. Meteorological Office mesoscale model. Boundary-

Layer Met. 41, 97-107.

Jones, J.A. (1986) The uncertainty in dispersion estimates obtained from the working group models. (Seventh report of a working group on atmospheric dispersion.) National Radiological Protection Board Report NRPB-R199.

Kretzschmar, J.G. & Mertens, 1. (1984) Influence of the turbulent typing scheme upon the cumulative frequency distribution of the calculated relative concentrations for different averaging times. Atmos. Env. 18, 2377-2393.

Lange, R. (1978) ADPIC - a three dimensional transport diffusion model for the dispersal of atmospheric pollutants and its validation against regional tracer studies. J. Appl. Met. 17, 320-329.

Lewellen, W.S., Sykes, R.I. & Oliver, D. (1982) The evaluation of MATHEW/ ADPIC as a real time dispersion model. Aeronautical Res. Assocs. of Princeton Inc., Rep. No. 442 for Div. Health, Safety and Waste Management, Office of Nuclear Regulatory Res., U.S. Nuclear Regulatory Commission.

Moore, D.J. & Lee, B.Y. (1982) An asymmetric Gaussian plume model. CERL Report RD/L/2225 N/81.

Paine, R.J., Strimaitis, D.J., Dennis, M.G., Yamartino, R.J., Mills, M.T. & Insley, E.M. (1987) User's guide to the Complex Terrain Dispersion Model. Vol. 1. Model description and user instructions. Atmos. Sci. Res. Lab., Office of Res. & Development, U.S. EPA.

Sherman, C.A. (1978) A mass consistent model for wind fields over complex terrain. J. Appl. Met. 17, 312-319.

Weil, J.C. (1985) Updating applied diffusion models. J. Clim. Appl. Met. 24, 1111-1130.

White, F.B. (ed.), Ching, J.K.J., Dennis, R.L. & Snyder, W.H. (1985) Summary of complex terrain model evaluation. Atmos. Sci. Res. Lab., Office or Res. & Development, U.S. EPA.

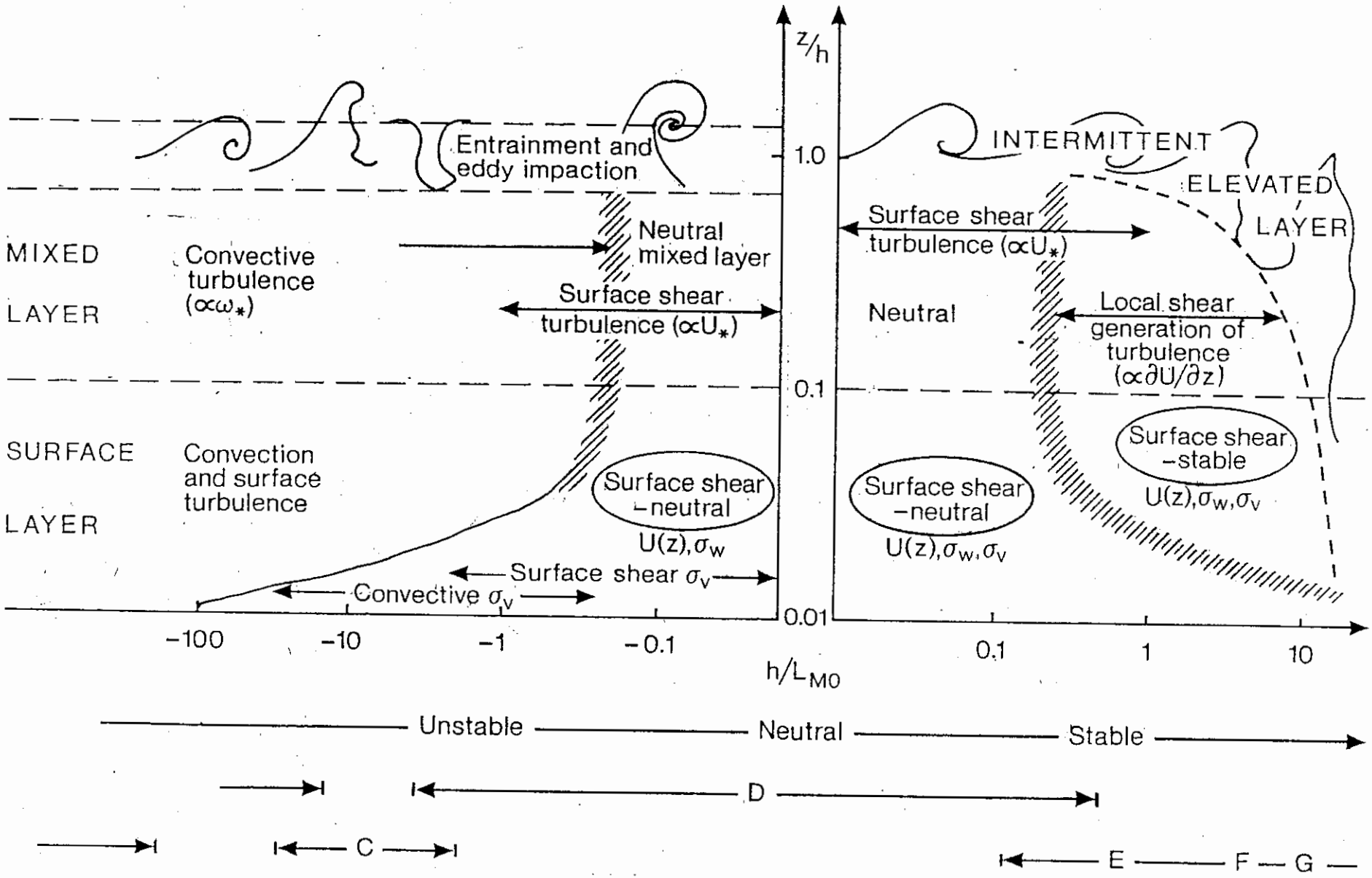

Fig.1 Structure of the atmospheric boundary layer as z/h and h/L_{MO} vary.

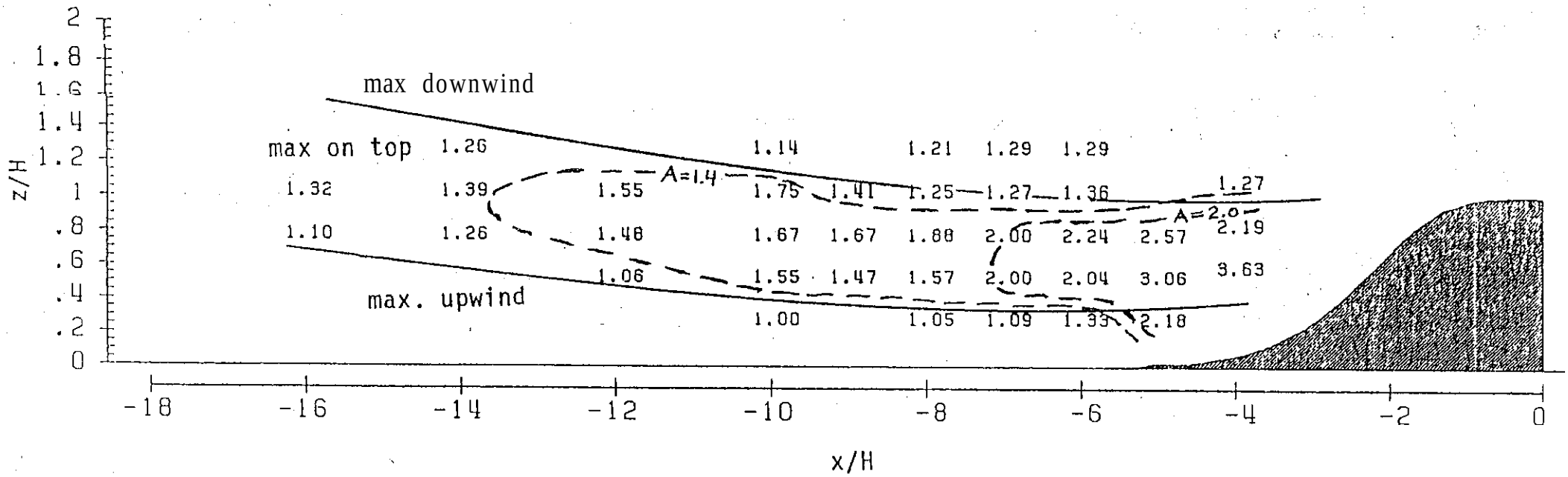

Fig.2 Terrain amplification factors for sources located upwind of an axisymmetric hill. The solid lines divide the region into areas where the source produces $C_{g\ell\,\mathrm{mx}}$ upwind of the hilltop, between the hilltop and the separation point on the lee slope, and downwind of the hill. Each number is the increase in $C^{(o)}_{g\ell\,\mathrm{mx}}$ for a source at that position.

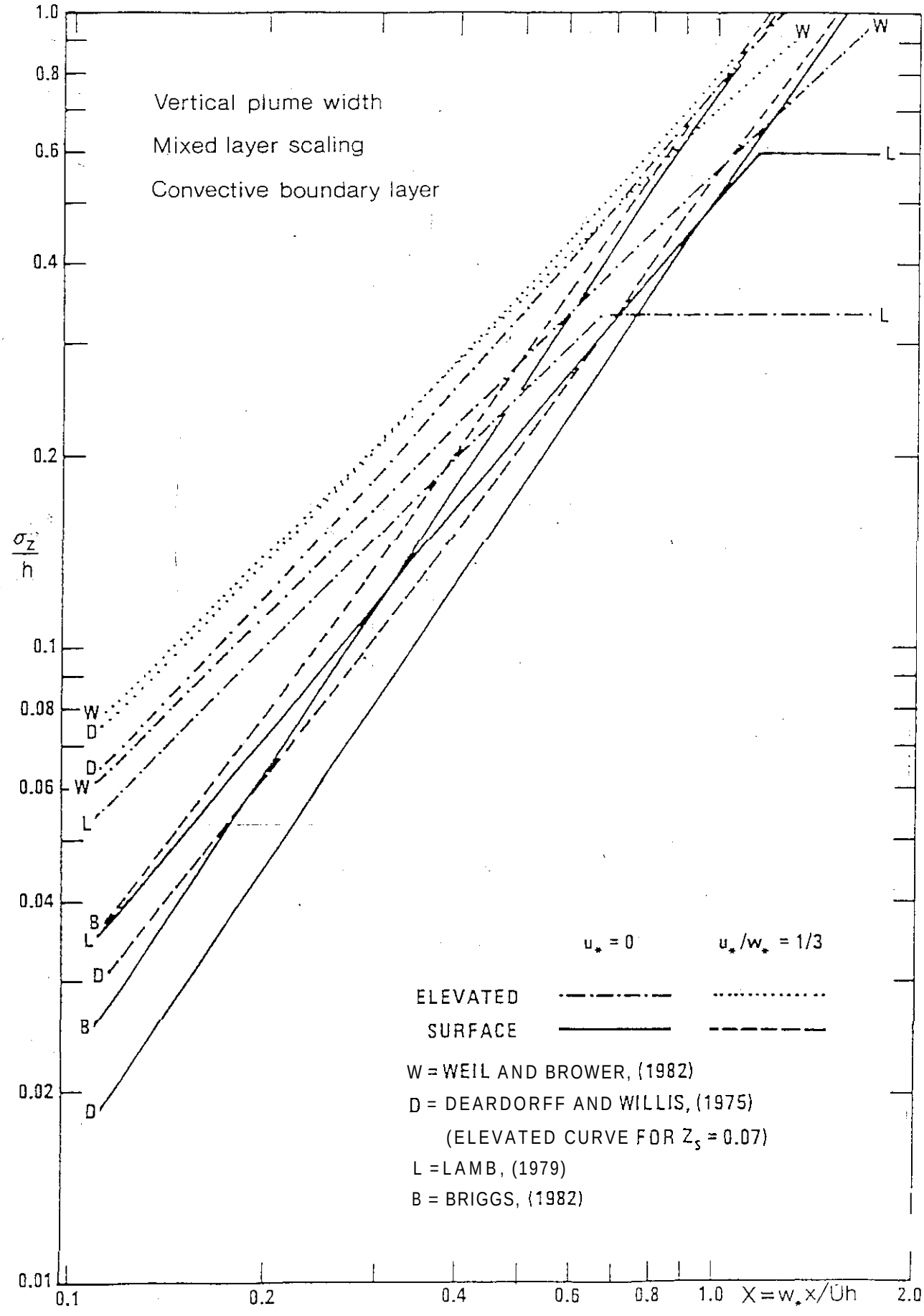

Fig.3 Variation of σ_z downwind of a source in a convective boundary layer expressed in similarity co-ordinates (from Briggs 1985).

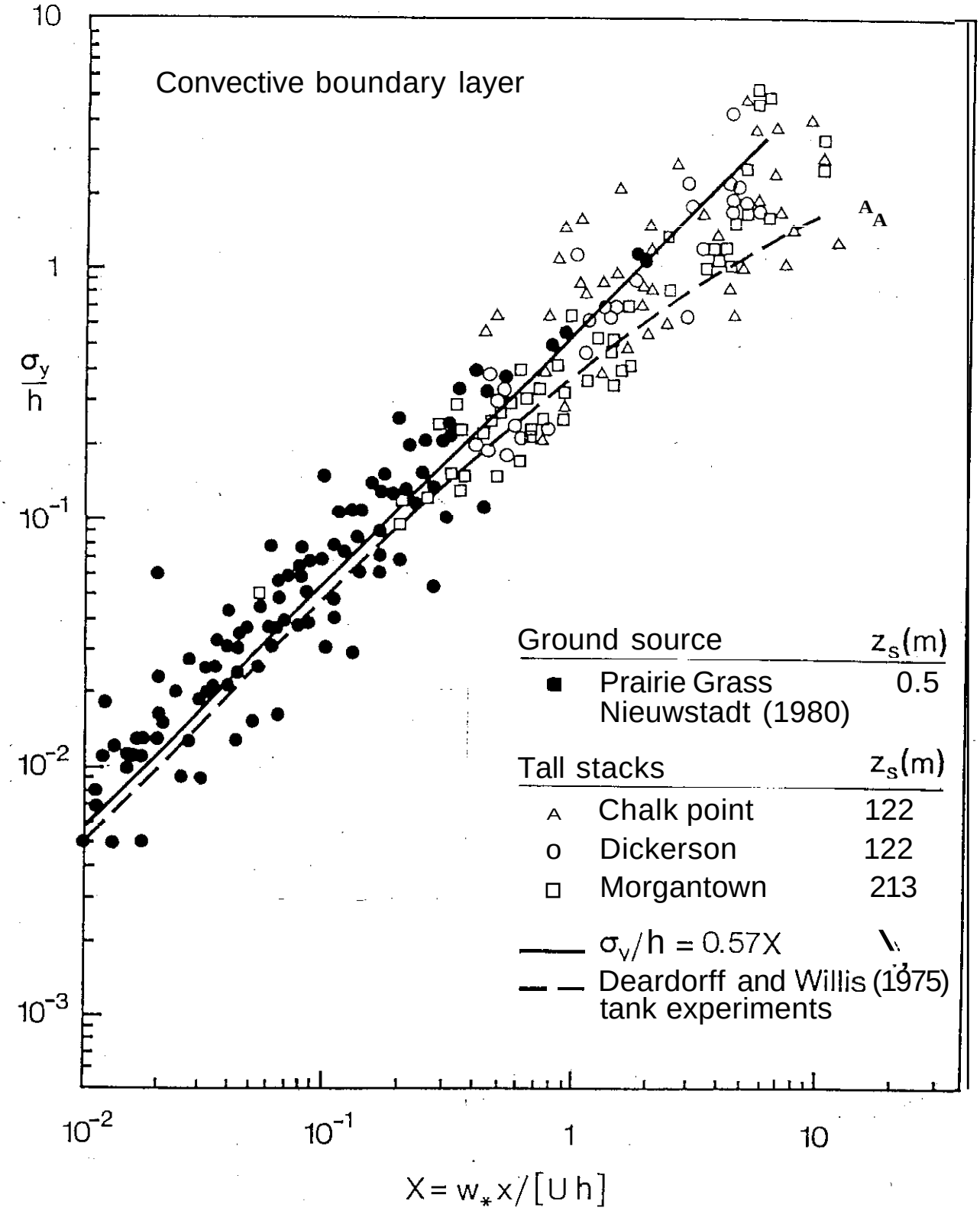

Fig.4 Variation of σ_y downwind of a source in a convective boundary layer expressed in similarity co-ordinates (from Weil & Brower 1984).

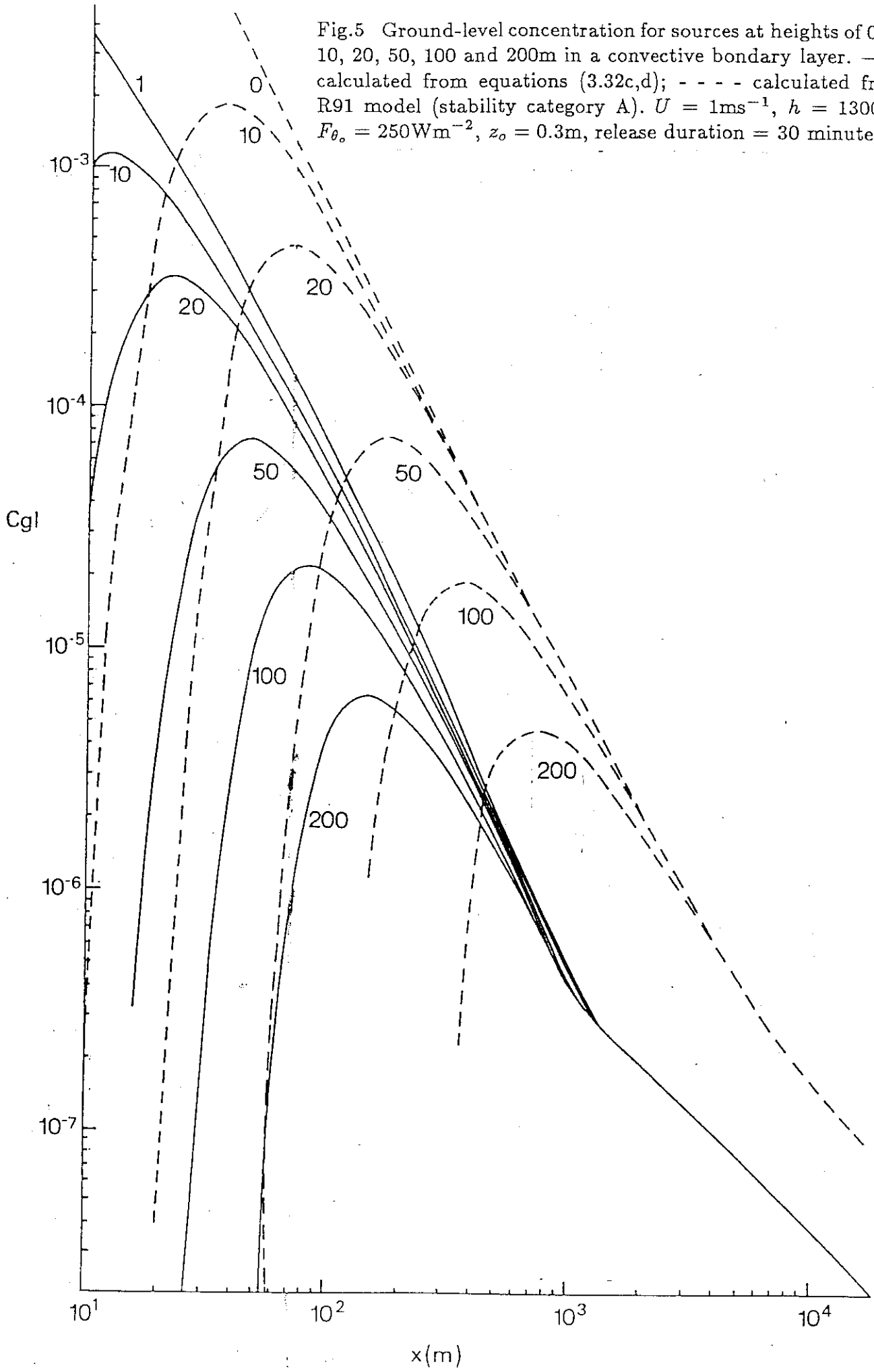

Fig.5 Ground-level concentration for sources at heights of 0/1, 10, 20, 50, 100 and 200m in a convective bondary layer. —— calculated from equations (3.32c,d); - - - - calculated from R91 model (stability category A). $U = 1\text{ms}^{-1}$, $h = 1300\text{m}$, $F_{\theta_o} = 250\text{Wm}^{-2}$, $z_o = 0.3\text{m}$, release duration = 30 minutes.

HB 9/88

Report to:
National Radiological Protection Board
Atomic Weapons Establishment
H.M. Inspectorate of Pollution
Health & Safety Executive

on

PREPARATORY STUDIES FOR A COMPLEX DISPERSION MODEL

by J.C.R. Hunt, R.J. Holroyd & D.J. Carruthers

Cambridge Environmental Research Consultants, Ltd.

November 1988

1. INTRODUCTION

1.1 Background to study

1.1.1 Limitations of current UK practical dispersion models

The current dispersion models widely used in the UK (similar to those described in R91) are based on simplifying assumptions about the wind field and the dispersion process. These models are generally suitable for flat uniform terrain (for low-level sources) in rather constant meteorological conditions, which are not far from neutral.

The report ADMLC(87)P1 highlighted situations where these models are inadequate, because the plume cannot be assumed to traevl in a straight line with uniform velocity from the source. Also, the dispersion is not a simple reflected 'Gaussian' plume, whose depth and width are defined by the meteorological conditions measured near the ground.

These situations where a more complex model is necessary can be stated in general terms as where there are large and/or abrupt changes in

(i) Roughness. e.g. from land to sea, or rural to urban;

(ii) Elevation. Changes in air flow over hills affect plumes, particularly in stable conditions, because they affect the direction of the wind. This is one way in which , plumes are strongly affected by topography; there are many others which are discussed later.

(iii) Temperature. These changes affect not only the turbulence and stability of the atmosphere, but also the mean wind speed and direction, as in sea breezes, slope winds and in urban/rural winds.

The dispersion models are also inadequate even over level ground when the sources are high (of the order of 100m) and the atmospheric boundary layer is quite unstable or quite stable. A number of practical procedures have been suggested and tested for these situations which could be applied in the U.K. (as reviewed in a recent U.S. workshop by Weil (1985) (to which Drs. Hunt and Britter of CERC contributed)).

Since a number of organisations in the U.K. are not aware of these limitations to current models, they are explained and illustrated in this report.

The current model developed by the UK ADWG (described in the report NRPB-R91, Clarke 1979, hereafter referred to as R91) also covers situations other than a steady dry atmosphere, e.g. diurnal variations, wet deposition, etc. The limitations and possible developments of these aspects of the ADWG model are not discussed in this report.

1.1.2 Reason for proposed study

Many research groups and agencies in the U.K. and Europe are well aware of these limitations and are developing new models to allow for them. But as yet there has been no agreed methodology for the next stage in modelling beyond the 'Pasquill-Gifford' Gaussian plume phase – with the possible exception of the use of new but simple descriptions of diffusion in the convective conditions (Weil 1985).

Although there are different uses of these models, e.g. real-time modelling, post-accident reconstruction, etc., one of the first aims of the next generation of modelling should be to improve probabilistic risk assessment. In such PRA studies, of the order of 10^3 to 10^4 computations might be necessary at any given site to take account of a full range of meteorological conditions and release accident scenarios. Consequently a model taking more than 5 to 10 minutes per run on a 'modest' computer system is not acceptable.

Cambridge Environmental Research Consultants Ltd. has been engaged to bring forward recommendations for the development of a complex dispersion model which can be used in situations not allowed for in the present model, and to meet the above criteria in terms of run time and computing power. The range to be considered is about 30km from the source.

There are some realistic grounds for believing that better models are possible and practical. It is the aim of this report to explore these models and bring forward recommendations for their practical development and implementation.

1.2 Objectives and the work plan of the study

The objectives as agreed by the Atmospheric Dispersion Liaison Committee in May 1987, are stated below, together with brief comments about them and about the work done towards achieving them.

(I) To review current wind-field models for use in dispersion models and make recommendations

We have interpreted this brief to include appropriate models of the boundary-layer structure, as well as models of air flow over complex terrain. In order to explain the models, an extensive review has been written, based on recent research of these flow fields. Models of all degrees of complexity have been considered, but we have assumed that the aim is to focus on those models that can be used with dispersion

codes in regulatory agencies, government and industry. In general, this means that models can only use modest computer resources (both human and hardware).

During the course of the project, the work by CERC on the first stage of its own wind-field model FLOWSTAR was completed. (This work was supported by CEGB.)

(II) To consider advanced dispersion models valid up to 30km from the source, and make recommendations for developments

We have reviewed different models (used in both practical and research work) which account for dispersion throughout the boundary layer and in wind flow over complex terrain. An extensive literature survey and review is an important part of this report.

Since the current modelling methods in the U.K. are based mainly on the approach described in the report R91, the algorithms and nomograms in that report have been programmed (in FORTRAN) to run on an IBM PC AT to act as a baseline for comparison with other models. Some specific comparisons have been made.

(III) To analyse the benefits and costs of more complex models

The aim of this section of the report is to justify the recommendations made in Sections 2 and 3 for developing improved models for the boundary layer, for complex wind fields, and for dispersion processes. The justification is made on scientific and practical grounds, and an estimate of cost of proceeding with the development is given.

2. WIND FIELD MODELS

2.1. Air motion and other processes affecting dispersion in the boundary layer

2.1.1 Defining the range of interest

Matter is dispersed in the atmosphere by the movement of the air which carries it from the source, diffuses it into larger volumes of air by turbulent eddies and molecular motions, and deposits it onto the ground. This dispersion is affected by density differences between matter and atmosphere, i.e. by buoyancy, and also by precipitation, such as snow or rain. The matter can change either by chemical reactions with other species in the atmosphere or by nuclear reactions.

Therefore the first problem in modelling atmospheric dispersion is describing, understanding and, if necessary, modelling those aspects of atmospheric motions that affect dispersion. In this report, we are concerned with dispersion within a distance of about 30km from the source and within the lowest 2km of the atmosphere (because on average very little matter disperses above this height over a distance of 30km). This lowest layer of the atmosphere is referred to as the atmospheric boundary layer. The processes of deposition by precipitation and change of concentration by chemical reaction can occasionally be significant over this distance but are not considered here.

2.1.2 Factors determining the air motions in the boundary layer

The motions and the temperature distribution in the atmospheric boundary layer are governed broadly by three groups of factors (see Figs.2.1a,b);

(i) the 'roughness' and changes in elevation of the earth's surface near and for some distance upwind of the region of interest. The 'roughness' effect is caused by many small surface protrusions obstructing the air flow; these may range in scale from grass to buildings or even ranges of hills. A roughness length z_o characterises the effect of these obstructions on the flow above them (typically z_o is about 1/30 of the height of randomly scattered promontories). So, for the examples given, z_o ranges from 0.01m to 1m to over 10m. The effects of changes in elevation on the air flow are characterised both by the height H and the length scale L of the terrain features, which are both much greater than $30z_o$ to distinguish them from roughness changes (see §2.2);

(ii) the air flow above the boundary layer, free from the influence of ground roughness and is usually termed the geostrophic wind speed U_g. Temporal and horizontal gradients in U_g are important and, in general, lead to convergence/ divergence of the horizontal flow and thence to upward/downard motion above the boundary layer.

(iii) the heat flux F_{θ_o} (Watts $m^{-2}s^{-1}$) into the atmosphere at the surface. This is determined by such factors as the solar radiation reaching the surface (which may be land or the sea), the absorption and release of latent heat by water vapour near the surface, especially around vegetation, and heat either absorbed by or released from the surface. As with the other factors, the temporal and spatial variations of F_{θ_o} are also important in determining the structure of the boundary layer. Important examples of the atmosphere affected by spatial gradients are urban heat islands and the sea breezes (see §2.2). An important example of the temporal variation in F_{θ_o} is that caused by the regular diurnal changes in solar radiation.

Plate (1982) contains a full discussion of air flow in the atmospheric boundary layer.

2.1.3 Ideal boundary layers with similar structure

Since the structure of the atmospheric boundary layer is determined by so many varied factors, does this mean

(i) that the structure changes as these factors change, and

(ii) that describing or modelling the wind field in the boundary layer requires a detailed computation for each meteorological condition?

If the answer to both questions was 'yes', it would be impossible to model atmospheric dispersion with small computational resources. In fact, for much of the time and for many locations, the atmospheric boundary layer does have an approximately similar structure over defined ranges of meteorological conditions.

Three ranges can be clearly identified, corresponding to unstable convective, neutral and stable boundary layers. Typical conditions characterising these ranges are: light winds and high surface heat flux; high winds and small positive or negative surface heat flux; and night time conditions of light winds and negative surface heat flux respectively. The parameters defining the structure of these boundary layers are quite different for each case.

It has been one of the major results of recent research in micro-meteorology to demonstrate this similarity in fairly ideal circumstances such as over terrain that is nearly flat and in slowly-changing meteorological conditions. Much current meteorological research is also directed towards identifying and modelling situations when the boundary layer has a spatial structure dependent on local topography and

local meteorology.

What 'similarity' means is that the vertical profiles of the mean wind speed, turbulence and temperature (and other quantities) can be described by the same mathematical functions of height above the ground z, or graphs, when each of these quantities is divided by (or 'normalised' by) a value at a particular height (say 10m or a surface value). For similarity the height co-ordinate also has to be divided by a particular length (usually the roughness length z_o or the boundary-layer depth h). We now illustrate and justify this approach for the three different types of boundary layer.

2.1.4 Convective Boundary Layer (CBL)

Figure 2.2a shows two examples of the convective boundary layer. In the first case, the mean wind speed 10m above the ground, U_{10} is 2ms^{-1} and the depth is 1.5km, while in the second case, U_{10} is 4 ms^{-1} and the depth is only 400m. Note how the profiles of mean velocity U, potential temperature θ, heat flux F_θ and the r.m.s. value of fluctuations in the vertical velocity σ_w (a measure of the vertical turbulence), all have approximately same shape. These two sets of profiles and others like them are replotted as 'similarity' profiles in Fig.2.2b, using (z/h) as the vertical 'similarity' co-ordinate. The wind speed is 'normalised' by U_{10}, and the turbulence is normalised by a characteristic value (w_*) of its magnitude at the mid-height of the boundary layer.

In thermal convection the turbulence is mainly determined and then driven by the heat flux at the surface (F_{θ_o}) which produces hot thermals of air that rise from the surface. Since the thermals gain in scale and speed as they rise, the depth h of the layer is also important. By dimensional analysis (Deardorff 1985) it follows that this characteristic velocity is

$$w_* = [g\ F_{\theta_o} h/(\rho c_p T_o)]^{1/3} \tag{2.1}$$

where T_o is the temperature at the surface $(z = 0)$, g the acceleration due to gravity, ρ the density and c_p the specific heat at constant pressure.

This similarity plot using z/h as the vertical co-ordinate, does <u>not</u> lead to the mean velocity and vertical turbulence profiles being the same as each other in the 'surface layer', which in the CBL extends from the ground up to about 1/10 of the boundary-layer height. The reason is that near the surface the air flow is strongly affected by the turbulence generated by the wind shear near the ground. This gives rise to a shear stress stress τ which, at the surface $\tau(z = 0)$, is usually expressed in terms of a friction velocity u_* as ρu_*^2. Very close to the surface the mean wind speed is solely determined by u_*, the roughness length z_o and the distance z above the surface, i.e.

$$U(z) = \frac{u_*}{\kappa} \ln(z/z_o), \tag{2.2a}$$

where κ is a constant, known as von Karman's constant, whose value is about 0.4 while the vertical turbulence is given by

$$\sigma_w \simeq 1.3 u_*. \tag{2.2b}$$

It is important to realise that the horizontal components σ_v, σ_u are determined by both the convective and the shear turbulence in this surface layer (Panofsky et al. 1977). The dynamical reasons for this are discussed by Hunt (1984)*. (A formula is given in §2.1.7.)

The height at which the fluctuating buoyancy stresses dominate over the shear-induced stresses and drive the turbulence is the Monin-Obukhov length

$$L_{\rm MO} = \frac{-u_*^3}{\kappa g F_{\theta_o}/(\rho c_p T_o)}. \tag{2.3}$$

More specifically, it is the magnitude of $L_{\rm MO}$ that is important since, for convective conditions F_{θ_o} is positive and, hence, $L_{\rm MO}$ is negative. For $z \geq |L_{\rm MO}|$ the mean velocity and temperature profiles and the turbulence are changed from the form given by (2.2). In other words for $z < |L_{\rm MO}|$ the shear stresses are strong enough for the flow to be locally effectively neutrally stable. Thus in the CBL there are different regions with quite different dominant processes.

In the surface layer these profiles can be expressed as general functions of $z/L_{\rm MO}$. This means that profiles for different situations, such as those in Figs.2.2a, which can be expressed as single functions of z/h in the surface layer, differ from each other depending on the ratio $h/L_{\rm MO}$.

By substituting the value for $g\ F_{\theta_o}/(\rho c_p T_o)$ from (2.1) into (2.3), it follows that

$$h/L_{\rm MO} = -\kappa\ \frac{w_*^3}{u_*^3}. \tag{2.4}$$

Therefore the ratio $h/L_{\rm MO}$ also characterises the relative importance throughout the CBL of the buoyancy-generated turbulence to the surface shear-generated turbulence. In fact $h/L_{\rm MO}$ has been chosen by most researchers as the most appropriate ratio for defining the state of the boundary layer for dispersion calculations (Holtslag & Nieuwstadt 1986; Gryning et al.1987). We present a modified form of their diagram in Fig.2.3, which describes these different regions of the boundary layer.

Many field experiments in several countries have now confirmed this general picture of the CBL, namely that over most of the depth of the boundary layer the quantities are functions of the non-dimensional height co-ordinate z/h. This is demonstrated in Figs.2.2c(i) and (ii) which shows profiles of vertical and horizontal turbulence measured over rolling terrain near the Rocky Mountains in Colorado

* Unless indicated by an initial, references to Hunt relate to J.C.R. Hunt.

by Kaimal et al. 1976) and in Malvern, England by Caughey & Palmer (1979). In §2.1.5 we discuss the question of when the boundary-layer structure is likely to diverge from this idealized or general structure.

As the wind speed increases and/or the surface heat flux decreases, there is a greater relative contribution to the turbulence in the boundary layer by surface shear stresses characterised by u_* than by the thermally-generated turbulence characterised by w_*. Thus the characteristic ratios w_*/u_* and $h/|L_{MO}|$ decrease. When these ratios fall below about 1.0 the structure of the boundary layer begins to change as the surface layer (where $z/|L_{MO}|$ is the relevant vertical co-ordinate) increases in thickness. The typical structure of thermal eddies produced by thermal instability continues to dominate even when $h/|L_{MO}| < 1$ (Hunt, Kaimal & Gaynor 1988), and the turbulent diffusion can be affected (Nieuwstadt 1978).

It is only when $h/|L_{MO}| < 0.3$ that thermal effects are generally small and the boundary layer can be regarded as neutral. (There is some difference of opinion between researchers as to when the bulk of the layer ceases to be affected by thermal effects – is it $h/|L_{MO}| = 0.3$ or 1.0?; Gryning et al. 1987.)

Typical values for these parameters are given in Table 2.1 which is an extended form of Table A2 in R91.

2.1.5 Neutral Boundary Layer (NBL)

Vertical profiles of the principal variables in the NBL and their variation with z_o are sketched in Fig.2.4. The mean wind velocity profile (Fig.2.4(ii)) increases continuously to its maximum value of U_g at the top of the layer. Over the lowest 100m the profile is logarithmic and depends on roughness the length z_o (Panofsky 1974), while in the upper part of the boundary layer, the profile depends on (z/h). The power-law profile

$$U/U_G = (z/h)^p \tag{2.5}$$

is a useful (and widely-applicable) approximation, where p depends on the roughness length. Other mathematical forms of the profiles are reviewed by Plate (1971).

When the boundary-layer dynamics are controlled by the Coriolis acceleration, there is a systematic turning of the wind with height (to the left for an observer facing away from the wind in the northern hemisphere), ranging from about 5° to 20° (Plate 1971). The direction and magnitude of this turning is quite sensitive to changes in surface roughness and upper-layer conditions.

In marked contrasts to the CBL, turbulence in the NBL is largely controlled by the surface shear stress so that $w_*/u_* \lesssim 0.7$ and $h/|L_{MO}| \lesssim 0.1$. Most of the turbulence is generated close to the surface (70% within the lowest 30m for a 500m thick layer over roughness of 0.03m) and so the magnitude of the vertical and horizontal fluctuations decreases with height (Fig.2.4(v,vi)). An important feature of this tur-

bulence is that it may also contain large roller eddies whose axes are aligned nearly parallel to the wind, with lateral scales of the order of h. These appear as slow fluctuations in surface wind speed and wind direction (typically on a time scale of $h/U_g \sim 50$ secs, for $h = 500$m and $U_g = 10$ ms^{-1} (Mason & Sykes 1980).

The depth h of the NBL may be determined by a balance of frictional forces and the Coriolis force, but it may equally well be limited by how much the mechanically-generated turbulence can entrain the stable air above the boundary layer during a period of strong wind (Deardorff 1972). In the former case $h \sim 0.2u_*/f$ where f is the Coriolis parameter ($\sim 10^{-4}$s^{-1} for U.K. latitudes), but in the latter case no simple formula is available. However, is is clear that, as with the CBL, defining the motions in the NBL depends on knowing its depth h.

2.1.6 Stable Boundary Layer (SBL)

In steady or slowly-varying conditions the SBL over land usually exists when the surface heat flux, F_{θ_o}, is negative. Overland this usually occurs between the hours of sunset and sunrise. An SBL can also occur when there is a heat flux to the ground, for example when warm air flow over the sea is advected over cold ground. It is the most variable of the three kinds of boundary layers as it is usually in a continuous state of evolution or even slow oscillation. Unlike the CBL and NBL, it is very sensitive to the slope and undulations of the local terrain and to the properties of the air flow above the boundary layer.

In the SBL the stable density gradient (formed by the cooler air near the ground) leads to a damping of the large scales of turbulence and thence to a higher dissipation of turbulent energy (for a given level of turbulence). This leads to a lower intensity (i.e. σ_w/U) of all components, and a smaller turbulence length scale (Caughey et al. 1979; Hunt, Kaimal & Gaynor 1985). As in the neutral boundary layer, the main source of turbulence is the air flow over the ground, but this diffuses up so slowly that the upper reaches of the SBL are dominated by turbulence generated locally rather than by the eddies emanating from the ground (Wyngaard 1985).

The boundary layer begins to change from its neutral form when the stabilising buoyancy forces are comparable with shear stresses. This occurs when

$$h/L_{\mathrm{MO}} \geq 0.3$$

(note that L_{MO} is now positive because F_{θ_o} is negative). Even when the boundary layer is stable, there is still a nearly neutral layer very close to the surface where $z/L_{\mathrm{MO}} \leq 0.1$. When $h/L_{\mathrm{MO}} \geq 1.0$ the local generation of turbulence begins to be the primary source of turbulence above the surface layer (Fig.2.3).

Because of the small levels of turbulence (or diffusivity), the SBL is more

responsive to Coriolis accelerations. This leads to the direction of the wind changing over the depth of the layer, typically by 25° - 40° (Nieuwstadt 1984; Hunt et al. 1985). van Ulden & Holtslag (1985) showed that the mean deviation between 20m and 200m increased from 12°±12° to 40°±20° as the stability increased from neutral to stable ($h/L_{MO} = 10$). This change in angle of the mean wind is important for estimating lateral dispersion and is poorly defined in general. The fact that the angle is fairly large means that the transverse component of the wind velocity becomes increasingly significant with height (see Fig.2.5a(i)).

The other feature of the SBL is that its mean vertical density or temperature gradient makes the air flow very sensitive to the mean slopes; for example, if there is slope of even 0.002 at an angle to the wind, the profile can be changed considerably (Garratt 1982). In undulating terrain the profiles are even more sensitive.

The temporal variability of the SBL is most frequently caused by the the fact that it appears in the late afternoon and evening after the vigorous convective turbulence dies down. For this period the air above the SBL is still well mixed, and so $d\bar{\theta}/dz$ is negligible for $h_{SBL} < z \leq h_{CBL}$ (see Fig.2.5a(ii), curve E). Later in the night the radiative processes may lead to a stable stratification above the SBL.

In ideal conditions the height of the SBL slowly evolves during the night to a steady state with a height of

$$h \sim (u_* L_{MO}/f)^{1/2} \tag{2.6}$$

where $f = 10^{-4} s^{-1}$, and u_* and L_{MO} are measured at the surface. Typical values are given in Table 2.1.

The turbulence velocities σ_u, σ_v and σ_w decrease with height above the surface (see Fig.2.5a(iv)) but they only decay to zero at the top of the SBL (where $z = h$) if there is neither wave motion nor shear above it, as has been found over the Netherlands (Nieuwstadt 1985) (see Fig.2.5b). Over more rolling terrain, or with typical wave motion, a weak level of turbulence is found above the SBL (i.e. above the level $z = h$ where $U = U_G$).

Despite the variability in the SBL caused by variation in surface and upper-layer conditions, there is still sufficient similarity in many kinds of SBL for it to be worthwhile defining typical mean velocity and turbulence profiles. These are given in §2.1.7.

2.1.7 Formulae for the mean velocity, temperature and turbulence profiles in the convective, neutral and stable boundary layers

It has been explained in §§2.1.4-2.1.6 that the structure of the atmospheric boundary layer, so far as the profiles of mean velocity, temperature and turbulence

are concerned, is most effectively defined by the ratio of the boundary-layer depth h to the height $L_{\rm MO}$ at which unstable or stable buoyancy forces dominate over shear stress (Gryning et al. 1987). In this section we present some parametric relationships for these profiles. The formulae are by no means definitive ones and others have been proposed (see, for example, Arya 1984). However, such differences as do exist are not inconsistent with the spread of data from which they are derived.

The boundary layer is significantly affected by unstable buoyancy forces when

$$h/L_{\rm MO} \leq -0.3 \tag{2.7a}$$

and strongly affected when

$$h/L_{\rm MO} \leq -1.0. \tag{2.7b}$$

This is the Convective Boundary Layer (CBL).

On the other hand, stabilising buoyancy forces can significantly affect the boundary layer velocity profile when $h/L_{\rm MO} \geq 0.3$, say by 6%. This is the Stable Boundary Layer (SBL).

Between these two extremes is the Neutral Boundary Layer (NBL), where

$$-0.3 \leq h/L_{\rm MO} \leq 0.3, \tag{2.8}$$

(i) **Mean velocity profile.**

Let $\mathbf{U}(z=0) = (U,0)$ at the surface (this defines the x direction), and $\mathbf{U}(z) = (U,V) = (U, U\tan\alpha)$ at height z, where α is clockwise (looking down in the northern hemisphere) so that $|\mathbf{U}| = (U^2+V^2)^{1/2}$. $U_g = |\mathbf{U}(z=h)|$ is the gradient wind speed which is not necessarily in the same direction as the ground wind.

For the CBL,

$$U(z) = \frac{u_*}{\kappa}[\ln(z/z_o) - \psi_m(z/L_{\rm MO}) + \psi_m(z_o/L_{\rm MO})] \tag{2.9a}$$

where ψ_m is an empirical function the commonest form of which for the $h/L_{\rm MO} < 0$ is

$$\psi_m(\zeta) = 2\ \ln(\frac{1+x}{2}) + \ln(\frac{1+x^2}{2}) - 2\ \tan^{-1} x$$

$$\text{and} \qquad x = (1-16\zeta)^{1/4}. \tag{2.9b}$$

Panofsky & Dutton (1984, Chap.6) discuss the merits of this and two other forms.

For the NBL $\psi_m = 0$. Note that (2.9b) reduces to this value as $|L_{\rm MO}| \to \infty$ and, in consequence $\zeta \to 0$.

No general formula is available for $V(z)$, but following Plate (1971) and van Ulden & Holtslag (1985), it is suggested that

$$V \simeq 2u_*[1 - \exp(-z/h)]. \tag{2.9c}$$

For most dispersion purposes, though, this can be neglected. In principle, (2.9a) is valid only for the surface layer, but in fact it is a useful approximation for the CBL and NBL over most of the depth of the layer (van Ulden & Holtslag 1985).

A simpler but less accurate alternative to (2.9a) is the power-law profile

$$U(z) = U_{\rm ref}(z/z_{\rm ref})^p, \tag{2.10}$$

where $z_{\rm ref}$ is the reference height.

Following the review of van Ulden & Holtslag (1985), who had also used the ideal conditions at the Cabauw tower in the Netherlands to validate their recommendations, the mean velocity profile in an ideal SBL is

$$U = \frac{u_*}{\kappa}[\ln z/z_o - \psi_m(z/L_{\rm MO}) + \psi_m(z_o/L_{\rm MO})] \tag{2.11a}$$

where

$$\psi_m(\varsigma) \simeq -17\{1 - \exp(-0.29\varsigma)\}. \tag{2.11b}$$

This is similar to the recommendation by Carson & Richards (1978) at the U.K. Meteorological Office.

The turning of the wind direction with height is given by

$$\alpha(z/h) \simeq \alpha_{\rm max}\,[1 - \exp(-z/h)], \tag{2.12a}$$

where for

$$\begin{aligned} &0.3 \le h/L_{\rm MO} \le 1.3 && \alpha_{\rm max} \sim 0.3 \\ &1.3 \le h/L_{\rm MO} \le 2.5 && \alpha_{\rm max} \sim 0.53 \\ &2.5 \le h/L_{\rm MO} && \alpha_{\rm max} \sim 0.7 \end{aligned} \tag{2.12b}$$

The standard deviation in each case is of the order of $0.5\alpha_{\rm max}$. Note that (2.12a) differs from the theoretical form given by Nieuwstadt (1985) and the Minnesota measurements of Caughey et al.(1979) which may have been influenced by the weak slope at the measurement site.

Equation (2.11a) may also be represented by the power-law profile (2.10). A graph, taken from Snyder (1981), showing the variation of the exponent p with z_o and $L_{\rm MO}$ for $z_{\rm ref}$ = 100m is shown in Fig.2.6. It should be noted that if the

alternative forms of ψ, are used when $h/L_{\rm MO} < 0$, values of p can differ by up to 20% for a given value of $h/L_{\rm MO}$.

(ii) Mean temperature gradient

In the SBL turbulent diffusion can most effectively be estimated from the turbulence statistics if the mean temperature gradient at the surface is known (Hunt 1982a; Venkatram et al. 1984). The value of $d\bar{\theta}/dz$ near the surface can be determined from the heat flux, F_{θ_o}

$$\frac{d\bar{\theta}}{dz} = \frac{-F_{\theta_o}}{u_* \rho c_p} \frac{1}{z}\left(1 + \frac{\alpha z}{L_{\rm MO}}\right),$$

where $\alpha \approx 5$. Thence typical values of the buoyancy frequency $N = \sqrt{g(d\bar{\theta}/dz)/\bar{\theta}}$ for different stability conditions can be estimated by using the values for F_{θ_o} and u_* in Table 2.1. For $0.3 \leq h/L_{\rm MO} < 1.3$

$$\begin{aligned} N &= 0.01 \left(\frac{50}{z}\right)^{1/2} && z \leq 50m \\ &= 0.01 && z \geq 50m \end{aligned} \qquad (2.13a)$$

and for $1.3 \leq h/L_{\rm MO}$

$$\begin{aligned} N &= 0.02 \,(\frac{10}{z})^{1/2} && \text{for} \quad z \leq 10m \\ &= 0.02 \left(1 - \frac{1}{2}\,\frac{z}{h}\right) \Big/ \left(1 - \frac{5}{h}\right) && \text{for} \quad z \geq 10m \end{aligned} \qquad (2.13b)$$

(iii) Turbulence intensity profiles

In the CBL above the surface layer, it is a reasonable approximation to assume that the variances of the horizontal turbulence components are constant to the top of the boundary layer i.e. $0.1h \leq z \leq h$, with a magnitude defined by

$$\sigma_u^2 = 0.3w_*^2 \quad \sigma_v^2 = 0.3w_*^2 \qquad (2.14)$$

(Kaimal et al.1976).

It is useful to have a formula for σ_u, σ_v that extends both to the ground and to the case of the neutral boundary layer. In the NBL the horizontal turbulence decreases with height to the top of the boundary layer. Therefore suitable interpolation formulae for the CBL and NBL are

for $h/L_{\rm MO} < -0.3$

$$\sigma_u^2 = 0.3w_*^2 + 6.25\ T_H^2(z)u_*^2 \qquad \sigma_v^2 = 0.3w_*^2 + 4.0\ T_H^2(z)u_*^2 \tag{2.15a}$$

and for $-0.3 < h/L_{\rm MO} < 0.3$

$$\sigma_u = 2.5T_H(z)u_* \quad \sigma_v = 2.0T_H(z)u_* \tag{2.15b}$$

where

$$T_H(z) \simeq (1 - 0.8z/h) \quad \text{for} \quad z/h \leq 1.2.$$

This is a generalisation to the whole boundary layer of the results of Panofsky et al.(1977), based on the assumption that the two forms of turbulence (buoyancy and shear) are independent of each other (Hunt 1984).

The intensity of the vertical turbulence varies because the large eddies impinge on the inversion layer and the ground. Experimental (and theoretical) arguments lead to the result that for $h/L_{\rm MO} < -3.0$ and $0.1 < z/h < 1$

$$\sigma_w^2 = 1.8\ w_*^2 \left(\frac{z}{h}\right)^{2/3} \left(1 - 0.8\frac{z}{h}\right)^2, \tag{2.16}$$

(Lenschow & Stephens 1980).

For neutral conditions in the surface layer we make the same interpolation as for the horizontal components based on the analysis of Panofsky et al.(1977) and Hunt (1984). For $-3 < h/L_{\rm MO} < -0.3$

$$\sigma_w^2 = \left(0.4T_{W(C)}^2(z) + \left(1.3T_{W(N)}\frac{u_*}{w_*}\right)^2\right) w_*^2 \tag{2.17a}$$

and for $-0.3 < h/L_{\rm MO} < 0$,

$$\sigma_w = 1.3u_*T_{W(N)} \tag{2.17b}$$

where

$$T_{W(C)} = 2.1(z/h)^{1/3}(1 - 0.8z/h) = \sigma_w(z)/\sigma_w(h/2) \tag{2.17c}$$

$$T_{W(N)} = (1 - 0.8z/h). \tag{2.17d}$$

In the inversion layer at the top of the CBL and in the stable layer above it, internal wave motions produce vertical and horizontal fluctuations that are small but may be significant for dispersion. There are several different kinds of distribution depending on the nature of the stratification. As a general estimate it may be taken that for $1.0 < z/h < 1.2$

$$\sigma_w^2 = 0.04\left(2.0w_*^2 + 1.3^2u_*^2\right) \tag{2.18}$$

(Lenschow & Stephens 1980; Carruthers & Hunt 1986).

The theory of the ideal SBL shows that all the turbulence components decrease from their maximum value at the surface to near zero at the top of the layer. This almost zero level in fluctuation near $z = h$ accords with most observations at the flat Cabauw site (Nieuwstadt 1984) (Fig.2.5(iv)). But it does not accord with many other atmospheric measurements at less ideal sites (especially those which do not filter out wave-like fluctuations which may be significant for diffusion (Hunt, Kaimal & Gaynor 1985)). Therefore it would be appropriate to define profiles of turbulence depending on whether the SBL is 'ideal' or 'disturbed'. We suggest the following:

$0 < h/L_{\rm MO} < 1.0$ take the neutral values in (2.15b) and (2.17b)

$1.0 \leq h/L_{\rm MO}$; ideal,

$$\sigma_v = 2u_*(1 - 0.9z/h)^{3/4} \tag{2.19a}$$

$$\sigma_w = 1.3u_*(1 - 0.9z/h)^{3/4} \tag{2.19b}$$

$1.0 \leq h/L_{\rm MO}$; disturbed,

$$\sigma_v = 2u_*(1 - 0.5z/h)^{3/4} \tag{2.20a}$$

$$\sigma_w = 1.3u_*(1 - 0.5z/h)^{3/4}. \tag{2.20b}$$

(iv) Effects of length scales on diffusion

Diffusion depends on the turbulence length scales, such as $L_x^{(w)}, L_x^{(v)}$, but in the CBL and NBL this dependence is significantly weaker and generally less well defined theoretically. In addition, the nature of the eddying motion of the turbulence (how it changes from the thermals and down drafts in the CBL to sheared eddies diffusing upwards from the surface in the NBL, to weakly produced, wave-like eddies in the SBL) also affect diffusion.

Some models for vertical diffusion in the CBL (see §3) and Weil (1985) depend on the probability distribution of the eddying motion or higher moments (such as the third moment w^3) (see §3.2). Models for vertical diffusion in the SBL depend on estimates of other kinds of length scales (the distance over which fluid particles move) and the rate at which fluid particles mix or change their density. These estimates depend on $N(z)$ and the local heat flux F_θ (Weil 1985; Hunt 1982a) (see §3.2).

All the turbulence quantities $L_x^{(w)}, L_x^{(v)}, T_L^{(w)}, T_L^{(w)}, p(w), \overline{w^3}, N, F_\theta$ vary with (z/h) in the boundary layer and vary as a function of $h/L_{\rm MO}$ (e.g. Kaimal et al. 1976; Nieuwstadt 1984; Hunt, Kaimal & Gaynor 1985,1988). There remain some

uncertainties about the form of these functions in different conditions, but new models and remote sensing should enable them to be defined more accurately in the next few years.

2.1.8 Boundary layers in changing conditions

We stated in §2.1.2 that the boundary layer is affected by the spatial and temporal changes both at the surface and in the air flow above the top of the layer. In the succeeding sections we have shown that there are a wide range of situations where the motion and temperature distribution have the same form without specifying anything about the changing conditions.

In this section we consider briefly when it is possible to ignore such changes in classifying, describing or modelling the boundary layer to changing conditions over flat terrain and what the consequences of doing so are.

(i) **Diurnal changes:**

Figure 2.7 shows the variation of the height of the boundary layer in convective conditions. Note how the depth h can double in a period T_h of the order of 10^4 seconds ($\approx$3 hours). The mean velocity and turbulence structure remain similar when expressed in terms of (z/h) if the turbulence can adjust to this rate of increase of h. This requires the natural time scale of the eddies $T_L \sim h/w_*$ to be less than the time T_h. For typical convective conditions $T_L \sim 10^3$s so that $T_L << T_h$ and therefore there is local adjustment.

On the other hand, when the surface heating is reduced so much that the heat flux reverses, the structure of the boundary layer is no longer described by any of the ideal cases of the CBL, NBL, SBL we have considered. In fact, the surface layer is stable while the upper regions slightly are unstable – leading to plumes 'lofting'. If, in such a situation, the whole boundary layer is described by surface meteorology, there is a sudden unrealistic switch from an unstable to a stable form.

Conversely in the morning when the heat flux changes from negative to positive, the surface layer is typically unstable while the upper layers are stable.

Note that where the boundary layer is stably stratified, the natural time scale for adjustment of the layer is about $h/(\sigma_w^2 N)$ ($\geq 10^4$secs), which is much larger than T_L because the eddy length scale is much less than h (being about σ_w/N). During the evening and night however, the conditions change more slowly than by day, so it is possible for the SBL can retain an approximately similar form.

In an 'ideal' day over flat terrain, these periods when the boundary layer does not fall into any category may only be about 15% of the total.

(ii) Spatial changes

Significant changes in the temperature over horizontal distances of about 100km give rise to vertical gradients of mean velocity above and within the boundary layer and also lead to significant changes in the wind direction with height. These changes may be caused by air flow over sloping ground, by large-scale weather systems, or by land-sea temperature changes. Figure 2.8a shows the kind of difference in the wind profile of a convective boundary layer that might be expected for variations in temperature at one level of about 1 K in 100km (10^5 Km^1). (In this case it is caused by convection over ground with slopes of about 10^{-2}.) In Fig.2.8b profiles are given for the stable boundary layer over a slope of less than 10^{-2}. (This estimate derives from the 'thermal-wind' equation $f\ \partial U/\partial z \simeq g\ (\partial\theta/\partial y)/T_o$. Thence, over a height of order h, if θ changes by $\Delta\theta$ over a lateral distance L, the change ΔU in U is estimated from

$$\Delta U \sim g\ h\ \Delta\theta/(f\ L\ T_o).$$

In the boundary layer V is changed by shear stresses affected by ΔU.)

The importance of synoptic changes on the dispersion of pollution is that they affect the depth of the boundary layer within which pollutants are confined. However, the rates of changes of h are usually sufficiently slow enough for the boundary layer to adjust so that 'similar' profiles can persist during such changes.

Rapid spatial and temporal changes associated with weather phenomena (e.g. fronts, clouds, thunderstorms) can change the structure of the boundary layer. The vertical profiles of mean velocity and direction, temperature and turbulence then change rapidly and are quite different to their forms in slowly-changing conditions. The kind of changes in profiles are similar to those shown in Fig.2.8. There is, of course, a finite but low probability of, say, a front passing between a source and a receptor in a dispersion situation and it may be feasible to develop simple models to cope with such possibilities.

Mesoscale models of varying levels of complexity are available for these situations and are reviewed in §2.2.

2.1.9 Comparison of boundary-layer meteorology classification schemes with surface-layer schemes

The current method for defining the meteorological state of the (ideal) atmospheric boundary layer for the purpose of estimating atmospheric dispersion is given in R91. Its underlying concept is essentially that of Pasquill (1961) who suggested that the atmospheric boundary layer in the U.K. could be defined by the surface meteorological variables of wind speed (at an appropriate height, say 10m) U_{10}, the surface heat flux F_{θ_o} and the roughness of the surface z_o. This concept was

further refined and quantified by Smith (1973)*, and led to a classification of the boundary layer into different states (denoted by the letters A to G, or the numbers 0 to 7) corresponding to the stability changing from unstable to neutral to stable. (For a general review of their methods in context of other approaches, the reader is referred to their book, Pasquill & Smith 1983).

A valuable feature of both Pasquill's and Smith's work was to derive simple estimates or nomograms to enable F_{θ_o} to be calculated from more easily measured variables, such as cloud cover (Pasquill 1961) or incoming solar radiation R (Smith 1973), as given in R91. In the latter calculation, assumptions are made about the amount of 'sensible' heat flux that is released, as compared with that absorbed or converted to latent heat, which implies an assumption about the surface (in fact it is assumed to be slightly wet vegetation) (details are given by Smith & Blackall 1979; other methods are reviewed by van Ulden & Holtslag 1985).

The important point about this surface method of classification compared with that set out here in §2.1.2 to §2.1.6 (which is based on methods suggested and developed by researchers in other countries), is that it does not make any use of information about the depth of the boundary layer. There are two objections to this omission:

(a) the strength of thermally-generated turbulence cannot be estimated correctly (since w_* depends on $h^{1/3}$);

(b) the variation of the turbulence and velocity profiles with height is not known.

We have looked at some typical cases of U.K. boundary-layer meteorology to compare the surface (Pasquill-Smith or R91) approach (A-G) with the 'boundary-layer scaling' approaches where the classification parameter is $h/L_{\rm MO}$ (or w_*/u_*).

In Table 2.1 (adapted from Table A2 in R91), we have given ranges for typical U.K. values of the boundary-layer depth h corresponding to the different Pasquill-Smith stability categories. Using this information and the Smith nomogram (R91, Fig.2) we have calculated values of w_* and $h/L_{\rm MO}$ for the 'mid-point' of each of the stability categories, and given a range of values at the boundaries between the stability categories. It is found that the latter correspond to a range of values of $h/L_{\rm MO}$ greater than a factor of two.

Using the formulae of §2.1.7, these correspond to a range of values of turbulence intensity (or ratios of σ_w/U or σ_v/U), which is the most relevant quantity for estimating dispersion as a function of distance from the source, for neutral and unstable cases. For the very unstable cases (more unstable than B), the lateral turbulence intensity σ_v/U may change by up to a factor of 2, using $h/L_{\rm MO}$ scaling, but in the mildly unstable and neutral boundary layer the variation in σ_v/U is small.

Thus the 'boundary-layer' approach probably gives a better prediction of the

* Unless indicated by an initial, references to Smith relate to F.B. Smith.

turbulence intensity than the present 'surface-meteorology' approach, when the boundary layer is significantly unstable (A,B) or stable (F,G).

The 'boundary-layer' approach, however, gives a significantly more accurate estimation of the variation with height of the turbulence intensity. As Moore (1975) has shown for plumes from tall CEGB power stations, this approach is essential for sources which are well above the surface layer. For example, using the formulae of §2.1.7, in A-B conditions, the vertical turbulence intensity σ_w/U increases from about 0.14 near the surface to values in the range 0.5 to 0.9 in the centre of the boundary layer, say at 300m, depending on $h/L_{\rm MO}$. As will be shown in §3, this increase in σ_w/U by a factor of 3 to 6 means that the initial vertical dispersion varies by this same factor.

The surface-layer classification of the boundary layer leads to further uncertainty in the estimate, because any one category includes a significantly large range of values of w_*/U and $h/L_{\rm MO}$.

Several other schemes have been proposed for defining the state of the boundary layer for dispersion calculations. An extensive review of them by Kretzschmar & Mertens (1984) reveals wide variations in their predictions for a specific meteorological condition. For example, the Belgian and R91 systems predict neutral (D) conditions to exist at Mol (Belgium) for 20-25% and 72% of the time. The reason is almost certainly that the state of the boundary layer cannot be defined by insufficient information, taken only at the surface.

Although no comparable studies have been made using the boundary-layer parameter $h/L_{\rm MO}$, the fact that the same profiles of velocity and turbulence are found using this scheme suggests that it will lead to much less variability between countries and between users of the scheme.

It would be possible to use the stability of existing surface-meteorology schemes to estimate the boundary-layer parameter and see if the variability was reduced. The current variation does not provide an acceptable basis for international comparisons of dispersion and thence for risk estimates, even over flat terrain in rather ideal situations.

2.1.10 Implementation of a boundary-layer meteorology classification scheme and comparisons with the R91 scheme

In the present R91 scheme for defining the state of the boundary layer, three variables are required, namely;

(i) the wind speed at 10m, U_{10};

(ii) the sensible heat flux into (or out of) the atmosphere at ground level F_{θ_o};,

(iii) the roughness length z_o.

Usually, F_{θ_o} is not known, so a method is provided to estimate it from the incoming solar radiation (R). In other surface-meteorology schemes, different methods are given for estimating the effects of heat flux on the boundary layer. For example, in the U.S. Nuclear Regulatory Commission System, the temperature difference at two heights is used as a raw criterion (a procedure that is less defensible scientifically than the U.K. scheme). However, F_{θ_o} can be derived from a local measurement of U_{10} and the difference in temperature at two heights in the surface layer (say at 2m and 10m) (cf. van Ulden & Holtslag 1985).

If *no measurements* of either heat flux, radiation or temperature are available, R91 provides a method of estimating F_{θ_o} for the U.K. from the day of the year and cloud cover. (Either F_{θ_o} needs to be given or this estimate is used in the code CERC R91.)

The procedure for calculating the Pasquill-Smith stability class following R91 is set out as a flow chart in Table 2.2a. This is also the basis of CERC R91.

Because the current R91 classification method is based on surface measurements, *no use is made of information about the depth* h of the boundary layer. However, a method for estimating h is given in R91, because it is required in the calculation of the dispersion, once the type of boundary layer mean flow and turbulence have been defined.

In a boundary-layer classification scheme, the depth of the layer would be required for defining h/L_{MO}. Therefore it would be quite straightforward to implement such a scheme using the same or similar algorithm. This algorithm for estimating h during the daytime uses the following information:

- accumulated heat flux during the day in question;
- surface wind speed;
- estimated cloud cover.

A similar model is used by the Netherlands Meteorological Office (KNMI).

R91 (Fig.4) also has an algorithm for estimating h at night.

However the boundary-layer depth is often measured directly at some meteorological stations using sodar or radiosondes. In several countries h is measured continuously at major nuclear installations (in the U.S.) and power stations (France). In the U.K. h is one of the meteorological variations that are given every three hours as part of the PACRAM data package although usually it is derived from other data by using the aforementioned nomograms. The CEGB dispersion studies (Moore 1975) used values of h defined from the Meteorological Office and specially instrumented towers.

Therefore, we conclude that essential data is available, either indirectly, using the R91 algorithms, or directly from the Meteorological office data, for implementing a boundary-layer classification scheme based on the parameter (h/L_{MO}).

CERC has made sample calculations for dispersion based on boundary-layer similarity variables (z/L and $h/L_{\rm MO}$), which are given in §3. We have shown that it is straightforward to implement the R91 algorithm to derive the boundary-layer variables variables. [These two approaches are given schematically by the flow chart in Table 2.2a,b.]

We conclude that it would be quite possible to develop a suitable software for defining the boundary-layer state and appropriate profiles on a personal computer-based system. Either indirect estimations of $L_{\rm MO}$ would be involved similar to the R91 or van Ulden & Holtslag (1985) algorithms, or some suitable use of data packages, such as PACRAM.

2.2 Wind field models for complex surface conditions

2.2.1 Why complex terrain affects dispersion

The aim of this section is to describe how changes in surface elevation (i.e. hills), surface roughness (e.g. rural/urban), and surface temperature (e.g. land/sea) affect the air flow in the boundary layer and how their effects can be modelled. Collectively, these effects are referred to as complex surface conditions.

Such conditions can give rise to large changes in the dispersion from both localised and area sources and, in particular, can induce large surface concentrations. For regulatory purposes, infrequent meteorological and topographical circumstances, when extreme values may occur have to be considered, as well as more frequent circumstances. Usually, we consider the location of the source to be fixed, but in fact the effective height of a buoyant discharge can be changed drastically by complex air flow over hills, because the plume rise is affected by changes both in horizontal and vertical velocity and in stratification.

To illustrate the kinds of changes that can occur, we give a few specific examples. As a measure of the effects of the change we use three parameters

- ⋆ the ratio $A_{g\ell}$ of the ground-level maximum concentration $C_{g\ell{\rm mx}}$ to the corresponding quantity over level ground in neutral conditions $C^{(o)}_{g\ell{\rm mx}}$; so $A_{g\ell} = C_{g\ell\ {\rm mx}}/C^{(o)}_{g\ell\ {\rm mx}}$;
- ⋆ the ratio A_p of $C_{g\ell\ {\rm mx}}$ to the maximum value in the plume at the same distance from the source $C^{(o)}_{p,{\rm mx}}$; so $A_p = C_{g\ell\ {\rm mx}}/C^{(o)}_{p,{\rm mx}}$;
- ⋆ the ratio A_x of the distance of $C_{g\ell\ {\rm mx}}$ from the source $(x_{\rm mx} - x_s)$ compared with the distance over level ground $(x^{(o)}_{\rm mx} - x_s)$: $A_x = (x_{\rm mx} - x_s)/(x^{(o)}_{\rm mx} - x_s)$.

(i) Neutral conditions: wind blowing pollution from a source onto a ridge or a round hill

Consider a typical situation of a 200m high ridge with slope of 1/4 and a source of height 100m, located 1km from the foot of the hill sketched in Fig.2.9a (Source S_1). In this case, wind-tunnel experiments (Khurshudyan et al. 1981) indicate that the average surface concentration near the foot of the hill can increase by a factor of 2; i.e. $A_{g\ell} \simeq 2$. If the hill slope is both steeper, say with a slope greater than 1/2, and rounded in shape, and the source is close to the foot of the hill (see Fig.2.9a, Source S_2), the surface concentration can be increased even more; then $A_{g\ell}$ may be as large as 4. In fact for this latter situation $A_p \simeq 1$ and $A_x \sim 1/2$.

The values of the A_{gl}, A_p, A_x coefficients only differ from 1.0 when the height and location of the source lie within a certain space, or a 'window' (Hunt, Puttock & Snyder 1979).

Field experiments in neutral conditions by Maryon et al. (1986) from low sources on rounded hills showed some effect of A_x being reduced, but little effect on $A_{g\ell}$. C.E.G.B's full-scale SO_2 dispersion studies (Moore & Lee 1982) have shown that A_x changes by about 1.5 for hills that have slopes of less than 1/4. There is much photographic evidence of plumes impacting onto hills in neutral conditions (e.g. Scorer 1968).

(ii) Neutral conditions: sources downwind of hills

Consider the same 200m ridge with slope ($\simeq 1/4$), but now a 200m high source 1km downwind (Fig.2.9b, Source S_1). The downwash in the wake can lead to significant changes such that $A_{g\ell} \simeq 1.5$ and $A_x \simeq 1/2$. To ensure that $A_{g\ell} \simeq 1.1$, it may be necessary for the source to be raised by a significant fraction of the hill length (Moore & Lee 1982).

The plume from a low-level source sited downwind of a hill with large slope may be brought to the ground by the recirculating flow that exists in the lee of that hill. For example, with a source 50m high placed 100m downwind of a hill of slope $\frac{1}{2}$, $A_{g\ell} \simeq 8$, $A_x \simeq 1/2$ (Castro & Snyder 1982).

The effect of a ridge induced downwash is currently allowed for in the CEGB dispersion model of Moore & Lee (1982). This same effect has been found in plume studies by Eliseyev (1977), and a photograph of it is given by Scorer (1968).

(iii) Neutral or unstable flows below elevated inversions

The situation sketched in Fig.2.9c is of particular interest for medium-to-long

range dispersion especially when a thick plume fills the mixing layer whose upper limit is fixed by an inversion (or temperature rise). The depth of such a layer changes considerably over hills; the wind speed increases, there is an increased likelihood of either precipitation or a change in the type of precipitation (Carruthers & Choularton 1983), and wet and dry deposition can be enhanced (as happened over the U.K. after the Chernobyl accident (Smith 1988)). On the lee side of a hill the air flow can be quite disturbed with lee waves and rotors forming, which also have a strong effect on deposition (Hunt, Weng & Carruthers 1988).

(iv) Stably stratified flows

Figure 2.10a shows some typical plumes flowing over a ridge in stably stratified conditions, for different source heights. Low-level plumes can stagnate, turn and flow parallel to the ridge as they impact (Strimaitis et al. 1988 ; Egan 1984) so that $A_{g\ell}$ is large and $A_p \simeq 1.0$. High-level plumes can be swept down over the ridge by lee-wave formations* and maximum surface concentrations can then occur on the lee side of the summit. The downwash associated with lee waves can effectively suppress the plume rise, from power station chimneys and cooling towers (Schiermeier 1978).

Another E.P.A.-sponsored field experiment at Cinder Cone Butte has shown how, for stable flows around a low isolated hill, the plume may impact onto the hillside leading to high surface concentration where $A_p \simeq 1.0$, and such a plume can divide so that part of it passes on either side of the hill. This behaviour is sketched in Fig.2.10b. Clearly the concept of a simple laterally-spreading Gaussian plume is not appropriate then! When either the air flow is slightly less stable, or the source is higher, the centre-line of the plume passes over the top of the hill but its lower extremities can touch the surface on the slope. A striking feature of these experiments was that during a one-hour period, plume behaviour could alternate between these two states (Lavery et al.1982).

In very stable conditions such as are found in valleys or near mountains, the air flow is not only frequently blocked by the mountains, but is also more stably stratified than over level terrain. Then stable air, draining down the valley sides, 'pools' in a valley bottom. Buoyant plume rise is suppressed; plumes can drift slowly onto hill sides, and a whole valley can become polluted (Fig.2.10c). The concentration depends on the duration of the meteorological conditions, source strength and the valley scale. This situation is certainly observed in Welsh and Pennine valley systems. It has also been studied in detail in valleys in the U.S.A., Australia and Austria. In strong winds on the other hand, there may be significant air motion in a valley, which may completely 'scour out' any pollutants emitted there (Fig.2.10d), or there may be recirculating 'rotors' in the air flow which lead to strong downwash and maximum surface concentrations near the source (i.e. $A_{g\ell}$ and A_x are affected).

---

* Such lee-wave formations over hills in New Mexico have been photographed by the US EPA. They have also been observed in this country by J.C.R. Hunt.

(v) Surface roughness and temperature changes

The most important effect on atmospheric dispersion of roughness changes at the surface is that it changes the wind speed and thence the effective local stability. At coastal with the wind coming over the relatively smooth sea surface, the wind speed is typically 50% more than over a site 50 miles inland, which has a high roughness. Consequently, for the same synoptic conditions, the value of the Pasquill stability category, for example, is likely to be changed by at least one 'letter'. Changes of wind speed are also important for plume-rise calculations. Danish field experiments by Gryning & Lyck. (1978) and recent wind-tunnel experiments by Pendergrass & Arya (1984) have shown that abrupt changes of roughness have rather little direct effect on the dispersion pattern from elevated sources placed near the roughness change; the dispersion is essentially determined by the wind conditions at the source.

However, the presence of surface temperature changes can lead to significant changes in dispersion patterns and surface concentration. For example, stable air over cool sea water passing onto warmer land causes the upward dispersion to be limited by an internal boundary layer (Fig.2.10e). Since h is limited, w_*, σ_v and therefore in lateral dispersion are reduced. Typically, the maximum surface concentration may be doubled and the distance to the maximum reduced (i.e. $A_p \sim 2$, $A_x \sim 1/2$). A model for this effect is given in the report NRPB-R157 (Jones 1983, hereafter referred to as R157) (see also van Dop et al. 1979; Raynor et al. 1975).

2.2.2 Factors affecting dispersion over complex surface conditions

The large changes that occur in the concentration and the dispersion patterns can be understood by first identifying in detail the flow features – which we call 'diffusion factors' – that affect dispersion and consider in what circumstances these factors occur in flow over hills, and changes in surface roughness and temperature.

Depending on the nature of the source and its location relative to both the region of complex surface conditions and the receptor point, quite different aspects of the mean air flow and turbulence are important. In other words, the 'factors' are strongly source-dependent and no general rules can be given for all sources. (These factors are defined quantitatively in §3.1.2.)

(i) Localised source

Figure 2.11 shows a plume from a localised source near a region of hilly terrain or near a change in surface roughness or temperature. The 'diffusion' factors are

most conveniently defined relative to the mean streamline through the source ψ_s (see Hunt 1985a). This is defined by the mean flow averaged over a period τ either greater than the travel time T_H for the air flow to pass over the change in surface conditions, or the characteristic time of the turbulence T_L; the greater of these two should be taken but τ should be less than the time over which the wind speed and direction change (typically of the order of 20 minutes to 1 hour). For example, over a 1km hill in stable conditions ($U \sim 3\text{ms}^{-1}$) τ would be at least 5 minutes but less than, say, 30 minutes if the wind is varying on this time scale (Egan 1984).

The location of the mean streamline is defined by its deflection in the vertical δ_z and horizontal δ_y from the mean wind horizontal direction through the source (see Fig.2.11). The principal diffusion factors are as follows.

The height n of ψ_s above the ground is especially important when estimating ground-level concentration. Fig.2.9b shows a source S_2 situated in a region of turbulent recirculating flow. In that case it is more useful to consider the mean streamline to be the average distance between the centre line of the plume and the ground.

The variations of the mean flow either side of and above and below the mean streamline. Wherever the mean flow changes, the streamlines converge and diverge thus narrowing or widening the plume from a source. For plumes impinging onto hills or being deformed by thermal fronts, they diverge in both directions, but over hill tops the narrowing in the vertical direction of a plume is associated with widening in the perpendicular horizontal direction (Hunt, Puttock & Snyder 1979; Maryon et al. 1986).

The vertical gradient of the mean velocity or shear $(\partial U/\partial z)$. Both over hills, especially in their wakes, and over roughness changes, $(\partial U/\partial z)$ is increased. This tends to lower the height of the position of maximum concentration in the plume (Hunt 1982a). Downwind of structures or hills with large slopes, the mean flow can change direction and recirculate. Then the shear is very strong and has a correspondingly marked effect on the dispersion, especially in the recirculating region. The dispersion is even more strongly affected, with strong dispersion downwards into the recirculating region.

The turbulence on and near the mean streamline. For an elevated source it is particularly important to know about the turbulence between ψ_s and the ground for estimating surface concentration. In some cases the mean streamline approaches the surface (i.e. n decreases) but the turbulence intensity is also reduced by the accelerating flow or increasing stable stratification. In that case the surface concentration may not be changed very much by the reduction in n. On the other hand, enhanced thermal convection on the slopes of a hill can combine with a decrease in n to increase the concentration at the surface. Since as explained in §2.1, the turbulence structure can only be understood when the thermal stratification in the boundary layer is known, the change in stratification with changes in surface conditions needs to be understood and modelled.

(ii) Area sources

A region of complex conditions affects diffusion from either an area source or a source that is far upwind (more than 20km) of such a region. The matter is vertically well mixed throughout the boundary layer, but even so there can be significant gradients in concentration in the vertical direction associated with deposition at the surface, with chemical reactions of the dispersed matter, and with veering of the wind direction. There are the usual variations of the concentration in the lateral direction.

Although the whole flow in the boundary layer affects the dispersion; less precision is required in the modelling than for a localised source. This is because small changes in the flow do not now lead to large changes in the dispersion. The key flow parameters of importance are again:

- ⋆ wind profile and streamline pattern especially near the mean streamline ψ_s through the source area;
- ⋆ the changes in the depth of the boundary layer;
- ⋆ the changes in turbulence and stratification.

Other parameters that depend on the flow are also important, such as surface deposition, precipitation, chemical reactions.

(iii) Effects of changes in the flow field

There are three main kinds of fluctuation in the flow field that affect the diffusion in the boundary layer, synoptic, turbulent and mesoscale 'fronts' (including sea breezes). The synoptic fluctuations lead to changes in the direction of a plume over a period of the order of one hour, while turbulence eddies in the boundary-layer fluctuate randomly in direction and increase the plume's thickness. Even in a boundary layer over flat terrain, there are moving regions in which the average temperature and velocity differ, on scales of 1km to 100km, from their values in the rest of the boundary layer. These may be produced by intermittent precipitation, surface temperature variation, and coastal or hilly regions far from the site and can lead to quite rapid changes in mean wind direction, say over a period of about 1 minute (see Fig.2.12).

In complex surface conditions, both turbulence and mesoscale fronts are affected (Pedgley 1971). One needs to know the typical changes in wind speed, direction, turbulence and stratification.

2.2.3 Physical processes and key parameters governing complex wind fields

In this section we describe the essential processes governing the changes in boundary-layer flow over complex surface conditions (changes in surface elevation, roughness and temperature), and derive approximate estimates for the changes. Thence it is possible to define parameters based on atmospheric conditions which define these changes. This is the first step in deciding when it is necessary for dispersion models to take complex flows into account. The important aim of this section is to provide the background against which different wind-field models are assessed in §2.2.4. Some of this review is based on Hunt & Simpson (1982), but different results are also included, especially where new data and models have led to new concepts.

(i) Changes in elevation

Changes in the elevation or slope of the ground affect the boundary-layer flow in different ways depending on the relative importance of the inertia of the oncoming flows to the buoyancy forces (which we denote by a parameter F). In convective conditions the relative magnitudes of the mean velocity and the turbulence are important and may be assessed from the ratios U/w_* and h/L_{MO}.

(a) Neutral – ($h/L_{MO} = 0$, $F \to \infty$, Pasquill Class D)

Consider flow over an isolated hill of H and length L_1.L_1 is defined, for convenience, as the horizontal distance from the summit to where the surface elevation is $H/2$) (see Fig.2.13). For most hills, the ratio of H/L_1 is less than about $1/3$, though of course there are steep hills, mountains and cliffs where this is not true. When $H/L_1 \lesssim 1/3$, the air flow passes over and round the hill and does not reverse its direction. The streamlines are deflected vertically by the slope of the hill ($\frac{1}{2} \approx H/2L_1$) up to a height h_m which is of the order of L (or slightly lower for a short hill). Because the approach wind speed $U(z)$ increases with height, the vertical velocity W over the hill increases with height up to h_m but above this level the deflection of the streamlines decreases. The change in the horizontal velocity at height h_m, ΔU is of order $(H/L_1)\ U(h_m)$, and this gives rise to a change in mean pressure $\Delta p \sim p(H/L_1)U^2(h_m)$. As in conventional boundary-layer theory, this upper-level pressure acts on the flow near the surface where the approach velocity is weaker, so that the change or perturbation in the horizontal velocity increases quite sharply near the surface to an approximate value at a height Z of $\Delta U \sim (H/L_1)\ U^2(h_m)/U(Z)$.

Very close to the surface within an inner region of thickness ℓ, the changes to the mean velocity field are strongly affected by the turbulent shear stress, whereas above ℓ the mean flow perturbations are, to a good approximation, independent of the turbulence. Downwind of the hill the turbulent inner region becomes the wake and grows in thickness, but at the same time the maximum velocity perturbation slowly decreases. Above this wake there is a systematic downward flow of air which has an important effect on the dispersion of pollutants from elevated sources.

Typically, the height ℓ of the inner region is about $L/20$ or about 10m for a hill with half length of 200m. Over a hill top the maximum velocity occurs at a height of about $\ell/3$ (or 3m in this case) and the typical increase in ΔU is about 2 H/L_1 for rounded hills.

The graph in Fig.2.14a,b shows measurements of how $\Delta U/U$ varies over a hill (in fact, the low hill Askervein on the Hebridean Island of South Uist and with height. Note that ΔU can be negative on the upwind and downwind slopes, and reaches a maximum at the hill top.

Once the mean velocity distribution has been defined (by modelling or measurement), the mean streamlines of the flow can be drawn. These pass close to the top of the hill where again for flow over Askervain Hill the flow speeds up (Fig.2.14a). There is an important difference between air flow over a long, effectively two-dimensional hill perpendicular to the flow and over a rounded three-dimensional hill – the distance between streamlines and the surface decreases more in the latter case (for hills with low slope by a factor of 2 – Hunt, Puttock & Snyder 1979; Hunt & Richards 1984).

For neutral conditions above hilly terrain, the lateral and vertical deflections of the flow are of the same order. Typically the mean lateral velocity V is about UH/L_1), so that the maximum change in angle of mean streamlines over the sides of a round hill is about $(H/L_1)\big/(1+1.5H/L_1)$. The maximum horizontal deflection of a streamline $\delta y \approx H/3$ (Mason & Sykes 1979; Hunt, Richards & Brighton 1988).

The changes in turbulence over a hill have been studied in both the laboratory and the field (Britter, Hunt & Richards 1981; Mickle et al. (1988); Zeman & Jensen 1987; Mason & King 1985), and can now, broadly, be explained. Near the surface, within the inner region of height ℓ, the turbulence and the surface shear stress increase or decrease in proportion to the changes in the local mean velocity (e.g. over a rounded hill the change in σ_w or u_* is about $2H/L_1$ times its upstream value). In the wake there is also an increase in turbulence. Above this inner region, say 10-20m in typical cases, the vertical turbulence σ_w is slightly greater than its value upwind but the lateral component σ_v is not much changed. Consequently, the turbulence intensities σ_w/U, σ_v/U are not much changed in the inner region over the hill but are significantly increased in the wake, while above the inner region they are decreased over the top of the hill, and increased upwind and downwind of the hill crest.

The same kinds of changes occur over hills where H/L_1 is significantly greater than 1/3 (or maximum slopes greater than about 1/4). For flow over ridges the maximum increase of wind speed can actually decrease as the slope increases because the flow separates on the lee side and thence effectively reduces the curvature of the overall flow over the hill (Bouwmeester 1978). The main effect of steep slopes is to induce recirculating flow either on the upwind or downwind slopes. Usually, as shown in Fig.2.9b, these recirculating flows are helical. Strong turbulence in the wake region extends further downwind in these cases, as shown by wind-tunnel studies (Arya & Shipman 1981; Courtney & Arya 1980; Counihan, Hunt & Jackson 1974). Downward vertical deflection of streamlines can be significant over a distance of 20 H downwind of the crest which can affect surface concentration considerably (Hunt, Britter & Puttock 1979).

So far we have only considered isolated hills but usually they occur in groups. Field, laboratory and numerical studies of air flow over groups of hills and valleys (e.g. Mason & King 1984; Counihan 1974; Richards & Taylor 1980; Fackrell & Robins 1979) have shown that similar speed ups and streamline deflections occur over the hill tops, but that the wakes are changed by the presence of downwind hills; in particular, the extent of the wakes and recirculating regions are reduced. This can lead to simple models being better in this case than for isolated hills. When the wind is at angle to a valley with steep slopes, significant helical motions occur which may determine the large-scale turbulence associated with that valley.

(b) Slightly stable stratification - ($h/L_{MO} \geq 1/3$, $F \geq 2$, Pasquill Class D/E.

When the atmosphere is slightly stable, the turbulence is reduced and the shear in the mean velocity profile is increased when compared with the NBL. Since the mean velocity now increases more rapidly with height, the effect of deflecting the air flow at a height h_m well above the hill has a relatively greater effect on the surface wind. Therefore the relative increase in wind speed is greater and the vertical and horizontal deflection of streamlines is greater. (Typically ΔU might be increased by 50% – but U could not be increased much beyond 100% of its upwind value at the same height.)

In this category the stratification is great enough to affect the velocity profile approaching the hill, but not great enough for buoyancy forces to be comparable with the inertia associated with the mean flow over the hills. Consequently, the changes in U, δy and δz have a similar distribution over the hills as for neutral flows.

Hence the specific criteria for this category in terms of the height H_1 of the hill are:

- either $l_1 < h$, $L_1/L_{MO} \geq 1/3$ or $L_1 \gtrsim 500$m (as is usual), $h/L_{MO} \geq 1/3$;

• the inertia/buoyancy forces are sufficiently large that $F \geq 2$, where

$$F^2 = U^2(L_1) \Big/ \frac{g}{T_o} \int_o^{L_1\sqrt{2}} Z \, \frac{\partial \theta_B}{\partial z} \, dz$$

where θ_B is the potential temperature distribution of the upwind flow. (This definition allows for θ_B to increase gradually with z or sharply at an elevated inversion.)

By way of illustration, consider a hill for which $H = 150\text{m}$ and $L_1 = 500\text{m}$ with a slightly stable atmosphere in which $U_{10} = 1.5\text{ms}^{-1}$, $h = 300\text{m} = L_{MO}$, $u_* = 0.25\text{ms}^{-1}$ and $N \approx \{(g/T_o)(\partial\theta_B/\partial z)\}^{1/2} \approx 0.003$. The above criterion yields $F = 3$. Changes in the velocity profile may be sufficient to increase the perturbation of the wind speed by up to 50%.

In neutral conditions the wind speed increases by about 60%, so in these slightly stable conditions it increases by about 90%. For a field experiment see Bradley (1983) and for wind-tunnel experiments see Bouwmeester (1978).

(c) Moderately stable stratification ($h/L_{MO} \geq 1$, $F_L \geq 2$, $F_H > 1$)

(Pasquill Class E/F).

In these conditions the stratification or stable density gradient is large enough, and the wind speed low enough for the buoyancy forces to be significant compared with inertial forces of the air flow over the hills. The whole distribution of the flow then begins to change. With changes depending on both the magnitude of the Froude parameter F and on the potential temperature profile $\theta_B(z)$.

Consider first of all a uniform temperature gradient with a strong inversion layer. When $F \cong 1$, the waves appear in the flow, especially lee waves, and downwind of a hill the mean wind speed near the surface alternately increases and decreases with downwind distance. The wind speed at the crest decreases but it increases on the lee slopes. If the waves are strong enough, stagnant or recirculating regions (called 'rotors') may form on the lee slopes (see Fig.2.9c).

As the stratification increases and F decreases, waves do not affect the flow near the surface. If the stratification is approximately uniform with height, there is a general reduction of the wind speed on the upwind and an increase on the downwind slopes. However, if the air flow is neutral and there is a strong inversion, the wind speed may reach a maximum value at the hill top. For hills with low slopes the maximum increase in wind speed is given by

$$\Delta U_{\max} \simeq U(h_m)\ F_L^{-1}\ H/L \ .$$

A graph giving the form of $\Delta U_{\max}/U(h_m)$ for a two-dimensional or ridge-like hill is given in Fig.2.15.

The distance between a mean streamline and the hill surface changes from its upwind value n_∞ to a local value n which can be calculated in terms of ΔU from

$$\frac{n}{n_\infty} \simeq \frac{1}{1+\Delta U/U(z)} \quad \text{or} \quad \frac{n_\infty - n}{h} = \frac{\Delta U}{U(z)}.$$

Examples of streamline variation over hills for various types of stratification are given in Fig.2.16.

For three-dimensional hills the downwind vertical deflection is greater. An important feature of stably stratified flow is that the streamlines diverge laterally on the lee slopes much more markedly than in neutral flow. Typically the maximum of δy is about $0.8H/F_L$ (R.B. Smith, 1980; Hunt, Richards & Brighton 1988).

Where the hill slopes are large enough for there to be separated recirculating regions in neutral conditions, these regions can be suppressed by strong downflow on the slope (Hunt & Snyder 1980; Sykes 1978). Even for these large slopes the magnitude of the maximum velocity perturbation is approximately given by Fig.2.15. There are some important changes (involving wave-breaking) in the upper layer flow well above the hill associated with very strong downflows (Rottman & R.B. Smith 1987).

An equally common situation where the stable stratification affects flow over hills occurs when there is a strong elevated inversion, i.e. there is a jump in temperature $\Delta\theta_B$ across the inversion at height h_i. Then

$$F^2 = F_i^2 = U_o^2 \Big/ [g\ \Delta\theta_B\ h_i \Big/ T_o].$$

This kind of stratification can lead to a maximum velocity perturbation ΔU and streamline deflection $(n - n_\infty)$ at different places over a hill; either at the crest when $F < F_{i\ \text{crit}}$ and $F > 1$ or on the downwind slope when $F_{i\ \text{crit}} < F \leq 1$, where $F_{i\ \text{crit}} = 1 - \left(\frac{3}{2}H/h_i\right)^{1/2}$ and is small. Usually there is stable stratification above the inversion and this also affects the wind near the hill surface (Carruthers & Choularton 1982; Hunt, Richards & Brighton 1988).

This elevated inversion situation is commonly found over high ground in prevailing winds, e.g. over Cumbria in westerly winds (Carruthers & Choularton 1982).

Note that air flow at the surface may be unstable. It is the stability in the elevated inversion layer that controls the changes in the air flow.

(d) Strong stable stratification ($h/L_{MO} \geq 3$, $F_L < H/L, F_H < 1$), (Pasquill Class F/G)

When the stratification is even stronger, the hills higher and the wind speed low enough, the buoyancy forces are so strong relative to the inertia of the oncoming flow that all the air cannot flow over the top of the hills (Fig.2.10b). An approximate criterion for these conditions is

$$F_H = \frac{U}{N(H)H} \leq 1$$

where the relevant buoyancy frequency is defined by the temperature gradient at the hill top. This is equivalent to $F_L \Big/ (H/L) < 1$.

In fact some of the approaching air stream, above a critical height H_c, has sufficient kinetic energy to pass over the crest. Laboratory, field and numerical studies indicate that this critical height $H_c \approx H(1 - F_H)$ (Sheppard 1956; Snyder et al. 1985).

The importance of this situation for atmospheric dispersion is that, plumes released from sources below the critical height, H_c move approximately horizontally; they impact onto the hill and either 'split' as they pass each side of the hill, or they move around one side or the other. Upwind of a ridge the plumes below H_c can slowly drift onto the surface. Plumes released above H_c pass over the hill as if the ground level had been raised to H_c (in fact this hypothesis has been verified by Snyder in his stratified flow tank; it provides an approximate basis for modelling).

An important feature of these highly stable air flows is they often contain low-frequency horizontal fluctuations that can lead to streamlines surging from one direction to another around the hill. There may also be slow fluctuations, over a period of less than one hour, of the temperature gradient which means that the central height H_c can fluctuate. As the EPA experiments showed, plumes can pass first over and then around a hill during a one-hour period.

At present very little is known about the level of turbulence or slow fluctuations in strongly stable flows over and around hills. Often most of the turbulence in a plume may come from the source itself!

Another feature of the slow stable flow is that Coriolis effects can systematically affect the wind direction over distance of less than 10km. This can lead, for example to a west wind veering more to the north of a range of hills (Hunt, Leibovich, Lumley 1983).

(e) Strong stratification with drainage winds

So far we have considered the boundary-layer flow to be driven by the large-scale synoptic pressure gradients. It has been assumed that the wind speed well above the hills is the relevant speed for defining the flow regime. However, there are situations where this is not the case; in particular, when the wind speed is low enough, the stability is strong enough, and the height and slopes of the hills are large enough, the air flow over the hills can be *driven* by buoyancy forces produced by temperature differences between the surface of the hills and the air above. These are called drainage, downslope or katabatic winds when the slopes are cool, and upslope or anabatic winds when the slopes are heated. Estimates are given of these winds after we have considered the effects of change in surface temperature.

(ii) Changes in roughness

(a) Wind normal to roughness change

The change of roughness of terrain affects the air flow by increasing or decreasing the resistance to the flow near the surface. The quantity that defines the effect on the air flow of the roughness 'elements', such as buildings, trees, grass, water waves, etc., is the *roughness length*, z_o, as explained in §2.1.2; this is *typically* about 1/30 of the actual height of the roughness elements.

Since the mean velocity $U(z)$ in the boundary layer just above the roughness elements has the form (given in (2.2a))

$$U(z) = \frac{u_*}{k} \, (\ln \, z - \ln \, z_o),$$

it follows that the *effect* of a change of roughness varies *approximately* in proportion to the log of the roughness length $\ln z_o$. Therefore, a measure of the effect of a change in roughness from terrain (L) to terrain (2) is the parameter R_{21}

$$R_{21} = \ln(z_{o2}/z_{o1}) = \ln \, z_{o2} - \ln \, z_{o1}.$$

This ratio is positive when the air flows towards the rougher terrain. Also as the air flows over such a roughness change, the surface shear stress u_* *increases.*

For example, in near neutral conditions (Pasquill Class D or $h/|L_{\rm MO}| \leq 0.1$), the effect of a change in roughness length by a factor of 30 from a coastal site ($z_o = 0.01$m) to a suburban site ($z_o \approx 0.3$m) leads typically to a *decrease* in surface wind speed at 10m of about 33%, but at the same time, the surface srear stress u_*

increases by about 25%. Therefore the turbulence intensities $\sigma_w/U(z)$, $\sigma_v/U(z)$, which are proportional to u_*/U, increase by a factor of about 2.

The reason why the change in roughness at a site has to be considered is because the changes in the conditions at the surface do not extend right through the boundary layer. In fact, the change in z_o affects the mean flow and turbulence in the boundary layer within an *internal* layer, whose height is ℓ_U, which extends downwind from where z_o change (at $x = x_o$). This internal layer is thickest in unstable conditions and thinnest in stable conditions (see Fig.2.17a). Typically in neutral conditions $\ell_U \simeq 1/20(x - x_o)$.

Because the changes in roughness have an effect on u_*, and because the structure of the boundary layer and the intensity of turbulence depend on L_{MO} which, being proportional to u_*^3, is very sensitive to u_*, the changes in roughness can have a significant effect on the local stability. (R91 shows how z_o affects the stability category for a fully developed boundary layer.) With a change in roughness, the stability within the internal layer may be different from that above it and so for estimating the dispersion from an elevated source, the height of this layer needs to be known, as well as the mean flow and turbulence within and above it.

(b) Arbitrary changes in roughness relative to wind direction

So far we have considered an abrupt roughness change along a line, such as at a coastal site (where z_o may change from 3×10^{-4} to 10^{-1}m (Jensen & Peterson 1978). In general, however, roughness varies gradually and haphazardly, such as on the outskirts of large urban areas where housing, woods, open areas, highrise buildings, lakes and rivers, alternate. The particular distribution of roughness in the region upwind of a source affects the mean flow and turbulence at the site (Pasquill 1971). Some distance downwind of the source, it is sufficient to know the roughness length averaged over several intervening kilometres.

As shown in Figure 2.17b, the direction of the wind alters as the roughness changes. This is because the component of wind perpendicular to the roughness change is changed more than the component parallel to it.

As explained in §2.1.2, the wind direction in fully-developed boundary layers over uniform roughness backs near the surface (i.e. it turns to the left, or North for a Westerly wind) by an amount dependent on the roughness length. The order of magnitude of these changes in direction is about equal to the change in u_* divided by $U(z)$, which at most, for a rural/urban change of about 10°. This change may be significant because it can be of the same order as the increase in σ_y with x.

(iii) Effects of changes in surface temperature and surface heat flux on the air flow

Changes in the surface temperature or surface heat flux affect the air flow by changing the buoyancy forces acting on it. (For brevity we usually just refer to temperature changes hereafter.) Depending on the strength of these buoyancy forces relative to the inertia of the turbulent eddying motion and of the mean flow, the changes in surface temperature lead to changes in either changes in the turbulence, and in the mean flow *profiles*, or to large changes in the flow direction and the whole flow structure. As with our other discussions of wind fields, these changes are best defined by suitable dimensionless groups. Numerical examples are also given.

In section (iv) we discuss the important type of complex air flow where there are *both* changes in surface temperature and in elevation. For other reviews, see Hunt & Simpson (1982); Atkinson (1981).

(a) No effect of change in surface temperature

($h/|L_{MO}| \leq 0.3$, Pasquill Class D)

When the winds are strong enough or the heat flux very weak, the atmospheric boundary layer is neutral and is unaffected by buoyancy forces. Therefore *changes* in surface temperature also do not affect the air flow.

(b) Moderate winds/weak mean buoyancy forces ($h\Big/|L_{MO}| \geq 0.3, \Delta F > 10$,

Pasquill Classes B-C, E)

In this case, for moderate wind speeds (typically in the range of $5 - 10$ ms^{-1} in the U.K.), the presence of a typical heat flux affects the mean velocity profile and the turbulence. When there is a change in surface heat flux and $h/|L_{MO}| \leq 0.3$, the mean velocity profile and the turbulence change. As with the changes in the mean velocity and turbulence above a change in roughness, the change in the mean *temperature*, $\Delta\theta$, field downwind of a change in heat flux is confined within an internal layer of thickness $\ell_\theta(x)$.

This change in $\Delta\theta$ causes the buoyancy forces to damp (if L_{MO} increases) or enhance (if L_{MO} decreases) the turbulence. It takes a certain distance for these changes in turbulence to occur and to affect the mean flow. Therefore the thickness ℓ_U of the internal layer within which the mean velocity and turbulence is affected by the heat flux change is *less* than the thickness of the thermal internal layer. In general $\ell_U \propto (x - x_o)^{1/2}$ whereas $\ell_\theta \sim (x - x_o)/20$ (for $h/L_{MO} \geq 1$) (see Fig.2.1.8).

When the upwind turbulence is weak and there is a significant increase in

surface temperature, such as when the wind blows from a cool sea onto land, the two layers have about the same thickness (van Dop et al. 1979; see also R157).

For the moderate heat fluxes considered, the changes in temperature $\Delta\theta$ are not large enough for *mean* buoyancy forces to generate significant *horizontal pressure* gradients to affect the direction of the mean flow at, say, 10m. The approximate criterion for this state of affairs is that

$$\frac{g\Delta\theta\,\ell}{2T_o U_{10}^2} \leq 0.1 \quad \text{or} \quad \Delta F = \frac{U_{10}^2}{g\ell\Delta\theta/T_o} \geq 5 \ .$$

This is also approximately equivalent to specifying

$$h\Big/|L_{\rm MO}| \leq \frac{1}{10}\,\ell n(\ell/z_o) \ .$$

This category is similar to that of 'slightly stable stratification' for air flow over hills, where only the upwind profile is affected by buoyancy forces.

(c) Weak winds/strong buoyancy effects ($\Delta F \leq 10$) (Pasquill A-B, E-G).

In this case the changes in mean temperature, $\Delta\theta$, over horizontal distances L_θ are large enough to give rise to horizontal pressure gradients can drive horizontal mean motions (Fig.2.19) which are of order

$$\left(\frac{g\ell_\theta\ \Delta\theta}{2\ T_o}\right)^{1/2} \ .$$

This situation is common along coastlines or at urban/rural boundaries, where there may be changes in temperature of order 3K, and ℓ_θ may be 300m, so that the wind speed perpendicular to the coast line or boundary can be of the order of 4ms^{-1}. This can result in a change of direction of a strong wind parallel to the coast line *or* in still conditions it might be the only flow that exists, for example, a net flow into large urban areas at night. In general, these flows occur when $\Delta\theta$ is changing with time because of diurnal heating and cooling.

The lateral scale L_θ over which such thermally-driven motions extend is usually *time dependent.* In other words, once such a flow (e.g. a sea breeze) has been established, it can extend over an increasing distance inland (i.e. L_θ increases) until the driving force of the flow (the sea-level temperature difference) disappears at night.

The criterion for these buoyancy-driven flows to exists is that

$$U \leq \left(\frac{g\ell\Delta\theta}{2T_o}\right)^{1/2} \quad \text{or} \quad \Delta F \leq 5.$$

Note that over distances greater than about 10km, Coriolis effects begin to affect the direction of the flow. For example, a thermally-driven flow into cities tends to turn anticlockwise (looking down) (Hunt & Simpson (1982) review some of the experimental evidence for this effect).

(iv) Combined effects of changes in elevation and surface temperature

There are many situations where the air flow is affected by a combination of changes in surface conditions. By way of illustration, we consider briefly the effects on air flow caused by changes in surface heat flux/temperature over hills.

(a) Moderate to strong winds/small hills/very weak buoyancy effects ($\ell/|L_{MO}| \leq 0.1$ – Neutral inner layer)

In this case, the turbulence affects the mean flow and changes in surface heat flux affect the mean temperature within the inner layer (of thickness ℓ) over hills. However, the mean flow and shear stress are not significantly affected by any changes in surface heat flux.

(b) Moderate winds/large hills/weak-moderate buoyancy effects in inner layer ($0.3 \geq \ell/|L_{MO}| \geq 0.1$ for $L \leq 10h$ – Pasquill A-B, E-F-G)

When $\ell/|L_{MO}| \geq 0.1$ the upwind velocity profile and the effective eddy viscosity within the inner layer over a hill are affected by buoyancy forces. This means that the change in shear stress caused by the variation in wind speed over a hill and the change in heat flux which is determined by the slope of the hill lead to significant changes in the inner region. In particular, they can make stably stratified flows more likely to separate and unstable flows less likely to separate, because, in the latter case, the turbulent mixing is stronger (Hunt 1981; Hunt & Richards 1984; Frenkiel 1962).

The other effect of changes in heat flux on hills is to induce buoyancy-driven horizontal pressure gradients that drive flow up or down the slopes when they are being heated or cooled. These pressure gradients usually occur as a result of diurnal heating and cooling.

An order-of-magnitude analysis suggests that such buoyancy pressure gradients are comparable with the inertial effects (considered in §.2.2.3(i)) when the Richardson number

$$Ri = \frac{g}{\theta}\frac{\partial\theta}{\partial z}\Big/\left(\frac{\partial U}{\partial z}\right)^2 \simeq \frac{2\ell}{L_1}, \quad \text{at} \quad z = \ell. \tag{2.21}$$

Therefore, for typical hills where $\ell/L_1 \sim 1/20$, $Ri \simeq 0.1$, and $\ell/L_{MO} \sim 0.2$ provided $L_{MO} > 0$.

The effect of buoyancy forces may be largely to change the wind profile and turbulence over the hill when $0.1 \leq \ell/L_{MO} \leq 0.2$. For $\ell/L_{MO} \gtrsim 0.2$ more significant changes can occur, such as downslope drainage or upslope winds occurring near the lower parts of the hill where the wind speed driven by the upper air flow is weak (see Fig.2.20a). Quite weak drainage or upslope winds significantly affect the tendency for the air flow to separate (Scorer 1955).

The other important conclusion from (2.21) is that since ℓ/L_1 *decreases* as the length of hill slope *increases* (typically in proportion to $1/\ln(\ell/z_o)$), then over very long slopes the effects of horizontal pressure gradients produced by buoyancy forces dominate any slope flow acceleration.

(c) Weak winds/large hills or long slopes/strong buoyancy effects

either $\ell/|L_{MO}| \geq 0.3$, for $L \lesssim 10$km – (Pasquill Classes A-B; -FG)

or $h/L_{MO} \geq 0.01/(H/L)$ for $L \geq 3$km – (Pasquill Classes F-G)

In this situation the horizontal pressure gradients produced by the buoyancy forces are larger than the inertial forces driven by the upper flow. On hills less than about 10km in length, the mean velocities of the downslope drainage winds are larger than those driven by the upper air flow when the hill surface is cooling. The *magnitude* and *depth* of these downslope winds are controlled by local shear stresses and mixing at the top of the drainage wind layer. Field studies of drainage winds in mountainous areas in Australia and California have been reported by Manins & Sawford (1979)and by Neff & King (1985). The depth of a drainage layer can range from 10 to 100m, but over European hill sides typical depths are of order 10m (Geiger 1965; Cox 1977) and the wind speeds of order 3-4 ms^{-1}.

Just as with other flows induced by temperature changes, such as the sea breeze, these slope flows can continue over less sloping ground or level ground at the bottom of a hill. The 'front' of the air flow waves moves slowly, and so the drainage wind feeds into a gravity front (see Fig.2.20b). Scorer (unpublished) has reported such fronts 30km from the hills of South Wales. Blumen (1983) has measured such a front 30km from the Rocky Mountains with a depth of about 100m.

For almost flat but slightly sloping ground, the horizontal pressure gradient balances shear stress gradients and leads to a change in the direction of the air flow and in the velocity profile. As reported by Brost & Wyngaard (1978) and surveyed by Weil (1985), this effect can occur even when the slopes are as little as 0.003 for very stable, weak wind conditions. For typical conditions, an approximate criterion for significant effects to occur is $h/L_{\mathrm{MO}} \geq 0.01/(H/L)$.

2.2.4 Types and comparison of wind-field models for complex surface surface conditions

(i) Flat terrain plus warnings

The simplest and most widely used assumption about wind fields over complex surface conditions is that they are not very different from the flow over flat terrain. Therefore, the height, n, of the mean streamlines above the terrain does not change (Fig.2.21a); nor does the turbulence. Some models based on this simple approach employ a 'warning' or 'flagging' procedure, to indicate under what circumstances this model can lead to significant errors. This approach was recommended in R91 and discussed in more detail in the subsequent report NRPB-R199 (Jones 1986, hereafter referred to as R199) from which Table 2.3 is taken. in the associated warning document R-199, reproduced as Table 2.3

(ii) Simple deflection/impingement models

Our review in §2.2.1 – 2.2.3 of changes in dispersion and air flow over complex surface conditions showed that a characteristic feature of air flow over hills is that the mean streamlines become closer to the ground, and in very stable conditions can impinge onto the hillside. In both cases, this can lead to a significant increase in surface concentration.

For some regulatory purposes, it may be sufficient just to estimate a typical average affect of the terrain on the dispersion.

The CRSTER model and its derivatives COMPLEX I, COMPLEX II developed by EPA can be justified on this basis. In the model it is assumed that at a point (x, y) the height above the ground, n, of the mean streamline which passes through the source (at x_s, y_s) decreases by an amount Δn proportional to the change in ground level Δz_g between the points (x_s, y_s) and (x, y), i.e. $\Delta z_g(x, y) = z_g(x, y) - z_g(x_s, y_s)$: for unstable/neutral conditions $(h/|L_{\mathrm{MO}}| \leq 0.3)$ $\Delta n = -0.5\Delta z_g$; for stable conditions $(h/L_{\mathrm{MO}} \geq 0.3)$ $\Delta n = -\Delta z_g$ (i.e. the plume travels horizontally). If the change in ground level is great enough, the plume impacts on the hill (Fig.2.21b).

The dispersion process is assumed to be the same as that over level ground from a source with height n; in other words, any changes in turbulence are neglected.

To improve the coarse approximation that all streamlines in stable conditions are horizontal, an improved model, RTDM, was developed. This model uses the concept of the 'dividing' streamline to discriminate between streamlines that pass over the hill top and impact on the hill side. As explained in §2.2.3(c), for a source of height z_s which lies between the critical height z_c and the height of the hill H, the mean streamline passes over the hill. Effectively the flow pattern is similar to that over a hill of height $(H - z_c)$, so the 'half' height formula can be used to estimate n for those streamlines. For source heights below the critical height z_c, the plumes travel in straight lines to the hill.

Thus in RTDM, for unstable and neutral conditions, the air flow model is the same as COMPLEX I, II but in stable flow the deflection of the mean streamline through the source depends upon the relative heights of the sources z_s, the dividing streamline z_c, and the crest of the hill H. Referring to Fig.2.21c, the streamline is horizontal whatever the source height, provided $z_g \leq z_c$. Then

if $z_{s3} \leq z_c$, the plume impacts upon the hillside;

if $z_c \leq z_{s2} \leq H$, the height of the streamline above the ground is given by

$n = r_2 \left\{1 - \frac{1}{2}\frac{z_g - z_c}{H - z_c}\right\}$ where $r_2 = n_o - (z_c - z_{gs2})$;

if $z_{s1} \geq H$, $n = r_1 - \frac{1}{2}(z_g - z_c)$ where $r_1 = h_o - (z_c - z_{gs1})$.

Note that z_c is defined by the local mean velocity $U(z)$ and temperature $\theta(z)$ profiles at the source position:

$$(H - z_c) = U(z_c)\Big/N_c, \quad \text{where} \quad N_c^2 = \frac{1}{2}\frac{g}{T_o}\int_{z_c}^{H} z\frac{\partial\theta}{\partial z}dz.$$

For other regulatory purposes it may be sufficient just to estimate the *largest* effect of the terrain on the surface concentration. In the E.P.A. VALLEY model (see White et al. 1985), it is assumed that the worst effect that can occur can be estimated by assuming that a mean streamline is directed *straight* from the source to the hill side in stable conditions. A further assumption is that the plume is spread horizontally by a specified angle over a given period (as $22\frac{1}{2}^\circ$ in 24 hours). These assumptions are made irrespective of whether such an air flow *does* occur.

In many cases, such as air flow in a valley, this situation never occurs, and certainly not over a significant period (e.g. 3 hours). The later models such as COMPLEX I,II incorporate this plume impaction effect.

The use of the VALLEY model has been criticised widely (e.g. in the review by E.P.A. and the American Meteorological Society; White et al.1985) for the above reasons, and partly because of its other assumptions about the dispersion process

on to the hill side which can lead to unrealistically high predictions of concentration. The review by White et al.(1985), comparing models with field experiments, showed that RTDM was a reasonably successful model for predicting the impingement of plumes onto hills in stable flows and for accounting for many neutral and unstable flow conditions. Even so, they recommended that further developments were certainly needed.

The common feature of these deflection/impingement models is that they are based neither on the details of the shape of the hill, nor on any calculations for the flow over the terrain to assess the likelihood of these flows actually occurring.

(iii) Interpolation of the wind field using terrain data and stratification

In the 'aerodynamic' approach to wind-field modelling (described in the next section) an attempt is made to calculate the wind field over a region of complex terrain in terms of the air flow approaching the region. As the size of the region and the complexity of the terrain increases, the errors must also increase. However, over most land areas, as the size of the region of interest increases, there are a number of meteorological wind-measuring stations. Also, in some areas, such as urban areas with nearby mountains and coasts, e.g. Los Angeles or Athens, there may be a dense network of meteorological stations. Therefore, it is natural to develop methods of modelling wind fields which make optimum use of data available. This is the approach we describe here. It has been developed in the U.S., particularly for Lawrence Livermore National Laboratory (LLNL) by Sherman (1978) and for Rockwell's Rocky Flats Plant by Restrepo (1987); in Europe at Imperial College London by ApSimon et al. (1984), at Karlsruhe by Moussiopoulos & Flassak (1986), and in Greece by Lalas et al. (1983). For reviews and discussions, see Lewellen et al.(1982) and Hunt et al.(1984).

At its basic level, this method requires measurements of the horizontal wind speed (U_{H_m}) and direction (θ_m) (or the two components $u_m, v_m (= U_{H_m} cos\theta_m, U_{H_m} sin\theta_m)$) at a number ($N$) of measuring stations located at $(x_1, y_1;\ x_2, y_2; \ldots x_N, y_N)$. Usually u_m, v_m are measured at one level and the form of their vertical variation has to be assumed; occasionally, though, their vertical variation is measured. The height of the terrain $z_s(x, y)$ is assumed to be known everywhere in the flow region. Different models require different levels of input about the stratification. In the simplest case, a single parameter, α, roughly equivalent to an inverse Froude number, F_o^{-1}, is used but other models require input at four levels, and details of the strength of any inversion layers.

The method is to construct a three-dimensional velocity field $(u_c, v_c, w_c)(x, y, z)$ for the region that is mass consistent (i.e. there are no sources and sinks of fluid

within the region) in terms of (u_m, v_m) (x_m, y_m) and $z_s(x,y)$ without solving the momentum equations for the flow. It is assumed that values (u_c, v_c) of the constructed velocity field are as close as possible to the values (u_I, v_I) that would be obtained by interpolating between the measured values (u_m, v_m) (Fig.2.22a). So, it is first necessary to interpolate between the values of (u_m, v_m) and also assume how they vary with z at (x_m, y_m): then the velocity field can be constructed.

The minimisation of the error $\epsilon(x)$ between (u_c, v_c) and (u_I, v_I) over the whole field and the need to construct the unknown vertical component of the motion leads to an expression for the constructed velocity field in terms of the interpolated field $(u_I, v_I)(x,y,z)$

$$u_c = u_I(x,y,z) - \frac{\partial \lambda}{\partial x}, \quad v_c = v_I(x,y,z) - \frac{\partial \lambda}{\partial y}, \quad w_c = -\alpha^2 \frac{\partial \lambda}{\partial z}.$$

The parameter α determines the vertical motion and is generally assumed to vary with z, depending on the stratification.

The constructed wind field has now been reduced to a computation of a single scalar variable $\lambda(x,y,z)$, in terms of α and of the interpolated velocity field. λ must satisfy the modified Poisson's equation, i.e.

$$\left(\frac{\partial^2}{\partial x^2} + \frac{\partial^2}{\partial y^2} + \frac{\partial}{\partial z}\left(\alpha \frac{\partial}{\partial z} \right) \right) \lambda = \nabla . \underline{u}_I = \frac{\partial u_I}{\partial x} + \frac{\partial v_I}{\partial y} + \frac{\partial w_I}{\partial z}.$$

and the solution must satisfy the condition that takes into account the fact that the air flow passes over the hills, so that at a small height Z (less than the inner-layer height ℓ) above the surface

$$w_c = \frac{\partial z_s}{\partial x} u_c + \frac{\partial z_s}{\partial y} v_c \quad \text{on} \quad z = z_s(x,y) + Z, \quad Z \underset{\sim}{<} \ell)$$

and that far above the terrain the perturbations tends to zero, i.e. $\lambda \to 0$ as $z \to \infty$.

The essential mathematical point about this solution is that if the interpolated velocity field $\underline{u}_I$ is uniform and the hill symmetrical (e.g. a hemisphere), then the constructed flow field $\underline{u}_c$ is also symmetrical and the perturbed flow is just potential flow. No account is taken of wakes behind hills, surface roughness changes, thermal effects, or waves.

The usual computational procedure is to divide up the flow region into cuboids, with lengths Δx, Δy, Δz, reduce the differential equations to finite-difference equations, and represent the terrain on this cuboid grid. Typically the depths Δz of the boxes are small near the surface and increase up to the top of the domain ($\sim$ 5km). Note that Moussiopoulos & Flassak (1986) have developed the method to include a terrain-following co-ordinate system. (This is also the basis of the NOABL code

used widely for wind-energy calculations.) For realistic computations over a horizontal scale up to 100km (10^5m), 30^3 boxes are required, which implies a horizontal length scale of about 3km.

The typical time required for such calculations on a large mainframe computer (e.g. a CDC 7600) is a few minutes while storage requirements amount to about seven times the number of grid points. These facts have limited the use of mass consistent schemes on smaller computers.

A key feature in the use of these models is the assumed form of $\alpha(x, y, z)$. Opinions differ as to whether α should be determined simply by the atmospheric boundary layer, or also by the height and nature of the topography. In the LLNL scheme, α is primarily determined by the height of any elevated inversion ($\alpha =$ constant below the inversion, $\alpha \simeq 0$ at and above the inversion), and by the Pasquill stability category of the flow. For most of their complex terrain flows, LLNL take a fixed value of $\alpha = 10^{-2}$. and do not seem to vary α according to the nature of the topography.

The WAFT scheme (ApSimon et al. 1984) is similar to the LLNL approach in allowing for the inversion layer where $\alpha = 0$ but it differs from the LLNL scheme in that the definition of $\alpha(x, y)$ is determined by the height and nature of the hills, as well as by the stratification of the atmosphere over the measuring points. Thus in strongly stable conditions (described in §2.2.3), when the Froude number, based on the hill height H, is small ($F_H < 0.5$), the flow below the critical height $H_c = H(1 - F_H)$ is approximately horizontal (so $\alpha \simeq 0$), while above H_c it passes over the hill where $\alpha \simeq 1$. In regions with many hills of different heights, α would presumably vary with x, y. For most computations there will not be adequate spatial resolution to define H_c accurately.

The scheme has been calibrated against idealised inviscid uniform flow over a hemisphere (so that there is no wake effect) (Fig.2.22b), and experiments on strongly stratified flow over a bell-shaped hill. There has been no attempt to calibrate the model for moderately stratified flow when the lee side accelerates and lee waves occur.

The key features of the models are:

- the flow passes over the terrain, and it speeds up over the tops of the hills (typical of neutral flow);
- by reducing the vertical velocity parameter α, the vertical motion is suppressed, so the effects of stable stratification are broadly described;
- the velocities of the flow field are equal to the measured velocities at the measurement points and tend to vary smoothly in the spaces between them;
- as new data is obtained anywhere in the flow, it can be incorporated into the constructed flow field (which is not true for many other models);

- the mean flow can be computed about 10^2 – 10^4 times faster than directly solving equations of motion.

The key disadvantages of the model are:

- the change in the flow produced by topography is similar to 'potential' flow – so that there are no wake and downwash effects on the lee sides of hills, and none of the lee wave effects in stratified flows (such as streamlines approaching the surface on the lee side of hills);
- for the standard value of $\alpha \approx 10^{-2}$ used in the MATHEW code, the accuracy of the model for predicting flow over individual hills of the model for predicting flow over individual hills of slope greater than 1/10 is not great even in neutral or strongly stably stratified flows unless the value of α is tuned to each case. The errors are particularly large for length scales less than 3-5km.
- the model does not directly account for effects such as roughness changes, sea breezes, thermally-induced winds but if there are enough measuring points, then these effects are incorporated indirectly into the computed wind field.

The conclusion of many studies (including our own – summarised in Table 2.4) is that, provided certain conditions are met, mass consistent models can provide a satisfactory and fast approach to mesoscale wind field modelling on scales from about 5 to 100km. Ideally the spacing of the measuring stations should be about the same as the length scale over which the topography and surface conditions change. Given such circumstances comparative tests indicate that these interpolation models are as good as any other system requiring a mainframe computer (see discussion by Hunt et al. 1984). However, for complex flows on scales down to 300m, with sparse data, these methods are unreliable and it is necessary to compute the flow, without assuming ideal flow. We consider this next.

(iv) Predictive computations involving terrain data and differential equations

The predictive approach to wind field modelling is similar to that used in weather forecasting and in computational fluid dynamics.

(a) Equations

It is assumed that the differential equations governing the flow are known everywhere in the flow region R (see Fig.2.23). These equations are usually approximations to the full equation of fluid flow because only a few statistics of the flow field are required (for example either the mean flow itself or the mean flow and the second moments of the velocity fluctuations). For an accurate description of the changes of the air flow, temperature and turbulence in the atmospheric boundary layer, it is necessary to consider equations for

- ⋆ mass conservation or continuity;
- ⋆ rate of change of momentum for air, water vapour, and other species;
- ⋆ first law of thermodynamics (linking the temperature field to the velocity field $\underline{u}(\underline{x},t)$, water vapour, radiation; ...)
- ⋆ equations of state (temperature, density, pressure, ...).

The exact equations are recast into approximate forms for the mean values of the variables (e.g. $\underline{U}(\underline{x},t)$, $T(\underline{x},t)$ and for the moments of fluctuation (e.g. $-\overline{u_1 u_3}(\underline{x},t)$, $\overline{u_1^2}$, $\overline{\theta u_3}$, etc.). For modelling purposes the means of the variables are defined as the average over some period $T_{\rm av}$, typically 0.5 hrs. Pielke (1984) and Panofsky & Dutton (1984) give a full statement and review of the relevant equations. For our present purposes, it is sufficient to state a limited form of the equations, that is appropriate for the mean velocity field with components $U_i(\underline{x},t)$ and mean temperature field $T(\underline{x},t)$ of a dry atmosphere, assuming the perfect gas law and using the Boussinesq approximation for low altitudes:

$$\begin{aligned}
&\frac{\partial}{\partial x_i}(\rho U_i) + \frac{\partial \rho}{\partial t} = 0 \\
&\frac{\partial U_i}{\partial t} + U_j \frac{\partial U_o}{\partial x_j} = -\frac{1}{\rho_o}\frac{\partial p}{\partial x_i} - \rho g \delta_{i3} + \frac{\partial \tau_{ik}}{\partial x_k} \\
&\frac{\partial T}{\partial t} + U_j \frac{\partial T}{\partial x_j} = -\frac{\partial F_\theta}{\partial x_j} + S \\
&\rho = f(\rho, T)
\end{aligned} \tag{2.22}$$

The quantities τ_{ik} = Reynolds stress and F_θ = vertical heat flux have to be modelled by subsidiary equations S as a heat source (e.g. radiation, latent heat) and δ_{i3} is the Kroneker delta.

(b) Boundary conditions

The equations can be solved to define the flow, i.e. velocity, temperature, pressure field, in the region R after a time t_o provided (see Fig.2.23)

BC1 • the flow is defined everywhere in R at time t_o (e.g. $\underline{u} = \underline{u}_o(\underline{x},t_o)$ for $\underline{x} \in R$);

BC2 • the velocity and fluid properties are defined on the boundaries B of R – where there is a mean flow into the region R (i.e. where $\underline{U}.\underline{n}_B < 0$) and where there is a flow parallel to the boundary B.

Therefore the flow has to be defined both at an upper level surface (e.g. $z = z_B$), and at the ground, where $\underline{U} = 0$, and the temperature, heat flux, water vapour, radiation need to be defined explicitly or in terms of supplementary equations.

(c) Simplifications

No initial conditions required: if the elapsed time for the calculation, i.e. $t - t_o$ is much greater than either the time for the mean flow to pass over the region or the time T_B over which the upwind surface conditions change, i.e.

$$(t - t_o) >> L_R/U_o \quad \text{or} \quad (t - t_o) >> T_B,$$

then the initial state of the atmosphere does not have to be defined. In that case, it is only necessary to define the condition (BC2). For example, over a domain of 30km with an average wind speed U_o of 5ms^{-1}, neglect of initial conditions would be justifiable only after a period of 2 hours.

Quasi-steady: if the length L_o of the typical variations of surface conditions (e.g. hills, roughness, etc.) are small enough and if the time scales T_B of the approach flow, the upper level air flow and the surface conditions (such as temperature) are long enough for

$$T_B \geq L_o/U_o \ ,$$

then the unsteady terms, e.g. $(\partial\rho/\partial t, \partial U/\partial t, \partial T/\partial t)$ can be neglected. This leads to a considerable simplification. Of course, as the boundary conditions vary with time, so do the flow variables U, T, ρ. The assumption means that the flow responds to the instantaneous values of the boundary conditions.

Hydrostatic: if the typical length scale L_o is large enough in comparison with the typical depth h of the atmospheric boundary layer, air flow over the topography leads to weak, vertical velocities (of order $U_o h/L_o$) which extend above the boundary layer. Since the air above the boundary layer is weakly stably stratified (with buoyancy frequency N) these vertical motions lead to vertical hydrostatic pressure gradients (of order $\rho N^2 L_o$). For sufficiently large L_o these hydrostatic pressure gradients are greater than pressure gradients caused by the weak vertical accelerations (of order $\rho U_o^2 h/L_o^2$). Thus, if

$$\left(\frac{U_o}{N\ L_o}\right)^2 \cdot \frac{h}{L_o} << 1 \ ,$$

vertical acceleration can be neglected in the momentum equation.

By way of example, take $U_o \simeq 10\text{ms}^{-1}$, $N = 0.01\ s^{-1}$, $h = 1\text{km}$; this implies that $L_o >> 1\text{km}$. For many large-scale features of mesoscale flows, this approximation is satisfied and it is used in some well-known schemes such as that of Pielke (1984).

(d) Computational methods

(α) Perturbation/analytical/Fourier methods

A cursory look at computations or wind-tunnel measurements shows that usually an air flow does not significantly change its direction by more than 20% or its wind speed by more than 100% as it passes over hills or roughness changes. The reasons for this were given in §2.2.3(i) & (ii). Consequently, one approach to modelling air flow is to assume that the effect of hills and roughness changes is merely to give a small perturbation to the mean flow of $\Delta\underline{u}(= \Delta u, \Delta v, \Delta w)$. So if $\underline{U}(\underline{x},t)$ is the flow over flat uniform terrain in the same atmospheric conditions, the mean velocity is

$$\underline{u}(\underline{x},t) = \underline{U}(\underline{x},t) + \Delta\underline{u},(\underline{x},t).$$

The temperature and pressure fields, and Reynolds stress, are also perturbed

$$\begin{aligned}\theta(\underline{x},t) &= T(\underline{x},t) + \Delta\theta(\underline{x},t)\\ \tau_{ij} \quad &= T_{ij} + \Delta\tau_{ij}\end{aligned}$$

Form a mathematical point of view, it is assumed that these perturbations are small (e.g. $|\Delta\underline{u}| \leq |\underline{U}|/3$), but as in many analyses in engineering and science, perturbation methods gives useful results even when the perturbations are of the same order as the basic flow. (Examples are given later!) Then for a quasi-steady analysis, the equations (2.22) become

$$\frac{\partial \Delta u_j}{\partial x_j} = 0$$

$$U_j \frac{\partial \Delta u_i}{\partial x_j} + \Delta u_j \frac{\partial U_i}{\partial x_j} = -\frac{1}{\rho_o}\frac{\partial \Delta p}{\partial x_i} - g\frac{\Delta\theta}{T_o} + \frac{\partial}{\partial x_j}\Delta\tau_{ij}$$

$$U_j \frac{\partial \Delta\theta}{\partial x_j} + \Delta u_j \frac{\partial T}{\partial x_j} = -\frac{\partial \Delta F_{\theta_j}}{\partial x_j}.$$

plus model equations for $\Delta\theta_{ij}, \Delta F_\theta$.

In these equations $\underline{U}$ and T are assumed to be given (by measurement or modelling of the flow over flat terrain). Since they are varying functions, even for these linear equations, no general solution is known. However, analytical solutions to the equations have been found for certain typical profiles of $U(z), T(z)$ and for flow over regular sinusoidal hills

$$z_s = \tilde{f}_s(k_1,k_2)\cos(k_1x + \phi_1)\cos(k_2y + \phi_2),$$

and for flow over sinusoidal variations in surface roughness length

$$z_o(x,y) = \tilde{g}_r(k_1,k_2)\cos k_1x \cos k_2y.$$

The analytical solution is written as

$$\Delta\tilde{u}(z,k_1.k_2)\cos(k_1x+\psi_1)\cos(k_2y+\psi_2),$$

where

$$\Delta\tilde{u}(z,k_1,k_2) = G(z,k_1,k_2)\tilde{f}_s(k_1,k_2),$$

and G is independent of $\tilde{f}_s$ but not $\tilde{g}_r$. ϕ_1, ϕ_2, ψ_1, ψ_2 are phases. Earlier authors obtained approximate solutions for neutrally stable flow with logarithmic profiles for $U(z)$ (Jackson & Hunt 1975; Walmsley et al.1982). Later authors have obtained more accurate solutions for a wider class of profile and have allowed for the effects of stratification over the hills (Hunt, Leibovich & Richards 1988; Hunt, Richards & Brighton 1988). Effects of roughness changes have been introduced by Walmsley et al. (1986), and Xu & Hunt (1988).

Because the analysis is *linear*, it means that the perturbation is doubled by doubling the height of a hill; more significantly it also means that perturbations produced by several superposed sinusoidal hills or areas of roughness can simply be added! Therefore, since, by the usual method of Fourier analysis, the shape of any hill can be represented by adding many sinusoidal hills, the air flow over any hill can be calculated by adding the solutions for flow over each of its sinusoidal components. Roughness can be handled in the same way.

In other words, if the terrain $z_s(x,y)$ is represented by $N \times M$ sinusoidal hills in the two directions

$$z_s(x,y) \simeq \sum_{n=o}^{N}\sum_{m=o}^{M} \tilde{f}_s(k_{1_n},k_{2_m})\cos(k_{1_n}+\phi_{1_n})\cos(k_{2_m}y+\phi_{2_m})$$

then the perturbation flow $\Delta\underline{u}(x,y)$ is given by the addition of $N \times M$ known functions, i.e.

$$\Delta\underline{u}(x,y) = \sum_{n=o}^{N}\sum_{m=o}^{M} \underline{G}(z,k_{1_n},k_{2_m})\tilde{f}_s(k_{1_n},k_{2_m}\cos(k_{1_n}x+\psi_{1_n})\cos(k_{2_m}y+\psi_{2_m}) \ .$$

This result is represented diagramatically in Fig.2.24(a-d).

In general $z_s(x,y)$ is defined over a grid of $N \times M$ points and therefore representing z_s by a finite sum of sinusoidal hills is an approximation which is consistent with the data. So the first stage in the calculation is to derive the $N \times M$ values of $\tilde{f}_s$ which are now seen to be the coefficients of the terms in the Fourier series representation of the terrain. Once these are known and stored, Δu can be calculated at arbitrary points (x,y,z) for those boundary-layer conditions in which $G(z)$ is defined.

The advantage of this method is that, apart from being very fast on mainframe computers, it can be used on small personal computers. The storage required for

three velocity component is $N \times M \times 3$. Thus for a typical region, where the terrain is described by 64×64 points in the horizontal plane only 12500 or so points need to be stored. Since the perturbation quantities are given in terms of analytical functions $G(z, k, k_1)$, the vertical variation of $\Delta \underline{u}$ etc. can be calculated in either great detail or very little detail. This is useful for streamline calculations for a localised source since only the flow along and near the streamline through the source need be calculated. In the mass consistent interpolation models and full computational methods the whole flow has to be calculated. To compute flow along a typical streamline over a terrain where $\tilde{f}_s(k_1, k_2)$, $\tilde{g}_r(k_1, k_2)$ are defined for 32×32 points takes about 10 minutes on an IBM PC/AT. With the new array processors for personal computers now becoming available, it will be possible to employ much larger grids (say 256×256 points) and achieve a much better resolution in the same sort of time.

Computer codes for flow over terrain based on the perturbation approach for arbitrary terrain are now available from various organisations in Europe and the U.S.A. So far though only the CERC model FLOWSTAR allows for stratification. So far it has been compared quantitatively with field experiments of neutral and moderately stratified flow over isolated hills, and with numerical computations and laboratory experiments for many neutral and stratified flows. Some of these are described in §2.2.4(ii).

The disadvantages of this method are

- there are errors if the slopes of the hills are greater than about 1/4–1/3; the predictions for the maximum increase in speed over hills may be as great as 20% but the error for the total velocity is typically only about 10%. More seriously, the model underpredicts the slow down in the wind speed, the formation of reverse flow, and downwash on the lee slopes and in the wakes of hills. This error, which extends over a larger volume of the flow for isolated hills than for rolling terrain, has been analysed and discussed in detail by Britter et al. (1981) and by Mason & King (1985). Formulae or particular computational schemes developed specifically for wake regions have been proposed by Counihan et al.1974 and Weng et al.1988. CERC is working to incorporate these methods as corrections into a perturbation approach;

- there are errors if the stratification is strong (i.e. if the Froude numbers based on the hill height $F_H < 1$) (see §2.2.3(i)(d), Fig.2.10b). In this case the air flow below the critical dividing height H_c moves in approximately horizontal planes around the hill. Therefore at each level z, below h_c, there is a point on the hill where the velocity of the flow approach is zero, and a significant zone where the velocity is much less than $U(z)$; the flow, in fact, changes direction by up to 90° and moves parallel to the high side. Above the critical height the air flow passes over the hill as if it has a height $H^* = (H - H_c)$ with a Froude number $F_{H^*} \simeq 1$. Unlike the mass consistent interpolation methods (such as WAFT) or the equivalent-ideal-shape method (such as CTDM described next), current

perturbation codes (such as FLOWSTAR) do not describe this flow regime; but it would be straightforward to incorporate a procedure similar to CTDM into them for individual hills.)

- The model does not allow for drainage or other thermally-driven winds, described in §2.2.3(i)(e).

(β) Constructed non-linear flow model for idealised terrain features

If the primary goal of an easily computable wind field model is to represent strongly stratified flow (i.e. $F_H < 1$) over and around isolated hills and mountains, it is necessary to have a non-linear flow model to account for the large changes in flow speed and direction associated with this kind of flow (§2.2.3(i)(e)). The only non-linear stratified flows that can be approximately modelled by analytical methods are flows around idealised shapes such as ellipsoids (Fig.2.25). Based on this concept, Paine et al. (1987) from Environmental Research & Technology and Sigma of Boston have developed a computer code CTDM for flow and dispersion impinging into isolated hills and mountains.*

The first step is to approximate the actual terrain by a set of ellipsoids or, in some versions of the code, bell-shaped hills. The second step is to define the Froude number F_H for each hill and if $F_H < 1$, the critical dividing streamline height $H_c = H(1 - F_H)$. Below H_c the flow is modelled as a potential flow in horizontal planes. For streamlines starting upwind above H_c, the flow is modelled approximately as a moderately stratified flow over a hill of height $H^* = H - H_c = HF_H$. If $F_H > 1$, the flow is modelled as a perturbation solution for flow over the idealised shape. In CTDM none of these solutions is a mathematically correct solution even in an an asymptotic sense, and there is no matching with the surface boundary-layer flow. Wake effects are also ignored.

In general, the emphasis of the CTDM code has been on choosing and patching theories together to ensure a very good fit with the air flow and dispersion measurements in three field experiments – an isolated 100m hill (Cinder Cone Butte), a long ridge about 85m in height (Hog Back Ridge), and amongst mountains rising up to 1km over 7km near Reno, Nevada (Tracy experiment). The main aim has been to produce a dispersion model for studying the high concentrations associated with plumes impacting on hills; it is not appropriate for the air flow over rolling terrain in near neutral conditions. In addition, it does not allow for interaction between flows over neighbouring hills. However, the model may be of some use in occasional UK situations associated with low winds and strong stable stratification.

The current operational status of this model is that it is being tested by many organisations in the U.S. Training courses are being held by the E.P.A. who envis-

* Dr. J.C.R. Hunt of CERC was a consultant on this project, which makes use of several studies initiated at Cambridge.

aged that it will become a regulatory model, replacing the streamline impingement model VALLEY, in about 1990-91. However, doubts have been expressed about this model, on scientific and practical grounds; it is not yet clear whether it will be accepted as a practical model for general use.

(γ) Finite-difference computations of non-linear equations

Mesoscale models used by meteorological organisations are based on current methods of forecasting synoptic scale weather using the 'numerical' computation of solutions to the governing equations for asymptotic motion. 'Numerical' means that the computations are performed on approximate estimates of differential coefficients based on finite sets of values of the flow field defined either at points (as in finite-difference methods), or in columns (finite-volume methods), or as particular mathematical functions (Fourier series).

Despite these approximations modern numerical methods and computational resources ensure that, for a given region of space and over a given time interval, 'numerical' solutions are close approximations, on the scale of the discretisation, to the correct solutions given the assumptions employed when in deriving the differential equations (such as those for shear stresses, thermodynamics, etc.). In other words, the finite-difference solutions $\underline{u}_s(\underline{x},t)$ obtained at a spacing of $\Delta x, \Delta y, \Delta z, \Delta t$ is a close approximation to the actual solution $\underline{u}(x,y,z)$ when averaged over both a volume $\Delta x \Delta y \Delta z$ and a time interval Δt. The only way of checking the correctness of the numerical solution is by reducing Δx until there is no change in the solution. As with weather forecasting, it is important to realise that, given approximate initial data for the flow in entering a flow region (or boundary conditions BC1 and BC2), the inherent numerical errors build up with time and distance (Pielke 1984).

In most finite-difference mesoscale models there is a uniform spacing $(\Delta x, \Delta y)$ in the horizontal direction which is present in about 10 to 15km but which may reduce to 3km over the next 5 years. The spacing Δz in the vertical varies, ranging from $\Delta z_{\min}$ to $\Delta z_{\max}$. All models have to assume some form for the profiles of mean velocity, turbulence and fluxes below a height of $\Delta z_{\min}$. Within the computational domain $(z > \Delta z_{\min})$ many atmospheric processes have to be approximately modelled when averaged over a volume of $\Delta x \Delta y \Delta z$, and this is a rather uncertain affair, especially when modelling cloud processes, wave radiation, etc.

Numerical and physical approximations can interact, because, depending on the mathematical form taken for the model of a physical process, it may or may not contribute to the stability of the numerical solution. For example, it appears that reducing both the finite-difference scale and the numerical 'diffusion' or smoothing which should increase accuracy, in principle may, in fact, prevent the solution converging, i.e. only occurs when physical diffusion is less than numerical diffusion.

Clearly these models incorporate sometimes more and sometimes fewer physical processes than the smaller-scale models described before – for example, in the atmospheric water cycle and thermodynamics and interaction with mesoscale and synoptic scale dynamics (such as fronts). They are the best models currently available for thermally-driven effects such as sea breezes and katabatic winds, and for interactions between air flow, clouds and dispersion/deposition processes. On the other hand, they incorporate less detail than smaller-scale models; all terrain slopes (on a 10km mesh) are less than actual slopes (see Fig.2.26) which reduces the speed up and turbulence and wave generation over hill tops, and ensures that there is no reverse flow downwind of hills in near neutral conditions.

In the widely known and used model of Pielke (now of Colorado State University) eight levels for Δz are used with $\Delta z_{\max} \approx 2$km, with the top of the domain at 10 km. The equations are simplified by making the hydrostatic approximation. The topography is 'smoothed' by being represented as an 11km horizontal grid with the whole grid being deformed over the topography. The model has been tested for air flow over mountains in Virginia, hills in Israel (Mahrer & Pielke 1985), and for sea breezes off the U.S. coast. In the latter tests comparison of predicted and radar measurements of convergence zones, cloud growth and rainfall show reasonable agreement.

In the U.K. Meteorological Office model developed by Golding and others (1987), the horizontal grid interval $(\Delta x, \Delta y)$ is 15km, while vertically there are 16 levels, with Δz ranging from 10m near the ground to about 2km at the top of the domain at 12km. (Even this height may not include all cloud activity in summer.) This mesh is deformed over the filtered topography and the non-hydrostatic form of the equations are used to permit fine resolution. The model covers the whole of the U.K. with 5000 (see Fig.2.27) points and is used primarily for forecasting local weather. It is also available for use in making trajectories for dispersion or emergency response calculations. In 1989 it is planned to extend the model to 15000 points at 32 levels. However, the 15km horizontal grid spacing will be retained so as to take in a greater area of topography surrounding the region of interest.

Other non-hydrostatic mesoscale models have been developed. For example, the French scheme developed under the auspices of Electricité de France EDF (Caneill & Buty 1988) is interesting in that it has a nested system of air flow models. PERIDOT, the French Meteorological office Model, gives a 24 hour forecast on a 35km horizontal grid spacing. This provides the boundary conditions to the EDF hydrostatic model HERMES which has a grid of 5 to 10km; this is used over a regional scale of, say, 300km × 300km. Then for local scale predictions, say over an area of 30km × 30km, they have developed a small-scale numerical model MERCURE, whose grid spacing is 0.5km to 5km.

For on-line use (NOWCASTING) they use data from a network of ground-level and remote-sensing measurements in the areas of interest, such as near power stations. This data is used to construct a mass consistent flow field on a region

on a scale of about 100–300km using the code MINERVE which employs methods similar to those described in §2.2.4(ii). This flow field may then be combined with the local predictive model MERCURE.

Small-scale/micro-meteorological numerical models are used to describe flows when the respective horizontal and vertical scales are less than a few metres and one metre. They are useful in local situations where the terrain-induced effects on the air flow are on a scale less than 10km. Given typical computing resources with, say, 32^3 points this means that the horizontal scale of the domain may be 10km $\times$ 10km and extend to about 2km vertically.

In the usual form of such models, they are used for quasi-steady analysis of the mean flow quantities. Making the usual approximation for the Reynolds shear stress and fluxes of heat, water vapour, etc., it is not necessary to assume the form of profiles near the ground; they are derived naturally from the solution. These models have been used to predict air flow over hills and escarpments with large slopes where there may be reverse flow and the perturbation approach does not work well, e.g. Deaves (1976); Hunt, Newley & Weng (1988), Mason & King (1985), Weng, Carruthers & Richards (1988). There are some considerable differences in the estimates of how long it takes for these calculations to converge ranging from 10 minutes to 10 hours! These methods require careful handling and significant computer power.

If the very fast and 'user-friendly' schemes like PHOENICS or FLUENT are used, our experience is that the solutions are rather dependent on the mesh size that is chosen and on the use of 'wall-functions' to define the flow near the ground. The interpretation of the results is not at all straightforward!

Later developments will incorporate these nonlinear results involving more complex models than mixing length into FLOWSTAR.

2.2.5 Conclusions and recommendations about modelling complex wind fields

We have shown that there are several possible levels of complexity for modelling air flow over complex terrain in complex meteorological conditions. Different methods are appropriate for different applications.

The "warnings" for when complex terrain effects may be important, given in R199 (Table 1) are a useful first approximation, but in the light of more recently available models should be reviewed. R157 gives estimates for the changes in the

boundary layer near coast lines where there are significant changes in surface temperature and roughness.

The simple deflection and plume impingement approach developed by EPA with their codes CRSTER and VALLEY are not accurate enough for regulatory use according to the EPA themselves, and to other reviewers, including ourselves. They are only useful for giving an indication of the possible increases in concentration and changes in dispersion associated with complex terrain.

The interpolation models using on-line data, such as MATHEW, WAFT, MINERVE, can give the general flow on a regional scale, including its time evolution. Clearly these models are useful for dispersion over scales longer than about 15km. They can also provide input to smaller-scale numerical models but with a typically sparse data network, these models do not, at present, account for many of the flow features found in flow over hills on scales less than 15km. It is possible that new algorithms can be constructed to improve these models and to make their results more consistent with those from numerical models. An important limitation on the widespread use of this approach for large numbers of predictive calculations is that these methods will require large computers, and intensive data handling facilities.

Current computational models for complex air flow, based on solving the differential equations of fluid motion for each case are not, at this stage of computer development and software writing, suitable for widespread use on small computer systems. The results from such models are available from large meteorological research/forecasting groups such as the Meteorological Office or EDF, etc. Such information is essential for on-line large-scale emergency response dispersion calculations, and for detailed post-event analysis.

There are many agencies and research groups involved in dispersion modelling who need to be able to perform many calculations of air flow and dispersion for both typical and exceptional situations using modest computer systems and data handling resources. At present the only suitable approach for them to account for complex terrain effects is to use a simplified method that can run on a small computer system.

Two current methods for flow and dispersion over hills have been described here.

The CERC code FLOWSTAR does not, at present, account for strong stratification, ($F_H < 1$) or thermally-driven winds. It allows for rolling terrain where the hills affect each other, computes the changes in turbulence over the surface, allows for variation in the shear in the wind profile, and also models changes in roughness. It naturally matches to a correct description of the boundary layer approaching the terrain. There are plans for adapting this code in various ways: to account for the case of $F_H < 1$, using a technique similar to the CTDM code; to account for

changes to the boundary layer at a coast line, and to model flow over terrain with greater slopes.

The EPA code, CTDM, does account for strong stratification, but it does not account for interactions between hills (and could not describe the typical case of rolling terrain). Nor does it account for changes in turbulence, roughness, or incident shear. It is possible that it could be developed in the direction of FLOWSTAR, but we do not know of any plans.

Our recommendation is that for modelling air flow and dispersion on modest computer systems, the use of codes similar to FLOWSTAR is the most appropriate method when dispersion calculations are to be made over distances from the source of less than about 30 km. However there will need to be further testing and developments to the existing codes before they can be relied on to cover most of the meteorological and topographic situations of practical importance.

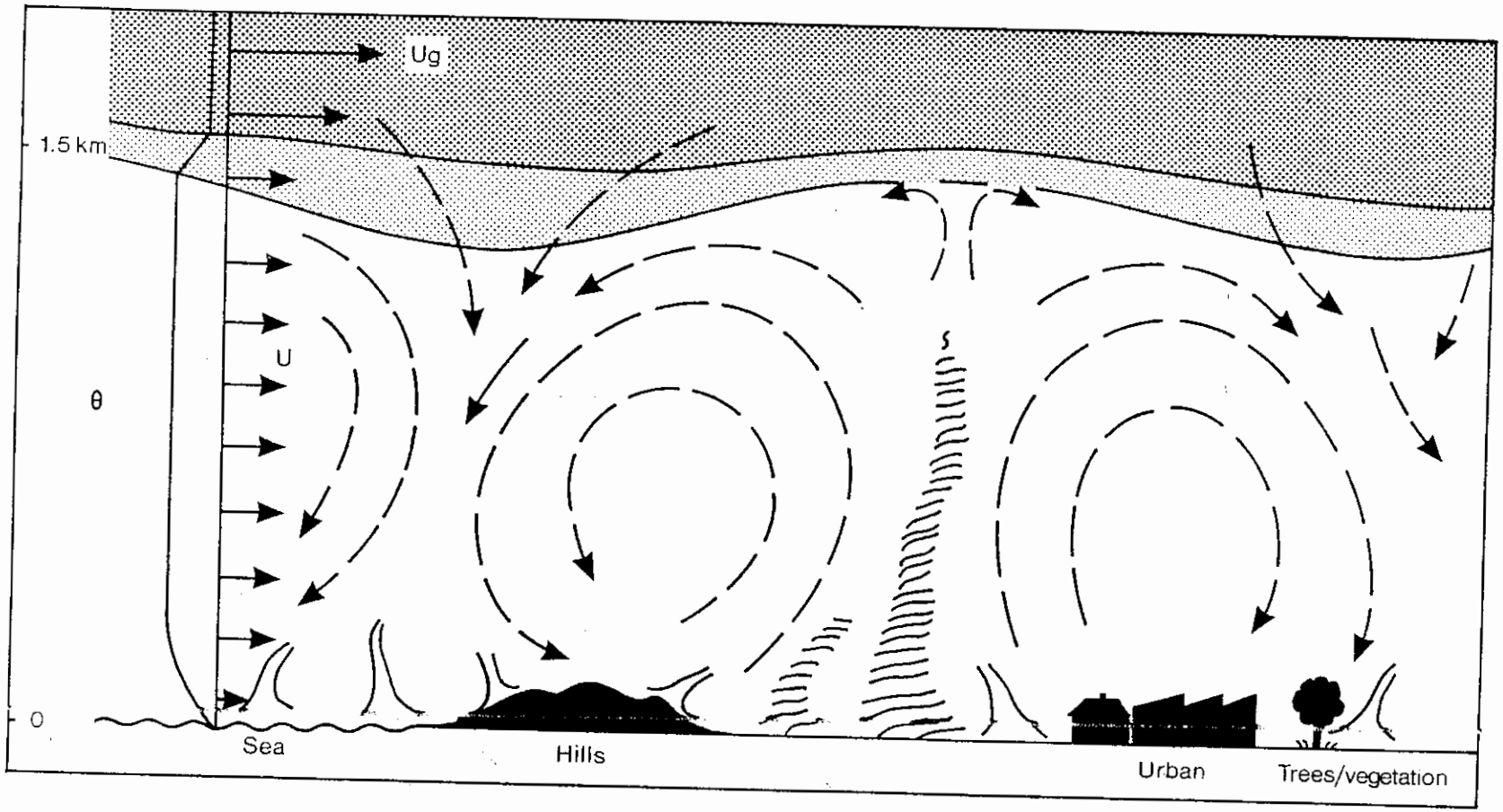

Fig.2.1a Sketch of unaveraged, local structure of a convective boundary layer showing its large convective eddies, plumes and sharp capping inversion (from Wyngaard 1985 with modifications).

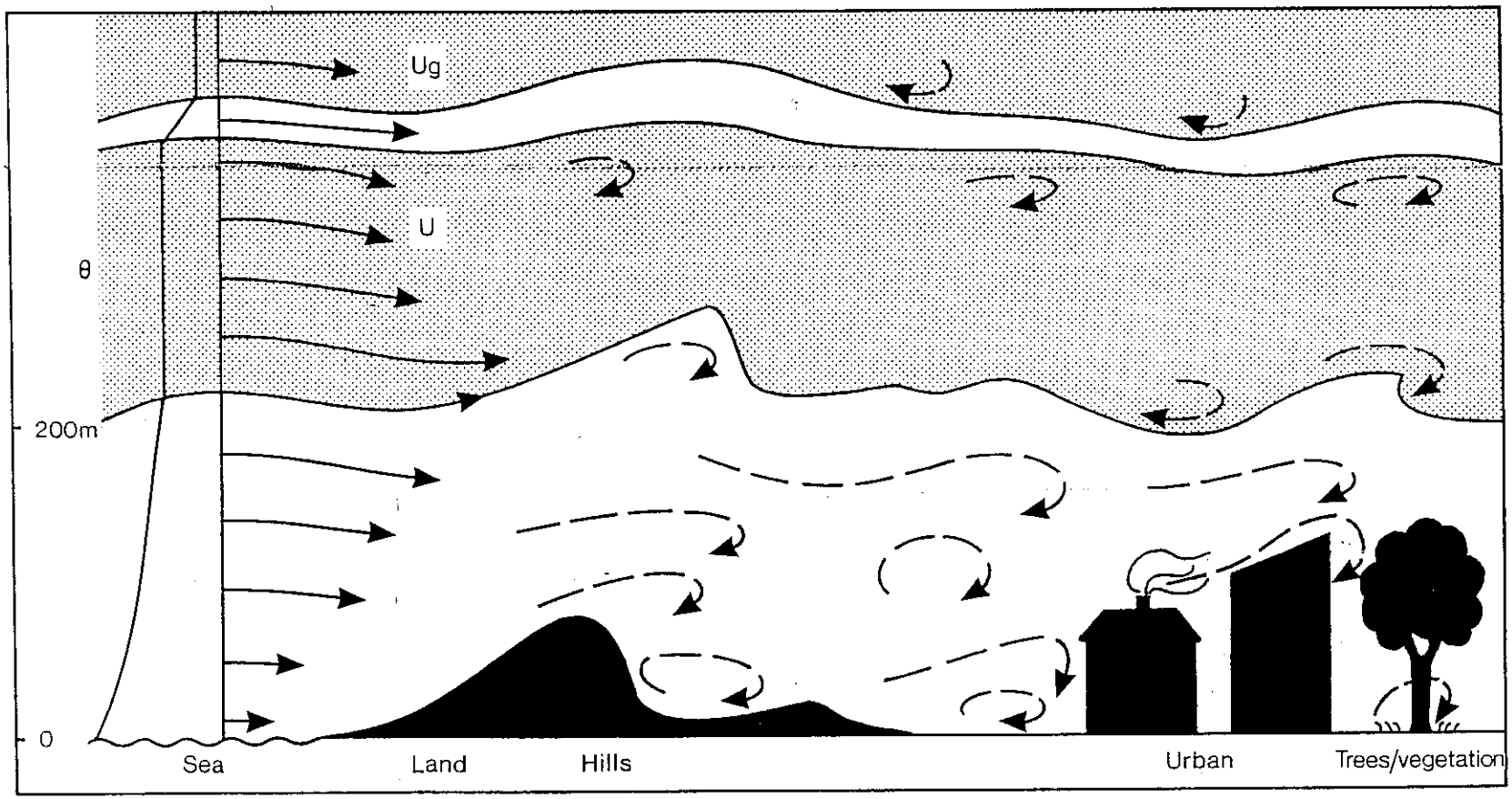

Fig.2.1b Sketch of unaveraged, local structure of a stable (nocturnal) boundary layer showing its relatively thin turbulent layer, small eddies, wind jet, and wave motion (from Wyngaard 1985, with modifications).

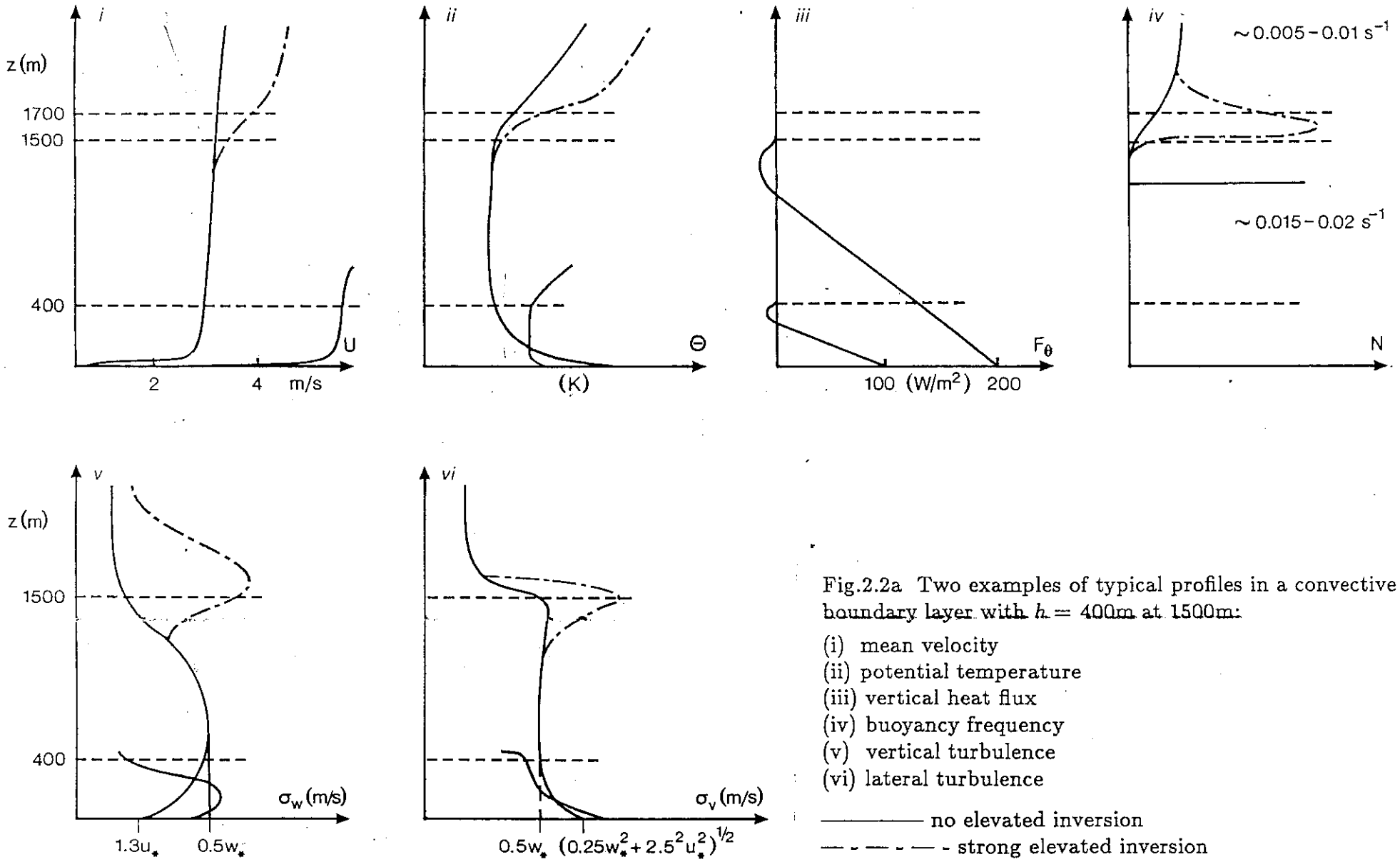

Fig.2.2a Two examples of typical profiles in a convective boundary layer with $h = 400$m at 1500m:

(i) mean velocity
(ii) potential temperature
(iii) vertical heat flux
(iv) buoyancy frequency
(v) vertical turbulence
(vi) lateral turbulence

———— no elevated inversion
— - — - — - strong elevated inversion

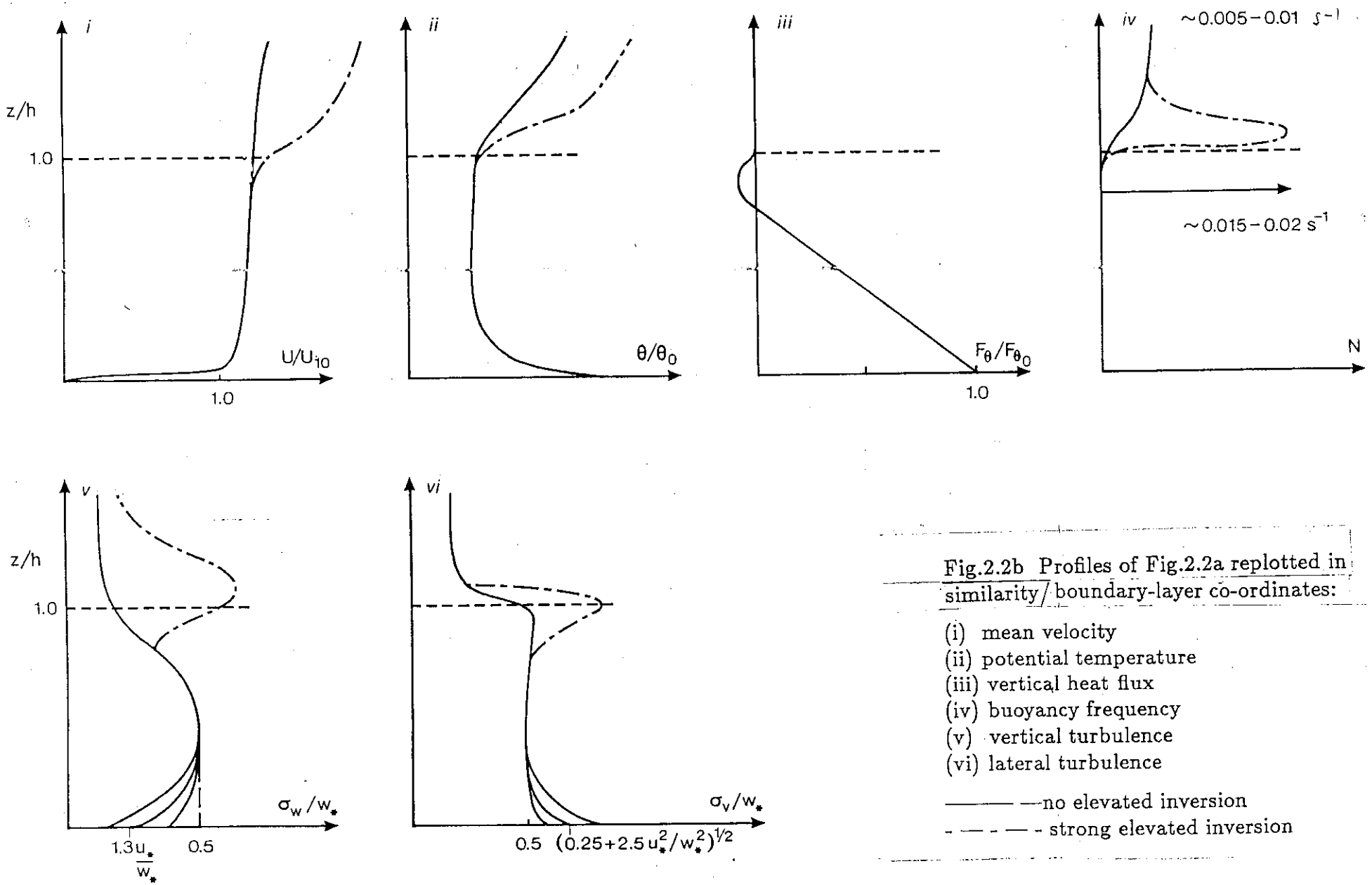

Fig.2.2b Profiles of Fig.2.2a replotted in similarity/boundary-layer co-ordinates:

(i) mean velocity
(ii) potential temperature
(iii) vertical heat flux
(iv) buoyancy frequency
(v) vertical turbulence
(vi) lateral turbulence

——— —no elevated inversion
- — - — - strong elevated inversion

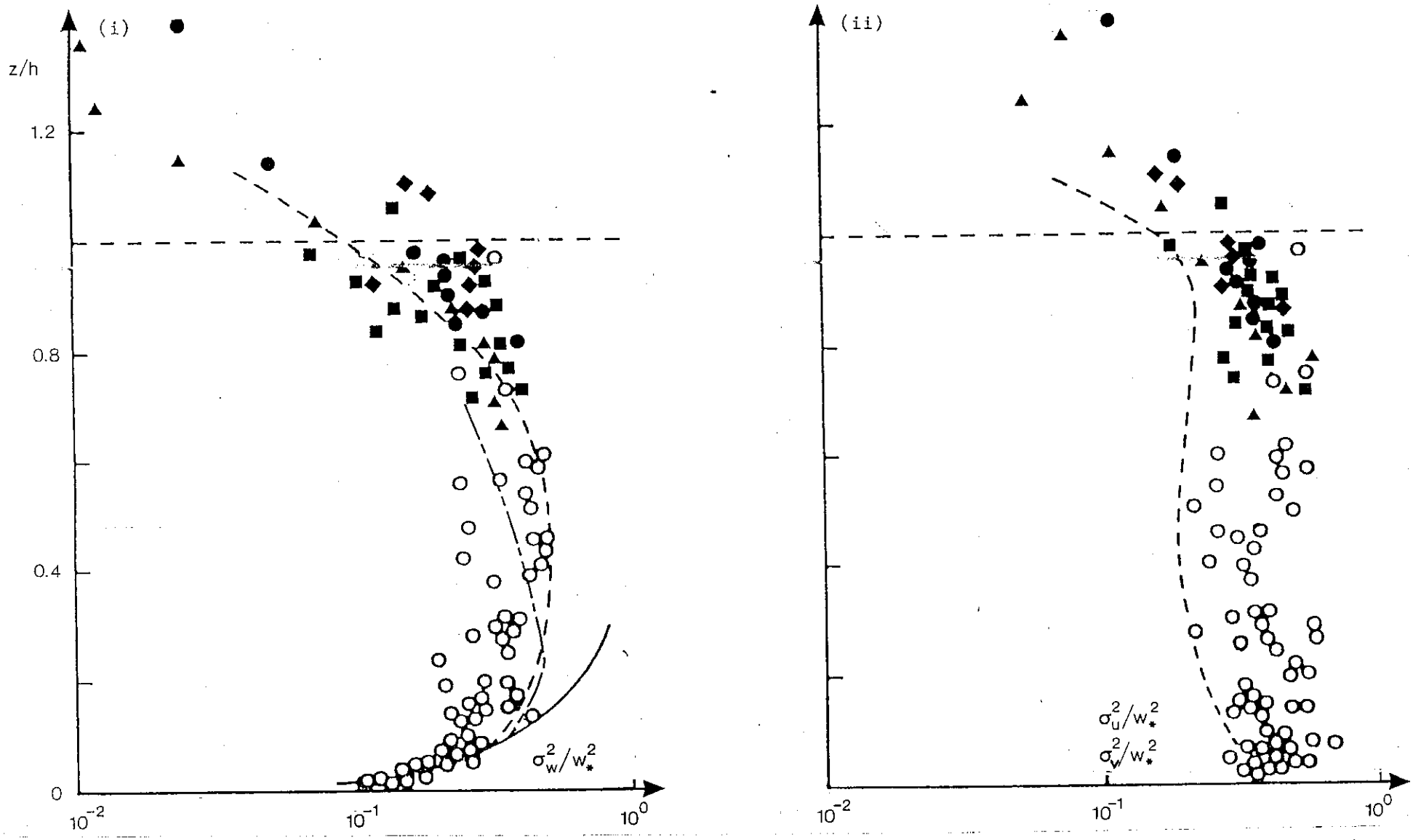

Fig.2.2c Vertical (i) and horizontal (ii) turbulence data from field experiments plotted in similarity/boundary layer co-ordinates. Closed symbols - Malvern, England on different days (Caughey & Palmer 1979); open symbols - near Rocky Mountains, Colorado (Kaimal et al 1976); - - - - - summary of results from aircraft flights (Lenschow 1970); - —— - —— summary of other results (Lenschow et al 1980); ———— $\sigma_w^2/w_*^2 = 1.8(z/h)^{\frac{2}{3}}$ = theoretical prediction for free convection.

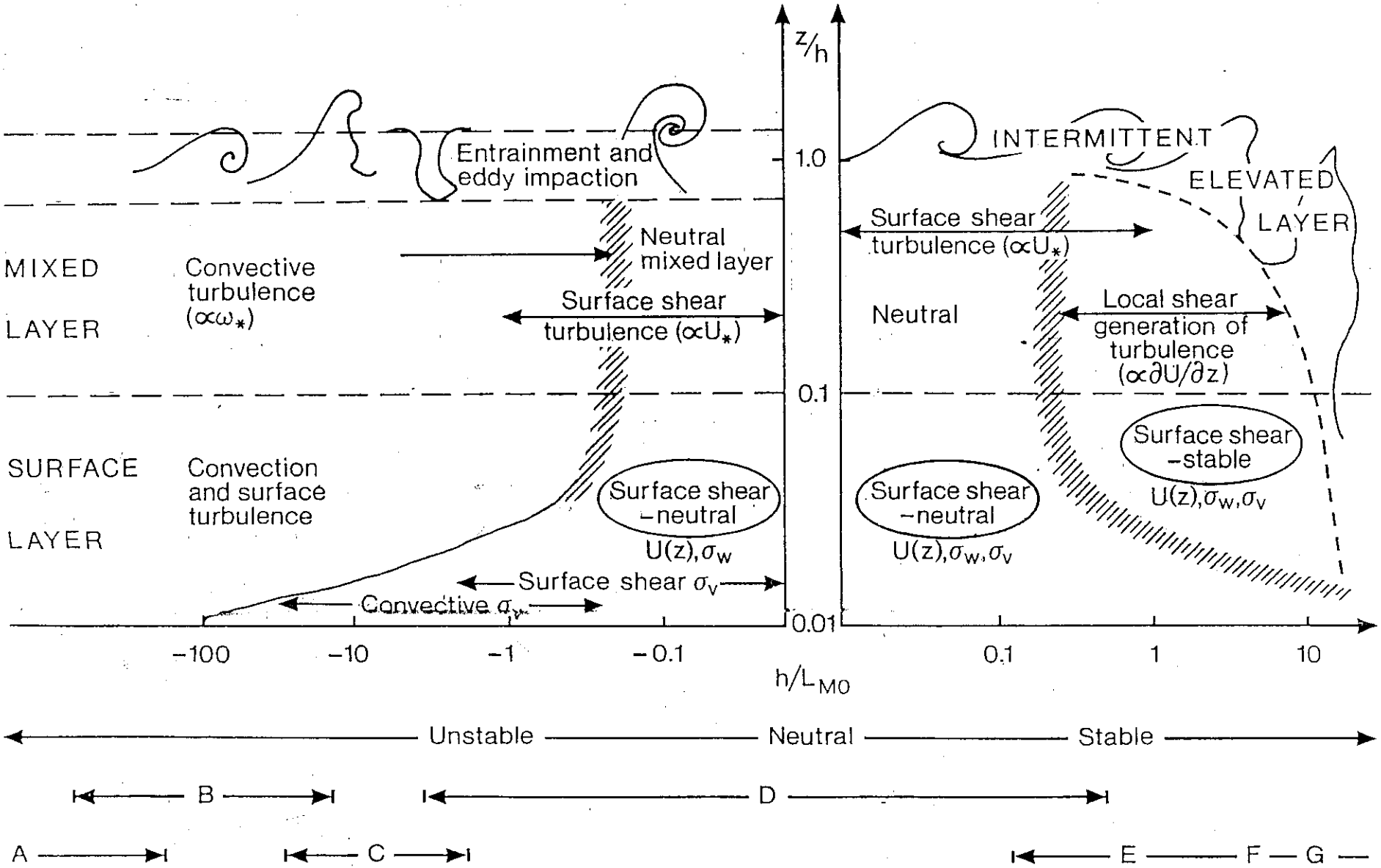

Fig.2.3 Structure of the atmospheric boundary layer as z/h and h/L_{MO} vary. Modified and elaborated form of diagram by Holtslag & Nieuwstadt 1986 and Gryning et al.1987.)

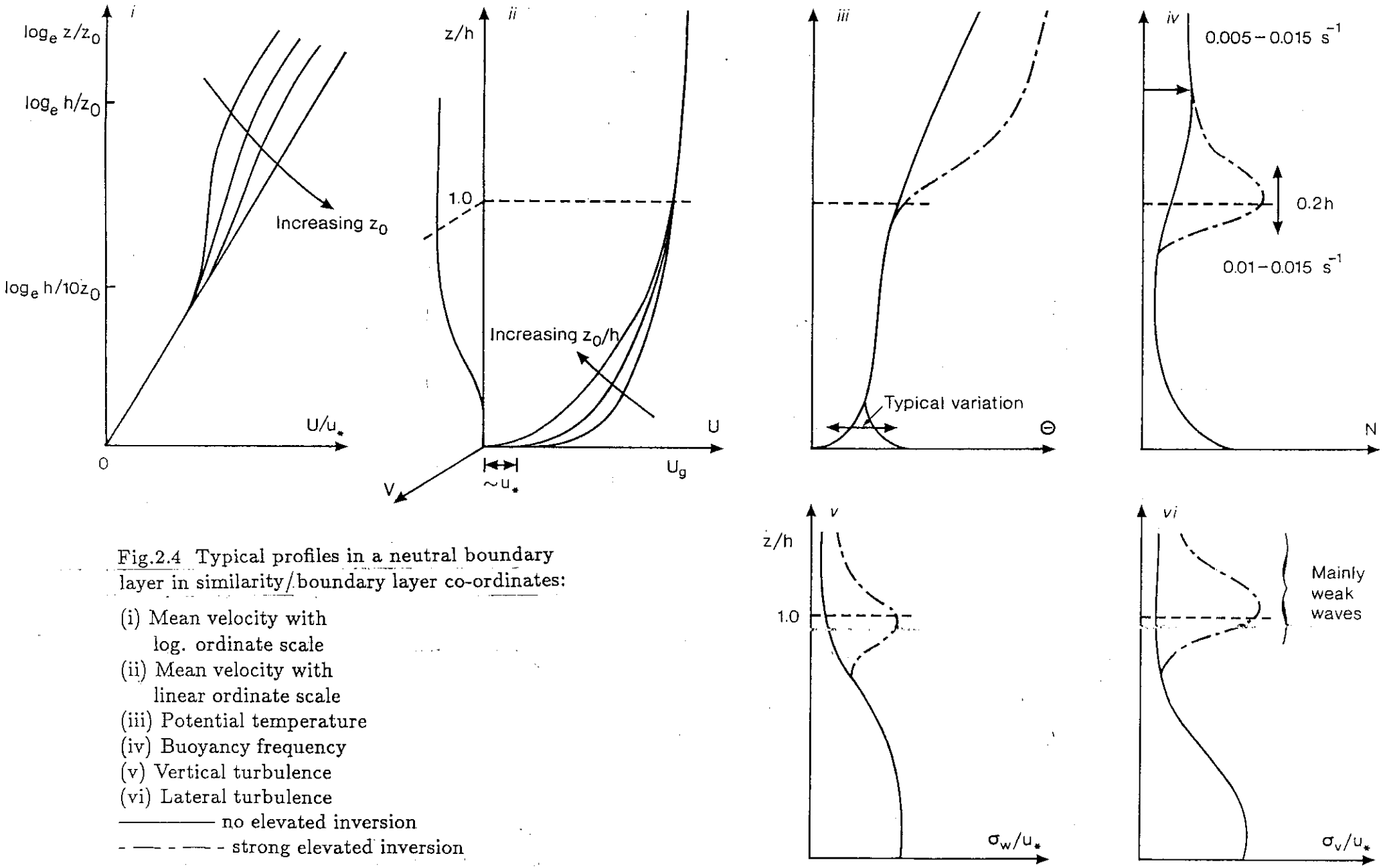

Fig.2.4 Typical profiles in a neutral boundary layer in similarity/boundary layer co-ordinates:

(i) Mean velocity with log. ordinate scale
(ii) Mean velocity with linear ordinate scale
(iii) Potential temperature
(iv) Buoyancy frequency
(v) Vertical turbulence
(vi) Lateral turbulence

———— no elevated inversion
- — - — - strong elevated inversion

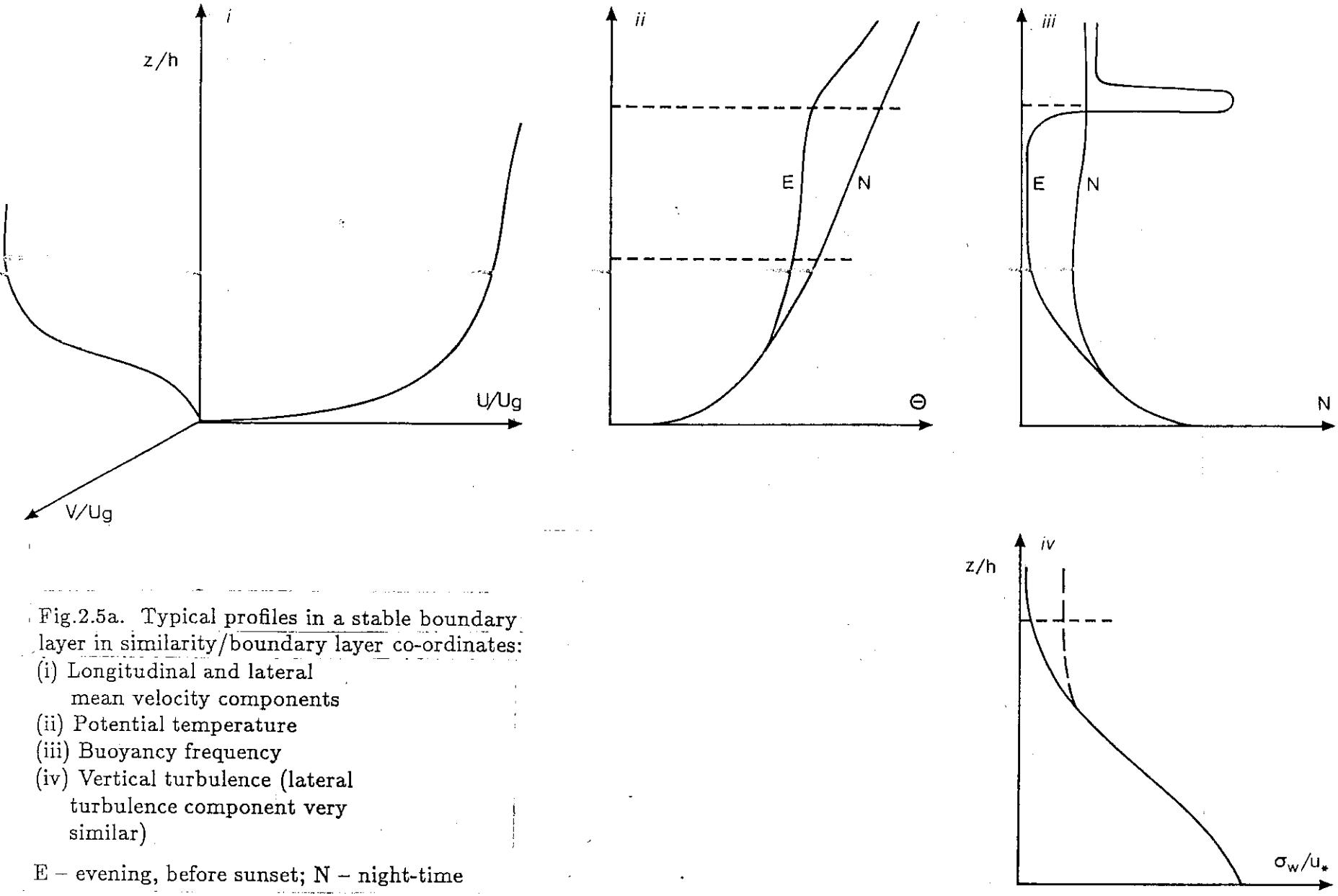

Fig.2.5a. Typical profiles in a stable boundary layer in similarity/boundary layer co-ordinates:
(i) Longitudinal and lateral mean velocity components
(ii) Potential temperature
(iii) Buoyancy frequency
(iv) Vertical turbulence (lateral turbulence component very similar)

E – evening, before sunset; N – night-time

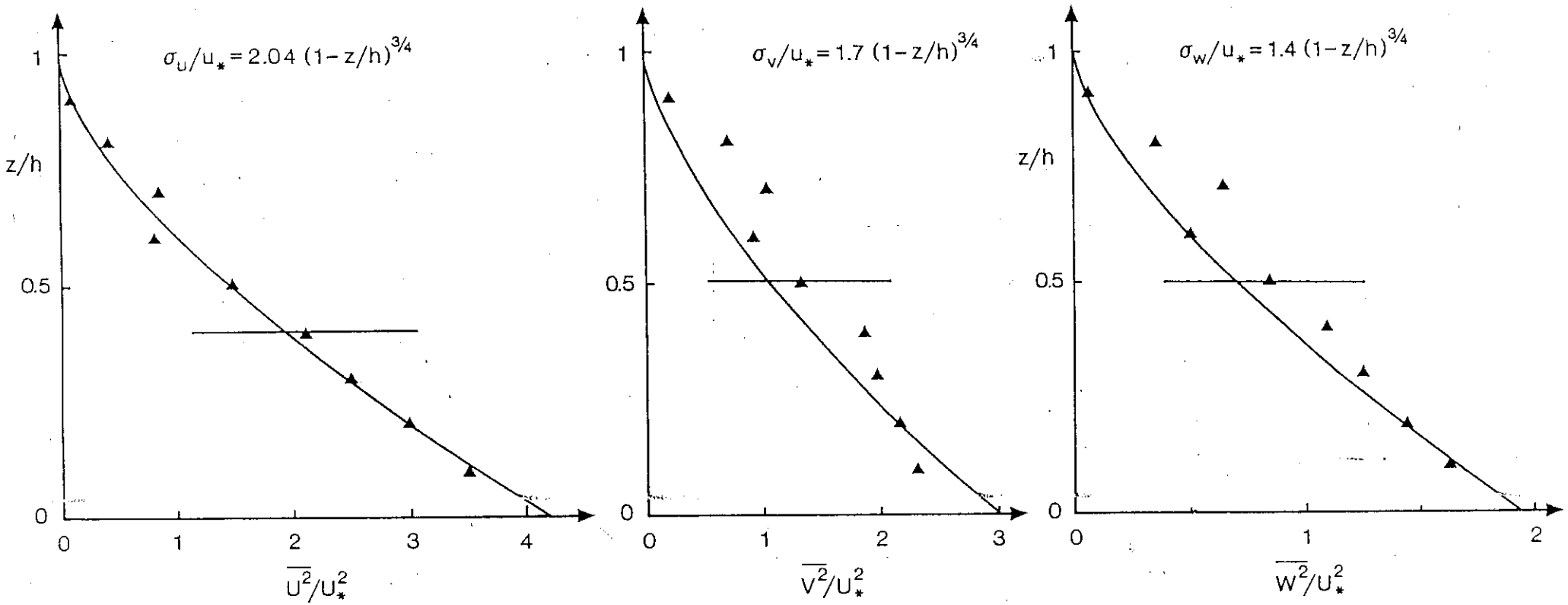

Fig.2.5b Field measurements at Cabauw, The Netherlands, of turbulence components in a stable boundary layer. Data recorded on seven consecutive clear nights over height range 20 - 200m. Sampling frequency 5Hz; data sampling period 30 mins.; high pass filter setting 0.01Hz (from Nieuwstadt 1985).

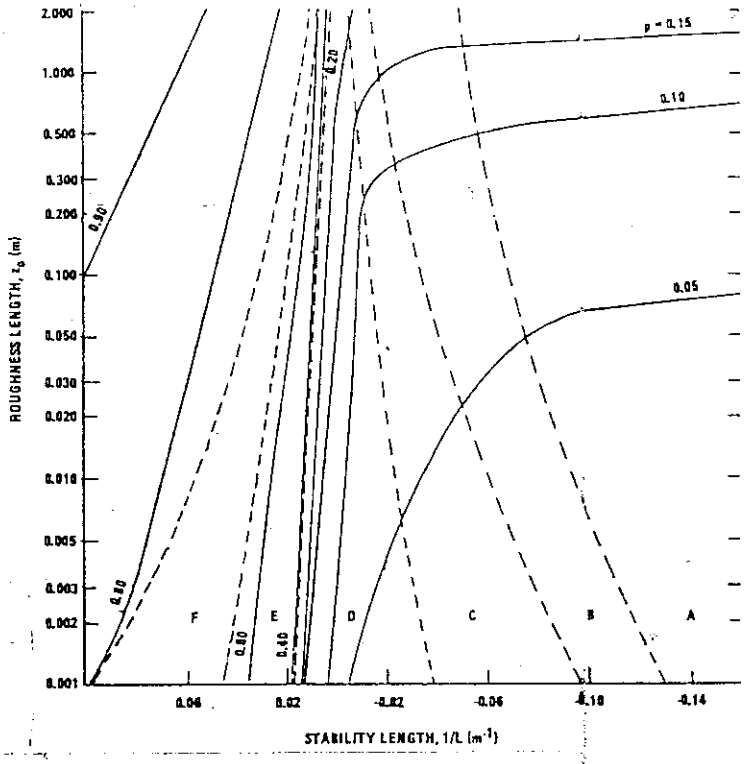

Fig.2.6 Theoretical variation of power-law exponent p with z_o and L_{MO} for $z_{ref} = 100$ derived from equations (2.9)–(2.11). Dashed curves are limits of Pasquill stability classes as adopted by Turner (1964) defined by Golder (1972). Calculations by Irwin (1979). Figure taken from Snyder (1981).

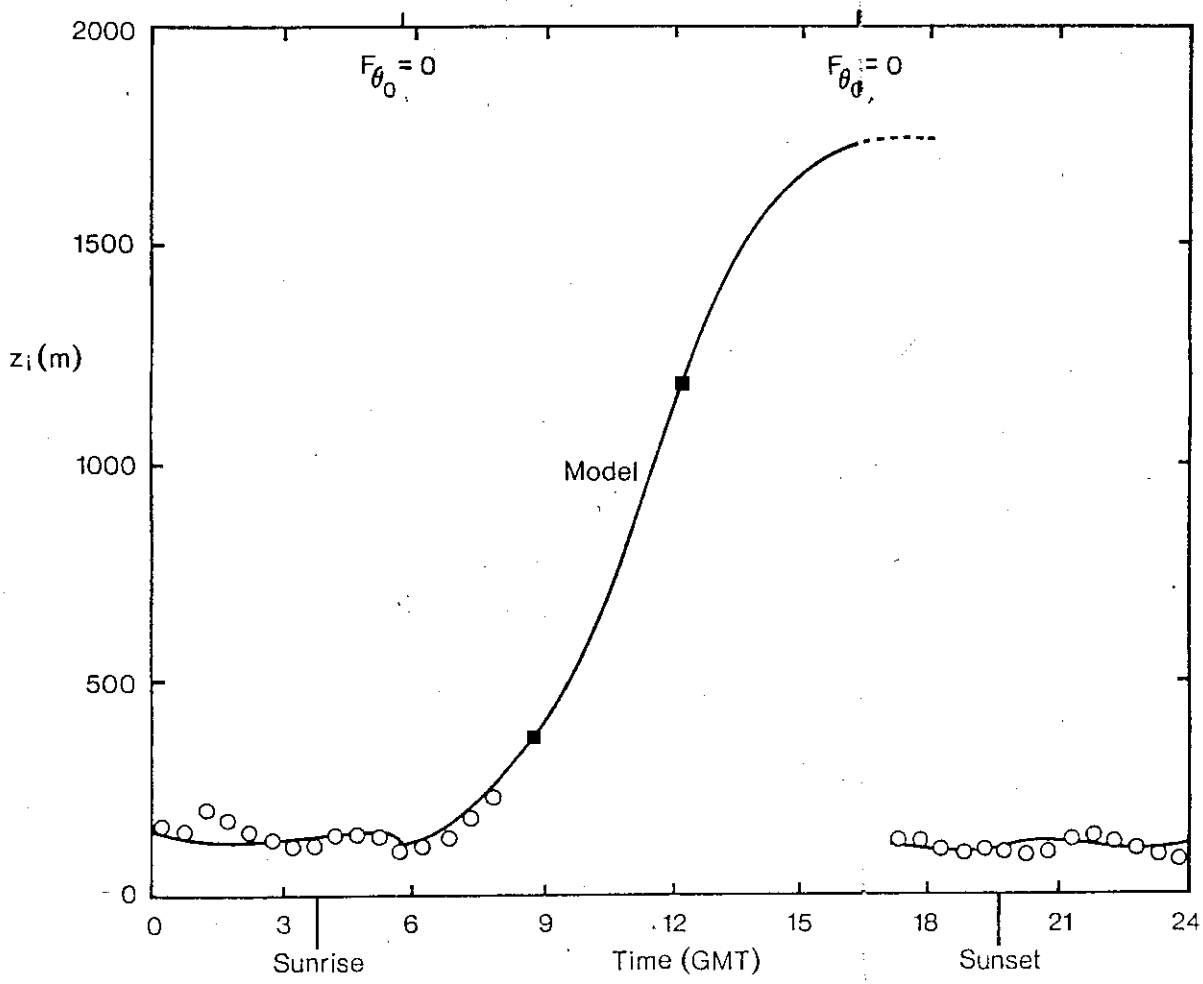

Fig.2.7 Diurnal variation of boundary-layer depth at Cabauw (The Netherlands), 31 May 1978. ○ – solar measurements (Nieuwstadt 1984), ■ – radio soundings. Curve calculated from equations given by Van Ulden & Holtslag (1985).

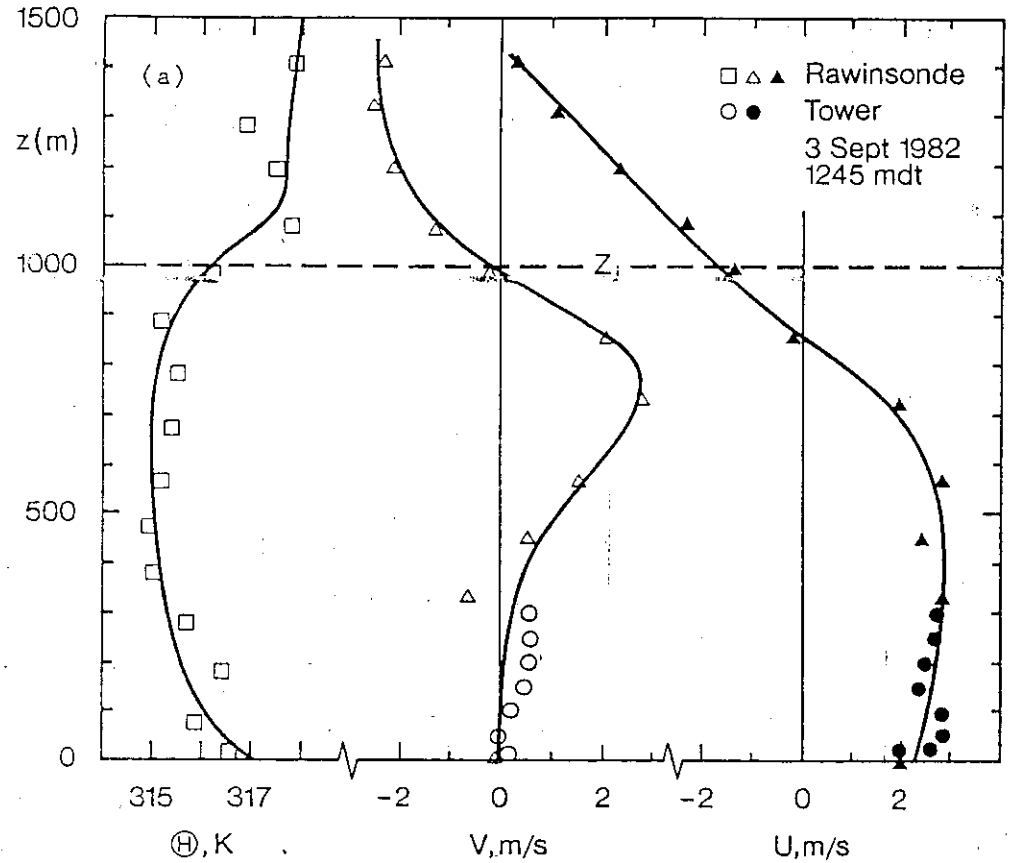

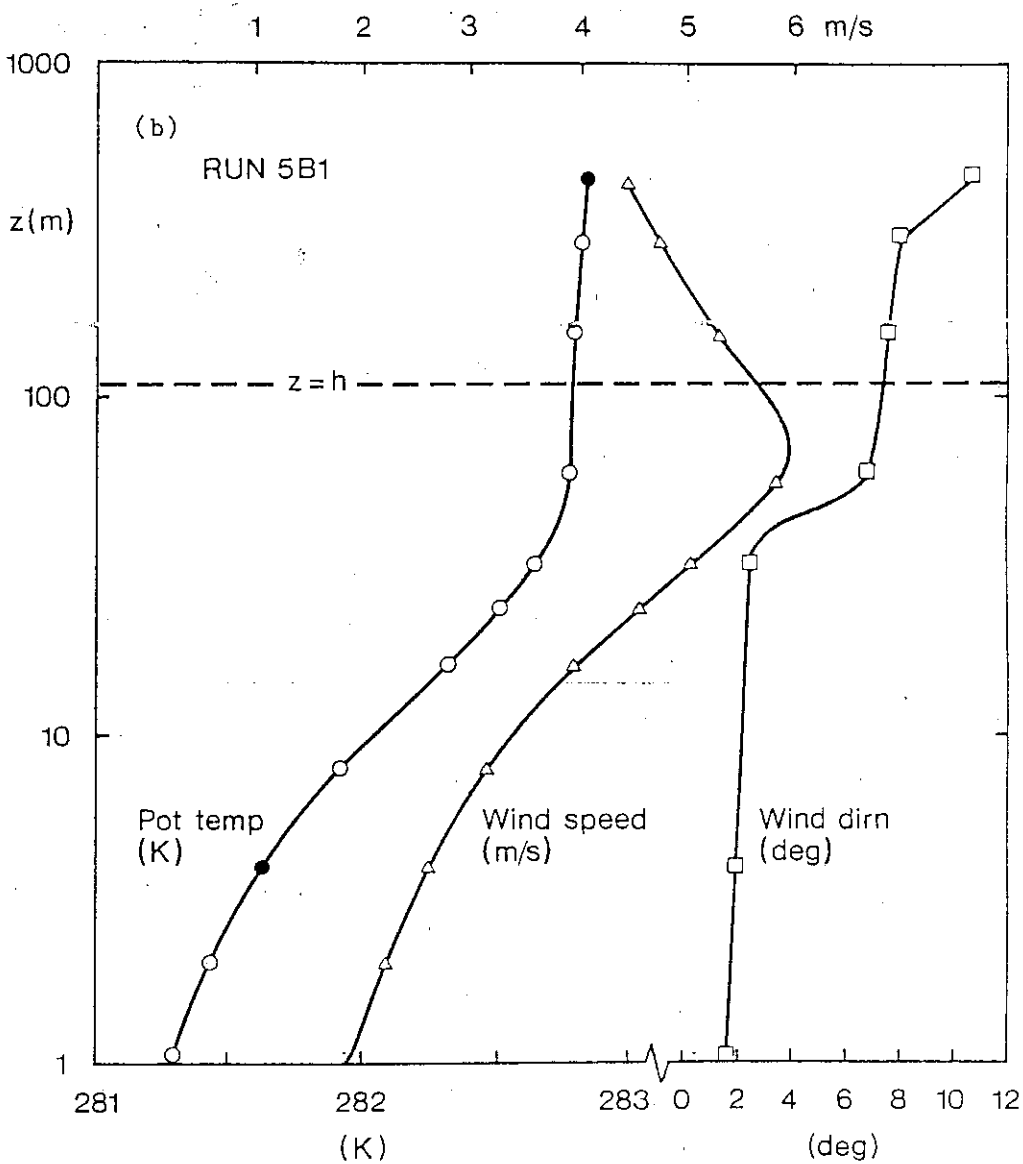

Fig.2.8 Profiles of mean wind speed and potential temperature in boundary layers over gently sloping (i.e. less than 0.01) terrain where there are *horizontal* temperature gradients.
(a) Convective boundary layer ($h/L_{MO} \approx -250$) at the Boulder Atmospheric Observatory, Colorado (from Wyngaard 1985).
(b) Stable boundary layer near the Rocky Mountains, Colorado (from Caughey et al.1979).

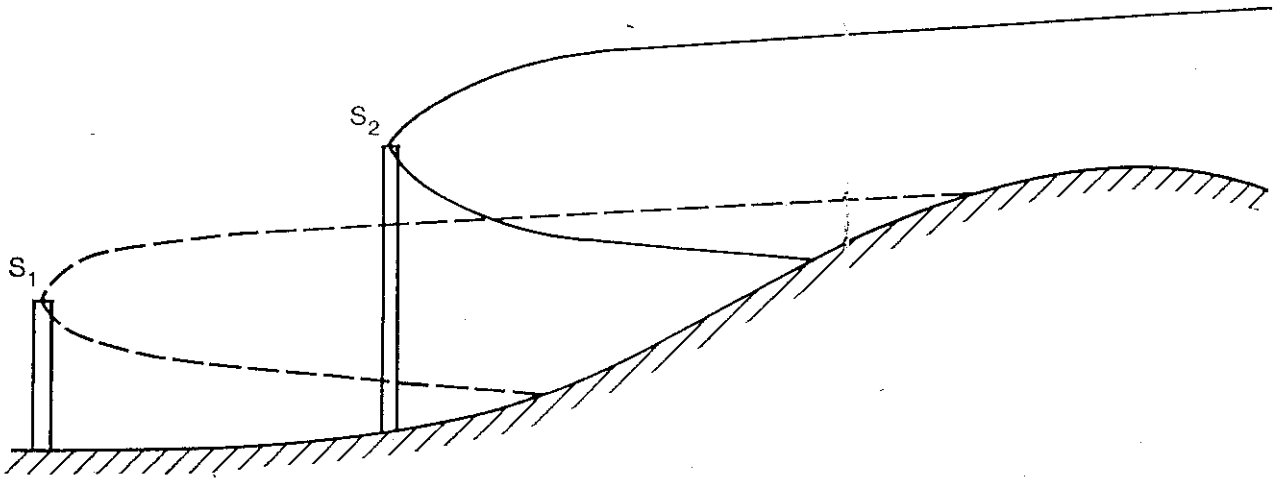

Fig.2.9a Plumes emanating from sources upwind of a hill in neutral conditions.

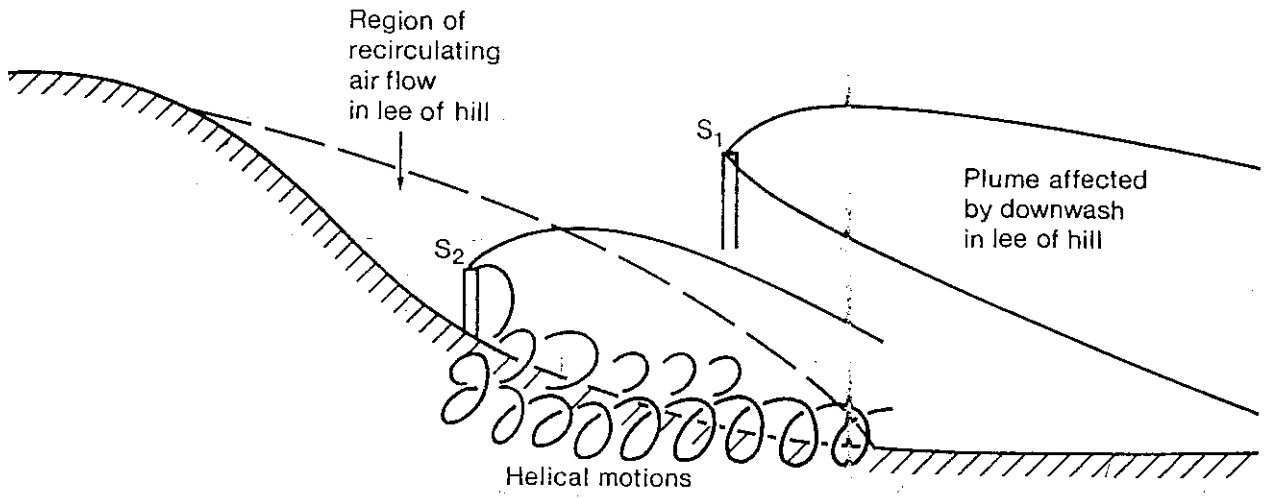

Fig.2.9b Plumes emanating from sources downwind of a hill in neutral conditions.

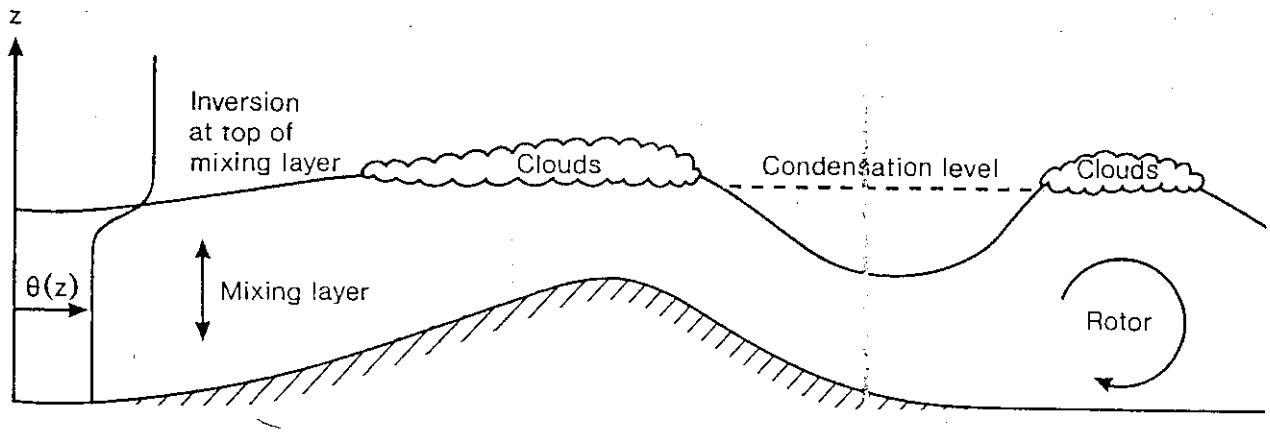

Fig.2.9c Neutral/unstable mixing layer capped by an elevated inversion over hilly terrain.

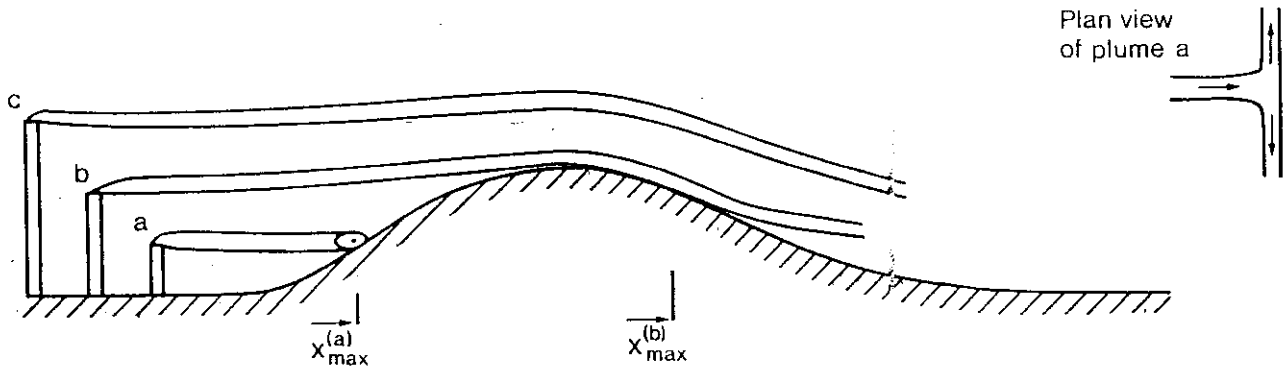

Fig.2.10a Plumes emanating from sources upwind of a hill in stable conditions.

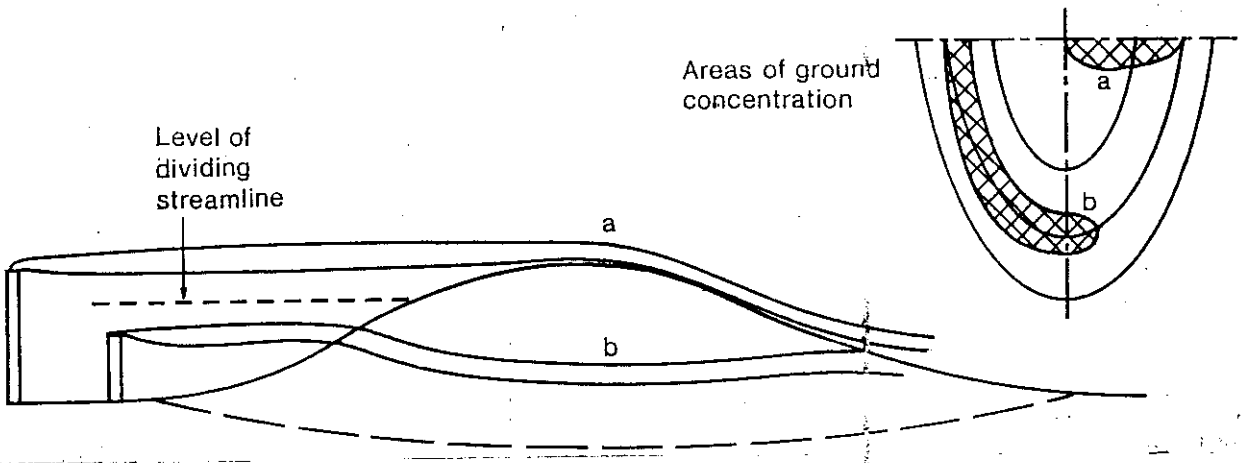

Fig.2.10b Sketch of plumes in stable conditions. Plumes below the level of the dividing streamline impact on the hillside, divide and pass around the flanks of the hill. Plumes above the dividing streamline flow over the top of the hill and give rise to a maximum ground-level concentration on the lee slope.

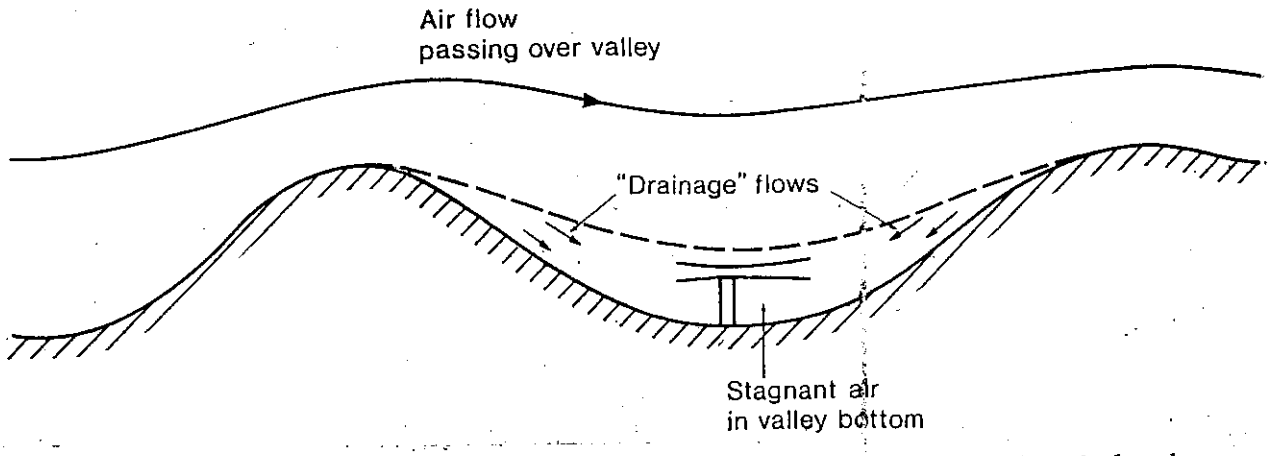

Fig.2.10c Plume trapped in valley in very stable conditions with light winds when drainage flows pool in valley bottom.

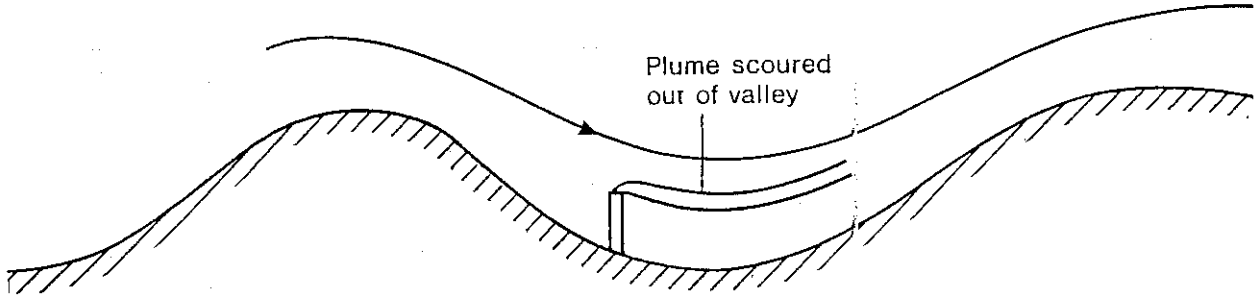

Fig.2.10d Plume scoured out of valley bottom by stronger winds.

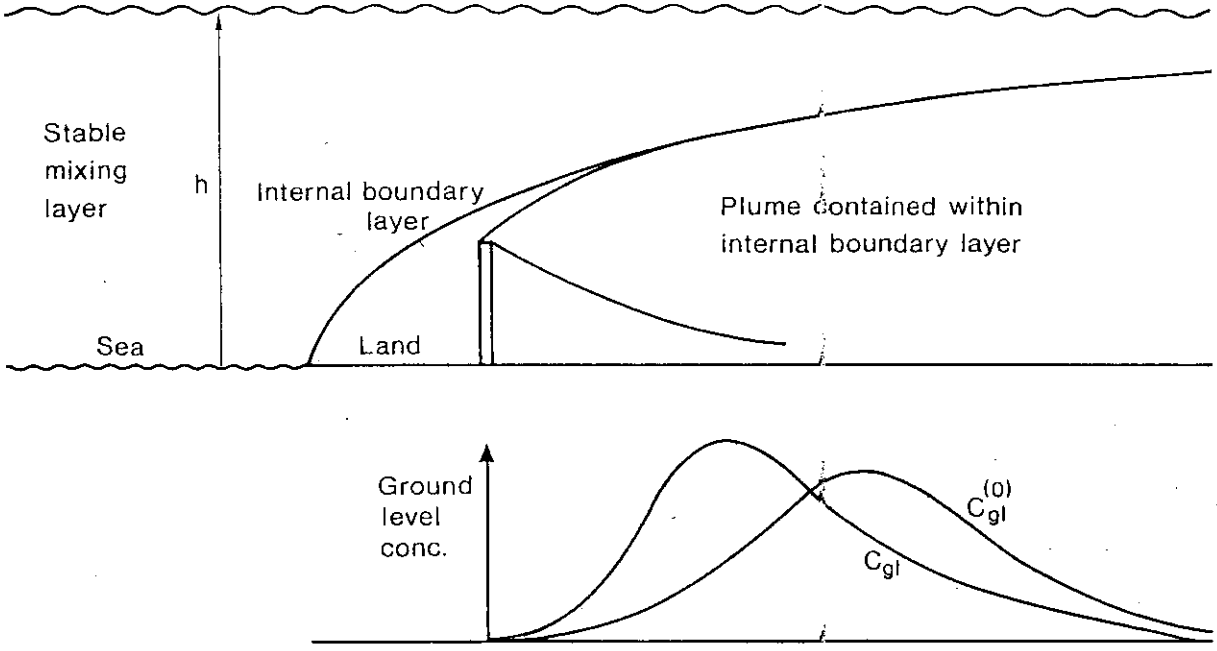

Fig.2.10e Internal boundary layer formed in stable mixing layer as air flow over cool sea passes over warmer land. Upward extent of plume limited by internal boundary layer.

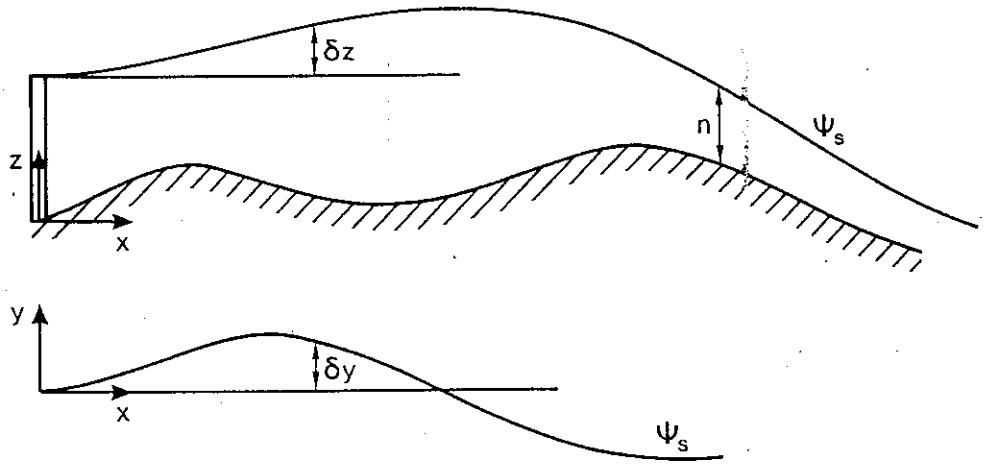

Fig.2.11 Co-ordinate system for source and plume in hilly terrain. ψ_s is the mean streamline through the source.

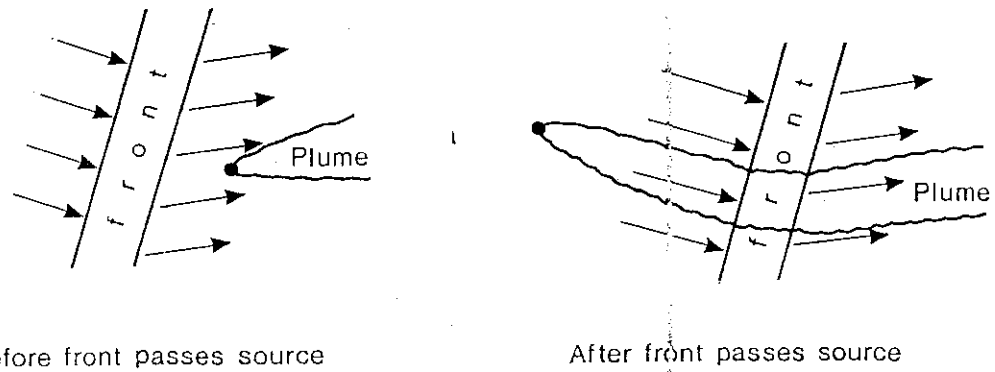

Before front passes source

After front passes source

Fig.2.12 Effect of front on direction of a plume.

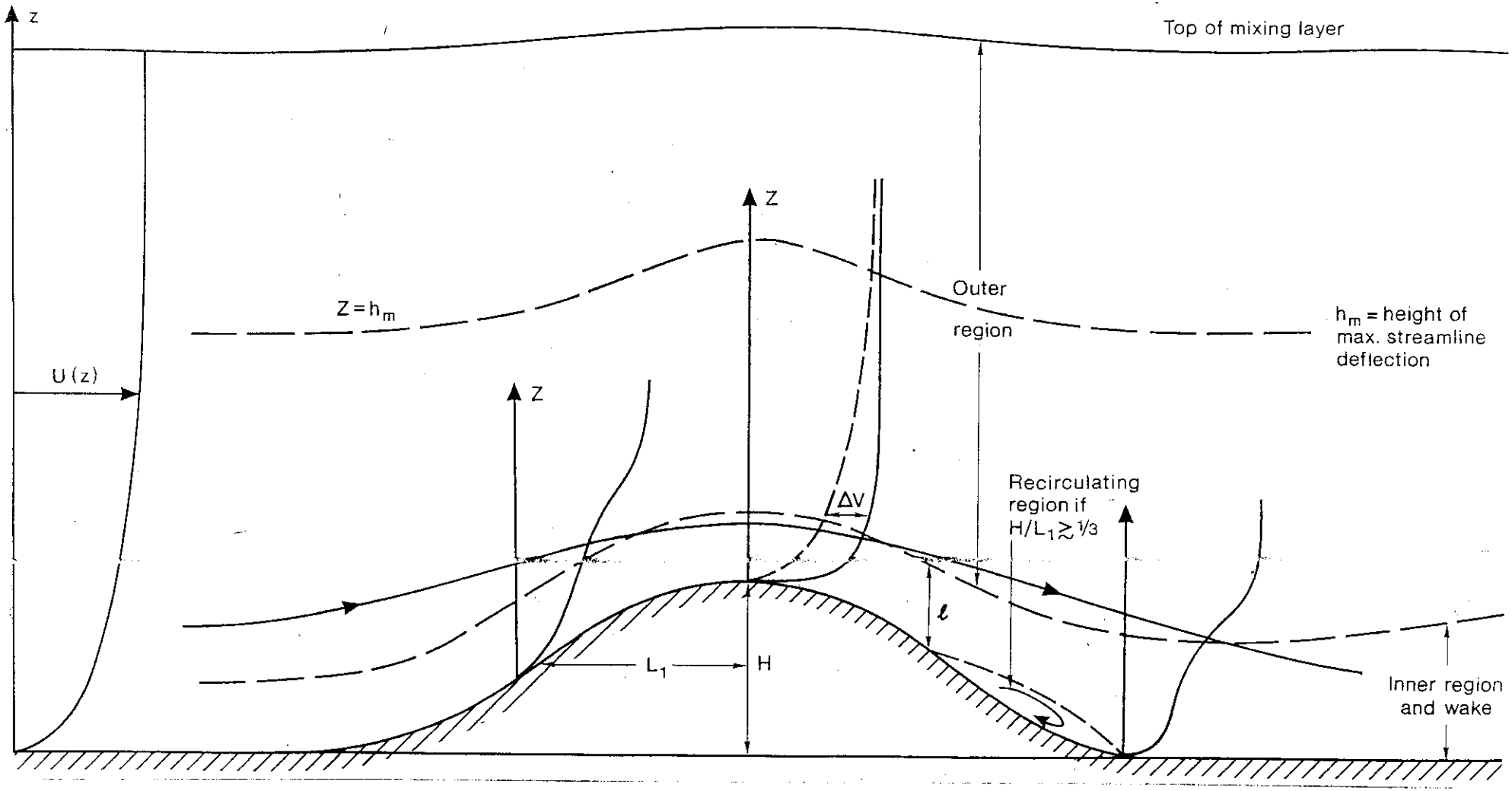

Fig.2.13 Sketch of air flow over a rounded hill showing: sub-division of boundary layer into different regions used in theoretical analysis of flow; typical velocity profiles at various points; principal dimensions and co-ordinates.

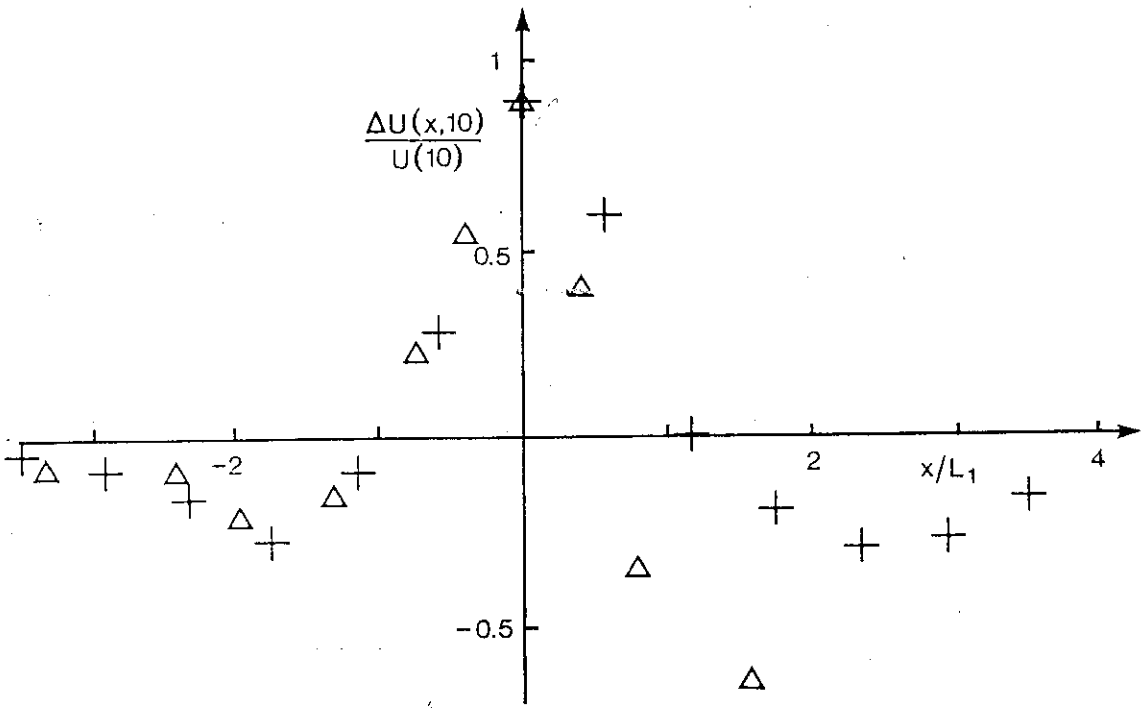

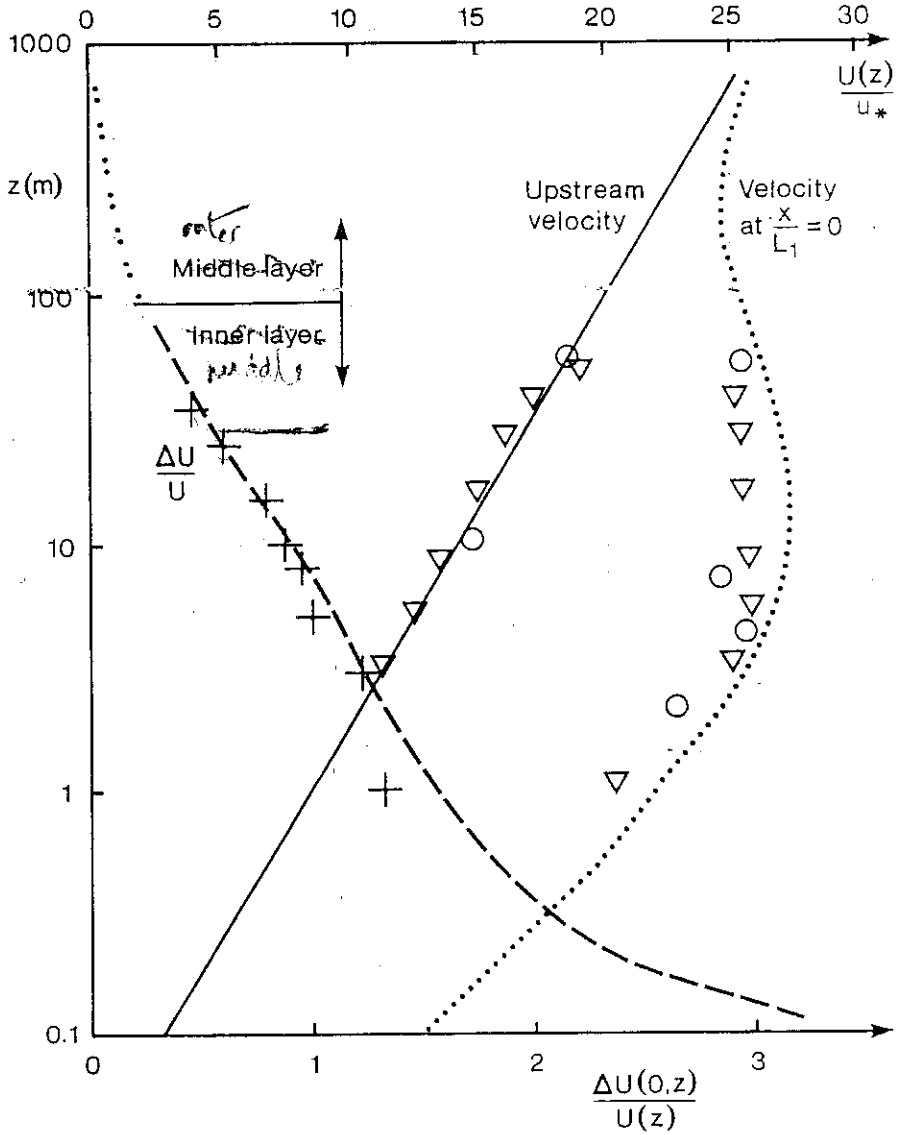

Fig.2.14 Neutral air flow over Askervein Hill. $L_1 = 250$m, $H = 85$m, $z_o = 0.03$m, $U(z)$ = upstream velocity profile. $\Delta U(x,z)$ = difference between velocity profile and $U(z)$ at some height above ground.
(a) Variation of $\Delta U(x,10)/U(10)$: $\triangle$ – data from field measurement (Raithby et al.1987); + – results from FLOWSTAR computations.
(b) Comparison of FLOWSTAR computations (circles) with field measurements (symbols): ∇,$\bigcirc$– velocity profiles recorded at same time (Zeman & Jensen 1987); + – data presented by Raithby et al.(1987).

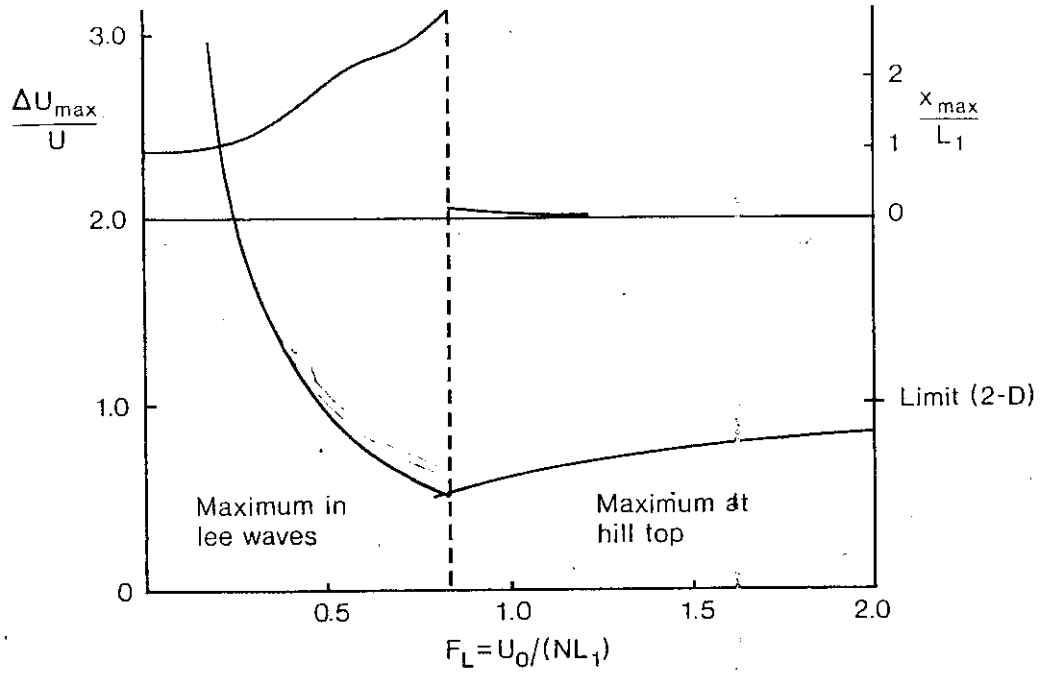

Fig.2.15 Location and magnitude of maximum surface velocity for uniformly stratified flow over a two-dimensional or ridge-like hill (from Hunt, Richards & Brighton 1988).

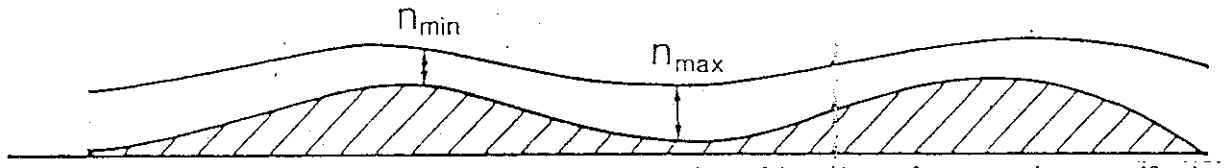

either $F_L >> 1$ (weak stratification) or $F_L < 1$ with strong elevated inversion and no upper-layer stratification

$F_L < 1$ (uniform strong stratification)

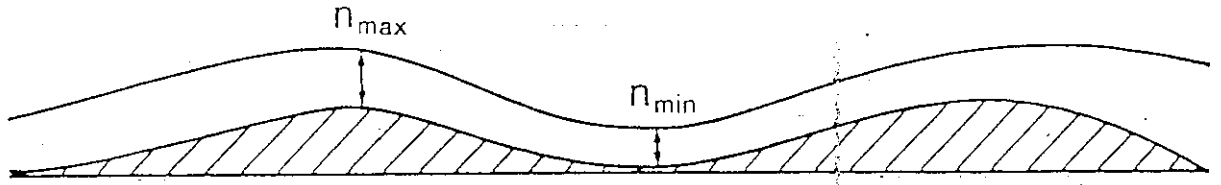

$F_L > 1$ with either an elevated inversion and no upper-layer stratification or decreasing stratification

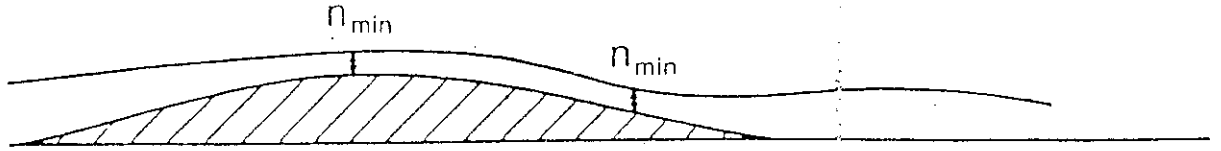

single hill, $F_L \approx 1$ and uniform stratification

Fig.2.16 Effects of type of stratification on mean streamlines over low hills (from Hunt, Richards & Brighton 1988).

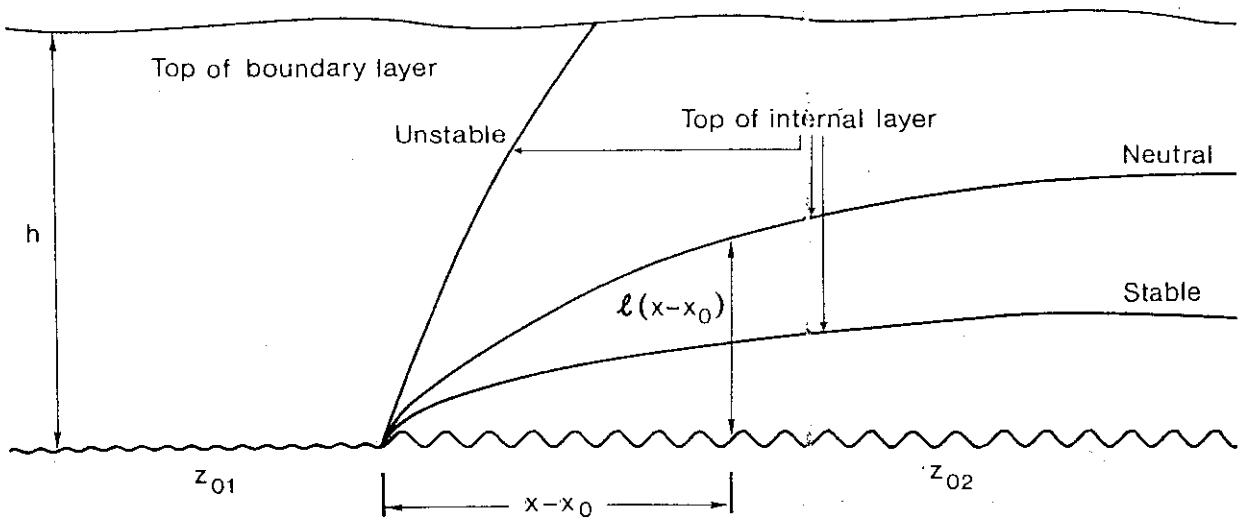

Fig.2.17a Variation of velocity internal layer formed at a change of roughness with stability.

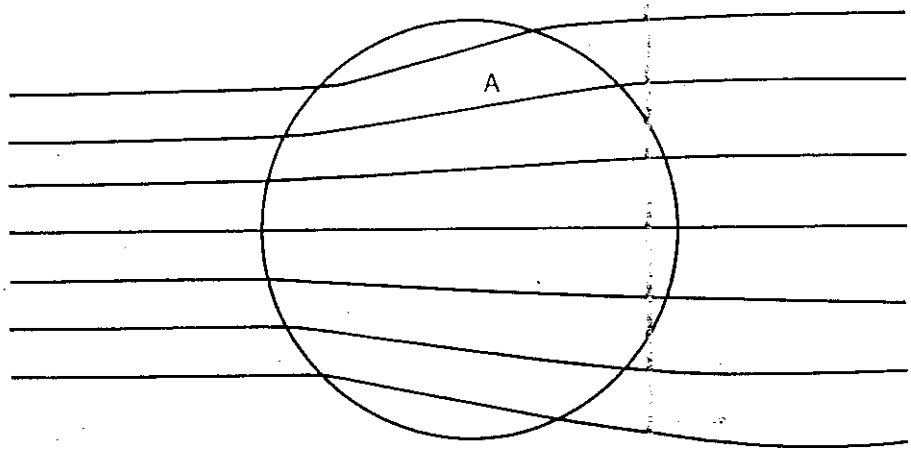

Fig.2.17b Lateral deflection of mean streamlines over circular area A of different roughness.

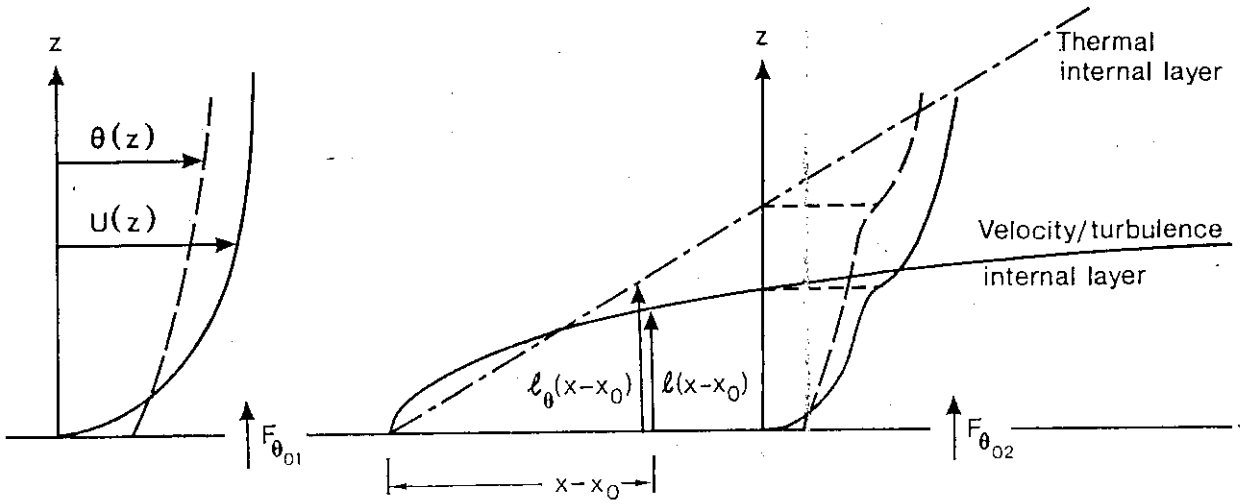

Fig.2.18 Variation of velocity and thermal inner layers formed at a change of surface heat flux.

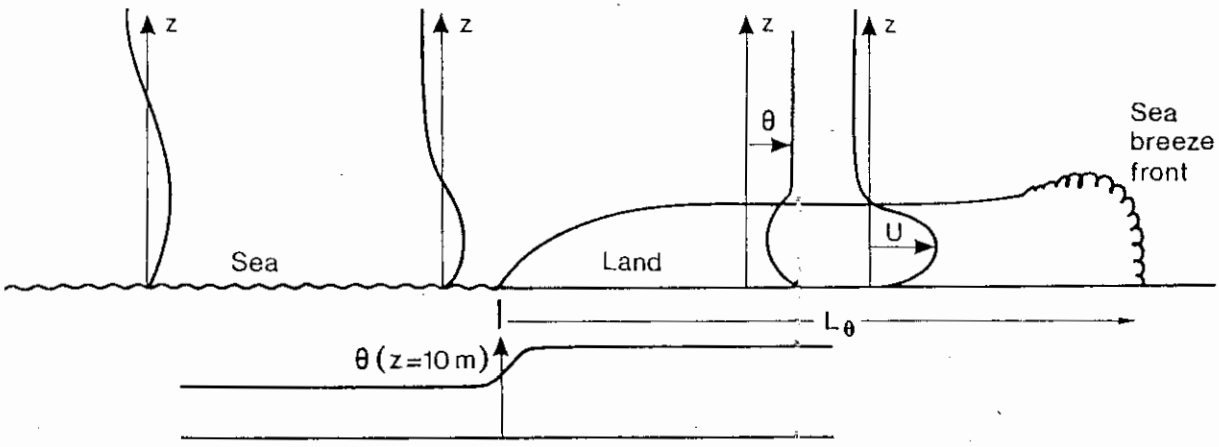

Fig.2.19 Formation of sea breeze (an air flow driven by a temperature difference).

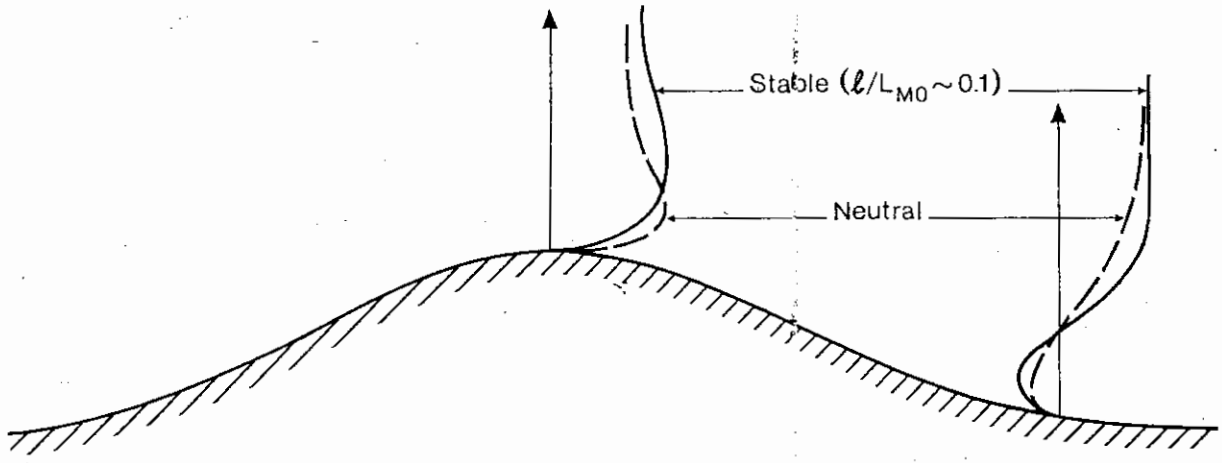

Fig.2.20a Effects of weak buoyancy forces on velocity profiles over a hill.

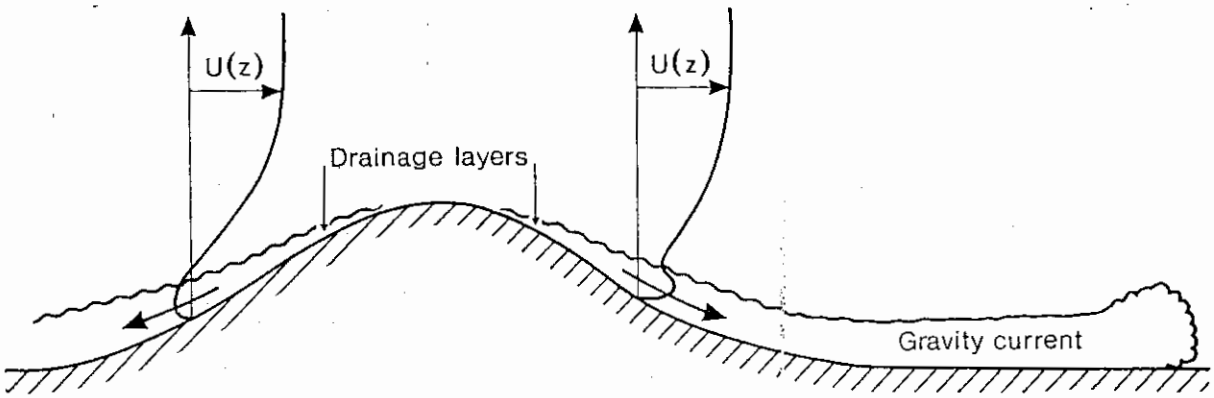

Fig.2.20b Effects of strong buoyancy forces on velocity profiles over a hill. A lee-slope drainage flow continues over level ground and feeds into a gravity front.

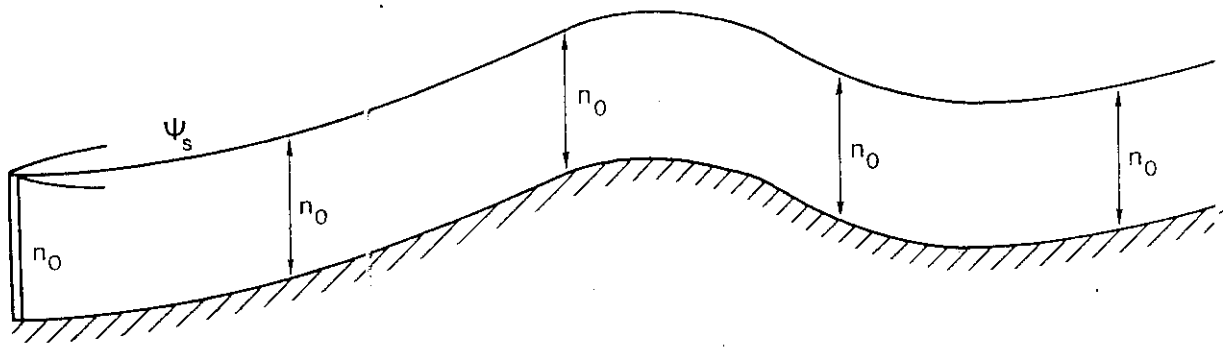

Fig.2.21a Mean streamlines stay at same height above ground if no allowance is made for changes to air flow.

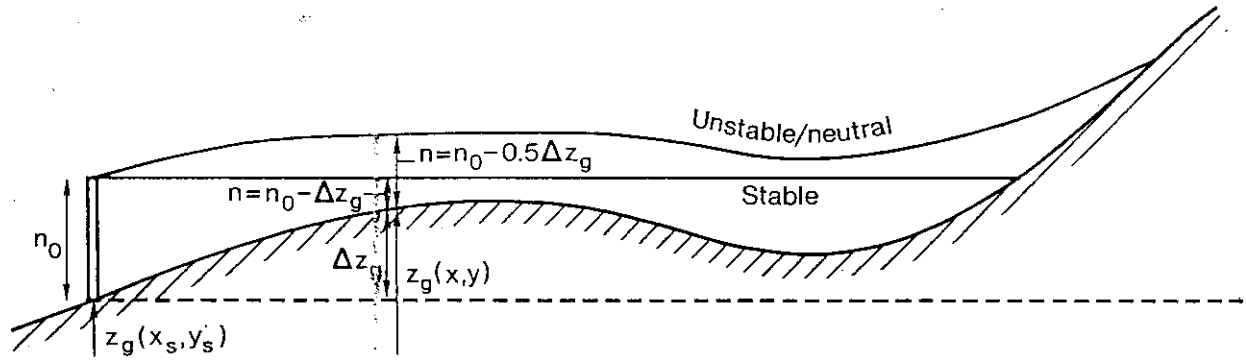

Fig.2.21b Path of mean streamline through source above hilly terrain for unstable/neutral and stable boundary layers after models COMPLEX I AND II. In latter case streamline is horizontal.

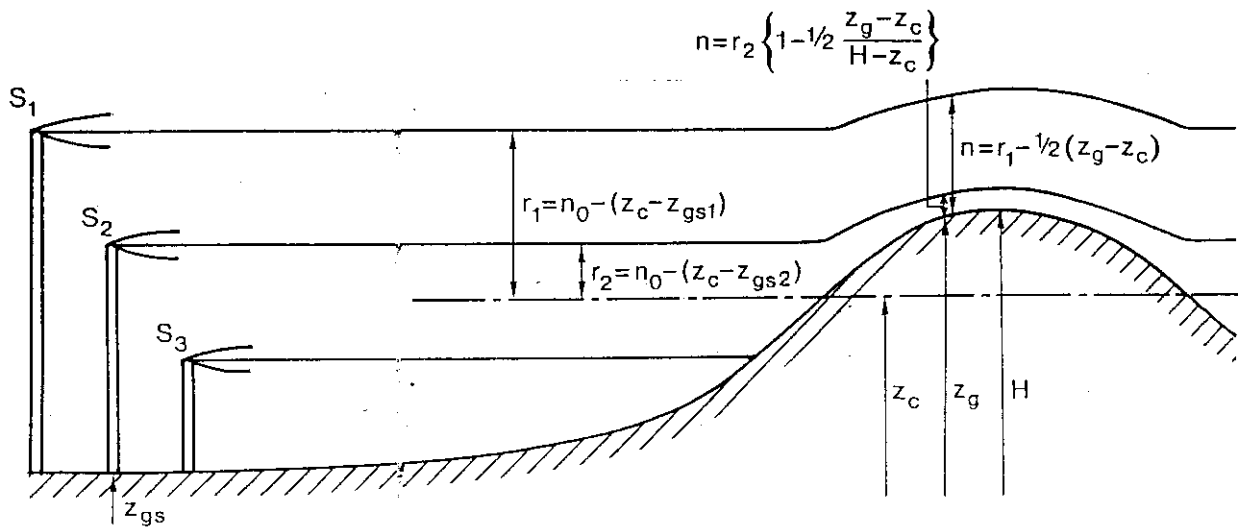

Fig.2.21c Effect of source height on path of mean streamline through source above hilly terrain in stable atmosphere after model RTDM.

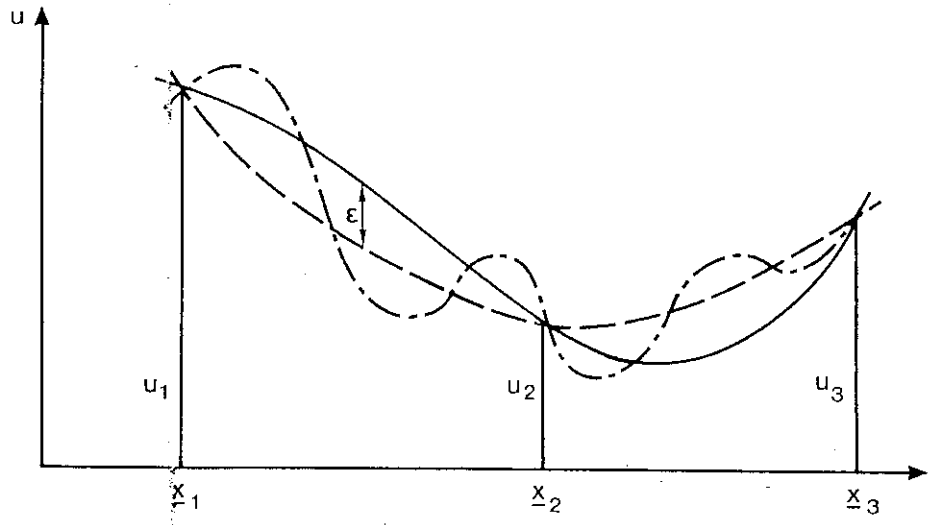

Fig.2.22a Interpolation of wind field between measured values at $\underline{x}_1$, $\underline{x}_2$ and $\underline{x}_3$. ——— constructed mass consistent wind fields u_c, v_c, w_c; - - - - interpolated wind field u_I, v_I, w_I .ϵ error between interpolated and constructd wind fields; - — - — - an unacceptable constructed wind field because ϵ then too large.

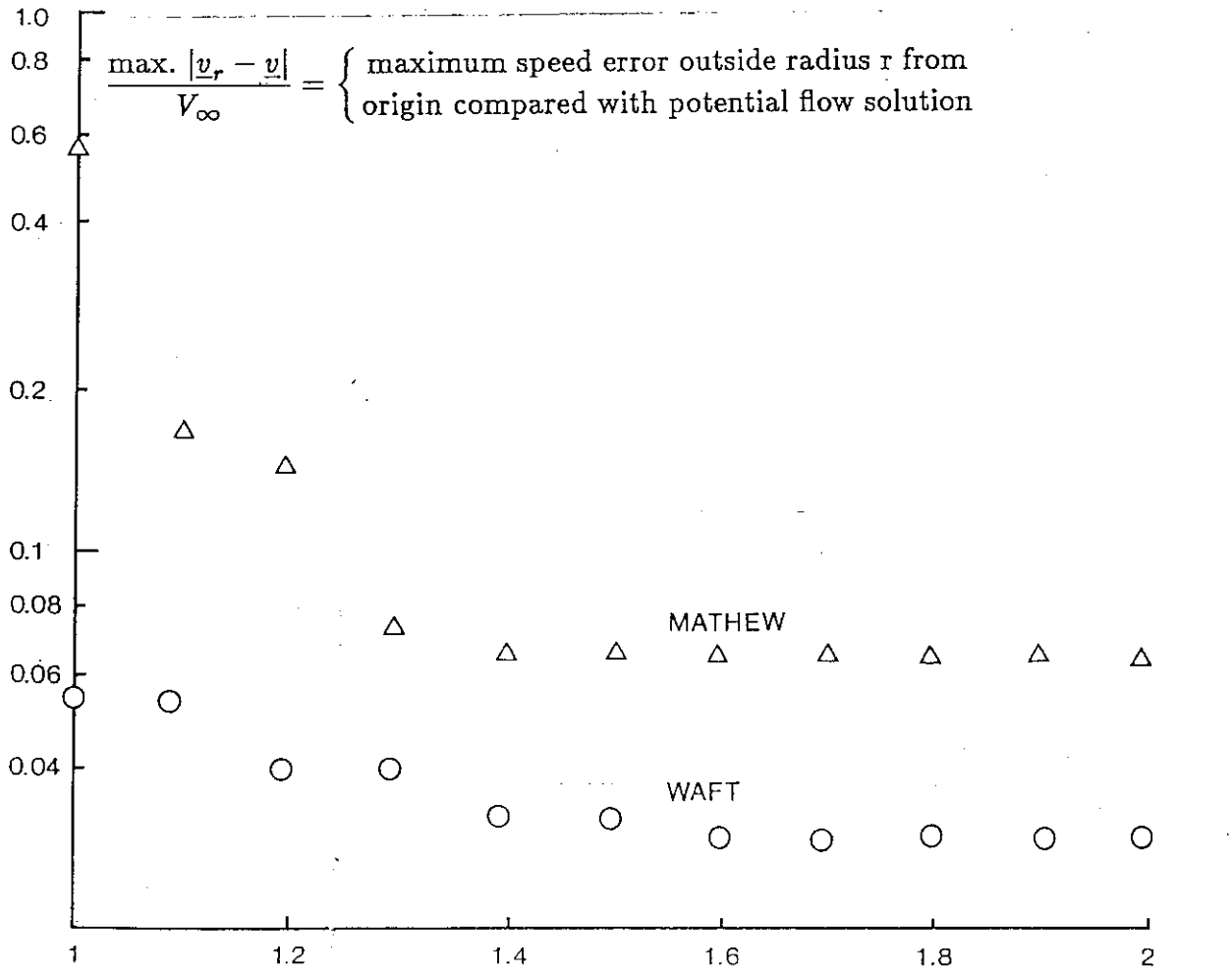

Fig.2.22b Comparison of flow fields over a hemisphere on a plane surface predicted by wind field models WAFT and MATHEW. The results are compared with the corresponding potential flow. V_∞ = magnitude of uniform velocity upstream of hemisphere.

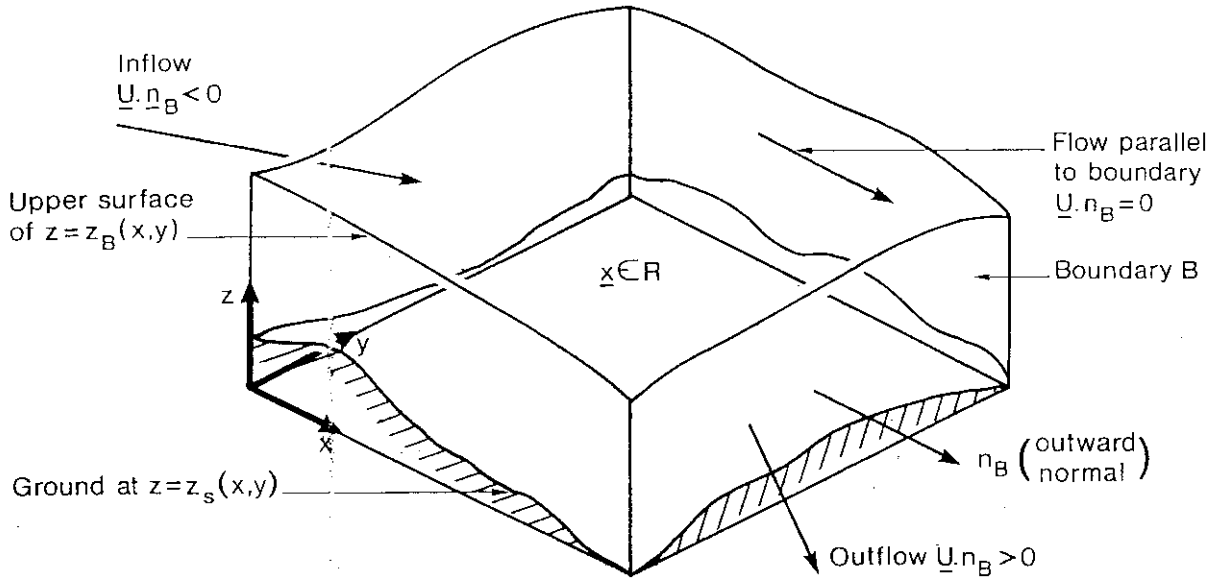

Fig.2.23 Notation used when computing flow in a region R above complex terrain.

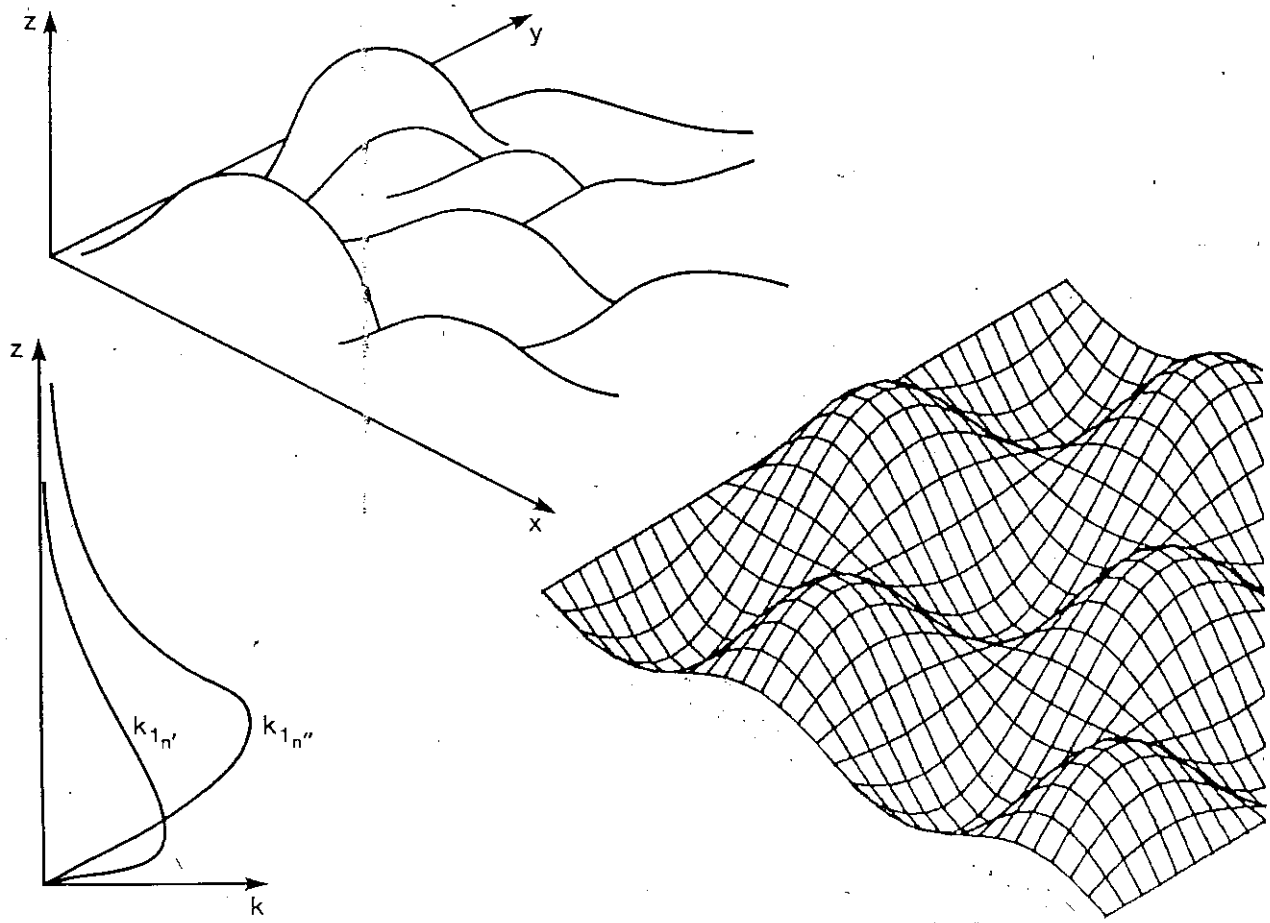

Fig.2.24 Illustration of method of solution by linearised Fourier analysis.
(a) Actual terrain.
(b) One component of Fourier transform of terrain with a single component of a streamline above it.
(c) Typical vertical profile of amplitude of perturbation velocity for different wave numbers.

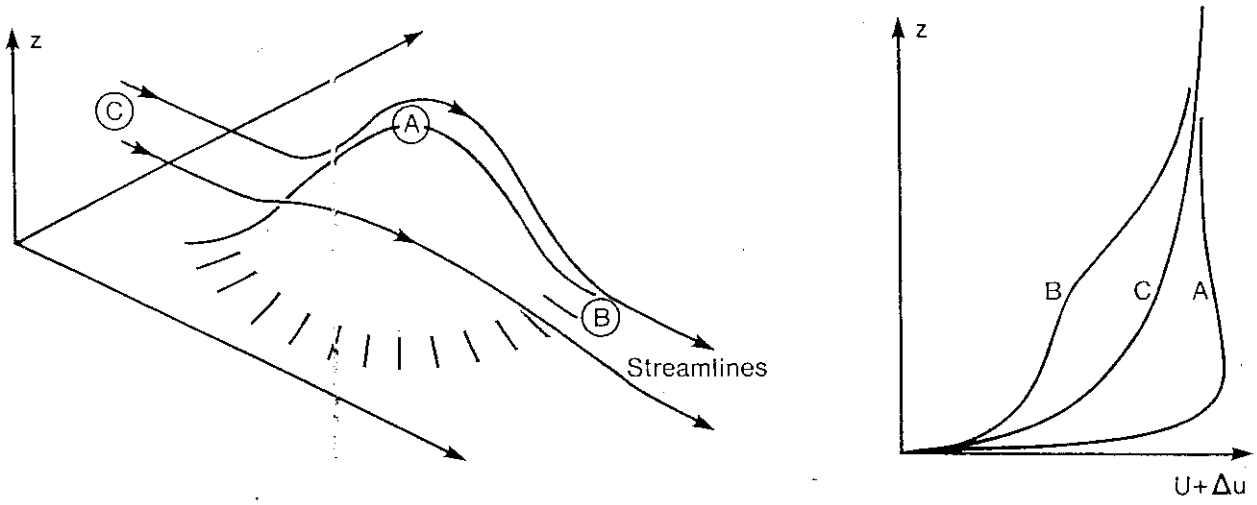

Fig.2.24d Illustration of method of solution by linearised Fourier analysis – typical streamlines and velocity profiles after superposing solutions like those in Fig.2.24b.

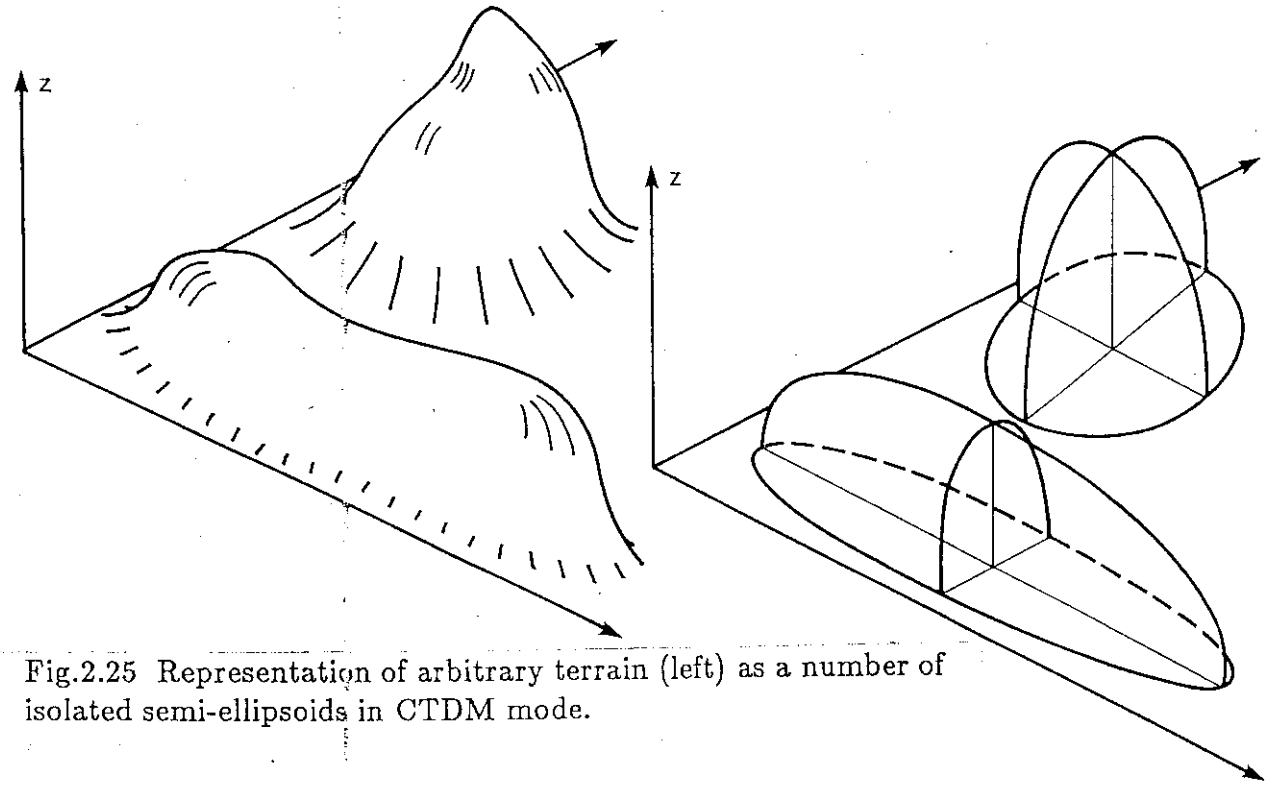

Fig.2.25 Representation of arbitrary terrain (left) as a number of isolated semi-ellipsoids in CTDM mode.

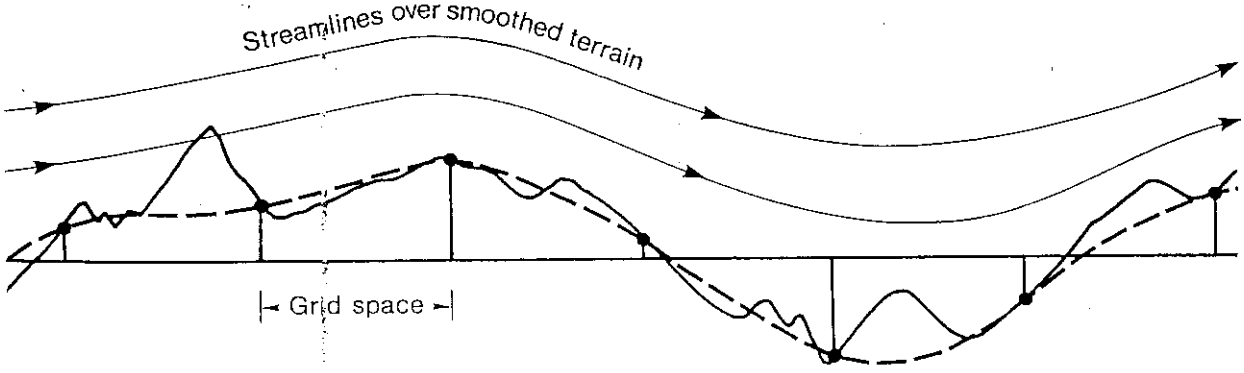

Fig.2.26 Effect of grid size on terrain representation: ——— actual terrain; - - - - terrain as seen by model, effectively a low pass filtered version of the actual terrain.

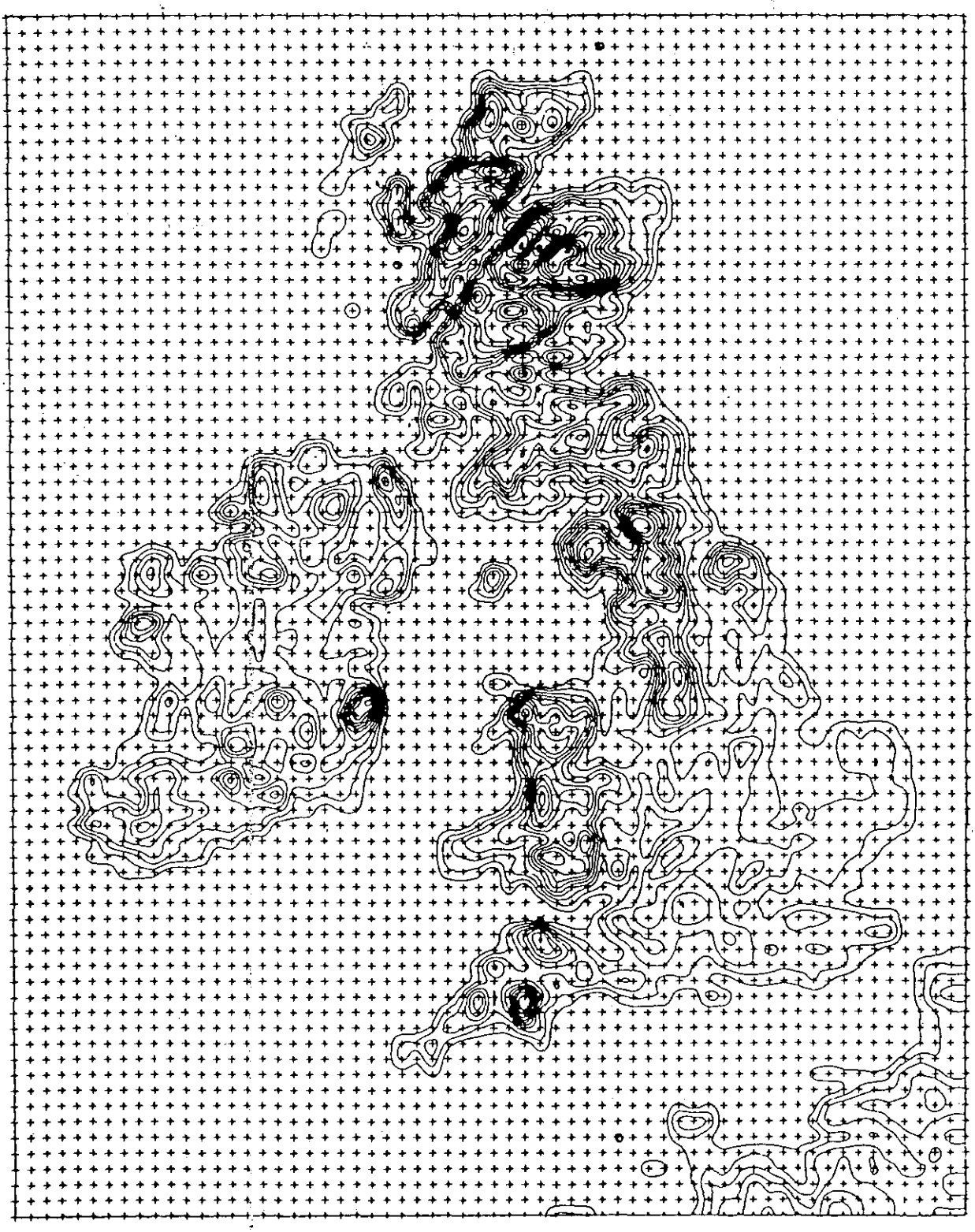

Fig.2.27 Model domain and orography for the Meteorological Office mesoscale model (from Golding 1987). Grid point spacing is 15km. Contours represent 50m steps.

Pasquill Stability Category P	Smith Numbers	% Frequency	Mean wind speed-up (ms^{-1})	Surface heat flux $F_{\theta_o}(Wm^{-2})$	h(km)	Friction velocity u_* ms^{-1}	Convection velocity w_* ms^{-1}	Monin-Obukhov length L_{MO}(m)	$h/\|L_{MO}\|$	σ_v/U_{10} $z = 10m$
A	*0.5*	*0.125*	*0.625*	*250*	*1.3*	*0.11*	2.2	0.4	3330	1.7
A-B	*1.0*	*1.25*	*1.25*-3	*180*-250	*1.08*-1.5	*0.17*-0.41	1.8-2.3	1.44-28	180-474	0.4-0.7
B	*1.5*	*3.8*	*2.0*	*150*	*0.92*	*0.24*	1.66	6.8	136	0.5
B-C	*2.0*	*2.6*	*3.37*-5	*125*-200	0.5-1.0	*0.33*-0.5	1.6-1.9	13-73	13-46	0.2-0.3
C	*2.5*	*15.0*	*4.12*	*90*	*0.84*	*0.38*	1.36	44.7	19	0.26
C-D	3.0	—	5-7	50-150	0.6	0.3-0.5	0.94-1.35	61-500	3-5	0.2-0.3
D	*3.6*	*62.4*	*4.12*	*0*	*0.5*	*0.36*	0	∞	0	0.17
E	*4.5*	*6.7*	*3.4*	-10	*0.4*	0.3	—	200	2	0.17
—	—	—	3.0	-20	*0.1*	0.3	—	100	1	0.19
F-G	*6.0*	*8.4*	*1.2*	—	0.05	0.03	—	0.1	10	0.05

Estimates of h are based on he work of Carson (1973) and Smith & Carson (1977).
A surface roughness $z_o = 0.1$m is assumed when calculating u_*.
The standard deviation of h about the mean is expected to be about 250m for each Pasquill category P (A-D).

Table 2.1 Meteorological parameters as a function of stability class.
(Based on Table A2, R91 with extensions (original parts in Italics).)

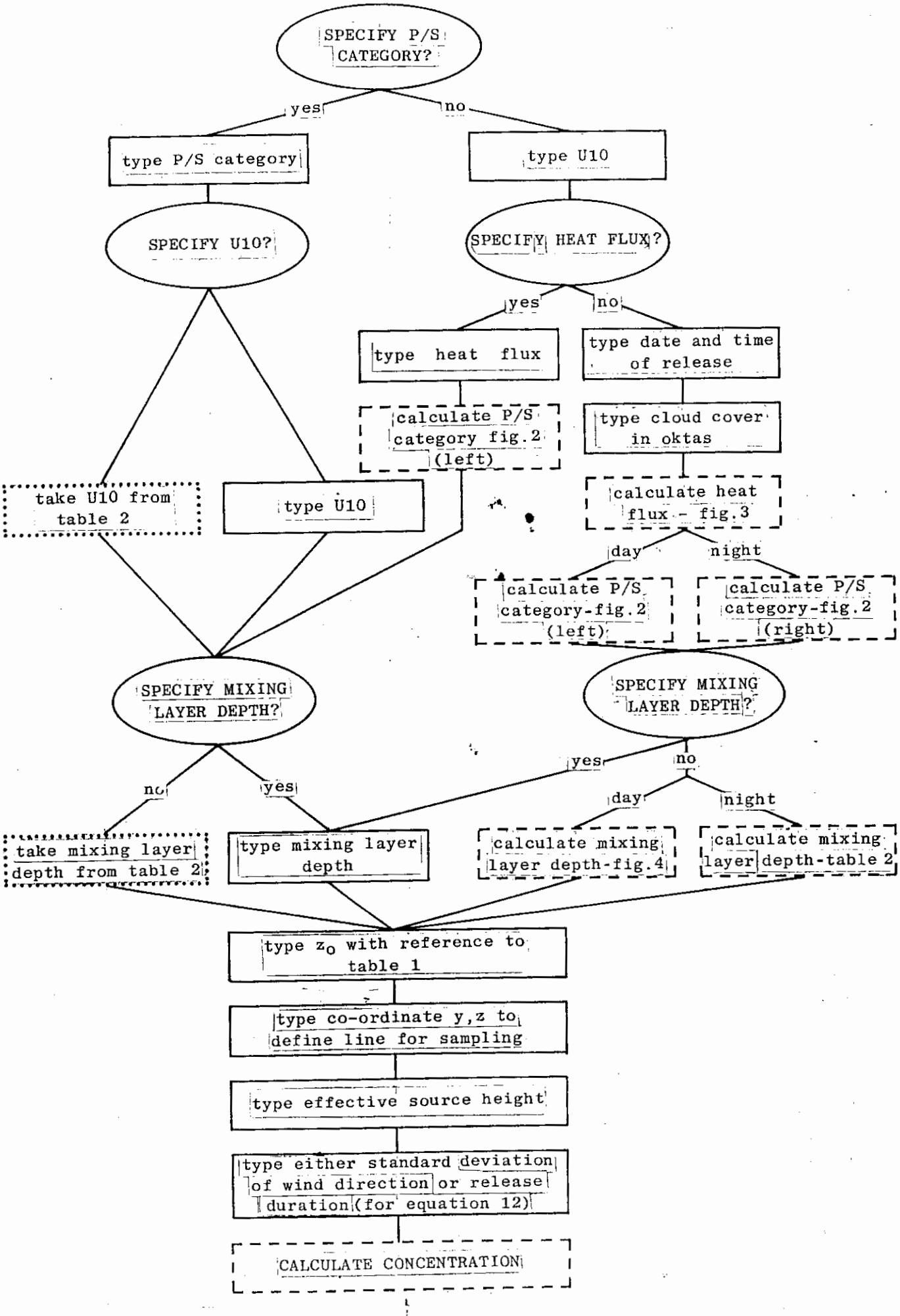

Table 2.2a Flow chart for calculation of concentration by R91 model.

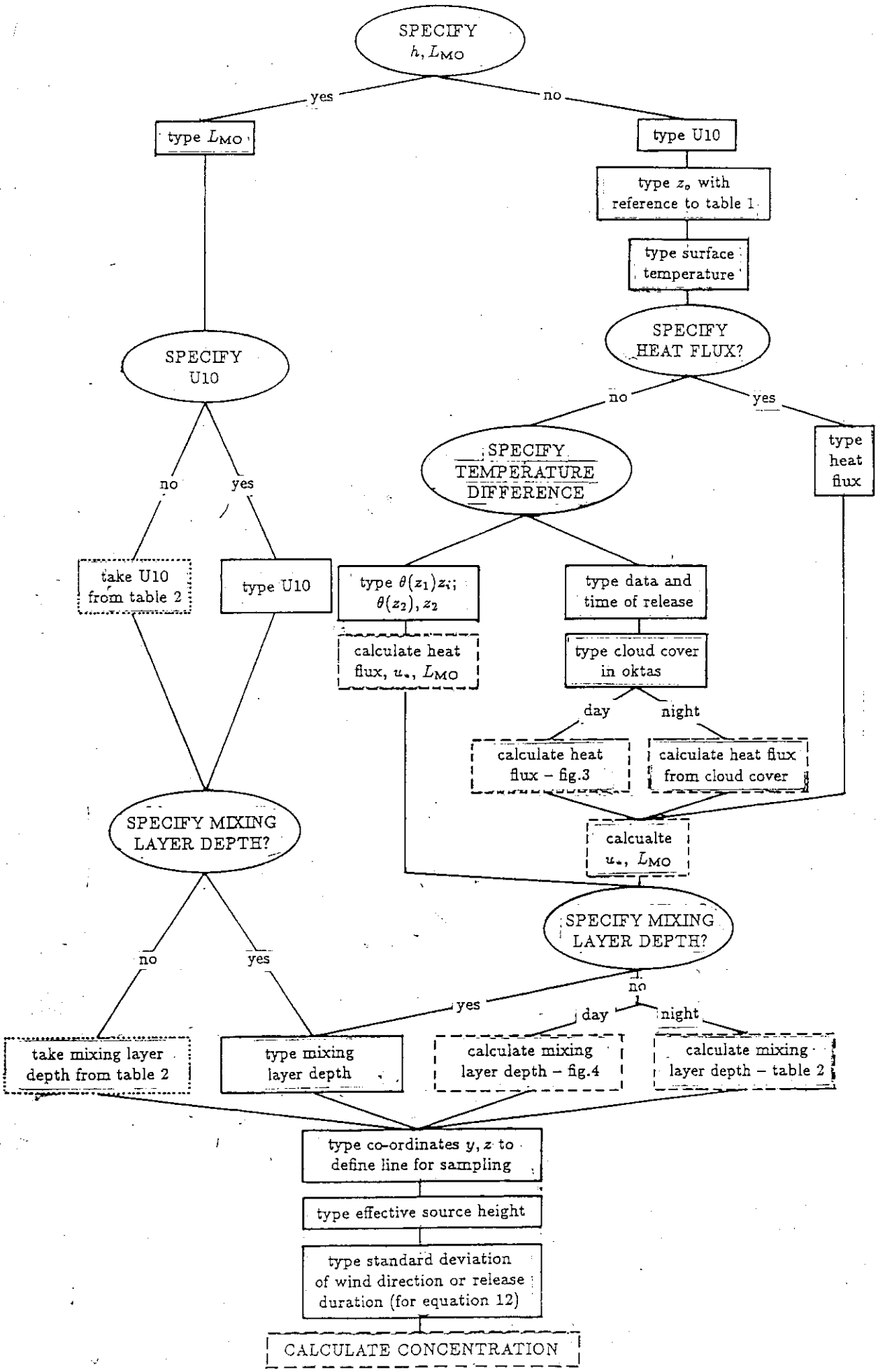

Table 2.2b Flow chart for calculation of concentration by boundary-layer model.

In neutral and unstable conditions

- the gradient of the surrounding terrain should be less than about 1 in 10

- for a ridge upwind of the source
  either $h > 1.5\ H$
  or $x > 20\ H$ in neutral conditions
  $x > 10\ H$ in very unstable conditions

- for an islated hill upwind of the source
  either $h > 1.5\ H$
  or $x > 7\ H$

- for a hill or ridge downwind of the source
  either $h > H + \sigma_z\ (x)$
  or $\sigma_z\ (x) > H$

In stable conditions

- the gradient of the surrounding terrain should be less than about 1 in 100.

- for an obstacle upwind of the source
  either $h > H$
  or $x > 40\ H$ in slightly stable conditions
  $x > 100\ H$ in very stable conditions

- for an obstacle downwind of the source
  either $h > H + \sigma_z\ (x)$
  or $\sigma_z\ (x) > H$

Notes:

The criteria are based on a change of 30% in the wind speed between flat and complex terrain.

The 10 m wind speed must be at least 1 m s^{-1}.

h = the release height.

H = the obstacle height.

x = the distance between obstacle and source.

$\sigma_z\ (x)$ = the vertical plume standard deviation.

Table 2.3 Criteria for neglecting orographic effects (Table 1, R199).

TYPE OF MODEL	Mass consistent/ interpolation		Linearised Fourier		Nonlinear/ "ellipsoids"	Finite difference	
NAME OF MODEL	(a) MATHEW (b) WAFT		(a) MS3DJH (b) FLOWSTAR		CTDM	(a) MET. OFFICE MESOSCALE (b) PIELKE, E.D.F.	
Computer Resources	($<10^7$ bytes storage) ($<10^2$ to converge)		Personal computer or mainframe		Personal computer or mainframe	Large mainframe ($>10^8$ bytes storage) ($>10^3$ to converge)	
INPUTS TO MODELS	(a)	(b)	(a)	(b)		(a)	(b)
1. *Surface Conditions*							
1.1 Elevation changes:							
Horizontal scale km	5	3-5	0.1	0.1	1-5	1-5	2
No. of vertical levels	30	30				16	8
Maximum slope	0.1	0.3	0.25	0.25	arb.	0.1	0.5
Complexity	arb.#	arb.#	arb.	arb.except for strong strat.	idealised isolated hills	arb.#	arb.#
1.2 Roughness changes:	no+	no+			no	arb.	arb.
Max. z_{02}/z_{01}			< 10	< 10			
Horizontal scale km			0.1	0.1			
1.3 Surface temperature/ flux changes:	no	no			no		
ΔF				5*		arb.	arb.
Horizontal scale km				0.1*		15	2
2. *Upwind Conditions:*							
Mean velocity profile	arb.	arb.	log.	arb.	surface layer Monin-Obukhov log.	arb.	arb.
Temperature profile		**		4 types of profile	N = constant	arb.	arb.
3. *Use of Local Data*	yes	yes	no	no	only for turbulence	no	no
OUTPUT FROM MODELS							
1. *Flow Field:*							
Mean flow	yes	yes.	yes	yes	no	yes	yes
Turbulence	no	no	no	yes*	no	yes	yes
Mean temperature	no+	no+	no	yes	no	yes	yes
2. *Conditions Covered*							
2.1 Elevated effects							
Neutral stratification	yes	yes	yes	yes	yes	yes#	yes#
Weak stratification	no	no	no	yes	no	yes#	yes#
Moderate stratification	no+	no+	no	yes	yes	yes#	yes#
Elevated inversion	no	no	no	yes	no	yes#	yes#
Strong stratification	yes	yes	no	yes*	yes	yes#	yes#
2.2 Roughness change	yes+	yes+	yes	yes	no	yes#	yes#
2.3 Temperature effects	yes+	yes+	yes	yes	no	yes#	yes#
Drainage winds	yes+	yes+	no	no ++	no	yes#	yes#
Sea breeze	yes	yes	no	no ++	no	yes#	yes#
3. *Input to dispersion model*	yes	yes	no	yes*	yes	yes	yes

* *to be implements*

\+ provided detailed local data available

** Simple Pasquill category used to F_H for particular hills

++ Other simple models available

\# at filtered scale

Table 2.4 Summary chart of air flow models.

3. ADVANCED DISPERSION MODELS

3.1 Physical effects to be considered

3.1.1 Initial motions of discharged gases and particles

In this section we give a general introduction to the current ideas about how air flow over and around a source begins the process of transporting and then dispersing a pollutant, be it gaseous or particulate, that is discharged into the flow.

When a stream of pollutant is discharged or a volume of pollutant is released it does not immediately travel with the velocity of the air flow, because of its own inertia. Initially there must be a sharp difference between the velocities of the pollutant and air flow, which is confined to a thin cylindrical vortex sheet or layer round the former. The small-scale eddying motions induced by the velocity gradients cause this vortex sheet to thicken as it deforms and set the pollutant into motion in the direction of the air flow (see Fig.3.1). Usually the vortex layer rolls up into vortices, which in a cross flow induce a motion against the flow and upwards as the stream of pollutant is bent over, and initially delay its mixing with the air flow (Rottman et a1.1987; Coelho & Hunt 1989).

Eventually the mixing is completed and the pollutant follows the motions of the air flow even at the smallest scales. (Reaching this final stage of initial mixing is poorly understood.) Then the pollutant may be regarded as an assemblage of "marked particles", whose motion can be analysed entirely in terms of the air flow.

The time and/or distance x_m required for this total mingling and the distribution of the pollutant when it is completed depend on a number of factors: the initial density of the pollutant at its discharge point together with either the height, velocity, direction, and volume flow rate of the discharge if it is continuous, or the height, volume and density of a fixed volume discharge; and finally the nature of the atmospheric air flow around the source; its velocity, turbulence etc. For recent reviews of many of these factors, see Britter & McQuaid (1988) and Briggs (1984).

In general the greater the inertia of the pollutant or the greater the difference in its momentum either at the source or produced by buoyancy forces associated with differences in its density with the surroundings, or the less the environmental turbulence, the longer it takes for mixing to occur. For large plumes from tall chimneys, it may take 1-2km; for weakly buoyant discharges near the ground, the distance may be less than 100m. Some progress in understanding comes from recent laboratory and field study research by Venkatram (1988). The CEGB is currently making use of remote sensing to give detailed cross sections of dispersing plumes. Further progress in this aspect of diffusion is likely soon.

When the mingling is complete, the 'plume' is distributed across an area, A_p, at a distance x_m from the source, (or in a volume V_p for a fixed volume). More precisely, the mean concentration of the pollutant C is significant over A_p or V_p (see §3.2.1). The usual procedure for modelling the subsequent transport, dispersion and advection is to assume that the plume (or cloud volume – we only refer to the case of a plume from a continuous source hereafter) disperses as if the pollutant had been released from a point source some distance upwind at a position x_s and height z_s as shown in Fig.3.2. Depending on whether the pollutant is lighter or heavier than air, this 'effective' source height z_s is above or below the actual source height z_s.

Estimating this effective source position (x_s, y_s, z_s) requires taking into account all the mechanisms affecting the plume's growth. Approximate formulae, such as those reviewed in the R157, are available for a number of cases (e.g. for very buoyant plumes which either impact on or break through elevated inversion layers, for plumes released in wakes of buildings and in very stable conditions) but they are widely acknowledged to be quite inaccurate (see the recent discussion by Venkatram 1988).

3.1.2 Qualitative aspects of the mechanics of dispersion

Consider now an ideal or effective source at $\underline{x}_s$ which discharges Q_m units per second of pollutant into an air flow having mean velocity U such that initially the cross-sectional area of the plume is A_s. Therefore the initial concentration

$$C = Q/(U\ A_s). \tag{3.1}$$

For a laminar air flow only molecular diffusion would occur downstream of the source, and the mean concentration, C, would tend to the form given by

$$C = \frac{Q}{2\pi U \sigma_y \sigma_z} \exp\left\{-\frac{1}{2}\left(\frac{y^2}{\sigma_y^2} + \frac{z^2}{\sigma_z^2}\right)\right\} \tag{3.2}$$

where $\sigma_y^2 = \sigma_z^2 = 2D(x - x_s)/U >> A_s$ and D = coefficient of molecular diffusion. Technically σ_y, σ_z are the lateral and vertical standard deviations of the concentration distribution (whatever its form) and as such are a measure of its spread. For convenience we will refer to them as the "widths" of the distribution or plume.

(i) Turbulent diffusion near the source in the NBL, SBL and CBL

If the external flow is turbulent particles of pollutant from the source are randomly displaced downwind of the source. Close to the source even if the turbulence is quite inhomogeneous, anisotropic or stratified (if the momentum flux of the source is small), the r.m.s. amplitude of these displacements in the horizontal and vertical directions $(\overline{Y^2})^{1/2}, (\overline{Z^2})^{1/2}$ are proportional to the rms of the turbulent velocity fluctuations σ_v, σ_w. This leads to the exact and very well verified result that, after a time of travel t from the source

$$\sqrt{\overline{Y^2}} = \sigma_v t, \quad \sqrt{\overline{Z^2}} = \sigma_w t. \tag{3.3a}$$

If the turbulence is weak compared with the mean velocity at the source, i.e. $\sigma_v, \sigma_w << U(z_s)$, then $t = (x - x_s)/U$ and

$$\sqrt{\overline{Y^2}} = \sigma_v (x - x_s)/U, \quad \sqrt{\overline{Z^2}} = \sigma_w (x - x_s)/U. \tag{3.3b}$$

Since the concentration of the pollutant at a point $\underline{x}$ is proportional to the probability of finding particles from the source at that point, and since the displacements of the source particles are proportional to the turbulent velocity fluctuations, it follows that the mean distribution of the pollutant, or its mean concentration profile $C(y, z)$ at a given value of x, is proportional to the joint probability distribution p_{vw} of the transverse velocity distribution:

$$C(x, y, z) = \frac{Q\ p_{vw}(v, w)}{U} \tag{3.4}$$

where

$$v = U(y - y_s)/(x - x_s), \ w = U(z - z_s)/(x - x_s).$$

In neutral and stable conditions p_{vw} is approximately a joint Gaussian distribution, i.e.

$$p_{vw} = \frac{1}{2\pi\sigma_v\sigma_w} \exp\left\{-\frac{1}{2}\left(\frac{v^2}{\sigma_v^2} + \frac{w^2}{\sigma_w^2}\right)\right\}$$

and so near the source the mean concentration is given by

$$C(x, y, z) = \frac{Q}{2\pi U\sigma_y\sigma_z} \exp\left\{-\frac{1}{2}\left(\frac{y^2}{\sigma_y^2} + \frac{z^2}{\sigma_z^2}\right)\right\} \tag{3.5}$$

where

$$\sigma_y = \sigma_v (x - x_s)/U, \ \sigma_z = \sigma_w\ (x - x_s)/U.$$

If the turbulence is strong relative to the mean velocity, i.e. $\sigma_v, \sigma_w >> U$, then the mean concentration may or may not reach a steady state (see Smith 1988; Hunt 1987a,b).

Thermal convection ($h/L_{MO} < -0.3$) gives rise to turbulence that is significantly non-Gaussian, because there is a high probability of weak down flow and a low probability of strong up flow. Consequently, the mode $\hat{w}$ of $p_w(w)$ is negative, and the height z_{mx} at which there is the maximum concentration (for given x) decreases with x although the height $\bar{z}$ of the spatial mean concentration increases with x (Fig.3.3). Based on recent atmospheric measurements of $\hat{w}$ by Hunt, Kaimal & Gaynor (1988), where it was found that $\hat{w}(z) \simeq 1.5(z/h)^{1/2} w_*$ for $z/h < 0.1$ and $\hat{w}(z) \simeq 0.5 w_*$ for $z/h \gtrsim 0.1$

$$z_{mx} \simeq z_s - 1.5 \frac{w_* x}{U} \left(\frac{z_s}{h}\right)^{1/2}. \tag{3.6}$$

So, for a source 100m above the ground the height of maximum concentration decreases by about 80m over 1/2 km when $w_* = 1\,\mathrm{ms}^{-1}$, $U = 3\mathrm{ms}^{-1}$ and $h \approx$ 1000m. This is a significant departure from the Gaussian profile.

(ii) Diffusion far from the source in unstratified turbulence

Since turbulence consist of many scales of eddies which are weakly correlated with each other, the different parts of the pollutant discharged into the turbulent air flow move in different directions. Also, the direction taken by each part changes with time. In order to calculate the mean concentration, only the random displacements of the individual fluid elements by the turbulence need be considered. (The relative movements of different parts of the stream or cloud of pollutant determine its fluctuations which are not discussed here.)

Because of the random velocity fluctuations of the individual fluid elements, their root-mean-square displacements $\sqrt{\overline{Y^2}}$, $\sqrt{\overline{Z^2}}$ do not continue to increase linearly with time (as in 3.3a). In a homogeneous turbulent flow (such as a wind tunnel) with a particular scale of turbulence L_x, (and a turbulent time scale $T_L \simeq L_x/\sigma_w$) it is found that when the travel time $t > 3T_L$,

$$\sigma_y = \sqrt{\overline{Y^2}} \propto (t\, T_L^{(v)} \sigma_v^2)^{1/2}, \qquad \sigma_z = \sqrt{\overline{Z^2}} \propto (t\, T_L^{(w)} \sigma_w^2)^{1/2} \tag{3.7a}$$

$$\propto (x\, L_x)^{1/2} \sigma_v / U \qquad \propto (x\, L_x)^{1/2} \sigma_w / U. \tag{3.7b}$$

Equation (3.7a) shows that σ_y, σ_z increase with $t^{1/2}$, and therefore at a slower rate than that given in (3.3a). The transition between these two limits depends on the spectrum of the atmospheric turbulence.

In the ideal limit defined by (3.7) the distribution of mean concentration is equivalent to that calculated by assuming turbulence has a diffusivity

$$K \propto \sigma_w L_x. \tag{3.8}$$

It is now recognised that this limit is seldom found in the atmosphere for three main causes.

(a) Unsteadiness of the plumes and large-scale unsteadiness of the flow

The expressions in (3.7) and (3.8) describe how the mean widths σ_y, σ_z of a plume vary with distance or travel time from the source when the concentration is averaged over a time greater than that of the largest turbulent eddies in a boundary layer ($h/\sigma_w \sim 10^3$secs). On the other hand,they say nothing about the mean widths $\hat{\sigma}_y, \hat{\sigma}_z$ at a particular moment in time. Near the source, say at $x < UT_L$, where the plume has a thin meandering form $\hat{\sigma}_y, \hat{\sigma}_z << \sigma_y, \sigma_z$ but further downstream $\hat{\sigma}_y, \hat{\sigma}_z$ and σ_y, σ_z are comparable.

At any instant the concentration profile within a plume is highly irregular and this contributes significantly to the variance of concentration but this is not treated here (Stapountzis et al. 1986; Mylne 1988).

The idealised flow of a turbulent boundary layer in a statistical steady state seldom corresponds to the actual state of the atmospheric boundary layer. Therefore lateral spreading of a plume does not follow the form (3.3), (3.7) primarily because of large mesoscale eddies, fronts and synoptic-scale variations. It is necessary to use either actual measurements of the variation of the wind direction over periods (T) longer than, say, 20 minutes, or some local climatological estimate. On the basis of Moore's work (summarsied by Moore & Lee 1982), it is recommended in R91 that σ_y^2 is calculated from the contribution by the turbulence $\sigma_{y_{(\text{turb})}}$ and by the long-term fluctuations $\sigma^2_{y(T)}$, i.e.

$$\sigma_y^2 = \sigma^2_{y(\text{turb})} + \sigma^2_{y(T)} \qquad (3.9a)$$

where

$$\sigma^2_{y(T)} = A\, x^2 t/U_{10} \qquad (3.9b)$$

with $A \simeq 0.04$ for the U.K, t in hours

A review of a more detailed approach than (3.9) based on a statistical analysis of the wind in a particular location is given by Hanna (1986), from whose paper Fig.3.4 is taken.

(b) Effects of inhomogeneity in the boundary layer

As was explained in §2.1, the turbulence in the boundary layer varies in inten-

sity and scale across it. In neutral and convective layers the eddy scales are of the same order at a height z above the surface. Thus if a pocket of gas is dispersed downwards from an elevated source it is mixed into small-scale eddies with a low diffusivity, but if it is dispersed upwards it is diffused further by large eddies. This inhomogeneous dispersion affects the growth of $\overline{Z^2}$ in a way not described by (3.7a); it can lead to

$$\sqrt{\overline{Z^2}} \propto t \,. \tag{3.10a}$$

Also the mean height

$$\bar{Z} = \int_{-\infty}^{\infty} \int_{o}^{h} zC dx\, dz \Big/ \int_{-\infty}^{\infty} \int_{o}^{h} C dy\, dz \tag{3.10b}$$

of a plume begins to increase according to

$$\frac{d\bar{Z}}{dt} \propto \frac{d}{dz}(\sigma_w L_x(w)) \tag{3.10c}$$

with downwind distance from an elevated source once the particles have had a time T_L to diffuse from the source (Fig.3.3). (Typically in the neutral boundary layer this is about 1/2km for a 100m high source.)

It is because the vertical eddy scale reduces to zero at the surface that the vertical diffusion flux F_{z_c} at the surface is effectively zero unless there is a chemical/physical deposition process. For molecular diffusion at an impermeable surface $F_{z_c} = \partial C/\partial z = 0$ but with inhomogeneous turbulence it is possible to have $F_{z_c} = 0$ but $\partial C/\partial z \neq 0$ because of the variable scale of eddies at the surface (it is assumed that $\partial C/\partial z$ is defined on a length scale of the order of 1m, not 1mm.)

Vertical diffusion is also prevented by an elevated inversion layer at the top of the boundary layer where both the turbulence scale and the diffusivity K_z decrease to zero. At this level $F_z = 0$, but $\partial C/\partial z \neq 0$ (Brost & Wyngaard 1978).

(c) Effects of wind shear

In the NBL and SBL there is a significant vertical variation of the mean horizontal velocity components U and V, i.e. $\partial U/\partial z \neq 0$, $\partial V/\partial z \neq 0$. The effect of $\partial U/\partial z$ on the distribution of mean concentration is illustrated in Fig.3.5 in terms of the expansion of a sequence of puffs emitted from the source. As they diffuse vertically into the layers of faster and slower moving fluid, they are bent over; in the faster stream their ends are separated, but in the slower stream they hardly move apart. Therefore at a given value of x, the concentration below the source is greater than above it and so the position of maximum concentration z_{mx} in and

the mean height of the plume both decrease. Hunt (1982a) shows that, to a good approximation, the decrease of $z_{\rm mx}$ is given by

$$z_{\rm mx} \approx z_s - \frac{\sigma_z^2}{2U(z_s)} \frac{\partial U}{\partial z} \,. \tag{3.11}$$

The transverse wind shear, $\partial V/\partial z$, moves pockets of gas that diffuse upwards in a direction parallel to V and those downwards in the opposite direction. Thus the cross section of the plume acquires the shape of an elipse whose principal axes are neither vertical nor horizontal. σ_y is effectively increased with the increase depending on both $\partial V/\partial z$ and σ_z. A simple estimate of σ_y due to turbulence and shear-induced dispersion after a time T is

$$\sigma_y^2 \approx \sigma_{y_{\rm turb}} + \frac{1}{6}\,\sigma_w^2 \left(\frac{\partial V}{\partial z}\right)^2 T^3 T_L^{(w)} \tag{3.12}$$

(Pasquill & Smith 1983; Weil 1985).

(iii) Molecular diffusion and surface concentration

The most important feature of dispersion by turbulence is that it is many orders of magnitude more effective than molecular diffusion. Consequently the molecular nature of a pollutant is not important in estimating its dispersion by turbulence except near a boundary when the turbulent velocity fluctuations are very small. Therefore, it is important to know whether molecular processes are significant and whether they have to be calculated in order to estimate concentrations and deposition at or on a surface.

Recent theoretical and experimental research at Cambridge reviewed by Hunt (1985) suggests that turbulent eddies transport the gas to very close to a surface, and, as they do so, they take a long time to slow down. During this period weak molecular processes can act and they have enough time to transport the matter (or heat) to the surface. For an impermeable surface the surface concentration is then dependent on molecular processes but approximately independent of the value of the molecular diffusivity of the gas or the mobility of particulate matter. For an absorbing surface this is not the case.

This concept is implied by many models, such as that of Misra (1982), Ley & Thompson (1983) for diffusion in which trajectories are computed from the source to the surface, without considering details of transfer processes at the surface.

(iv) Diffusion in stably stratified turbulent flows

In stably stratified boundary layers the scales of turbulent motion are much smaller than the boundary-layer depth (§2.1.6). Consequently diffusion is largely a local process and in that sense it is simpler than in neutral and unstable boundary layers. However, the effect of the density gradient on the neutral motions of fluid elements significantly changes the vertical diffusion of gases or particles introduced into the flow.

In turbulent flow with neutral and unstable density (or temperature) gradients there is no limit to how far fluid elements can move (as implied by (3.3), (3.7)). However, in a stably stratified boundary layer with a positive temperature gradient and a buoyancy frequency N which is typically 0.01 – 0.04 s^{-1}, the fluid elements experience a restoring force $\frac{1}{2}\rho Z^2 N^2$ when displaced vertically a distance Z. Consequently in very stable flows a fluid element with a kinetic energy $\frac{1}{2}\rho\sigma_w^2$, can only move a vertical distance of order $\sqrt{\bar{Z}^2}$ determined by

$$\frac{1}{2}\rho\bar{Z}^2N^2 \sim \frac{1}{2}\rho\sigma_w^2 \quad \text{or} \quad \bar{Z}^2 \sim \sigma_w^2/N^2 \,. \tag{3.13}$$

The question for estimating theoretical diffusion of a 'marked particle' is how much mixing between fluid elements occurs to enable fluid elements to change their density and escape from this limitation (Fig.3.6a). If the mixing is weak it means that the vertical spread of plumes, σ_z, reaches a nearly constant value given by (3.13). This is quite different to the expression for growing plumes in (3.7) (Csanady 1964; Pearson, Puttock & Hunt 1983; Hunt 1982a).

Recent research indicates strongly that this mixing can be quite intense in the surface shear layer but that it is weaker in the upper two-thirds of the SBL. Furthermore, it is quite variable and not well defined by overall boundary-layer variables (Weil 1985). Despite this uncertainty, the research has led to a better estimate for the typical range of values of σ_z to be expected in different conditions and at different heights in the boundary layer.

A formula for σ_z^2 that describes most existing laboratory field data for elevated sources when $t \gtrsim N^{-1}$ is

$$\sigma_z^2 = \left(\sigma_w^2/N^2\right)\,\left(\varsigma^2 + 2t\,\tau_m N^2\right) \tag{3.14}$$

where $\varsigma \simeq 1.0 \pm 0.5$ for most kinds of spectra. The value of τ_m depends on the mixing process and the presence of the ground and can be estimated as

$$\tau_m \sim \gamma^2/N, \tag{3.15}$$

where the parameter γ varies typically from 0.3 when $z/h << 1$ to about 0.1 when $z/h \gtrsim 0.5$ (see Fig.3.6b). Some researchers, for example Venkatram et al.(1984), take

a fixed value of γ of about 0.3 although our Fig.3.6c shows it is by no means clear that their data supports this value; which is also used in the CTDM model. On the other hand Hunt (1982a) has pointed out that there is significant variation in γ with height and recent large-eddy simulations by Derbyshire (1988) carried out at the Meteorological Office support this observation.

Equation (3.14) can be used for σ_z for different source heights by using the formulae for σ_w and N given in §2.1.7.

(v) Dispersion in complex wind fields

The variations in the level of maximum surface concentration $C_{g\ell\ \mathrm{mx}}$ caused by variations in the stability of the boundary layer over level terrain are typically not more than a factor of three. However the increases in $C_{g\ell\ \mathrm{mx}}$ over the surface of hills or buildings can be a factor of 30, and if the source is downwind of a large hill or structure $C_{g\ell\ \mathrm{mx}}$ may be increased by a factor of at least 10. As pointed out in §2.2.1 complex surface conditions also change the position of the maximum ground-level concentration and the distribution in space of the dispersed matter. There is now a broad understanding of what causes these large amplifications and when they occur (see reviews by Egan 1984; Snyder 1985; Hunt 1985a; A. Hunt & Castro 1984).

The first of these amplifications occurs where localised sources are upwind of hills (Fig.2.9a). There are three mechanisms that can make the surface concentration on a hill different to that on a plane:

* the mean streamlines approach the surface – which increases $C_{g\ell}$;
* the mean streamlines diverge or converge in a direction normal to the surface – which increases or decreases $C_{g\ell}$;
* the velocity on the mean streamline Q_s decreases.

All these mechanisms act in different directions on $C_{g\ell}$ in different flows;

* sources upwind of two-dimensional hills in neutral conditions – the maximum increases in $C_{g\ell\mathrm{mx}}$ are small and on the upwind slope – all the effects are positive.
* sources upwind of three-dimensional hills – the maximum concentrations may occur upwind or near the summit of hills, and the increases are generally greater; in the latter case the velocity is greater but the first effect of reducing n is even greater;
* stable flows – the maximum concentrations can occur upwind, on the top, or

on the downwind slopes of hills.

Theory, model experiments and field experiments all show that in the most extreme case the maximum surface concentration $C_{g\ell\ \mathrm{mx}}$ is about equal to the mean concentration at the centre of the plume both in the absence of the hill and at the same distance from the source $C_{CL}^{(o)}(x_H - x_s)$ (Snyder & Hunt 1984). This result is most easily understood by considering strong stably stratified flows ($F_H < 1$) when the flow below the critical height is approximately horizontal and the vertical diffusion is very weak (so $\sigma_z \simeq$ constant). Since the flux Q of the pollutant is constant the centreline concentration C_{CL} can be compared with its value without the hill from the continuity relationship

$$Q = 2\pi\sigma_z\sigma_y U C_{CL} = 2\pi\sigma_z^{(o)}\sigma_y^{(o)}U^{(o)}C_{CL}^{(o)}\ , \tag{3.16}$$

where the superscript $^{(o)}$ denotes the value over a flat surface. It is found that $\sigma_z \simeq \sigma_z^{(o)}$ in the approximately horizontal two-dimensional flow approaching the hill. As the horizontal streamlines diverge, U decreases, and it follows that σ_y increases proportionately. Therefore $\sigma_y U$ is approximately constant (in fact, $\sigma_y U$ is slightly less than $\sigma_y^{(o)}U^{(o)}$) and so

$$C_{CL} \simeq C_{C_L}^{(o)}.$$

(Note that there is no 'reflection' effect at a stagnation point to increase the concentration by a factor of two; this only occurs when the flow is parallel to a surface.)

The general features of the simple experiments on impinging plumes performed so far have been predicted by simple theory using the diffusion equation. Useful estimates have been obtained but detailed quantitative results have still not been adequately modelled. When plumes just touch the hill surface only the 'tail' of the vertical concentration profile is affected, so that quite small changes in turbulence near the hill surface have a large effect. When there is direct impingement of the plume the effects of low-level turbulence are of less importance.

When the sources are downwind of hills, the dispersion process can be classified according to whether the source is situated inside or outside the recirculating wake region W_R indicated in Fig.3.7.

If the source is located in the central part of W_R, the pollutant is dispersed vertically by the strong turbulence and carried around the region W_R by the mean flow. The important finding of recent research is that there are significant variations of concentration within this region. In other words, the turbulence and recirculating flow are never strong enough in practice to make the concentration uniform.

Over the upper boundary of W_R the pollutant is diffusing outwards, with the largest efflux near R_S. Therefore downwind of W_R a reasonable approximation to the concentration distribution is obtained by considering an effective point source

near the ground some distance upwind of the hill or building causing the recirculation as shown in Fig.3.7a. However, the position of this effective point source must be varied to achieve the best estimate for the concentration distribution downwind of the hill at a selected point (Hunt 1982b).

For low-level sources placed in the back flow (such as source S_o in Fig.3.7a), a reasonable approximation for the calculation for the maximum ground-level concentration is to assume that the source is in a boundary-layer flow in the reverse direction. There are, however, more sophisticated methods (reviewed in §3.6).

When a source is located in the upper part of W_R near to the mean attachment line (e.g. source S_1 in Fig.3.7b), the plume then tends to reach the ground by being carried directly downwards by the mean flow towards the rear stagnation point R_S at the downwind end of the region W_R. This is analogous to the plume being transported onto a hill side and correspondingly leads to high concentration at h_s – in fact $C_{g\ell\ \mathrm{mx}} \simeq C_{CL}^{(o)}$, where $C_{CL}^{(o)}$ is estimated on the basis of a plume in a uniform flow dispersing over a distance equal to that from the source point to the point R_S, and with a high turbulence level (typically 0.25 $U(H)$) (Turfus 1988; Castro & Snyder 1982).

If the source is outside the recirculating region, the dispersion is affected by:

* the downwash of the mean streamline in the wake of the hill;
* the change in mean shear $\partial U/\partial z$;
* the increase in turbulence in the wake;
* the special effect of the plume being entrained into the recirculating region W_R (if the mean streamline ψ_s is close enough to the boundary B_R of that region).

There is no entrainment from a high-level source such as S_2 in Fig.3.7b into W_R and the first three effects lead to an increase in $C_{g\ell\ \mathrm{mx}}$ and to a decrease in the distance to the maximum (i.e. A increases and A_x decreases). For example, for a 200m high source located 1km downwind of a 100m high hill, the increase in $C_{g\ell\ \mathrm{mx}}$ is equivalent to a reduction in $C_{g\ell\ \mathrm{mx}}$ of about 40m. while A_x is reduced by about 60%.

Figure 3.7c shows a plume from a lower-level source. Part of it is is entrained in, and consequently is usually well mixed throughout, the wake. Downwind of the recirculating region the plume has a double structure; one plume is a depleted plume of strength $Q(1-\alpha)$ from an elevated source (S_1) whose height is lower than the original source $(0 < \alpha < 1)$; the second plume of strength αQ is effectively the plume from a low-level source (S_2) upwind of the recirculating region. This 'second' plume is well mixed laterally across the width of the wake of a typical building or three-dimensional hill. If the hill is two-dimensional with height H, this plume has a width of the order of 2-3H. This model, originally suggested by Puttock (1978),

has been developed and validated against many wind-tunnel studies by Apsley et al.(1989).

(iv) Summarising the effects of complex terrain

A useful way to indicate how hills can significantly affect the ground-level concentrations is by defining a window of possible source locations in relation to a given hill. This concept, introduced by Hunt, Puttock & Snyder (1979), has been used extensively by Snyder (e.g. Thompson & Snyder 1985) to map out the effects of different kinds of hills and source locations in wind-tunnel and water-flume tests (Fig.3.8).

3.1.3 Diffusion factors

The discussion in the previous section has shown how, for different source heights in different atmospheric conditions, and in different kinds of complex terrain, the diffusion is controlled by a number of extra processes. It is also clear that in these various cases the extra processes are similar but their relative importance is different. For comparing models of dispersion, it is useful to quantify these extra processes and express them as 'factors' multiplying the natural diffusion processes in uniform homogeneous flow. Following Hunt (1985a), we will call these parameters "diffusion factors" and express them in the terms of

* $U(x,y,z)$ – the mean velocity of the wind which may vary in three principal directions in space;
* σ_w – the vertical turbulence velocity (technically the r.m.s. value of the vertical velocity fluctuations = $\overline{w^2}$);
* σ_z – the vertical width of the plume (technically the r.m.s. of the vertical displacement of pollutant with respect to the centre line of the plume);
* K_z – the vertical eddy diffusivity of the pollutant;
* $\overline{w^3}$ – the third moment of the vertical velocity fluctuations.

The diffusion factors are denoted by Δ with a subscript appropriate to the processes represented.

(i) **Diffusion to surfaces**

$$\Delta_n = \frac{\sigma_z}{n} = \frac{vertical\ plume\ width}{distance\ of\ the\ mean\ streamline\ above\ surface} \qquad (3.17i)$$

for plumes travelling parallel to the surface.

(ii) **Convergence/divergence of mean streamlines**

$$\Delta_{CD} = \frac{1}{U}\frac{\partial U}{\partial x} \Big/ \frac{1}{\sigma_z}\frac{\partial \sigma_z}{\partial x}$$

$$= \frac{the\ rate\ of\ mean\ streamline\ convergence/divergence}{plume\ growth\ by\ turbulence\ alone} \qquad (3.17ii)$$

important for plumes impacting onto hills or onto near stagnation region downwind of hills/buildings (R_S);

(iii) **Wind shear**

$$\Delta_{WS} = \frac{\sigma_z^2}{U}\frac{\partial U}{\partial z} \Big/ \sigma_z = \frac{\sigma_z}{U}\frac{\partial U}{\partial z}$$

$$= \frac{vertical\ deflection\ of\ plume\ by\ vertical\ wind\ shear}{plume\ width} \qquad (3.17iii)$$

with deflection being towards the lower velocity – important in stable boundary layer and in wakes.

(iv) **Turbulence inhomogeneity factors**

$$\Delta_{T2} = \frac{\sigma_z}{\sigma_w}\frac{\partial \sigma_w}{\partial z}$$

$$= \frac{mean\ drift\ of\ plume\ due\ to\ gradients\ in\ variance\ near\ source}{growth\ of\ plume} \qquad (3.17iv)$$

$$\Delta_{TS} = \frac{(\overline{w^3})^{1/3}}{\sigma_w} = \frac{departure\ of\ plume\ from\ Gaussian}{typical\ width\ of\ Gaussian\ profile} \qquad (3.17v)$$

$$\Delta_{T3} = \frac{\sigma_z}{\sigma_w^3}\frac{\partial \overline{w^3}}{\partial z} = \frac{\text{asymmetric plume growth due to non-Gaussian turbulence}}{symmetric\ growth\ rate} \qquad (3.17vi)$$

$$\Delta_K = \frac{\sigma_z}{K_z}\frac{\partial K_z}{\partial z} = \frac{variations\ of\ diffusivity\ across\ plume}{average\ diffusivity\ across\ plume} \qquad (3.17vii)$$

$$= \frac{mean\ drift\ of\ plume\ due\ to\ gradients\ in\ diffusivity\ far\ downstream}{growth\ of\ plume\ width}$$

Δ_{T2}, Δ_{T3}, Δ_{TS} and Δ_K are particularly significant in the convective boundary layer and in wakes. Note that Δ_K involves variation of the length scale as well as turbulence across a plume.

The factors have been expressed in such a way that when $\Delta << 1$ the effects are insignificant and when $\Delta \sim 1$ they are important. In general, the factors vary along the plume; for example, $\Delta_n << 1$ near the source but becomes significant downwind.

There are other factors which affect the concentration distribution from sources, such as

* variation of mean velocity along streamlines;
* deflection of streamlines;
* variable density gradients;
* reversing flows.

These effects are important if they affect the diffusion factors already listed.

The actual values of σ_w, σ_z, K_z, etc. used in (3.17) depend on the turbulent flows in each case, and in particular on the buoyancy effects.

3.2 Gaussian plume models

3.2.1 The basis of Gaussian plume models

Consider a turbulent flow in which the mean velocity U is uniform and the turbulence is homogeneous and has Gaussian statistics. If a source emits a pollutant at a steady rate Q into the flow at (x_s, y_s, z_s), then beyond a certain distance downwind defined by $(x - x_s) >> \sigma_z$, the mean concentration profile is described by

$$C(x,y,z) = \frac{Q}{2\pi U \sigma_y \sigma_z} \exp\left(-\frac{(y-y_s)^2}{\sigma_y^2}\right) G_z(x,z) \qquad (3.18a)$$

where for homogeneous turbulence

$$G_z = \exp\left(-(z-z_s)^2/2\sigma_z^2\right), \qquad (3.18b)$$

and

$$\left\{\begin{matrix}\sigma_y^2 \\ \sigma_z^2\end{matrix}\right\} = \int\int_{A_p} \left\{\begin{matrix}(y-y_s)^2 \\ (z-z_s)^2\end{matrix}\right\} C \, dy \, dz \Big/ \int\int_{A_p} C \, dy \, dz, \qquad (3.18c)$$

with the integral being taken over the plume cross section, A_p.

For this model it is immaterial whether σ_y, σ_z are obtained theoretically or experimentally.

The conditions for this model can be relaxed a little because it only requires that the assumptions to be valid *over the cross section of the plume*. Therefore, in quantitative terms, the diffusion factors defined by (3.17(i)-(viii) must be small.

The Gaussian plume model (G.P.M.) is also used in a modified form when the turbulence is confined by one or two plane boundaries. In fact, such boundaries change the structure of the turbulent eddies and therefore the form of the concentration profile. However, if the main purpose of a formula for $C(x,y,z)$ is that it should have approximately the correct first and second moments, and that the flux of source matter should be conserved, then the effect of one plane boundary at $z = z_b$ can be modelled as equivalent to adding another Gaussian plume into the flow with a source at the image point relative to z_s, i.e. at

$$z_i = z_b + (z_b - z_s) \tag{3.19a}$$

Then G_z in (3.18b) becomes

$$G_z = \exp\left\{-\frac{(z-z_s)^2}{2\sigma_z^2}\right\} + \exp\left\{\frac{(z-z_i)^2}{2\sigma_z^2}\right\}. \tag{3.19b}$$

If there are boundaries at $z_b = 0$ and $z_b = h$, then the vertical profile function G_z can be constructed as the sum of sources at image points

$$-z_s, \pm(2h \pm z_s), \pm(4h \pm z_s) \tag{3.19c}$$

the latter points in the series being images of images. However, sufficient accuracy can be obtained with only the first five image sources. Their layout is sketched in Fig.3.9.

These formulae for G_z are valid theoretically only if both $U(z)$ and $K_z(x,z)$ are constant with height, but these are never good approximations for the atmosphere. Another implication of these image formulae is that at $z = 0$ and $z = h$ $\partial C/\partial z = 0$. As we shall see, this is not a good approximation either!

For the G.P.M.s described in R91 the functions $\sigma_y(x)$, $\sigma_z(x)$ for the plume width and depth are taken to be independent of the source height z_s. For each stability category different functions for $\sigma_y(x)$, $\sigma_z(x)$ are defined. In other forms of G.P.M.s, some of which are reviewed later, $\sigma_y(x)$ and $\sigma_z(x)$ have different values for different source heights, and are dependent on the meteorological conditions in a way that differs from the simple 'stability category' approach of R91.

One of the difficulties and uncertainties of G.P.M.s is how the plume depth $\sigma_z(x)$ in (3.18b), (3.19b) should be calculated from actual concentration profiles $C_a(x,y,z)$ at different downwind positions. Near the source, when the plume has reached neither the ground nor the inversion at the top of the boundary layer,

$$\sigma_z^2 = \int_o^h \int_{-\infty}^{\infty} (z-z_s)^2 C_a dz\, dy \Big/ \int_o^h \int_{-\infty}^{\infty} C_a dz\, dy, \tag{3.20}$$

but further downwind when this is not the case and the effects of the image sources are significant in the Gaussian plume models, then (3.20) cannot be used to calculate σ_z from the actual concentration. Different procedures have been adopted; for example, by iteration, calculating the model value of σ_z such that the second moment of the G.P.M. is equal to the second moment of the actual concentration defined in (3.20). It is important to realise that the value of σ_z derived by this procedure is not the second moment of the particle displacement, but is an artificially constructed variable specifically for use in G.P.M.s with reflection!

The value for the wind speed U in the formula (3.18) is sometimes taken as the wind speed at the source height z_s, or, as in R91, taken as U at a reference height ($z_{\rm ref}$) independent of source height.

3.2.2 Review of Gaussian Plume Models in neutral boundary layers over flat terrain

(i) Limitations of current Gaussian plume models

For elevated sources in the neutral boundary layer the mean concentration profiles are Gaussian for a certain distance downwind of the source, say about $(x - x_s) \lesssim z_s U(z_s)/3\sigma_w$ or typically 1km for a 100m high source. Beyond that distance the effects of inhomogeneity of turbulence scale (or K_z) and, to a lesser extent, wind shear, affect the plume – leading to an increase in the mean plume height $\bar{Z} = \int_o^h \int_{-\infty}^{\infty} zC\,dy\,dz \Big/ \int_o^h \int_{-\infty}^{\infty} C\,dy\,dz$) and a slight decrease in the height $z_{\rm mx}$ of the height of the maximum concentration (i.e. the factors $\Delta_K \sim 1$ and $\Delta_{WS} \sim 0.1$).

At this stage the downward diffusion of the plume material leads to a rapid increase of the ground-level concentration $C_{g\ell\ {\rm mx}}$. Because the boundary is impermeable, this material later diffuses upward again – the reflection or image effect. In fact, the pollutant comes downwards in large pockets or 'sweeps' and then, by small-scale motion, diffuses up again, which is not at all the same as large-scale upward movement from an image source below the ground!

Since C varies with z in these descending pockets of pollutant (analogous to plumes impinging onto a hill), there is a finite mean gradient of C at the surface ($\partial C/\partial z > 0$) (Fackrell & Robins 1982). This is the stage at which $C_{g\ell\ {\rm mx}}$ reaches a maximum (i.e. when $C_{g\ell\ {\rm mx}} = C_{g\ell\ {\rm mx}}$, $\partial C/\partial z > 0$ at $z = 0$). Consequently, the precise value of $C_{g\ell\ {\rm mx}}$ must depend on the turbulent processes near the surface.

Further downwind, the build up of pollutant at the surface has continued so that the maximum concentration at a given value of x is on the surface. The form of the profile is now determined by variations in turbulence scale (or K_z); the

wind shear $\partial U/\partial z$ also has an effect (i.e. $\Delta_K \sim 1$ but $\Delta_{WS} \sim u_*/U(\sigma_z) << 1$). Sufficiently far downwind of the source, when $(x - x_s) \gtrsim 3z_s U(z_s)/\sigma_w$, the plume from an elevated source is similar to that from a ground-level source. Theory and wind-tunnel models show that the vertical concentration profile $G_z(s)$ has the form

$$\exp(-A(z/\sigma_z)^s)$$

where s is typically 1.5, and slowly decreases with distance downwind, in theory to a value of 1.0 (Pasquill 1974, p.350; Pasquill & Smith 1983, Chap.3).

The value of plume depth as a function of distance $\sigma_z(x)$ is not a sensitive function of source height z_s. When the source height is within the surface layer (i.e. for $z_s \lesssim h/5$ ~100m) the vertical turbulence, σ_w is within 20% of its surface value, and the mean wind profile is logarithmic. In fact, as a function of mean travel time t from the source, for a ground-level source, $\sigma_z(t)$ is about half the value of an elevated source; but since the matter from the elevated source travels faster, the values of σ_z at a given distance downwind are typically within 30% of each other (Hunt 1982a).

When the source height is above the surface layer ($z_s \geq h/5 \sim$ 100m), the vertical turbulence at the source height and the initial plume growth are progressively reduced. The scale of vertical turbulence does not increase with height and so $\sigma_z(x, z_s)$ decreases with z_s for all values of x.

The initial plume width $\sigma_y(x) = \sigma_v x/U$ in the boundary layer. In the surface layer, where σ_v is approximately constant with height, but $U(z)$ varies, the product $U(z_s)\sigma_y(x, z_s)$ in the denominator of the G.P.M. (3.2), (3.5) is approximately constant with height and equal to the value at a reference height $z_{\rm ref}$ which in R91 is taken as 10m. Therefore

$$U(z_s)\sigma_y(x, z_s) = U(z_{\rm ref})\sigma_y(x, z_{\rm ref}) \ . \qquad (3.21)$$

Above the surface layer σ_v decreases, but the turbulence length scale increases slowly. Near the source σ_y decreases with source height, but over longer distances σ_y is not very sensitive to source height, especially when the contribution by long-term variability (3.9b) is added to the turbulence component.

To summarise, the reflected Gaussian forms of the mean concentration profile from elevated or surface sources do not agree with the measurements. Therefore the concentration at a height of, say, $2\sigma_z$ below or above the plume centre line could differ by a factor of three between an assumed Gaussian plume profile and the actual profile. However, for an elevated source the maximum ground-level concentration is usually within a factor of two of that predicted by a G.P.M. because as Scriven (1969) showed theoretically $C_{g\ell\ {\rm mx}}$ is not very sensitive to either the variation of σ_y, σ_z or the form of the profile. (This is also implied the formulae derived by Sutton (1947) $C_{g\ell\ {\rm mx}} = 2Q/\ \pi e\ U(z_s)(\sigma_y/\sigma_z)h^2)$.) On the other hand, the location of the

ground-level maximum is sensitive to the variation of the plume width and height $\sigma_y(x)$, $\sigma_z(x)$, but less sensitive to the form of the profile.

The variation of σ_y, σ_z used in G.P.M. is less sensitive to source height than for stable or unstable boundary layers.

(ii) Possible revised Gaussian plume model formulae to account for some height dependent diffusion

Having outlined the defects of the current formulae based on Gaussian plume profiles and values of σ_y, σ_z for surface sources, we give some possible formulae that account for some of these defects (based, in part, on Briggs, 1985). There is still more work to be done to improve these formulae utilising advanced dispersion models, especially in deriving expressions for plume depth and plume profiles once the plume has touched the ground and the inversion layer.

For $z_s/h \lesssim 0.1$,

$$\sigma_z \simeq x\, u_*\, b \Big/ U(\bar{Z}) \tag{3.22a}$$

where

$$b = \frac{1.3\, T_{W(N)} + (0.6u_*/U(\bar{Z}))(x/z_s)}{1 + (u_*/(U(\bar{Z}))(x/z_s)}, \qquad T_{W(N)} = 1 - 0.8z_s/h. \tag{3.22b}$$

Thus, for a ground-level source $(x/z_s >> 1)$

$$\sigma_z \simeq 0.6xu_*/U(\bar{Z}) \tag{3.23a}$$

while for an elevated source for $(x/z_s << 1)$,

$$\sigma_z = 1.3\, T_{W(N)} xu_*/U(\bar{Z}). \tag{3.23b}$$

In these expressions $\bar{Z}$ is the mean plume height which changes with downwind distance. To allow for the image effect at the ground and at the inversion,

$$\bar{Z} \simeq z_s + 0.5S(\sigma_z - z_s) - 0.5S(\sigma_z + z_s - h) \tag{3.24a}$$

where $S(\varsigma)$ is a slope function defined by

$$\begin{aligned} S(\varsigma) &= 0 \quad \text{for} \quad \varsigma < 0 \\ &= \varsigma \qquad\quad \varsigma > 0. \end{aligned} \tag{3.24b}$$

Note that when $\sigma_z > h$, $\bar{Z} = h/2$.

For higher level sources, $z_s/h \geq 0.1$. Moore & Lee (1982) and others (e.g. Draxler 1976) have proposed forms for σ_z similar to those for homogeneous turbulence. (They have also suggested other changes which are discussed in §3.3.) Then the function b in (3.22a) becomes

$$b = 1.3T_{W(N)} \Big/ (1 + t/2T_L)^{1/2} \tag{3.25a}$$

where

$$t = \frac{x}{U(\bar{Z})}, \quad T_L = \frac{L_x^{(w)}(\bar{Z})}{\sigma_w(\bar{Z})}, \quad \frac{1}{L_x^{(w)}} = \frac{2}{\bar{Z}} + \frac{3}{h}, \quad \sigma_w = 1.3u_* T_{W(N)}(\bar{Z}). \tag{3.25b}$$

Note that when $x/z_s << 1$, (3.25) is equivalent to (3.22b). When $x/\bar{Z} >> 1$ and $z_s/h << 1$, (3.25) reduces to the same as (3.22b), i.e. $b = 0.6$. (Therefore (3.25) could be used for all source heights in place of Briggs' formula (3.22b).)

For the horizontal plume width, the component due to turbulence alone is approximately

$$\sigma_{y_{(\text{turb})}} = 2.0u_* T_{H(N)} x/U(\bar{Z}) \tag{3.26}$$

where from §2.1.7

$$T_{H(N)} \simeq 1 - 0.8\ z/h.$$

The component due to slow wind direction variability is give by (3.9b).

(iii) Comparison between R91 Gaussian plume model and proposed formulae

Figure 3.10 shows the computed ground-level concentration along a line through the source parallel to the mean wind direction for the R91 G.P.M. (which uses low-level σ_z, σ_y) and for the G.P.M. employing the formulae in the previous section (which allow for the variation of σ_z, σ_y with height). The R91 model results are taken from Fig.16 of that report, and the same values of $U = 5\text{ms}^{-1}$, $h = 800\text{m}$, $z_o = 0.3\text{m}$ and release duration = 30 minutes are used in the proposed formulae.

it can be seen that in all cases the position of $c_{gl\ \text{mx}}$, z_{mx}, is moved upwind relative to the R91 value by an amount that increases with source height. $z_{\text{mx}}/z_{\text{mx}}$ (R91) ranges from about 0.75 when $z_s = 20\text{m}$ to 0.6 when $z_s = 200\text{m}$.

For low-level sources, the R91 model predicts a large maximum ground-level concentration that our formulae but the opposite is true for high-level sources. The changeover occurs for sources just over 100m about the ground. $c_{gl\ \text{mx}}/, c_{gl\ \text{mx}}$ (R91) is about 0.7 for $z_s = 20\text{m}$ and about 1.15 when $z_s = 200\text{m}$.

3.2.3 Review of Gaussian plume models in stable boundary layers over flat terrain

(i) Limitations of current Gaussian plume models

In the stable boundary layer field experiments show that near the source the plumes do have a Gaussian concentration profile but further downwind (typically 500m for a 25m high source) the plume centreline may have descended by about 15-20m, whereas the G.P.M. shows no drop (Doran et al. 1978). This downward deflection is caused by wind shear (i.e. a large value of $\partial U/\partial z$) which can vary considerably from place to place. For example, it was not found in the field experiments reported by Strimaitis et al. (1985). In general, this shear-induced deflection may be sensitive to slopes as small as 10^{-2} (Hunt 1982a; Weil 1985).

Field measurements show that near the source $\sigma_z = \sigma_w x/U(z_s)$, and that both σ_w and $U(z_s)$ vary more rapidly with height in the SBL than in the NBL (as shown in §§2.1.6, 2.1.7. For example, in F conditions with $h/L_{\rm MO} \simeq 1$ and $L_{\rm MO} = 50$, $\sigma_w/U(z_s)$ varies from 0.06 at 10m, to less than 0.01 at 50m (Hunt 1982a, Strimaitis et al. 1985).

Further downwind the vertical growth of the plume is also determined by other parameters which are functions of z/h and of $h/L_{\rm MO}$. When the plume has travelled a distance of the order of $U(z_s)/N(z_s)$, (say 250m for $U = 5{\rm ms}^{-1}$, N = buoyancy frequency = $0.02{\rm s}^{-1}$) its growth rate is greatly reduced as explained in §3.1.2(iv). Thus the location of this change in growth depends on how $U(z), N(z)$ vary through the boundary layer. Typically $N(z)$ might decrease by a factor of three from the surface to the top of the layer (§2.1.7). Downwind of this point the plume growth is also quite variable; it may or may not exist. Some evidence and theory suggest that the growth is determined by a mixing rate time scale $1/\gamma N$ where γ is a factor whose value ranges from 0.1 to 0.6 (it is discussed in more detail in the next section).

As in the NBL, the effect of the ground on the plume profile is not equivalent to an image source for neither an elevated nor a ground-level source because of the variation with z of the diffusivity and velocity profile (see, for example, Hunt 1982a; Doran et al 1978; Gryning et al. 1983). In general the variation of the mean concentration is given by

$$C \propto \exp(-Az^s) \quad \text{where} \quad 1 < s < 2. \tag{3.27}$$

For a ground-level source the growth of the vertical plume depth has been analysed in terms of the Monin-Obukhov length $L_{\rm MO}$ and roughness length. The results can be expressed in functional form as

$$\sigma_z = x f(x/L_{\rm MO}, x/z_o) \tag{3.28}$$

(see Doran et al. 1978). This approach has not been related to that for vertical dispersion from an elevated release.

For the lateral plume width, σ_y, the contribution from turbulence $\sigma_{y(\text{turb})}$ is not well documented. Observation shows that $\sigma_v/U(z)$ decreases to less than 0.01, while $L_x^{(u)}$ increases to about $h/6$. Therefore near the source σ_y generally decreases with z/h. Further downwind the increase of σ_y is generally caused by the cross-wind shear, $\partial V/\partial z$, and vertical diffusion. Since $\partial V/\partial z$ reaches a maximum in the lower half of the layer and σ_z decreases near the top of the layer, then $\sigma_z\ \partial V/\partial z$ also decreases with z. Therefore the whole turbulence component $\sigma_{y(\text{turb})}$ decreases with (z/h).

The long-term variability of $V(t)$ and its contribution to σ_y for ideal flat terrain, $\sigma_{y(T)}$, has been reviewed by Larsen et al. (1985). It is likely that there are significant differences between different types of terrain and so in practice it is probably best to use a locally measured value for $\sigma_{y(T)}$.

(ii) Possible revised Gaussian plume model formulae

For elevated sources the consensus is that, in the absence of strong shear $((dU/dz)(\sigma_z/U) << 1)$ and near the source

$$\sigma_z = \sigma_w\ x/U(z_s). \tag{3.29a}$$

Further downwind, when $x >> U(z_s)/N$, (3.14a) may be used in a slightly modified form which, with $\zeta = 1$, is

$$\sigma_z = (\sigma_w/N)\left[1 + 2\gamma^2 N\ x/U(\bar{Z})\right]^{1/2}. \tag{3.29b}$$

To agree with diffusion data γ ranges from 0.6 to 0.1 and for data at source heights of 25m – 100m, γ typically ranges from 0.3 to 0.1. In ideal flat terrain this range corresponds approximately to z_s/h, varying from 0 to 1.0. To be specific, let

$$\gamma = 0.3\left\{1 + \frac{1}{1 + z/L_{\text{MO}}} - \frac{2}{3}\,\frac{z}{h}\right\}. \tag{3.29c}$$

For ground-level sources the growth of a plume is simply related to the diffusion of heat or any scalar (because of the high local shear and mixing). For $z_s << h$ and $z_s \lesssim |L_{\text{MO}}|$

$$\sigma_z \simeq \frac{\sigma_w x/U(z)}{(1 + t/2\tau_*)^{1/2}}\ , \tag{3.30a}$$

where

$$\frac{1}{\tau_*} = 1.3\ u_*\left(\frac{2}{\bar{Z}} + \frac{3}{h} + \frac{10}{L_{\text{MO}}}\right). \tag{3.30b}$$

This reduces to the form for the NBL when $L_{\text{MO}} \to \infty$ in (3.25).

In these formulae $U(z), N, \sigma_w$ are given as functions of z/h and/or h/L_{MO} in (2.11), (2.13) and (2.18b), (2.20b) respectively.

Because of the many factors affecting σ_y, it seems that the most reasonable general formula to adopt is (3.5b) with

$$\sigma_{y(T)} = \sigma_v x/U(\bar{Z}) \tag{3.31}$$

and σ_v given by (2.19a), (2.20a).

Three examples of the variation of σ_z with downwind distance for high- and low-level sources are shown in Fig.3.11. Values of $U, h, L_{\rm MO}$ and u_* are taken from Table 2.1 and the low- and high-level sources are assumed to be located 10m above the ground and 10m below the top of the boundary layer respectively. For comparison the curves for E, F and G conditions taken from Fig.8 of R91 are also shown.

For ground-level sources σ_z grows at gradually decreasing rate in a similar way to the R91 curves. This is because σ_w decreases with height and so as the plume grows, the average value of the turbulent fluctuations drops which reduces the rate of dispersion.

The behaviour of elevated plumes is quite different. They emerge into an air flow with a low level of turbulence. Initially the growth of σ_z is governed by σ_w through (3.29a). Then the growth slows down in line with (3.29b) but later it increases at an ever-increasing rate. Physically this is because at high levels there is very little dispersion of the plume and so it grows very slowly. As it does so, however, the average value of σ_w rises and so the rate of growth increases continually.

3.2.4 Review of Gaussian plume models in convective boundary layers over flat terrain

(i) Limitations of current Gaussian plume models

As explained in §3.1.2, the mean concentration distribution near a source is only Gaussian if the turbulent fluctuations are Gaussian. In the CBL the probability distribution of the vertical velocity fluctuations w is far from Gaussian; its skewness increases from nearly zero close to the surface to about 0.4 when $z/h \simeq 0.1$, and to about 1.0 near the top of the CBL while its mode is about half the standard deviation, σ_w, (Hunt, Kaimal & Gaynor 1988). Even when $-1/3 > h/L_{\rm MO} \gtrsim -1$ (e.g. C conditions), these non-Gaussian features are present over most of the boundary layer. Consequently the mean concentration profiles are not Gaussian (i.e. the skew diffusion factor $\Delta_{TS} \approx 1$).

Figure 3.12a, based on laboratory experiments (Willis & Deardorff 1981) and numerical simulations (Lamb 1982), clearly shows the height of the maximum concentration, $z_{\rm mx}$, decreases rapidly from the source due to the long-lived downdrafts in thermal convection. This effect is not very evident in the scatter of field measurements of plumes, but what is evident from these, other field measurements and

laboratory experiments is that the mean height of plumes rises steeply and at the same time they become increasingly asymmetric. This is caused by the inhomogeneity and non-Gaussianity of the turbulence (i.e. diffusion factors Δ_{T2}, $\Delta_{T3} \approx 1$). A notable feature of diffusion in the CBL is how material is rapidly carried high into the boundary layer (Fig.3.12b).

For elevated sources laboratory experiments have shown how either the height of the maximum concentration, $z_{\rm mx}$, falls to the ground and then rises again or $z_{\rm mx}$ may be on the ground but an elevated secondary maximum may occur (Poreh & Cermak 1984; Deardorff 1985). Weil (1988) has shown how these effects can be modelled using random-flight techniques.

In the CBL the inhomogeneity diffusion factors $\Delta_{T2} \sim 1$, when $\sigma_z \sim z_s$, and the asymmetry factor $\Delta_{T3} \sim 1$ when $\sigma_z \sim h$. Because of this inhomogeneity of the vertical component of turbulence, the vertical depths of plumes released into the CBL vary rapidly with source height z_s. Figure 3.13, taken from the Briggs (1985) review, shows that for ground-level sources $\sigma_z \propto (x - x_s)^{3/2}$ whereas for elevated source $\sigma_z \propto (x - x_s)$. Therefore, near the source the depths of elevated plumes are greater than those from ground-level sources (by a factor of three at most) whereas further down wind (when $x \sim 0.7hU/w_* \sim$ 1-2 km in A conditions) they become comparable with each other.

Plume concentration profiles also differ with source height. For surface releases the height of maximum concentration can rise, whereas for elevated sources it initially decreases.

The important point about Fig.3.13 is that the two bands of data for elevated and surface releases could only be correlated to this extent by using the 'mixed layer' or 'boundary-layer' variables, introduced in §2.1, i.e. by normalising σ_z on the depth h of the layer, and x on the convection velocity $w_* = (ghF_{\theta o}/\rho c_p T_o)^{1/3}$, h and U. This is only appropriate for σ_z when the boundary layer is sufficiently convective and the source height is above the surface layer (i.e. when $h/|L_{\rm MO}| \lesssim -1$ and $z_s/|L_{\rm MO}| \gtrsim 1$). Thus, for an elevated source $\sigma_z(x)$ might be determined by convective turbulence and the curve given by Fig.3.13 while for a surface release, at say $z_s \simeq$ 5m with $L_{\rm MO} = -50$m, the initial vertical plume depth would be given by the results for the neutral boundary layer since $z_s/|L_{\rm MO}| << 1$.

These two effects of source height on σ_z for a given stability category and on the effective stability category are features not present in the standard G.P.M.s.

Whereas $\sigma_z(x)$ is rather sensitive to z_s, $\sigma_y(x)$ is rather insensitive to it largely because σ_v does not vary much with height in the CBL. This aspect of the G.P.M. is therefore correct. However, the deficiency of a conventional G.P.M. with the Pasquill-Gifford surface meteorology-typing scheme is that it does not parameterise the meteorological conditions as accurately as using the 'mixed-layer' parameterisation. Fig.3.14 shows how plotting measurements of σ_y/h against $xw_*/(Uh)$ enables a wide range of experimental measurements to be corrected over a wide range of

stability. Recent numerical simulations by Mason et al. (1988) indicate that even when $h/L_{MO} \lesssim -0.3$ the growth of σ_y , except very close to the source, is effectively described by 'mixed-layer' convective scaling. The reason is that the large-scale convective eddies are approximately independent of the shear-induced eddies.

Figure 3.15 shows the results summarised in Fig.3.13 plotted as σ_z against z and compared with the appropriate curves given in Fig.8 of R91. Relevant values of U, h, w_* and u_* are taken from Table 2.1. The results for $u_*/w_* = 0$ are taken as being A conditions (although, in fact, super-A would be a more apt description for what are conditions of effectively pure convection), while those for $u_*/w_* = 1/3$ are considered representative of C conditions.

In the former case the experimental results from Fig.3.134 are about an order of magnitude greater than the corresponding values in R91 (but to a certain extent this difference is exaggerated by the very stable conditions represented in Fig.3.13). For the C conditions values of σ_z for elevated sources are again greater than the R91 values, by a factor of between two and three initially but more at greater distances downwind. Within about 250m of the source σ_z for a ground-level source is smaller than the R91 value but thereafter it becomes progressively larger.

Figure 3.16 shows a similar comparison between the results shown in Fig.3.14 and the corresponding curves drawn from R91. However, in this case the exact conditions under which the results in Fig.3.14 were obtained are not known, so the time $\sigma_y/h = 0.57X$ in that figure is expressed in terms of A,B and C conditions using values of U, h and w_* given in Table 2.1. In addition, it has been assumed that the duration of the release is 30 minutes when calculating the curves from R91 for comparison. (A longer release would reduce the discrepancies between the two sets of curves.) Unlike the results for σ_z, those for σ_y do not diverge from the R91 values, but in each stability category the results from Fig.3.14 are larger than those from R91 by a factor which increases as the stability decreases.

(ii) Possible revised Gaussian plume model formulae incorporating a neutral boundary-layer limit

For sources in the lowest part of the CBL, theory, numerical modelling and some field experiments all lead to a similar form for σ_z, namely

$$\frac{\sigma_z}{h} = X\,(0.4T_{W(C)}^2 + 0.25X)^{1/2}\,, \qquad (3.32a)$$

where $X = xw_*/Uh$ and $T_{W(C)}$ is given by (2.17c). Briggs (1985) has suggested a form for ensuring a smooth transition to the case of a ground-level source in the NBL, namely

$$\frac{\sigma_z}{h} = X\,\left(0.4T_{W(C)}^2 + 0.25X + \left(\frac{bu_*}{w_*}\right)^2\right)^{1/2}\,, \qquad (3.32b)$$

where b is given by (3.22b).

The striking feature of this form is that when $(x-x_s)$ is greater than about $h/3$ (say 300m), the graph of σ_z against x curves upwards (it is proportional to $x^{3/2}$) as it did in the original curves given by Pasquill (1961) for the A category. However, numerical modelling, theoretical arguments (already given) and field experiments show that when $z_s/h \gtrsim 0.1$, σ_z/h increases in proportion to x. Therefore we propose that (3.32b) be modified to

$$\frac{\sigma_z}{h} = X \left(0.4 T_{W(C)}^2 + 0.25X \, e^{-10 z_s/h} + \left(\frac{b u_*}{w_*} \right)^2 \right)^{1/2} . \qquad (3.32c)$$

Because they relate to plume behaviour near the source, the first and second terms on the r.h.s. of (3.32c) must use z_s for their arguments. On the other hand, the third term applies to conditions far downwind of the source and so the mean plume height $\bar{Z}$ should be used when evaluating it. For consistency with the NBL expressions given in §3.2.2. we have adopted (3.25a) for b, using the formulae for t and T_L given in (3.25b) but using (2.17a) for σ_w.

For the lateral plume width, σ_y, it is suggested that, as in the NBL,

$$\sigma_y = \sigma_v \; x/U(z) \qquad (3.32d)$$

where σ_v is given by (2.14).

A comparison between these formulae and results shown in Fig.13 of R91 for the ground-level concentration is shown here in Fig.3.17. As in Fig.3.10, c_{gl} is calculated along a line through the source parallel to the mean wind direction using the R91 values of $U = 1\text{ms}^{-1}$, $h = 1300\text{m}$, $F_{b_o} = 250\ \text{Wm}^{-2}$, $z_o = 0.3$ and release duration = 30 minutes.

The much larger values of σ_z, σ_y shown in Figs.3.15, 3.16 which form the basis for the above formulae indicate that a plume will spread more quickly than in the R91 model. This fact is borne out by the calculations which show that the differences between the present G.P.M. formulation and that of R91 increase with source height. When $z_s = 200\text{m}$, the distance to the position of maximum ground-level concentration decreases by a factor of five and $C_{gl\text{mx}}$ itself is 40% greater than the R91 value.

3.3 Modified Gaussian plume modelling

3.3.1 Generalities

In the previous section the limitations of G.P.M. were explained. It was also suggested how some of the limitations in the current uses of G.P.M. could be mitigated by changing the specification of the plume depth and width parameters σ_z, σ_y. These kinds of changes could be implemented readily.

In this section we review other kinds of modifications of the G.P.M. by which we mean that the concentration is given by a function of the form

$$C(x,y,z) = \frac{Q}{U(z_{ref})} G_y(y,x,z_s,h) G_z(z,x,z_s,h) \tag{3.33}$$

where

$$\int_o^h \int_{-\infty}^{\infty} U(z) C \; dy \; dz \; = \; Q \; .$$

The function G_z is no longer simply the sum of 'reflected' Gaussian profiles centred on the source height, z_s, and its image points, but the function G_y is made up of one or more Gaussian functions, and the mean velocity $U(z_{ref})$ is defined at at appropriate height z_{ref}.

However, one essential feature of other G.P.M.s has been retained, and that is that the wind conditions are approximately steady over the time of travel from the source to the receptor.

3.3.2 Moore & Lee's (1982) modified form for $C_{g\ell}$

Moore & Lee suggested a form for (3.33) to account for the variation in the turbulence and wind speed with height by allowing σ_y, σ_z, and U to have different values above and below the source height z_s, designated $\sigma_{y\uparrow}, \sigma_{y\downarrow}$, $\sigma_{z\uparrow}, \sigma_{z\downarrow}$ and $U_\uparrow, U_\downarrow$. They only gave a formula for the ground-level concentration $C_{g\ell}(x,y)$ rather than $C(x,y,z)$, and this was based on the 'image' source concept; it is

$$C_{g\ell}(x,y) = \frac{2Q \exp(-y^2/2\sigma_{y\downarrow}^2) \exp(-h^2/2\sigma_{z\downarrow}^2)}{\pi(\sigma_{y\uparrow}\sigma_{z\uparrow}U_\uparrow + \sigma_{u\downarrow}\sigma_{z\downarrow}U_\downarrow)} \; . \tag{3.34}$$

This formula was developed for ground-level concentrations (g.l.c.) out to a distance from the source of the order of $2x_{\rm mx}$, where $x_{\rm mx}$ is the distance to the position of max g.l.c., $C_{g\ell\ {\rm mx}}$. It does not account for reflection from an elevated inversion layer, and therefore is not appropriate for sources in the upper half of the boundary layer.

For many of the practical problems where diffusion modelling is required, it is necessary to model the actual distribution of concentration $C(x, y, z)$. Other modified G.P.M.s have been proposed, but none cover all the situations of interest covered by the existing one.

3.3.3 The elevated plume model of Venkatram & Paine (1985)

In this case the effect of shear on the plume shape is allowed for in the function G_z, by using different Gaussian forms above and below the source height.

$$\begin{aligned} G_z &= \exp\left\{-(z-z_s)^2/2\sigma_{z\uparrow}^2\right\}/\sqrt{2\pi}\sigma_{z\uparrow} \qquad \text{for } z > z_s \\ &= \exp -(z-z_s)^2/2\sigma_{z\downarrow}^2/\sqrt{2\pi}\sigma_{z\downarrow} \qquad \text{for } z < z_s. \end{aligned} \tag{3.34}$$

The model may be capable of extension but at present it is too limited for general application.

3.3.4 Ground-level sources

We pointed out in §3.2 that for ground-level sources the vertical profile of C does not have a Gaussian form. Consequently a number of authors have proposed modified G.P.M.s for near surface sources where G_y and G_z in (3.33) take the forms

$$G_y = \frac{\exp(-y^2/2\sigma_y^2)}{\sqrt{2\pi}\sigma_y}, \quad G_z = \frac{\exp(-A_1(z/\sigma_z)^s)}{A_2\sigma_z} \ .$$

s is usually taken to be 1.5 (e.g. Pasquill & Smith 1983) but in general $1 \leq s \leq 2$. The constants A_1 and A_2 are defined by the relationships

$$\int_o^\infty G_z dz = 1 \quad \text{and} \quad \int_o^\infty z^2\, G_z dz = \sigma_z^2 \ .$$

3.3.5 Possible developments in modified Gaussian plume model

There are certain well-established experimental and theoretical results that, in combination and suitable interpolation, might form the basis of a modified G.P.M. that would be a distinct improvement on current G.P.M. and the improvements suggested in §3.2. However, further research and development would be needed to produce a validated usable model incorporating the following features:

(a) near the source G_z approximately Gaussian for neutral and stable layers, but non-Gaussian for the CBL;

(b) where the shear is strong the height $z_{\rm mx}$, at which the concentration is maximum, changes and also the plume becomes asymmetric about that level;

(c) for sources released at or near either the surface or an elevated inversion G_z is not Gaussian but has the form (3.35b);

(d) for elevated sources $\partial C/\partial z \neq 0$ at either the surface or $z = h$.

These effects can be modelled approximately by a function of the form

$$G_z = G_s + G_g + G_h. \qquad (3.36a)$$

The source term G_s should be the sum of <u>two</u> functions centred at different heights (in order to allow for non-Gaussian profiles in convection)

$$G_s = \frac{A}{\sigma_{z_1}} \exp\left(-\frac{(z-z_1)^2}{2\sigma_{z_1}}\right) + \frac{B}{\sigma_{z_2}} \exp\left(-\frac{(z-z_2)^2}{2\sigma_{z_2}^2}\right) \qquad (3.36b)$$

where z_1, σ_{z_1}, and z_2, σ_{z_2} vary with x, and are chosen to satisfy conditions (a) and (b). The parameters A,B would vary with atmospheric conditions.

There are several reasonably simple ways of modelling the ground effect. The concept of an image source is only one of these. Usually source and image source have identical strengths but this need not be so. By allowing the position and strength of an image source solution to vary, it is possible to satisfy approximately condition (b), e.g.

$$C_g = A_g \exp\left(-\frac{(z-z_g)^2}{2\sigma_{z_g}^2}\right) \quad , \quad G_h = A_h \exp\left(-\frac{(z-z_h)^2}{2\sigma_{z_h}^2}\right) \quad . \qquad (3.37)$$

Presumably $\sigma_{z_g}, \sigma_{z_h}$ are similar to the values for near ground-level sources.

These functions must satisfy the condition that the net vertical flux through the ground or inversion is zero, which is equivalent to the horizontal flux constant, i.e.

$$\int_o^h \int_{-\infty}^{\infty} U(z) C(x,y,z) dy \; dz = Q \; . \qquad (3.38)$$

Functions such as these can be incorporated easily into a modified G.P.M. dispersion code.

Note that G.P.M.s have been extended to apply to convective conditions when the mean velocity U is much less than the turbulence velocities (σ_v, σ_w), (Hunt 1987b; Smith 1988).

3.4 Puff models

The major defect of the forms of Gaussian plume model reviewed in §§3.2, 3.3, is that they can 'only' be used to describe the distribution of concentration (averaged over a short time scale of T_c) between a source at x_s and a receptor at x if the wind direction remains constant over the period $T = (x - x_s)/U$ it takes the material to pass between them. By 'short' averaging time T_c we mean that $T_c \lesssim T/5$, but greater than the characteristic time scale h/u_* or h/w_*. Thus if $U = 5\text{ms}^{-1}$ the wind direction must stay constant over a distance of 20km for about 2 hours if the 20-minute average concentration is to be described by a G.P.M. (Such a calculation might be important for certain kinds of dose response.) If it does not stay constant a new model is required.

However, as explained in §3.1.2, if the G.P.M. is used to calculate the long-term mean concentration at the receptor, i.e. averaged over a period much longer than T, say 3 – 24 hours, then the changes in the wind direction can be modelled by increasing σ_y, for example, as modelled by (3.9). Later in this section it will be seen that this concept has been partially validated by detailed puff models.

Clearly this means that over long distances out to 100km or even 1000km, the travel time must be of the order of 10 hours or 100 hours if 3 hour or even 24 hour average concentrations are required in order to satisfy the condition $T_c \lesssim T/5$. Therefore a model is required that accounts for the variations in wind direction and speed.

Puff models are practical and computationally fast models that have been developed for this purpose. Many of them make use of the results of G.P.M.s, in particular for the classification of the meteorology σ_z, σ_y and a corresponding function for σ_x. We give a brief review here, to indicate the potential of practical dispersion models over a distance of up to 20km.

The essential concept, described in Fig.3.18, is to consider a source emitting a sequence of 'puffs' of pollutant at times $t_{s1}, t_{s2}, t_{s3}, \ldots$ rather than a steady stream. Because there is no assumption about the volume or mass of pollutant in each puff as it is released, the model can be used for continuous sources with varying strength, $Q(t)$ by setting $\delta V(t_{s_k}) = Q(t_{s_k}) \times (t_{s_{k-1}} - t_{s_k})$. Unlike the case of steady plume models, diffusion in the direction parallel to the mean wind has to be considered now because each puff, with constant volume $\delta V(t_s)$, diffuses outwards in all three directions as it travels from the source.

In the simplest form of the model the effects of shear along or across the wind (i.e. dU/dz, dV/dz) are not considered, and the puffs move as growing ellipsoids, with image puffs caused by the ground and the inversion. The concentration at

x, y, z at time t, for the puff released at t_{s_k} with volume $\delta V(t_{s_k})$ is

$$\Delta C(x,y,z,t-t_{s_k}) = \frac{\delta V(t_{s_k})}{2\pi\sigma_x\sigma_y}\left\{\exp\left(-\left[\frac{(x-X)^2}{2\sigma_x^2}+\frac{(y-Y)^2}{2\sigma_y^2}\right]\right)\right\}G_z. \quad (3.39a)$$

In the simplest case

$$G_z = \exp\{-(z-Z)^2/2\sigma_z^2\}\Big/(\sqrt{2\pi}\sigma_z) + \{\text{image solution}\}. \quad (3.39b)$$

but over long distances, much greater than 20km in unstable conditions and 100km in very stable conditions, the puffs fill the boundary layer and then $G_z = 1$. X, Y, Z is position of the centre of the puff and $\sigma_z, \sigma_y, \sigma_z$ are defined over a period T_c greater than the integral scale h/u_*. Then the mean concentration over that same period T_c, is obtained by summing the concentrations of all puffs released in time between t and some previous time, $t - \alpha T$, i.e.

$$t - \alpha T < t_{s_k} < t\ , \quad (3.40)$$

where T is the travel time from the source position (calculated from the long-term mean velocity), and α is a parameter that increases with variability of the 'mean' wind σ_u (i.e. over period T_c or 1 hr) compared with the mean velocity U. If $\sigma_u/U << 1$, $\alpha \simeq 1$ but if $\sigma_u/U >> 1$, $\alpha >> 1$.

Thus

$$C(x,y,z,t) = \sum_k \Delta C(x,y,z,t-t_{s_k}) \quad (3.41)$$

where t_{s_k} satisfies (3.40).

The location of the centres of the puffs (X, Y, Z) are calculated from the mean wind field (over the period T_c, e.g. 3 hrs), i.e. if the wind vectors are U, V, W at the location X, Y, Z, the changes $\delta X, \delta Y, \delta Z$ in the position are

$$\delta X = UT_c, \quad \delta Y = VT_c, \quad \delta Z = WT_c \quad (3.42)$$

(see Fig.3.18). The puffs can meander in significantly different directions over large distances from their initial directions.

Puff models based on these principles, especially the MESOS model of ApSimon et al.(1985), have been successful in modelling long-range dispersion over 100 to 500km from unsteady sources. They have also been used for modelling dispersion in unsteady conditions over distances less than 20km. Over such distances, however, the puffs do not fill the boundary layer and therefore it is necessary to consider the vertical distribution of concentration.

The various complex diffusion processes of steady straight-line plumes were explained in §3.1 and the difficulties of modelling them explained in §§3.2, 3.3. For

puffs additional complex processes have to be considered and modelled. Figure 3.19 shows the kind of problems and the idealisations that are made in modelling puffs omitted from ground-level sources. In neutral and stable boundary layers a spherical puff is sheared over by the strong velocity gradient (dU/dz) near the ground. These processes distort the initial spherical shape into an increasingly elongated kidney shape (Fig.3.19a). Measurements and smoke pictures demonstrate these shear effects in neutral and stable boundary layers, e.g. reviews and models by Chatwin (1968), Hunt & Weber (1979), Hanna (1980), Stretch, Hunt & Britter (1983). Figure 3.19b shows how these conditions are modelled by a series of spaced puffs.

A source in the CBL might lie beneath a downdraft (Fig.3.19c) or an updraft (Fig.3.19d). In the former case a puff is stretched laterally before leaving the ground as two sausage-like puffs, but in the latter case the initial puff is drawn up into the updraft. Figure 3.19d also shows what happens when a puff carried aloft in an updraft reaches the inversion. These events can be modelled by a growing ellipsoidal puff as shown in Fig.3.19e.

It is important to note that even though the modelling of individual puffs may be quite inaccurate large errors do not accumulate when a sequence of many puffs is added to constitute a continuous plume. To allow for the shear, segmented puff models are used. Each slice or segment travels with a different mean speed and in principle should have different rates of vertical and horizontal diffusion. In some formulations, discrete slices or segments are used while in others the segments are infinitesimal and a continuous model is used.

This is the approached used in the Riso 'puff-model' (Mikkelson et al. 1984), which is expected to be used over short distances for surface releases. The concentration at time t caused by puffs released at t_{s_k} has the form of (3.39) but now the centres $(X,Y)(z,t)$ of the 'segments' vary with height z, depending on the wind shear, i.e.

$$\frac{dX(z,t)}{dt} = U(X,Y,Z) \quad \frac{dY(z,t)}{dt} = V(X,Y,Z). \tag{3.43a,b}$$

They also allow for the non-Gaussian vertical concentration profile discussed in §3.2, by setting

$$G_z = A\exp(-b(z/\sigma_z)^s), \tag{3.44a}$$

with the constants A, b determined by the integrals

$$\int_o^\infty G_z dz = 1 \text{ and } \sigma_z^2 = \int_o^\infty z^2 G_z dz. \tag{3.44b}$$

and the exponent s derived from an approximate theoretical analysis of the surface layer; typically $s \simeq 1.5$. The Riso puff model was tested in a field experiment by releasing a continuous plume over level terrain; but the measurements were only

made out to about 500m. Continuous wind measurements at the source height were used to calculate the movements of the puff centres by assuming that the wind (averaged over a time of about 2 minutes) everywhere was the same as at the source point. During the experiment the wind changed rather suddenly by about 30°, leading to the instantaneous plume having a sharp bend. The model was satisfactory and obviously better than a straight line G.P.M. which does not allow for a change of wind direction during the travel time.

This kind of puff model is appropriate for detailed analysis of specific experiments or events. If used for probabilistic risk assessment it is not yet clear how the meteorological data would be fed into such a model – perhaps by defining typical wind changes in different conditions. The calculation time for one experiment with one wind direction over about 10km for this model is about one minute on a mainframe computer. No validated and generally accepted puff models yet exist for short-range dispersion from elevated sources.

Puff models have been used to examine the assumption in R91 that, over long averaging times, the effects of wind direction changes can be modelled by effective increases in σ_y. Mikkelson et al. (1984) find some differences compared with the R91 formula (3.9) of this report; but for most purposes their results confirm that (3.3) is a useful and simple approximation.

It should be pointed out that there is another way of considering wind direction changes in the context of Gaussian plume modelling and that is, to take the continuous plume solutions and allow for sudden wind changes (as in the Riso experiment). An algorithm for such a model was given by Hunt (1987b). Using typical wind changes, statistics for 'short' time samples ($T_c < T/5$) could be evaluated.

3.5 Research models

3.5.1 Overview

Since this report is concerned with the future development of practical models for atmospheric dispersion (over distances less than 20km), the main purpose of reviewing research models is:

(a) to indicate whether any of them are suitable for development into practical models;

(b) to review whether or how such models might help the development and validation of practical models;

(c) to review whether such models might be appropriate in *specific* situations

where practical models are not valid or accurate enough.

The important features of research models that have to be considered for the above purposes are:

(i) requirements of input data and assumptions. Some diffusion models differ greatly in the amount and type of data they can use;

(ii) ease of programming the models for computers;

(iii) ease of use and interpretation of computations;

(iv) computer power needed and type of computer;

(v) connections between research models and practical models;

(vi) use of the models for on-line, real-time calculations or off-line.

The research models we consider here are: in §3.5.2, stochastic models, including random flight/walk models and particle-in-cell; in §3.5.3 eddy diffusion models and 'second-order' models; and in §3.5.4 methods based on the numerical simulation of entire turbulent velocity fields.

Much of the required technical background of this review is available in Pasquill & Smith (1983) but it is also based on more recent research.

3.5.2 Stochastic models

The statistical theory of turbulent diffusion is based on G.I. Taylor's (1921) paper which forms the basis of current practical Gaussian dispersion modelling (as explained in §3.1). Taylor showed that for homogeneous turbulence the analytical results for the mean square displacement of fluid particles released from a source, $\overline{Z^2}(t)$, could also be calculated by considering the motion of a particle as a sequence of steps each of finite length (Fig.3.20). These steps differ from the simple drunkard's walk of elementary statistical theory because the velocity of each new step is determined partly by the velocity of the previous step. It is found that for the vertical turbulence:

$$dW = -\frac{W}{T_L}dt + \frac{\sigma_w}{\sqrt{T_L}}d\xi_t \tag{3.45}$$

where $d\xi_t$ is a Gaussian random variable, $d\xi_t^2 = dt$ and is uncorrelated with previous time, and T_L is the Lagrangian integral time scale (defined in §3.1.1). The concentration is calculated at a point by counting the number of 'particles' from the source that pass through a small box around that point.

The importance for diffusion modelling is that this computational approach can also be applied even when the source is in inhomogeneous turbulence. Therefore for a ground level or elevated source in the NBL (3.45) can be used to predict the

mean vertical height and dispersion of a plume. It has to be extended to take into account the correlation of horizontal and vertical fluctuations ($-\overline{uw}$). The method obviously uses information about $\sigma_w(z)$ and $T_L(z)$ in the boundary layer which may be supplied by measurement or computation. The programming of (3.45) (and its equivalent forms) is quite straightforward and there is always a remarkable degree of agreement about the answers amongst programmers from the least to the most experienced. To obtain, say 10% accuracy in σ_z, it is necessary to make at least 1000 particle trajectories.

In some turbulent flows such as the CBL, wakes downwind of hills and over roughness changes, the standard deviations of the turbulent velocity components change rapidly with height so that the diffusion factor $\Delta_{T2} = (\sigma_z/\sigma_w)\partial\sigma_w/\partial\sigma_z$ is significant. Also, the turbulence is non-Gaussian especially in the convective layer so that $\Delta_{TS} = (\overline{w^3})^{1/3}/\sigma_w \approx 1$ and $\Delta_{T3} = (\sigma_z/\sigma_w^3)\partial\overline{w^3}/\partial z \approx 1$. In such cases, (3.45) has to be modified, as shown by Thomson (1984) and van Dop et al. (1985), to

$$dW = -\left(\frac{W}{T_L} + \frac{\partial\sigma_w^2}{\partial z}\right)dt + \left(\frac{\sigma_w}{\sqrt{T_L}} + \left(\frac{\partial\overline{w^3}}{\partial z}\right)^{1/2}\right)d\xi_t. \qquad (3.46)$$

There remain some fundamental questions about the use of (3.45) and (3.46) in inhomogeneous turbulence. So far, though, these methods have shown very close correspondence both with detailed wind-tunnel and water-tank diffusion experiments and with field experiemnts (e.g. de Baas et al. 1986; Weil 1988; Durbin & Hunt 1980; Ley & Thomson 1983).

An advantagere of the stochastic simulations is that they can be programmed for use on personal computers. Also for a small number of runs, say less than 100, the simulations give a qualitative indication of the effect of small sampling time on the interpretation of the diffusion data.

Random flight models using two or more particles are also now used to predict concentration fluctuations, mixing and chemical reactions (Thomson 1988). Inhomogeneity effects have not yet been studied but Stapountzis & Britter (1987) have examined the significant effects of reducing fluctuations in shear. For homogeneous turbulence the results produce equivalent statistics to those obtained by puff model when many puffs are used. So, in some ways these models predict more and in other ways less than puff models.

In §3.1 we explained how, in stably stratified turbulence, the effects of density differences and changes of fluid particles have to be considered when calculating their vertical movements. For that reason and the fact that the form of the velocity correlation function is not an exponential function of t/T_L, the simple stochastic models (3.45), (3.46) are not appropriate. However other stochastic models have been derived which account approximately for the two major effects (see Hunt 1982b).

Stochastic random flight models are too computationally intensive to be used as practical dispersion models but they are now the most reliable means of testing any proposals for simple/fast practical models. They can be used for particular investigations where more accuracy is needed and also for real time investigations when the wind speed (averaged over turbulence time T_L) changes between source and receptor. These methods are being actively developed for different applications and will develop even more with faster, small computer systems.

A very similar approach to these random-flight methods called Particle-in-Cell, has been developed at the Lawrence Livermore National Laboratory by Lange (1978) for use on large main-frame computers. Although the code is available widely, because of its complexity it can neither be used readily on a small system nor easily make use of detailed local turbulence measurements. The whole code comprises the flow field model MATHEW (described in §2.3) and the dispersion model ADPIC. Although its predictions have been compared with the results of major field experiments, we have not seen any reports of runs of the models to compare in detail with standard diffusion experiments for different release heights and different stability conditions. Lewellen et al. (1982) have reviewed the model in detail and made a number of criticisms.

The ADPIC model is used in a different way to the purely stochastic modelling approach, because the widths of the distributions of the trajectories of marked particles from the source are used to compute diffusivities K_z, K_y. Then the concentration is calculated from the diffusion equation (described in the next section).

This model has been used in the U.S.A. particularly for post-event analyses. However, it is a long way from meeting the criteria for a practical regulatory code, and indeed has not been designed for that purpose.

3.5.3 Eddy diffusion methods

(i) K-models

The simplest concept of turbulent diffusion is that it is similar to anisotropic molecular diffusion and defined by turbulent diffusivities K_y, K_z. This implies that the mass fluxes of pollutant F_{cy}, F_{cz} in these directions are given in terms of the gradients of the mean concentration C by

$$F_{cy} = -K_y \frac{\partial C}{\partial y}, \quad F_{cz} = -K_z \frac{\partial C}{\partial z}. \qquad (3.47a,b)$$

With (3.47a,b), the distribution of mean concentration is then defined by the equation

$$U(z)\frac{\partial C}{\partial x} + V\frac{\partial C}{\partial y} + W\frac{\partial C}{\partial z} = -\left\{\frac{\partial F_{cy}}{\partial y} + \frac{\partial F_{cz}}{\partial z}\right\}. \qquad (3.47c)$$

In order for the model to be meaningful, the diffusivities should be independent of the concentration distribution; i.e. K_y, K_z are given functions of x, y, z for a given flow. Therefore K_y, K_z should be the same for point or area sources and the same for heat as for pollutants.

There are only qualitative guidelines as to when this approach is a good approximation, namely:

* the scale of the concentration field σ_y, σ_z, (be if for plume or puff) should be larger than the integral scale of turbulence L, i.e. $\sigma_y, \sigma_z > L$; (3.48a)

* the turbulence should be close to a Markovian process, i.e. the acceleration of fluid particles should be independent of the history of their motion; (3.48b)

* the probability distribution of the turbulent velocity field should be close to Gaussian $(\Delta_3 << 1)$ (3.48c)

Clearly (3.48a) cannot be satisfied near a small source placed away from a boundary in a turbulent flow, because at the source σ_y and σ_z are small whereas L is finite. Note also that only the second of these these criteria has to be satisfied by random-flight methods, when modelled by (3.45), (3.46).

As with random-flight models, the next question in the eddy diffusion method is how to define K_y, K_z. Equation (3.47) agrees with the results of the exact statistical theory far from the source (when $t >> T_L$) (see (3.7)), provided

$$K_y = \sigma_v^2 T_L^{(v)}, \quad K_z = \sigma_w^2 T_L^{(w)} \quad . \tag{3.49a,b}$$

In general the Lagrangian time scales $T_L^{(v)}$, $T_L^{(w)}$ are not known because they require the motions of particles to be tracked but by dimensional arguments (e.g. Tennekes & Lumley 1972) and wind-tunnel experiments, they can be estimated in terms of fixed point Eulerian measurements. For homogeneous turbulence and the NBL

$$T_L^{(v)} \simeq L_x^{(v)}/\sigma_v, \quad T_L^{(w)} \simeq L_x^{(w)}/\sigma_w. \tag{3.50a,b}$$

In the CBL, where the turbulence near the surface is very anisotropic, (3.50b) does not agree with heat flux measurements but Turfus & Hunt (1987) suggest that $T_L^{(w)} \simeq L_x^{(w)}/\sigma_u$ (Turfus & Hunt 1987). In the SBL, when little mixing occurs, (3.49b) may only be appropriate very far from the source for reasons given in §3.1, §3.5.2 and Hunt (1985b). Then

$$K_z \simeq \gamma \sigma_w^2 / N. \tag{3.51}$$

This is a good model for heat flux or for vertical diffusion from an area source.

In the atmospheric boundary layer over level terrain, these turbulence statistics have been measured in different stability conditions (see §2.1).

In complex environmental and engineering diffusion problems, the diffusivities K_y, K_z are usually derived from models of the mean flow and certain statistics of the turbulence. The simplest of these models assume the length scales $L_x^{(v)}, L_x^{(w)}$, and then use a single extra equation for the kinetic energy of turbulence, k. By also assuming the values of the ratios σ_w/k, σ_v/k, and using (3.49), K_z, K_y may be computed. A more widely used approach, especially for estimating vertical diffusivities of areas sources, is the (k-ϵ) method. This employs two equations: one for k and a second for the ratio $k^3/L_x^{(w)}$ which is proportional to the rate of dissipation per unit mass ϵ (e.g. Betts & Haroutunian 1988).

The eddy diffusion method has been applied to atmospheric dispersion from point or line sources in the atmospheric boundary layer over flat terrain in different stability conditions. It gives good results for the whole mean concentration field $C^{(\ell)}(x,z)$ of ground-level line sources in conditions not far from neutral because $L_x^{(w)}$ tends to zero at the ground so that condition (3.48a) can be satisfied. From (3.47c) $C^{(\ell)}$ satisfies

$$U(z)\frac{\partial C^{(\ell)}}{\partial x} = \frac{\partial}{\partial z}\left(K_z(z)\frac{\partial C^{(\ell)}}{\partial z}\right) \tag{3.52}$$

where

$$K_z \partial C^{(\ell)}/\partial z \to 0 \quad \text{as} \quad z \to 0 \quad \text{(zero flux gradient at ground)}$$
$$C^{(\ell)} \to 0 \quad \text{as} \quad z \to h \quad \text{(zero flux at inversion)}$$

and

$$\int_o^h U(z) C^{(\ell)} dz = Q.$$

Even if the conditions are quite unstable (i.e. $h/L_{\mathrm{MO}} < -1$ when the conditions (3.48a,b,c) do not apply) or quite stable ($h/L_{\mathrm{MO}} \gtrsim 1$ when conditions (3.48b) does not apply), the ground-level concentrations $C^{\ell}(x)$ are modelled rather well, based on the comparison with the U.S. Prairie Gray field experiments (Nieuwstadt & Van Ulden 1978). The theoretical reasons why the eddy diffusion method is appropriate are reviewed by Pasquill & Smith (1983).

Because the integral scale of the transverse fluctuations $L_x^{(v)}$ is finite even for a ground-level source, (3.41a) cannot be used. However, (3.47a) can be justified from the point of view of statistical theory. On the same grounds, therefore, it can be shown that the concentration near a ground-level point source, is given by

$$C = \frac{\exp(-y^2/2\sigma_y^2)}{\sqrt{2\pi}\sigma_y}\, C^{(\ell)}(x,z) \tag{3.53}$$

where $C^{(\ell)}$ is the solution for the line source, (3.52). In the case of the neutral boundary layer, $C^{(\ell)}(x,z)$ can be approximated by the form (3.35b).

For elevated sources, the eddy diffusion method is incorrect near the source. It predicts $\sigma_z = \sqrt{K_z x/U}$, whereas from (3.3), $\sigma_z = \sigma_w x/U$. Consequently, some empirical methods have been proposed for modifying (3.47), the most common being to allow K_z, K_y to be functions of distance from the source as well as functions of z in the boundary layer (e.g. Smith & Blackall 1979; Hunt 1985a), but this approach breaks down when there are multiple or areas sources. Even far downwind of the source, (3.47) does not give satisfactory answers for convective and stable plumes, without further special adaptation. There are now standard integration procedures for computing solutions of equations such as (3.47c), but considerable care has to be taken both near the ground where $K_z \to 0$ and near the source. To overcome such problems the statistical theory results are used, especially in the latter case. Because of these difficulties, the numerical integration of (3.47) for calculating the concentration downwind of a point or line source belongs to the domain of computational specialists.

The considerable limitations to the use of K-models for elevated sources in non-neutral atmospheric conditions rules out the approach either as a practical or regulatory model or even as a research method for testing and developing regulatory models. At one time it was thought that K-models might be appropriate for these purposes, but recent research has shown that not to be the case.

(ii) Higher-order models

To overcome the limitations of eddy diffusion or K-theory defined by (3.47), more complex equations for the mean eddy fluxes F_{cy}, F_{cz} have been developed. Included on the l.h.s. of these differential equations are changes in F_{cy}, F_{cz} following the mean flow (e.g. terms like $U\partial F_{cy}/\partial x$) and on the r.h.s. are terms involving fluctuations in concentration $\overline{c'^2}$. Various approximations and 'closure' assumptions are made; some call for extra equations to determine $\overline{c'^2}$ which in turn involve further approximations and input, depending on the type of turbulence and concentration field (Pasquill & Smith 1983, p.102).

Higher-order models have been applied to elevated and ground-level sources (e.g. El Tahry et al. 1981; Hunt, Leibovich & Lumley 1983) even in convective conditions and have also been used over complex terrain. Most models require some empirical adjustment near point sources. Rather large codes are required and they are far from straightforward to write. Really these models are still at the research stage. For elevated sources in the CBL or SBL we have the same reservations about their uses for practical modelling or verification studies as for K-models.

3.5.4 Validation methods by numerical and experimental simulation

(i) Background to validation methods

In the 'practical' methods of §3.2, §3.3 and the stochastic research methods of §3.5.2, the relevant Lagrangian statistics of the velocity of the marked particles that pass through the source that are needed (e.g. $\sigma_v, \sigma_w, \overline{w^3}, T_L, L_x$, etc.) were derived from either measurements at fixed points in the flow (i.e. 'Eulerian' data) or flow models which gave these statistics of the turbulent flow. Relations such as (3.50) are assumed in the Eulerian to Lagrangian conversion. It is also assumed that at a point the statistics of the fluctuating velocity of 'marked' particles coming from the source are equal to the statistics of all fluid particles which pass through that point (van Dop et al. 1985). When the change of density of fluid elements is important, derivations based on (3.50) and (3.51) are more doubtful.

In the K-theory and higher-order eddy diffusion methods of §§3.5.3, assumptions are made about the relations between different Eulerian statistics of the turbulence and the concentration fluctuations (e.g. between terms like K_z, $\overline{w^2 c}$, $\overline{wc^2}$ and $\sigma_w^2, L_x, \overline{c^2}, \overline{wc}$, etc).

We have shown in §3.5.2, 3.5.3 that, despite these uncertainties, many different models describe the mean concentration C satisfactorily but there are also conditions and source locations when the models do not agree with measurements. Without further information it is usually not possible to explain precisely why the models fail or to predict when they will fail in new situations. Further comparisons with concentration experiments are not sufficient; what is needed is information about and investigation of the questionable assumptions between Lagrangian and Eulerian statistics and mixing processes. This can be provided by direct measurements of fluid 'particles' in the turbulence (Snyder & Lumley 1971) and/or by computing the movements of particles using a numerical simulation of the full velocity field $\underline{u}(\underline{x}, t)$(Squires 1989).

The other contribution provides detailed data of the mean concentration field $C(\underline{x})$ in steady flows or $C(\underline{x}, t)$ in unsteady flows. With the availability in the U.K. (at the CERL) of a stratified wind tunnel and water flume, atmospheric flows and dispersion can be modelled. Therefore, by both numerical and experimental simulation, it is possible now to study the flow field and diffusion in many different kinds of meteorological conditions that would be impossible in field experiments.

Recent new techniques have been developed for photographing and analysing automatically the trajectories of particles in laboratory turbulent flows to enable Lagrangian statistics to be measured (e.g. Fung & Perkins 1988). In the past, such studies required huge amounts of labour, as in Snyder & Lumley's (1971) experiment, and consequently were not often attempted.

The use of stratified wind tunnels and water flumes for these fundamental studies is likely (in our opinion) to be the best way of improving the 'stochastic' models in current use for research application. Methods for measuring the mixing rate of fluid particles ('Lagrangian' mixing) are not yet available, but they are likely to be so soon. Because the Eulerian K-theory and higher-order models have assumptions dependent on the concentration field, they can only be improved by measuring higher-order Eulerian statistics, not only in many different kinds of turbulent flow, but also for many kinds of concentration distribution.

The different methods for the numerical simulation of turbulent flow fields are now reviewed briefly.

(ii) Direct numerical simulation

Using the largest computers in the world (e.g. CRAY II or FUJITSU 200), the highest Reynolds number Re for turbulent boundary-layer flows that can be reliably computed is about 10^4. This is, of course, much lower than the value for atmospheric flows where $Re > 10^8$. Although large-scale features of the high Re flows can be reproduced approximately, significant details of the mean flow such as the full logarithmic profile cannot. In addition, the turbulence of low Re flows is quite different. For all these reasons, and bearing in the mind the fact that full details of the flow in a channel took 500 hours on the CRAY computer at the NASA Ames Research Centre (Moin & Kim 1982), it can be appreciated that direct numerical simulation is not a suitable tool for atmospheric dispersion modelling. However, for its range of validity, it gives the most complete information of any simulation, such as the recent computations of Lagrangian statistics by Squires (1989).

To overcome these limitations, approximations are made. One approach being tried in Japan, is to modify the finite-difference form of the equations which leads to flows with much of the small-scale structure characteristic of turbulent flows. It is being used to simulate flows over hills and buildings (e.g. Tamaru & Kuwahara 1988). However, this method takes more than 100 hours on a FUJITSU 200!

(iii) Large eddy simulations

The most wide-spread approximate method for the numerical simulation of turbulent flows is to 'filter' the equations of motion; these are then used to compute motion at larger scales and the small scales are represented by an eddy viscosity acting on the large scale motion. Typically, the flow field is divided into a large number of cuboid cells of the order of 10^5, so not unexpectedly these methods require large mainframe computers and many hours of run time.

This method enables most of the large-scale features of the mean flow and turbulence to be modelled, such as the logarithmic profile and the vertical profiles

of σ_w, σ_v, $L_x^{(w)}, L_x^{(v)}$, etc. (e.g. Mason & Thomson 1987; Schmidt & Schumann 1989). Recently it has proved possible to compute the smaller-scales needed to model the SBL (Derbyshire 1988).

Lamb (1982) used large eddy simulations to compute the mean concentration field from sources in the CBL (without shear). His results agree well with the laboratory and field experiments where $C(x, y, z)$ for metal chaff was measured by radar (Deardorff 1985). Mason et al.(1988) have recently used large eddy simulation for the CBL with shear and shown how lateral dispersion varies as h/L_{MO} changes from 0 to about -3.

Large eddy simulation methods are also proving valuable for computing complex processes such as entrainment into the boundary layer (Wyngaard 1988). They have also been used to yield higher-order Eulerian statistics for heat; but so far not for concentration from sources. As yet large eddy simulations have not been used to provide Lagrangian statistics needed by stochastic models, perhaps because it does not model the small scales of turbulence well and because of the long run time needed to obtain the statistics. These small scales determine how fluid elements accelerate (or the 'jumps' dW in velocity in the random flight methods) and are especially important for modelling concentration fluctuations and mixing processes.

(iv) Kinematic simulation

Finally, we mention new methods currently being developed which might provide turbulence research with much cheaper and faster computational simulations. The turbulent flow field is represented as a series of given functions of space and time $\underline{\phi}_n(\underline{x}, t, \lambda_n)$ whose amplitudes a_n are random as is the parameter λ_n i.e. $\underline{u}(\underline{x}, t) = \Sigma\, a_n\, \underline{\phi}_n(\underline{x}, t, \lambda_n)$. ϕ_n is chosen to satisfy mean conservation while statistics of a_n and λ_n are specified from measurements or computations of spectra. In principle, the method is similar to deriving mass consistent mean flow fields. It enables the smaller scales (with -5/3 inertial spectrum) to be readily simulated which cannot occur in other methods (Fung & Perkins 1988). Hypotheses central to random flight and K-model can be explored by these techniques (e.g. Turfus & Hunt 1987).

3.6 Dispersion Models in Complex Terrain

The models for dispersion over complex terrain fall into the same categories as those for dispersion over flat terrain.

3.6.1 Practical regulatory Gaussian plume models

In §2.2 the models of air flow over complex terrain used for regulatory dispersion modelling were described briefly as

(a) flat terrain plus warning, e.g. R199.

(b) deflection/impingement models, e.g. CRSTER, COMPLEX I and II. These flow models are used in conjunction with Gaussian plume models, in the form

$$C = \frac{Q}{\sqrt{2\pi}U_o(z_s)\sigma_y} \exp\left(-\frac{y^2}{2\sigma_y^2}\right) G_z(z, z_\psi) \qquad (3.54a)$$

where

$$G_z(z, z_\psi) = \frac{1}{\sqrt{2\pi}\sigma_z}\left[\exp\left\{-\frac{(z-z_\psi)^2}{2\sigma_z^2}\right\} + \exp\left\{-\frac{(z-z_{\psi_i})^2}{2\sigma_z^2}\right\}\right] \qquad (3.54b)$$

where z_ψ is the height of the mean streamline ψ_s through the source. The image source at $z_{\psi_i} = z_\psi - 2n$, where $n = (z_\psi - z_s)$ is the distance from ψ_s to the surface where $z = z_s(x, y)$ (see Fig.2.11). Note that the plume is assumed to be straight and parallel to the wind at the source point. Formulae for the height z_ψ are given in §2.2.4(i)(b) and illustrated in Fig.2.21.

The limitations of these models are that they consider the change in the distance $n(= z_\psi - z_s)$ between the mean streamline and the surface (i.e. the diffusion factor Δ_n) but they ignore the counteracting effect of convergence and divergence of streamlines (i.e. the factor Δ_{CD}).

Therefore models such as COMPLEX I,II can predict the high surface concentration associated with plume impaction approximately (as in Fig.2.9a, Fig.2.10a for the lower source height) but for plumes passing over hills they are very unreliable because of the quite inadequate estimation of the plume height z_ψ (compare Figs. 2.9a, 2.10a with Fig.2.21).

In R199 a 'flagging' procedure was given warning when the R91 model is invalid because of hills. That warning could be revised to give an estimate of the magnitude of errors caused by ignoring terrain effects.

3.6.2 Gaussian plume model for complex terrain

(i) Thin plume approximation

To rectify two of the main deficiencies of simple plume deflection models, such as COMPLEX I,II, models have been developed which make use of calculations of the actual mean flow streamlines, their convergence and divergence and the variation of the turbulence along them, i.e. models in which the diffusion factors Δ_n and Δ_{CD} can vary. But, as with G.P.M.s on level ground, the plumes are assumed to be 'thin' in the sense that the effects of the variations of mean wind speed $U(z)$ and turbulence across the plume are assumed to be small, i.e.

$$\Delta_{WS},\ \Delta_{T2},\ \Delta_K,\ \Delta_{T3} << 1\ . \tag{3.55}$$

In fact, just as over level ground in the NBL, these factors may be of order unity, but only have a moderate effect on concentration profiles.

The general form for the mean concentration distribution in a plume that travels over a hill, but does not impact, is

$$C(x,y,z) = \frac{Q}{\sqrt{2\pi}U_\psi\sigma_y}\exp\left(-\frac{(y-y_\psi)^2}{2\sigma_y^2}\right)G_z(z_1,z_{\psi_i},z_\psi) \tag{3.56}$$

where U_ψ is the mean velocity along ψ_s, $y_\psi(x)$ is the y co-ordinate of the mean streamline (Fig.2.11), and G_z is given by (3.54b). This formula can be used in neutral, weak and moderately stable conditions, but it is only appropriate if the slope is small (say less than 1/3). For steeper slopes, local co-ordinates normal and parallel to the surface should be used to replace z and y. When the slope is steep enough for the mean to streamline impact onto the hill, (3.56) is not valid near the point of impaction.

Equation (3.56) was derived from statistical theory by Hunt & Mulhearn (1973) and generalised to three-dimensional flow by Hunt (1985a) for the situation where $n/\sigma_z >> 1$ and the conditions in (3.55) are satisfied. In that derivation σ_z, σ_y are related to correlations of the turbulent velocity field. If the travel time, t, of particles is long compared with the Lagrangian time $T_L(\simeq L_x/\sigma_w)$,

$$\sigma_\alpha^2 = \frac{2}{\beta_\alpha^2}\int_o^t \beta_\alpha^2(t')K_\alpha(t')dt' \tag{3.57a}$$

where K_α is the turbulent diffusivity defined in terms of correlations,

$$t = \int_{x_s}^x \frac{dx'}{U_u} \qquad \beta_\alpha = \exp\left(-\int_o^t \frac{\partial U_\alpha(t')}{\partial x_\alpha}dt'\right) \tag{3.57b,c}$$

and α may be y or z (so that $U_y = V$, $U_z = W$, $x_y = y$, $x_z = z$). For flat terrain this reduces to the homogeneous result of (3.7), i.e.

$$\sigma_\alpha^2 = 2\int_o^t K_\alpha(t')dt$$

(Hunt 1985a). Note that (3.57c) depends on $\partial V/\partial y$ and $\partial W/\partial z$ i.e. the rate at which streamlines converge and diverge in the horizontal and vertical directions.

The effect of the hill surface on the concentration is usually modelled by an image source at z_{ψ_i}. If the eddy diffusion model is applicable (3.1) (with small variations of K, i.e. $\Delta_K << 1$), then for certain ideal two-dimensional flows the image solution of (3.54b) is the theoretical solution (Hunt & Mulhearn 1973). Consequently this result is generally used, even for non-ideal flows.

For practical purposes, the expression for σ_z, σ_y, (3.57) is not convenient. Other expressions that are broadly consistent have been derived, based on the plume depth and width functions $\sigma_z(x), \sigma_y(x)$ for flat terrain, e.g.

$$\sigma_z^2(x) = \hat{\sigma}_z^2(t) - \frac{2}{U_\psi^2}U_o^2\int_o^t \hat{\sigma}_z^2(t')\frac{\partial W}{\partial z}(t')\beta_z^2 dt' \qquad (3.58)$$

where U_o is the wind speed over flat terrain at the source height z_s, and β_z is given by (3.57c),

$$t = \int_{x_s}^x \frac{dx'}{U_\psi(x')} \quad , \hat{\sigma}_z^2(t) = 2\int_o^t K_z(t')dt'$$

To obtain the correct result near a point or line source, K_z can be regarded as a function of travel time from the source. In general K_z changes over a hill with the change being a function of source height and capable of being estimated from models of mean flow and turbulence over hills.

To a first approximation the diffusivity is assumed to be the same as over level ground, so that

$$\hat{\sigma}_z(t) = \sigma_z^{(o)}(t). \qquad (3.59a)$$

but a better approximation is

$$\hat{\sigma}_z(t) \simeq \frac{\langle\sigma_w(t)\rangle}{\sigma_w^{(o)}}\,\sigma_z^{(o)}(t), \qquad (3.59b)$$

where $\langle\sigma_w(t)\rangle$ is the average value of σ_w along the plume centreline, and $\sigma_z^{(o)}, \sigma_w^{(o)}$ are the plume depth and vertical turbulence in the absence of the hill. Equation (3.59b) was found by Britter to give a good estimate of growing plumes impinging onto a body (Hunt, Britter & Puttock 1979).

It is certainly a poor approximation to assume no variation in σ_z over terrain, i.e. $\sigma_z(x) = \sigma_z^{(o)}(x)$, and simultaneously to allow for n and U_ψ to vary.

Results using (3.56), (3.58) and (3.59b) for plumes passing over hills were computed by Hunt & Richards (1980) and are given by Carruthers et al. (1989).

Formulae similar in form to (3.57) are used in the EPA CTDM model, but the principles behind the calculation of $K_z(t), K_y(t)$ are in general not clear. In that model the dispersion is source-height dependent in complex terrain but not over level terrain, because the model has to agree with the current standard EPA Gaussian plume model for flat terrain.

(ii) Extending the thin plume approximation by plume splitting

When the air flow is strongly stably stratified, i.e. ($F_H < 1$), it has a different structure below and above the dividing streamline where $z = H_c = H(1 - F_H)$ (see Fig.2.10 and §2.2.3d). Below H_c the air flow is approximately homogeneous and therefore a plume approaching a hill can split if some part of the plume is on the stagnation streamline (Fig.3.21a). Therefore downwind of the stagnation region at $x_{\rm stag}, y_{\rm stag}$ it is necessary to represent the original plume as two separate plumes and these can still be modelled approximately as Gaussian plumes with image plumes inside the hill. (We outline here the kind of approach that is used in the EPA code *CTDM* . It is our opinion that this simple approach could be implemented with a suitable flow field model for strong stratification.)

For $x < x_{\rm stag}$, C is given by (3.56); for $x > x_{\rm stag}, C = C^*$, where

$$C^* = \frac{Q^*}{2\pi U_\psi \sigma_n \sigma_z}\left[\exp\left(-\frac{(n-\alpha_\psi n_\psi)^2}{2\sigma_n^2}\right) + \exp\left(-\frac{(n+\alpha_\psi n_\psi)^2}{2\sigma_n^2}\right)\right] \times \exp\left(-\frac{(z-z_s)^2}{2\sigma_z^2)}\right) \qquad (3.60)$$

where

$$U_{\bar\psi} = U(n = n_{\bar\psi}) \qquad (3.61a)$$

is the mean velocity at $n_{\bar\psi}$, the mean plume displacement from the hill surface defined by

$$n_{\bar\psi} = \int_o^\infty nC\ dn \Big/ \int_o^\infty C\ dn, \qquad (3.61b)$$

In general $U_{\bar\psi}$ is not the same as U_ψ because $n_{\bar\psi} \neq n_\psi$. Also n_ψ is different for $y > y_{\rm stag}$, $y < y_{\rm stag}$. In (3.60), if $y_\psi - y_{\rm stag} > 0$ at $x_{\rm stag}$, for

$$\begin{aligned} y > y_{\rm stag}, \quad \alpha_\psi = 1, \quad Q^* = Q_1 \\ y < y_{\rm stag}, \quad \alpha_\psi = 0, \quad Q^* = Q_2 \end{aligned} \qquad (3.62a)$$

and if $y_\psi - y_{\rm stag} < 0$ at $x_{\rm stag}$, for

$$\begin{aligned} y > y_{\rm stag}, \quad \alpha_\psi = 0, \quad Q^* = Q_1 \\ y < y_{\rm stag}, \quad \alpha_\psi = 1, \quad Q^* = Q_2 \end{aligned} \qquad (3.62b)$$

The values of Q_1 and Q_2 can be calculated from the relation $Q_1 + Q_1 = Q$ and the fluxes of the plume that pass each side of the hill, i.e.

$$\left\{\begin{matrix} Q_1 \\ Q_2 \end{matrix}\right\} \simeq \int_o^\infty \int_o^\infty U_{\bar{\psi}} C^* \, dn \, dz \quad \text{for} \quad \left\{\begin{matrix} \mathrm{y} > \mathrm{y_{stag}} \\ \mathrm{y} < \mathrm{y_{stag}} \end{matrix}\right\} \tag{3.62c}$$

The growth of σ_n is determined by the oncoming turbulence, the turbulence generated at the hill surface and the convergence/divergence of the mean flow around the hill and may be calculated by approximate formulae of the form of (3.57). At x_{stag} the value of σ_n at x_{stag} for the two plumes depends on how much of the plume is on each side of the stagnation line.

A different split plume model is required when the source height is above the critical height H_c because that part of the plume above H_c passes over the hill, while that art below impacts on the hill and splits (Fig.3.21b). In this case, for $x < x_{\mathrm{stag}}$, C is given by (3.56) ; for $x > x_{\mathrm{stag}}$

$$\begin{aligned} C &= C_+^* \quad \text{for} \quad \mathrm{z} > \mathrm{H_c} \\ &= C_-^* \quad \text{for} \quad \mathrm{z} < \mathrm{H_c}. \end{aligned} \tag{3.63a}$$

where

$$C_+^* = \frac{Q_+^*}{2\pi U_{\psi+}\sigma_y\sigma_z} \exp\left(-\frac{(y-y_{\psi+})^2}{2\sigma_y}\right) G_z(z, z_{\psi+}, z_{\psi i}) \tag{3.63b}$$

and $z_{\psi+}$ is the same as z_ψ in (3.54b) and σ_y, σ_z are calculated as in (3.57). The mean streamline for the upper plume has to be defined by the mean height of dispersing material above $z = H_c$ near $x = x_{\mathrm{stag}}$. Thus, at x_{stag}

$$\left\{\begin{matrix} y_{\psi+} \\ z_{\psi+} \end{matrix}\right\} = \int_{-\infty}^\infty \int_{z_*}^\infty \left\{\begin{matrix} y \\ z \end{matrix}\right\} C dz \, dy \Big/ \int_{-\infty}^\infty \int_{z_*}^\infty C \, dz \, dy. \tag{3.64a}$$

where C is given by (3.56).

For $z < H_c, C_-^*$ is as defined in (3.60, 3.61, 3.62), with the mean streamline at x_{stag} defined by

$$\left\{\begin{matrix} y_{\psi-} \\ z_{\psi-} \end{matrix}\right\} = \int_{-\infty}^\infty \int_0^{z_*} \left\{\begin{matrix} y \\ z \end{matrix}\right\} C dz \, dy \Big/ \int_{-\infty}^\infty \int_0^{z_*} C \, dz \, dy. \tag{3.64b}$$

The strengths of the plume passing over the hill Q_+^* and around the hill, Q_-^*, are given by the flux crossing the stagnation line. As an approximation

$$Q_+^* \simeq \int_{-\infty}^\infty \int_{z_c}^\infty U_{\psi+}(x_{\mathrm{stag}}, y_{\psi+}, z_{\psi+}) C \, dz \, dy \tag{3.65}$$

and

$$Q = Q_+^* + Q_-^* \, . \tag{3.66}$$

(If Q^*_- is greater than Q^*_+, it would be preferable to compute Q^*_- and thence Q^*_+ from (3.66).)

Downwind of a hill in strongly stratified flow the plumes below $z = H_c$ are dispersed across the recirculating, turbulent flow region of the hill. At this stage and further downwind, the plume no longer appears as two plumes, but rather as three – the third being the plume associated with the recirculating region. Sufficiently far downwind these three plumes can be regarded as a single plume again (Snyder & Hunt 1984).

For these Gaussian 'split-plume' models it is necessary to know various aspects of the flow field. When a plume is below the dividing streamline in a strongly stable flow ($z_s < H_c$) and in consequence impacts on a hillside, it is necessary to know the mean flow and turbulence around the hill at the source height z_s.

If the plume is near or above H_c, the whole flow over the hill top above H_c must be modelled along with the flow around the hill at height z_s. This could be computed from an interpolated wind field model, a simplified theoretical model (such as a modified form of FLOWSTAR), or a full numerical solution of the differential equations (see §2.2.3). (It would be inconsistent to use a G.P.M. for dispersion together with a numerical or 'primitive' equation model, because having used a large computer for the flow field, it would be natural to compute the diffusion a code of similar complexity.)

In the CTDM approach, the whole hill shape is modelled as an ellipsoid and then a theoretical solution for an ellipsoid is used. For the proposed FLOWSTAR approach only the hill shape at z_s would have to be modelled as a simple shape. This would avoid the inflexibility of modelling the whole hill as an ellipsoid (as required by CTDM) and it would require less input.

When modelling plumes downwind of hills, the details of the flow over the hill are not usually necessary. Some bulk feature of the hill such as its height, length, breadth, etc. are sufficient to define approximate wake solutions and thence the downwash etc. (cf. the model of Moore & Lee 1982; Hunt, Britter & Puttock 1979).

In more complex terrain, plumes from sources may be dispersed around and over several hills. It is likely that the split-plume approach can be used in these situations, as well. (This is one kind of model to be studied in a forthcoming project at the University of Cambridge, funded by M.O.D.)

Note that in these plume impaction/ strongly-stratified flow models, account is taken of drainage winds. This is an important effect for large hills and mountains and leads to oncoming plumes being dispersed down the slope below the source height. Some K-theory models for this process have been developed, including an unpublished one by Hunt.

3.6.3 Gaussian puff models for complex terrain

When the speed, direction and stability of the wind vary significantly during the time of travel (T) from the source to the receptor, and also vary over time periods of interest for dose calculations, it is necessary to use unsteady diffusion models, such as puff models (cf.§3.4). There are conditions and situations when puff models may be very suitable in complex terrain, and others when they are not. For unsteady conditions in steady convective turbulence, with weak vertical shear (e.g. $h/L_{MO} < -1$ in A,B conditions) puffs are not significantly distorted as they move over scales of 10km or more. In such cases puff models are quite practical, provided the unsteady wind field is defined in space and time. A scenario that satisfies these criteria is an urban or developed area in complex terrain where there are many measuring points, situated in lower latitudes than the UK where strong convection is common. For example, in Los Angeles, Athens and in the area around Denver, Colorado, there are enough measurements for interpolating wind field models to be used (see §2.2.5(c)) (Restrepo 1987).

Many flows in complex terrain vary over the diurnal cycle because of up slope and downslope and sea breeze effects (§2.2.4(iv)). If the terrain is such that the pollution can be trapped over several diurnal cycles, then puff modelling can give some estimates provided the wind field is known. However, there are periods when the air flow is stably stratified and highly sheared (in two horizontal directions) and then the puff model needs careful consideration. In most cases where detailed wind fields are available for such complex flow situations, they have been computed on large main frame computer models with 'primitive' equations (e.g. using mesoscale models reviewed in §2.2.5d(iii)). Mesoscale models contain modules for computing the diffusion from sources, and therefore they are suitable for these situations over these larger length and time scales. (The U.K. mesoscale model is used for this purpose (Golding 1987).)

3.6.4 Research diffusion models for complex terrain

(i) Stochastic models (including random flight models)

The general principles of random flight models were discussed in §3.5.2. They require as input the mean flow $U(\underline{x},t)$ and certain statistics of the turbulence. Unlike some eddy diffusion models (§3.5.3), the assumptions are not dependent on the concentration distribution. In complex flow where the mean flow changes direction and the turbulence is highly inhomogeneous, all the required statistics (for equations of the form of (3.46) cannot be derived from most computational flow field models such as interpolating models, FLOWSTAR-type models, or mesoscale

models. In particular in wakes or recirculating regions, these quantities have not been studied adequately.

In the laboratory some random flight simulations were made by Frost (1981) for dispersion downwind of a source within a recirculating region. Only the r.m.s. turbulent velocities and length scales were provided from experimental measurements. Although he used the simple (but in principle less correct) form of the principal equation, (3.45), the agreement with measurements was satisfactory.

Thomson (1986) used a complex random flight model for diffusion in Welsh valleys, in conjunction with the mean flow obtained from a 'primitive' differential equation flow-field model of Mason & King (1984). He did not have all the information required for his full model so many estimates and approximations had to be made. Even so, the trends of his results agreed with the field measurements and he was able to draw some interesting general conclusions about how vertical and horizontal diffusion increased. However, it seems possible that many of these results could have been obtained by simpler approaches, because of the sparsity of the data and the methods of estimating required statistics.

Random flight methods could well be used to great advantage for the unsteady impaction of plumes onto hills stable conditions when there is some meandering of the wind direction. They are good for indicating the effects of the different scales of turbulence in the problem (in the approach flow, at the surface and in the wake). These methods could well help improve the practical Gaussian plume models for this type of problem.

(ii) Eddy diffusion (K-theory)

Criticism of these models made in §3.5.3 is less relevant in flow over complex terrain. The diffusion factors representing the effects of the convergence and divergence of the streamlines, Δ_{CD}, and inhomogeneity of the turbulence, Δ_{T2}, are particularly important in controlling the depth and width of the plume, so that provided reasonable estimates of K_z, K_y are made over the flow field, it appears that K-theory models can give useful estimates.

Effectively then K-theory is better in complex terrain than over level terrain. This surprising conclusion has been tested in the laboratory by comparing K-theory models with experimental measurements of plumes impacting onto hills/buildings and used for plumes in wakes. Except very close to the source, the agreement has been satisfactory, and comparable with the agreement from more complex models based on statistical theory or flow simulation of the particle trajectories (Hunt 1981, 1985a; Turfus 1986).

At present K models are used in many complex flow-field dispersion codes. It is our opinion that if the mean flow is correct, and if the distribution of the length scale and intensity of the three components of the turbulent velocities are

approximately modelled, so as to estimate K_x, K_y (and in some cases K_x), then most features of dispersion in complex terrain can be estimated.

This is the approach used in most mesoscale models (e.g. Pielke 1983) and by models based on mass consistent flow fields (e.g. Moussiopoulos & Flassak 1986). The parameterisation of K_y and K_z in these models is quite primitive and does not reflect recent research on turbulent diffusion in complex conditions, so there could be some improvement of these in future.

A feature of K-theory models is that they cannot use detailed turbulence statistics or models of eddy structure. Therefore these models may be superceded in the future.

If more detailed information can be obtained (such as spectra from measurements or statistical theory), then the larger scale lateral dispersion can be better estimated from statistical theory than from K-theory models.

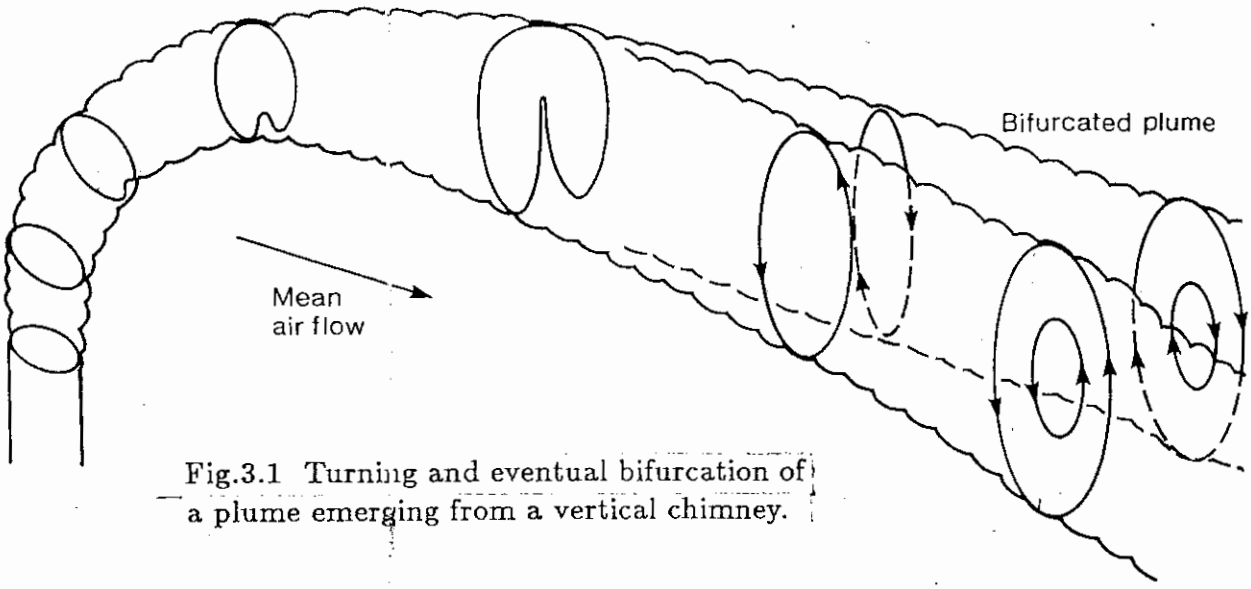

Fig.3.1 Turning and eventual bifurcation of a plume emerging from a vertical chimney.

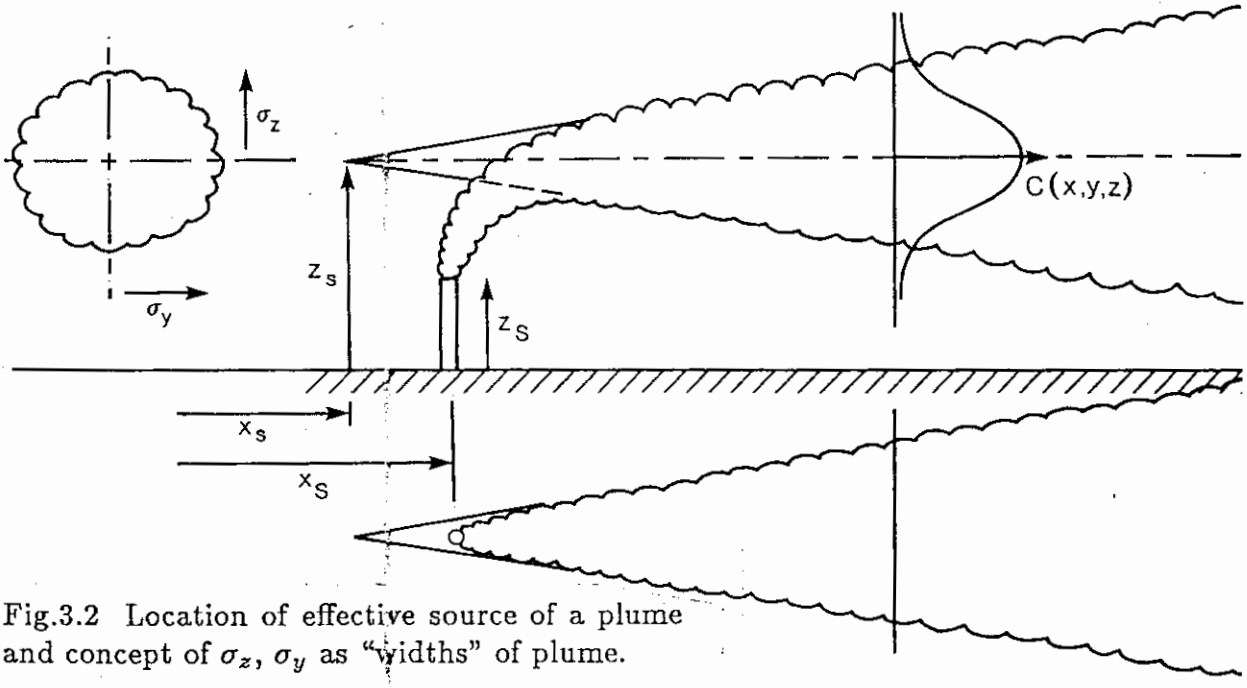

Fig.3.2 Location of effective source of a plume and concept of σ_z, σ_y as "widths" of plume.

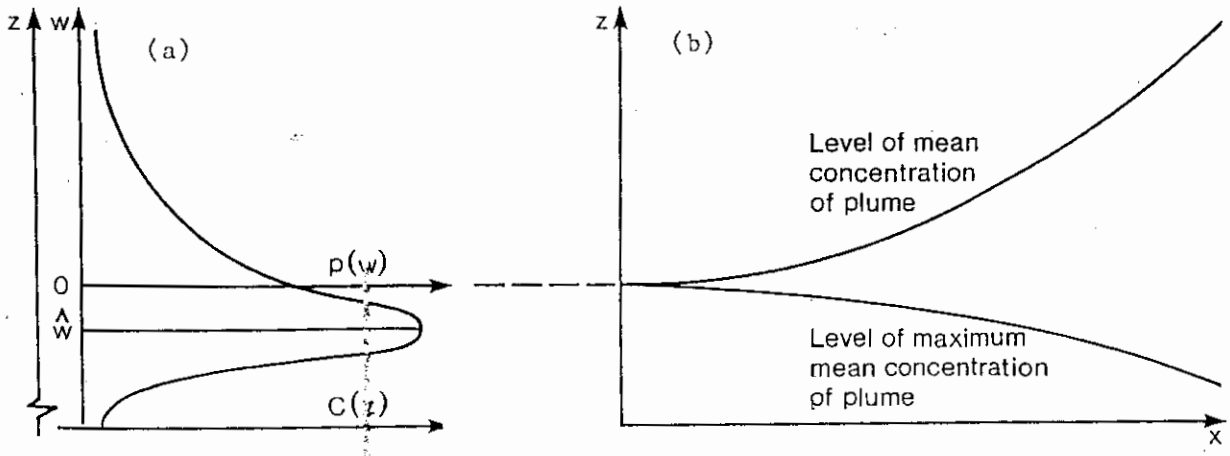

Fig.3.3a Probability distribution of vertical velocity fluctuations $(p(w) - w)$ and vertical profile of concentration $(C(z) - z)$ for plume in convective boundary layer. $\hat{w}$ = mode of $p(w)$.

Fig.3.3b Variation of level of mean concentration and maximum concentration of plume downwind of source (from Hunt 1982a).

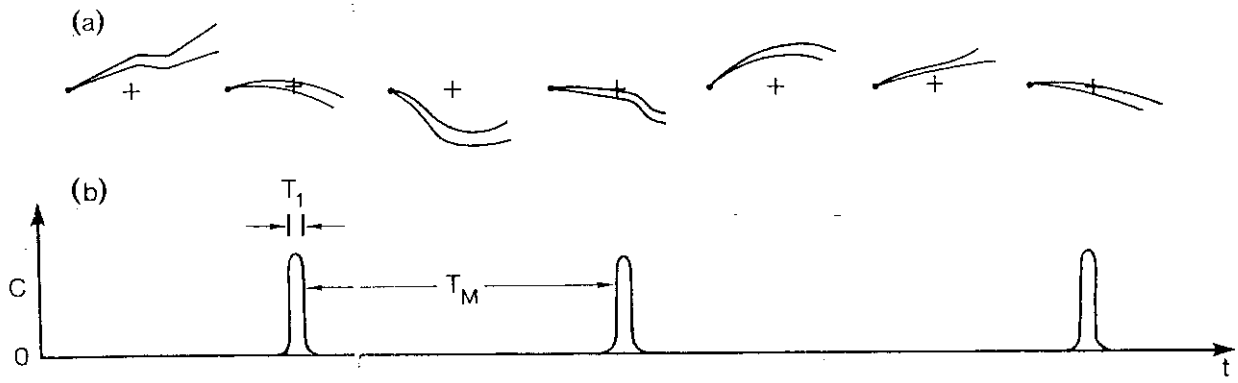

Fig.3.4 Time series of a meandering narrow plume. (a) "Snapshots" of plume at different times (+ is receptor point where concentration C is measured). (b) Variation of C with time. $T_1 \approx$ time during which plume is swept across receptor; $T_M \approx$ meander period of plume. (From Hanna 1986.)

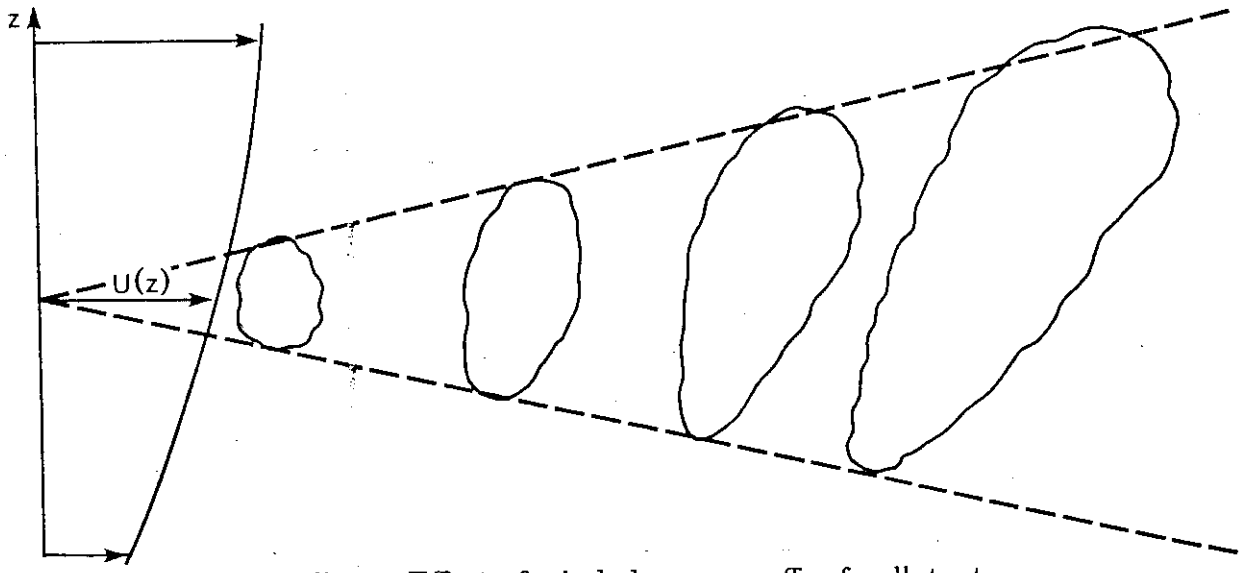

Fig.3.5 Effect of wind shear on puffs of pollutant.

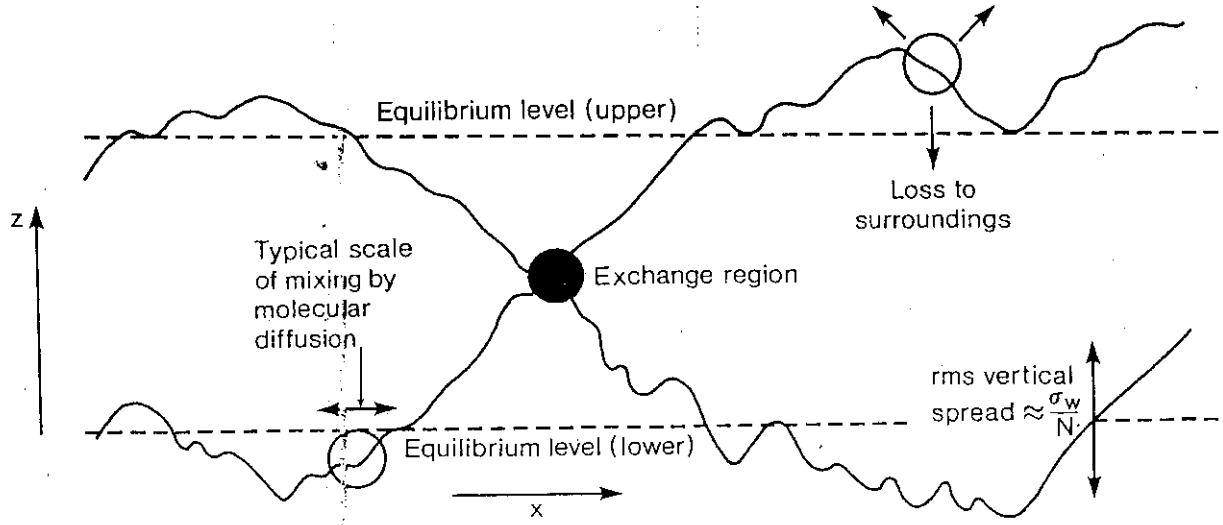

Fig.3.6a Transfer of heat or density between fluid elements when they have restricted vertical motions in strong stable stratification (from Hunt 1982a).

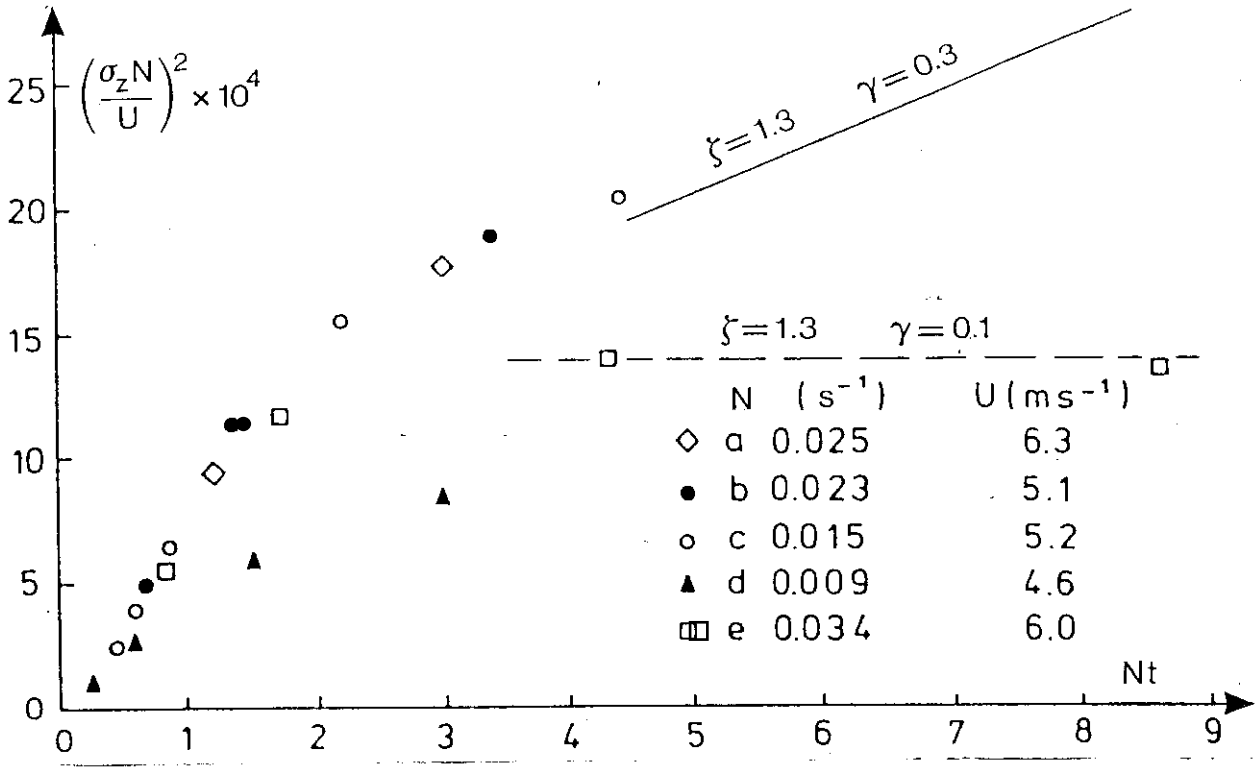

Fig.3.6b Field measurements of $(\sigma_z N/U)^2$ (by Hilst & Simpson 1958) plotted against Nt and compared with prediction of equation (3.14).

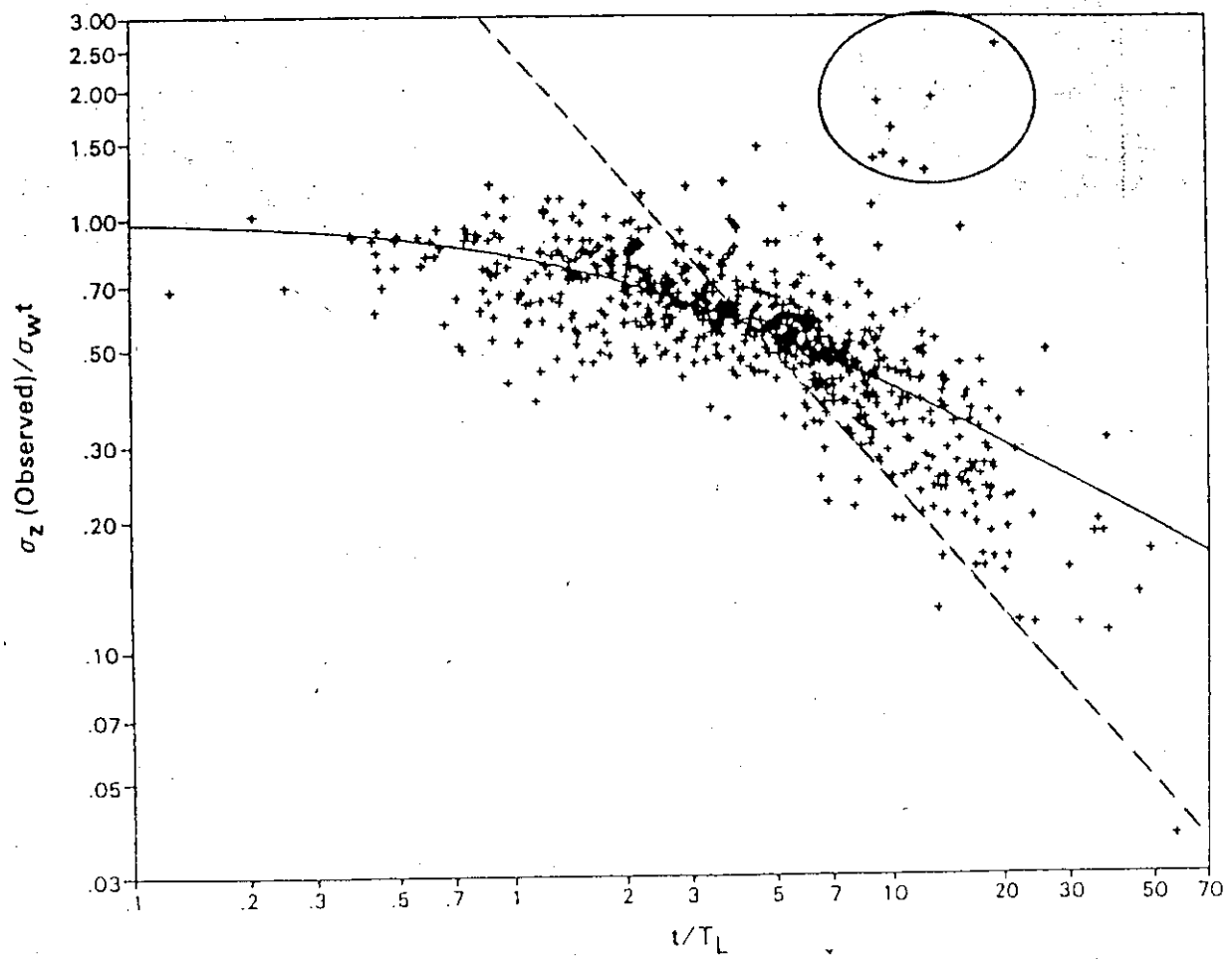

Fig.3.6c Variation of $\sigma_z/\sigma_w t$ with t/T_L where $t = x/U$ and $T_L = 0.27/N$. ——— theoretical prediction of Venkatram et al.(1984); - - - - prediction of equation (3.14).

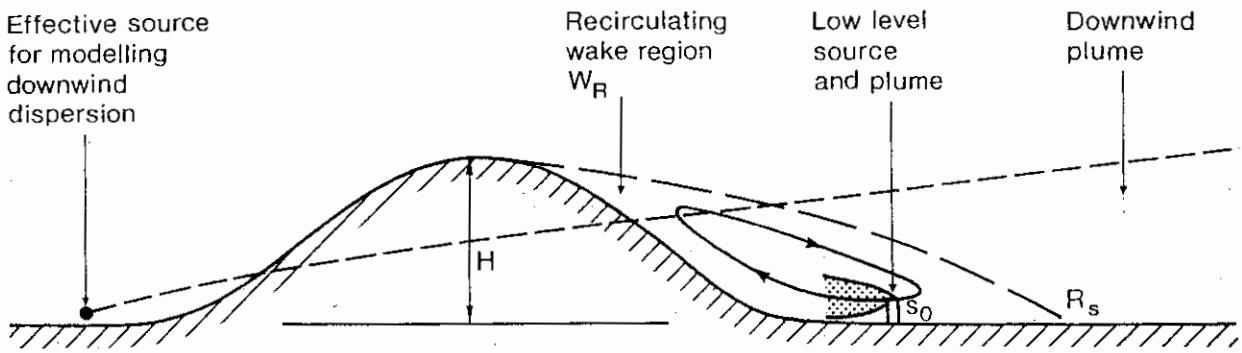

Fig.3.7a Position of effective source for modelling dispersion from a source located in the central part of the recirculating wake region W_R downwind of a hill and the plume from a low-level source in W_R.

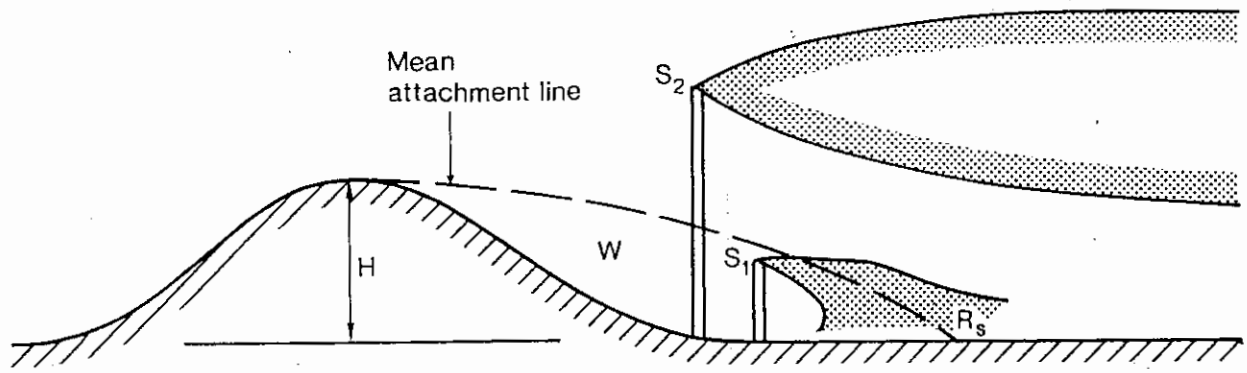

Fig.3.7b Effect of W_R on a source S_1 located near but below the mean attachment line which forms the upper boundary of W_R and on a source S_2 located far above the mean attachment line.

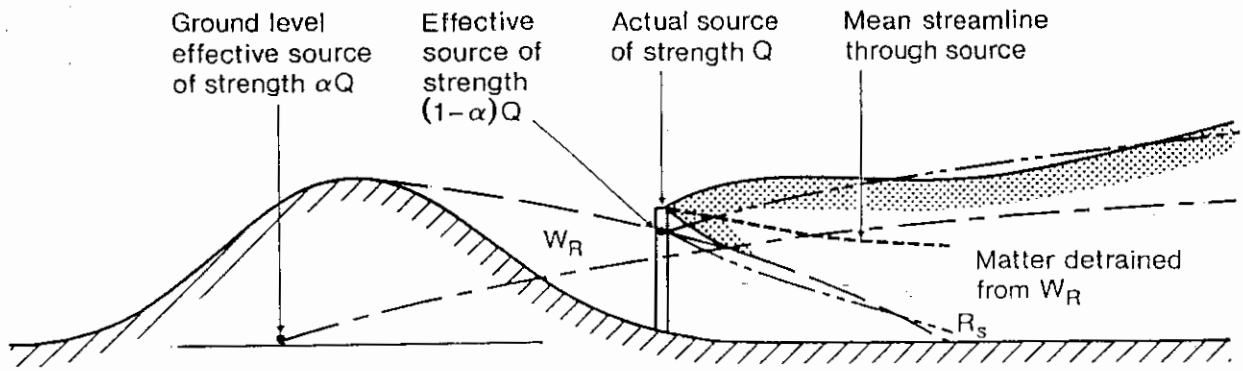

Fig.3.7c Modelling a plume from a source of strength Q located just above the mean attachment line by a source of strength $(1-\alpha)Q$ located below real source and a ground-level source of strength αQ located upwind $(0 < \alpha < 1)$.

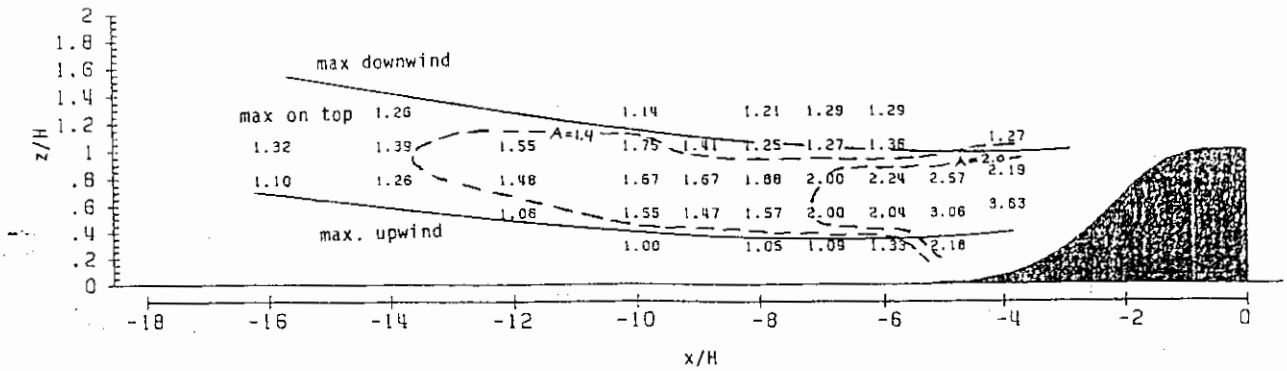

Fig.3.8 Terrain amplification factors for sources located upwind of an axisymmetric hill. The solid lines divide the region into areas where the source produces $C_{g\ell\ \mathrm{mx}}$ upwind of the hilltop, between the hilltop and the separation point on the lee slope, and downwind of the hill. Each number is the increase in $C^{(o)}_{g\ell\ \mathrm{mx}}$ for a source at that position.

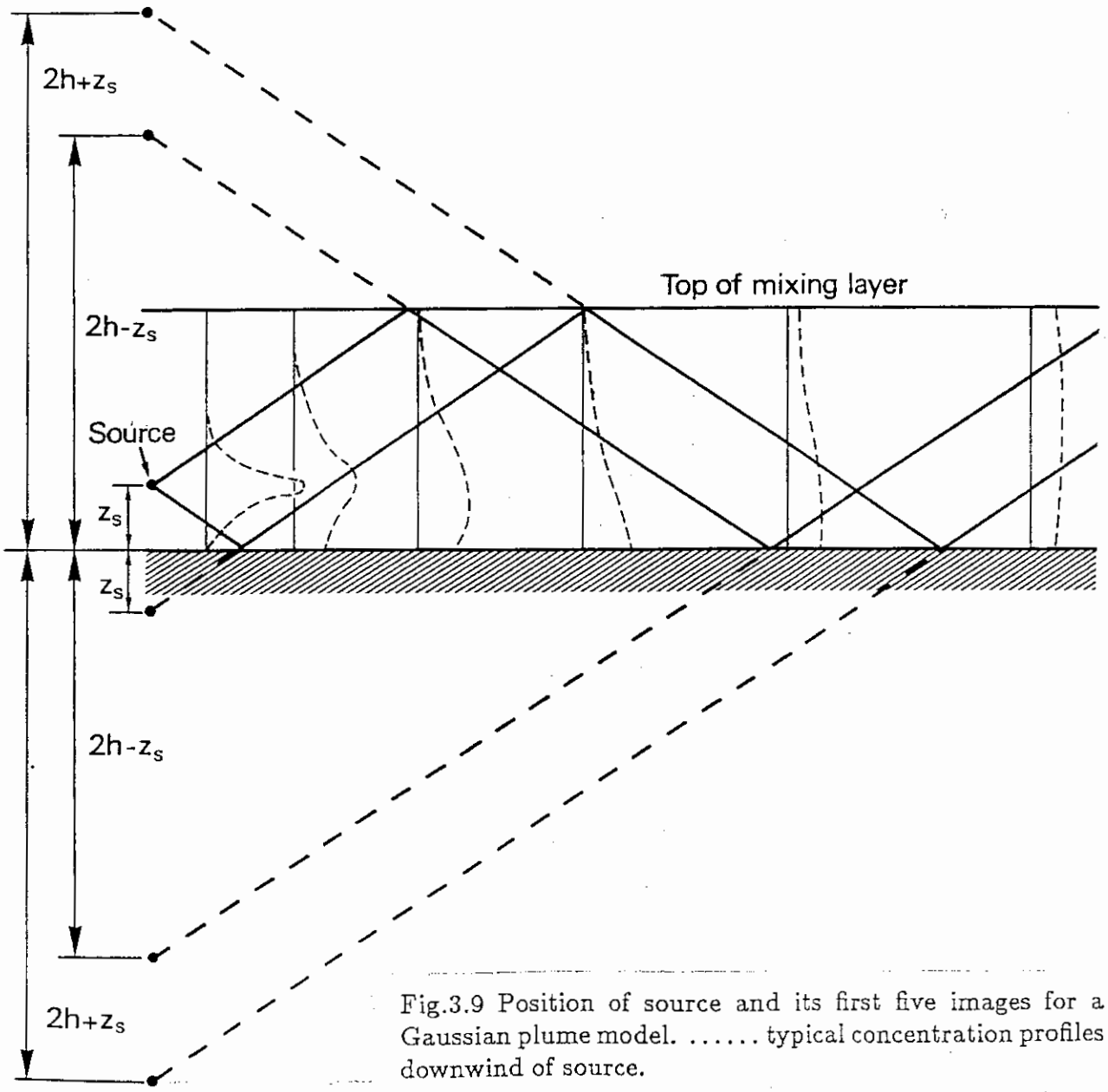

Fig.3.9 Position of source and its first five images for a Gaussian plume model. ..... typical concentration profiles downwind of source.

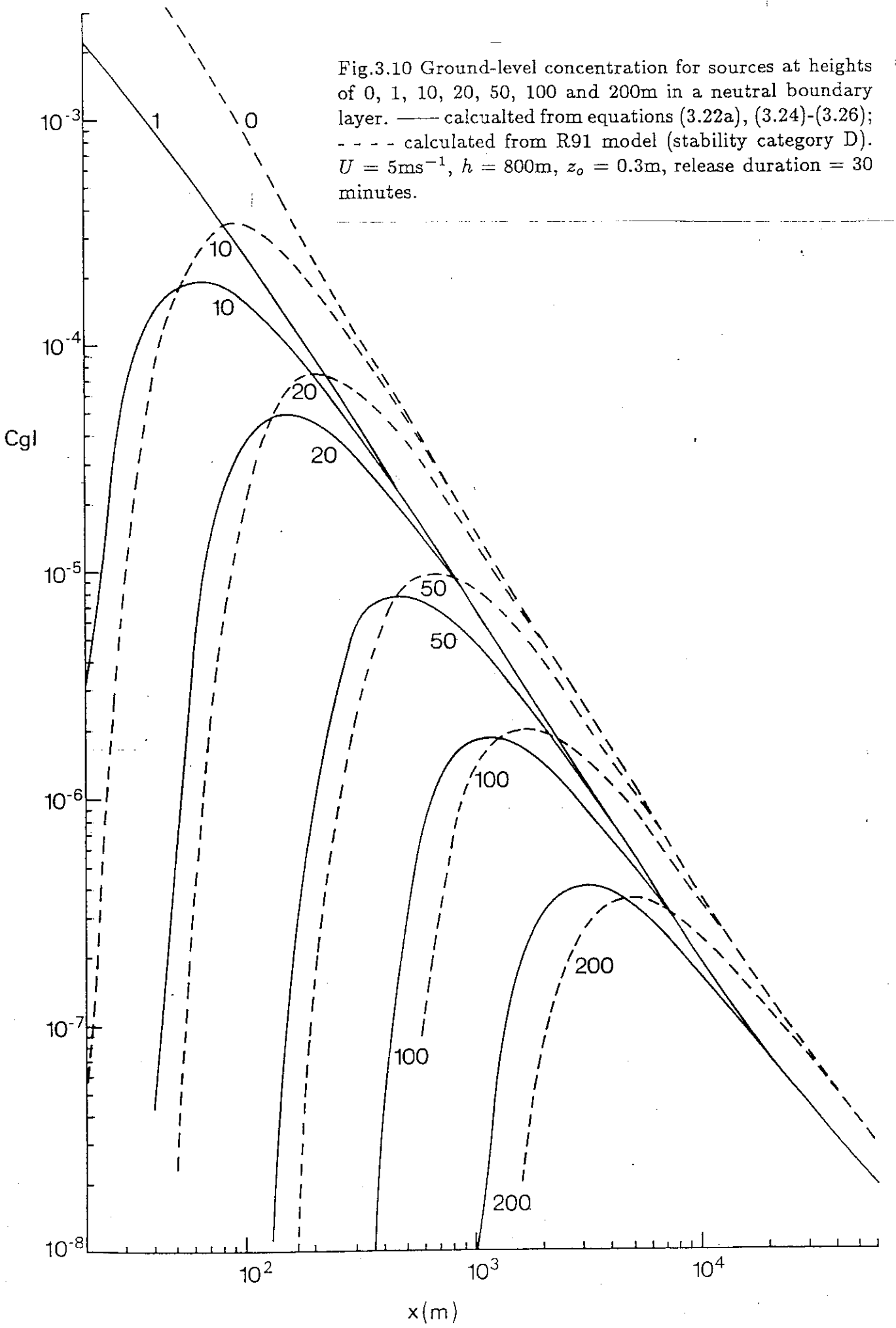

Fig.3.10 Ground-level concentration for sources at heights of 0, 1, 10, 20, 50, 100 and 200m in a neutral boundary layer. —— calcualted from equations (3.22a), (3.24)-(3.26); - - - - calculated from R91 model (stability category D). $U = 5\text{ms}^{-1}$, $h = 800\text{m}$, $z_o = 0.3\text{m}$, release duration = 30 minutes.

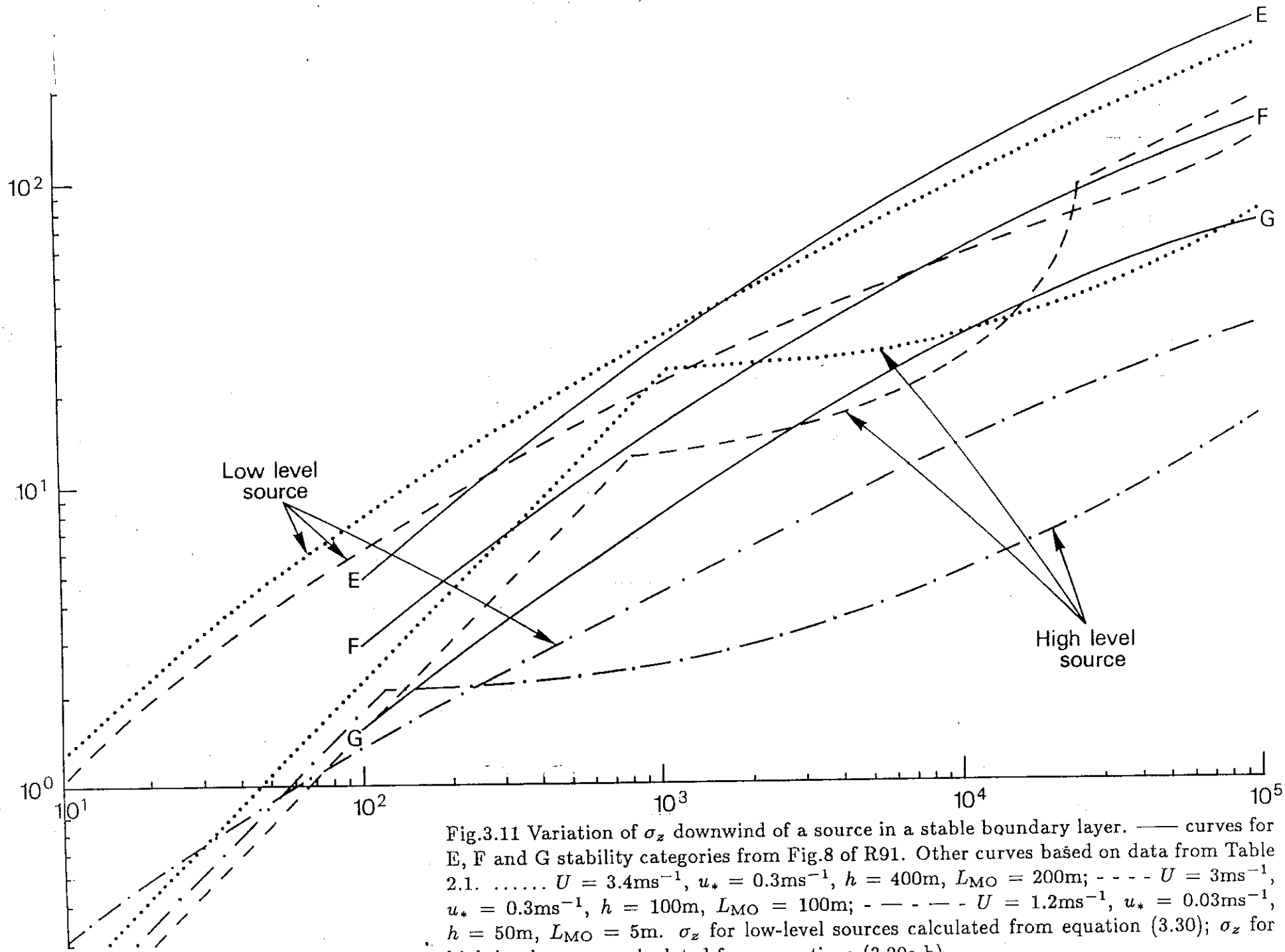

Fig.3.11 Variation of σ_z downwind of a source in a stable boundary layer. —— curves for E, F and G stability categories from Fig.8 of R91. Other curves based on data from Table 2.1. ..... $U = 3.4\text{ms}^{-1}$, $u_* = 0.3\text{ms}^{-1}$, $h = 400\text{m}$, $L_{MO} = 200\text{m}$; - - - - $U = 3\text{ms}^{-1}$, $u_* = 0.3\text{ms}^{-1}$, $h = 100\text{m}$, $L_{MO} = 100\text{m}$; - — - — - $U = 1.2\text{ms}^{-1}$, $u_* = 0.03\text{ms}^{-1}$, $h = 50\text{m}$, $L_{MO} = 5\text{m}$. σ_z for low-level sources calculated from equation (3.30); σ_z for high-level sources calculated from equations (3.29a,b).

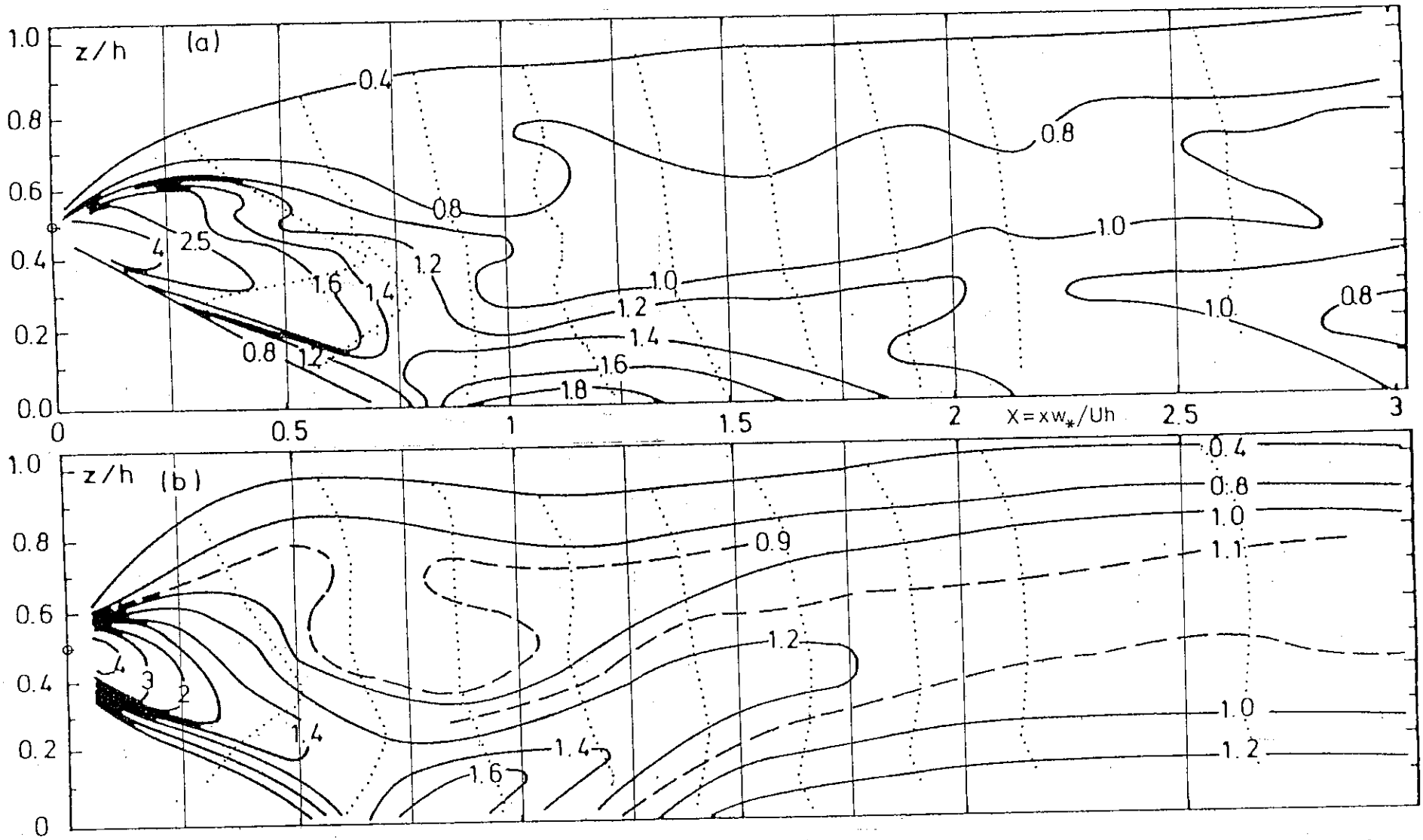

Fig.3.13 Contours of cross wind integrated concentration C' in a convective boundary layer. ..... vertical profile of C'. (a) Calculations by Lamb (1982); (b) Laboratory experiments by Willis & Deardorff (1981).

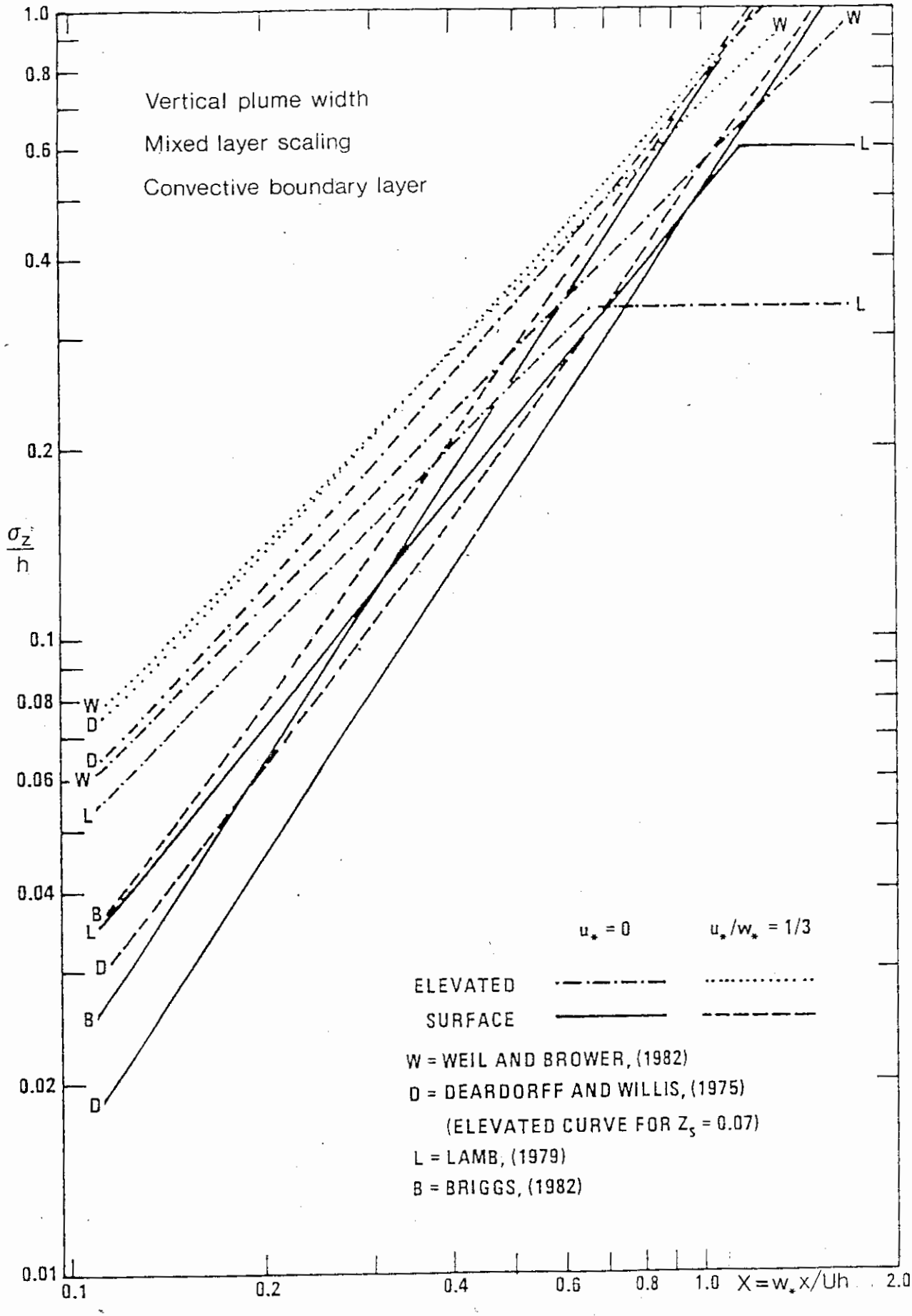

Fig.3.13 Variation of σ_z downwind of a source in a convective boundary layer expressed in similarity co-ordinates (from Briggs 1985).

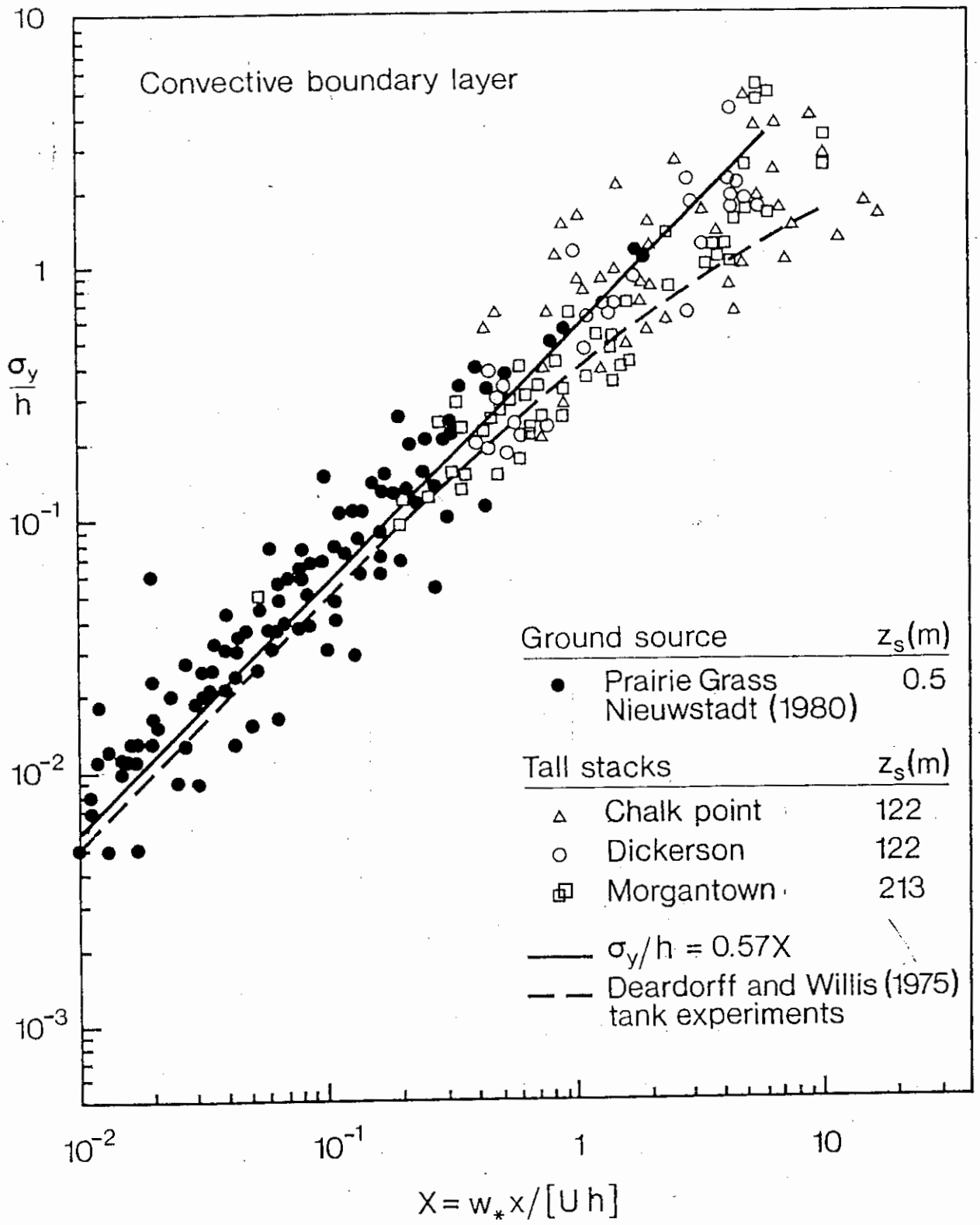

Fig.3.14 Variation of σ_y downwind of a source in a convective boundary layer expressed in similarity co-ordinates (from Weil & Brower 1984).

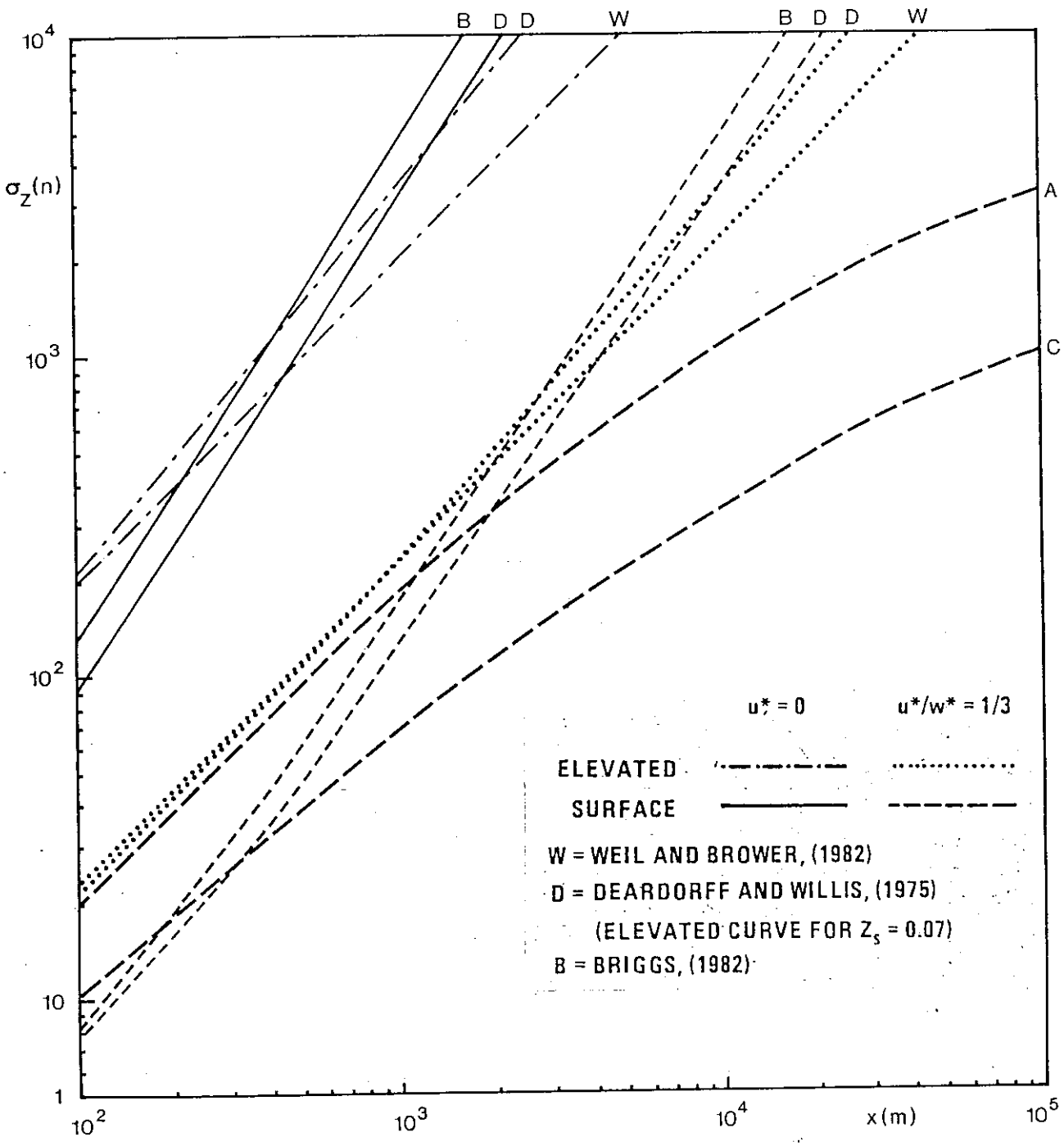

Fig.3.15 Results of Fig.3.13 plotted as σ_z against x and compared with distributions shown in Fig.8 of R91.

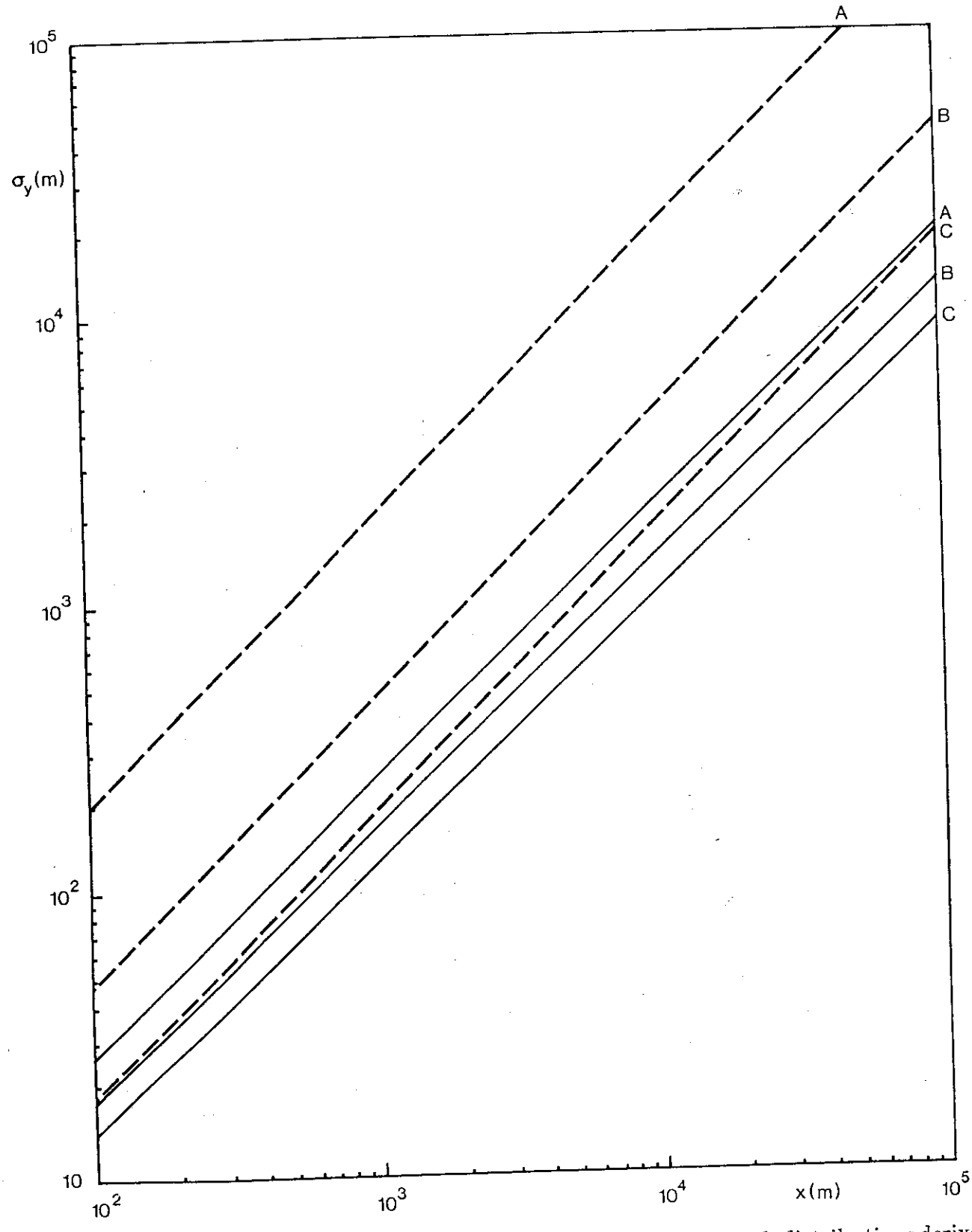

Fig.3.16 Results of Fig.3.14 plotted as σ_y against x and compared with distributions derived from Fig.10 of R91 for a 30-minute release period.

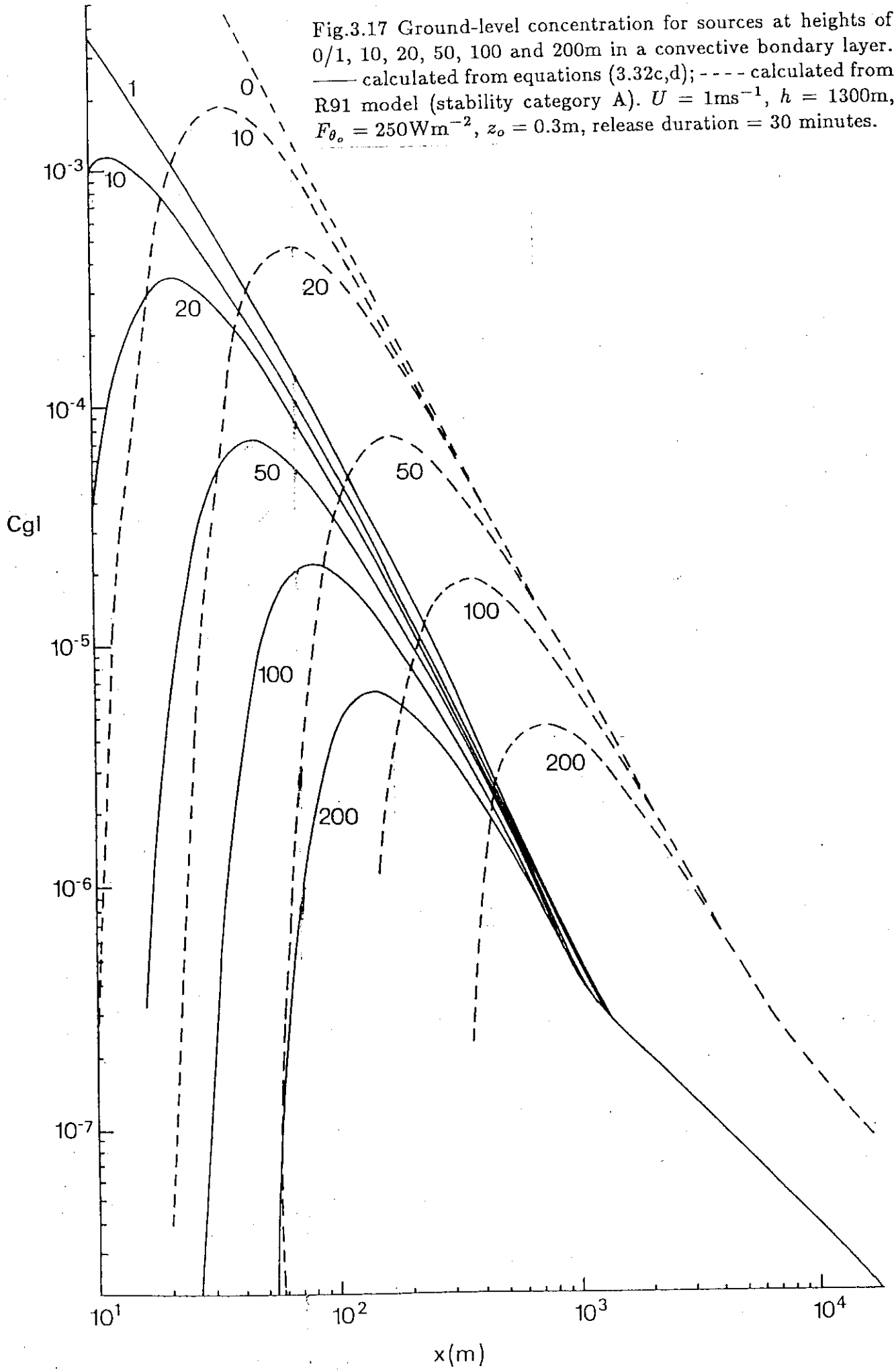

Fig.3.17 Ground-level concentration for sources at heights of 0/1, 10, 20, 50, 100 and 200m in a convective bondary layer. —— calculated from equations (3.32c,d); - - - - calculated from R91 model (stability category A). $U = 1\text{ms}^{-1}$, $h = 1300\text{m}$, $F_{\theta_o} = 250\text{Wm}^{-2}$, $z_o = 0.3\text{m}$, release duration = 30 minutes.

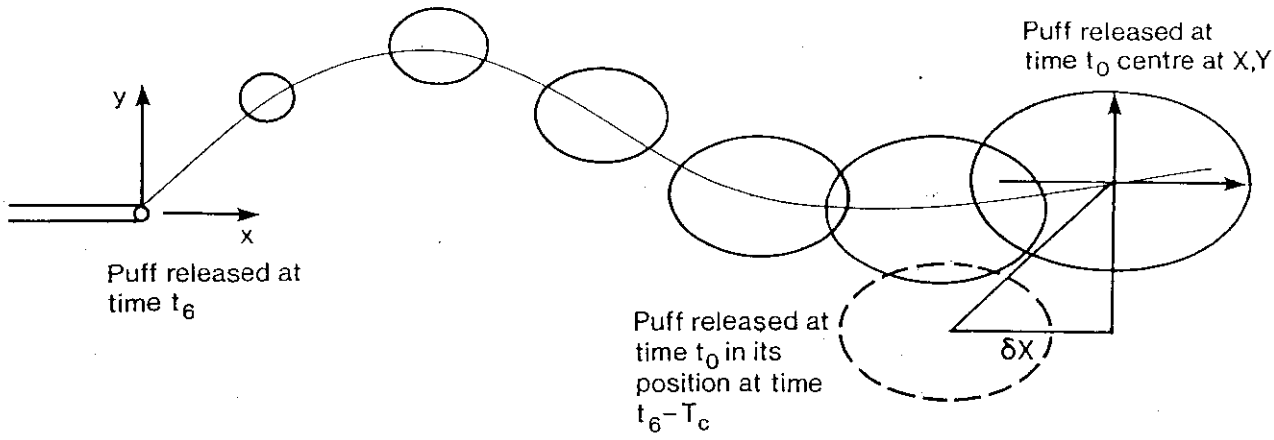

Fig.3.18 Distribution and growth of a sequence of puffs emitted from a source.

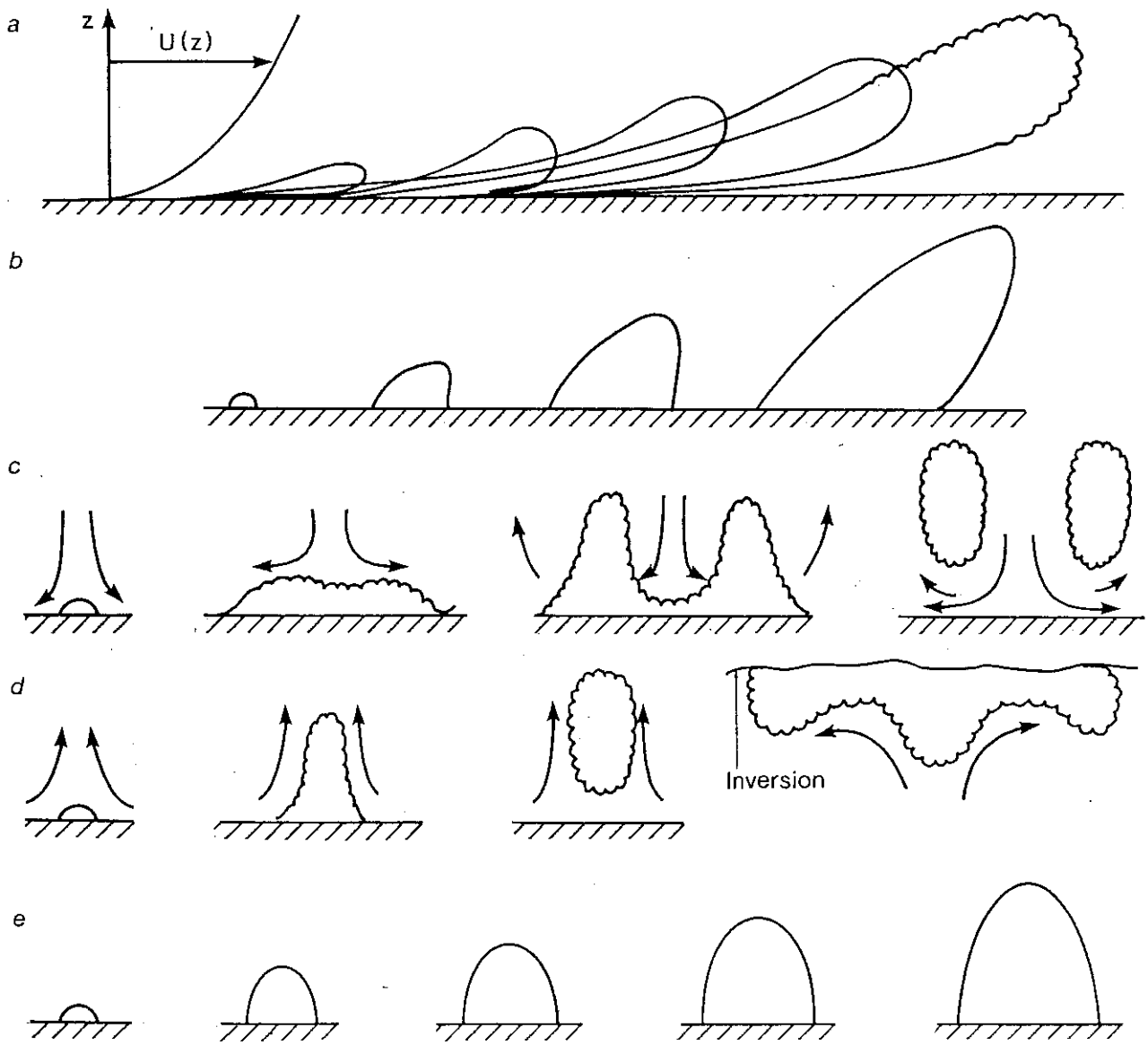

Fig.3.19 (a) Distortion of puffs from a ground-level source by shear in neutral and stable boundary layers. (b) Model of puffs shown in Fig.3.19a by a number of idealised puffs. (c) Behaviour of a puff located beneath a downdraft in a convective boundary layer. (d) Behaviour of a puff located beneath an updraft in a convective boundary layer including its distortion when it reaches the inversion. (e) One way of modelling behaviour of puffs in a convective boundary layer.

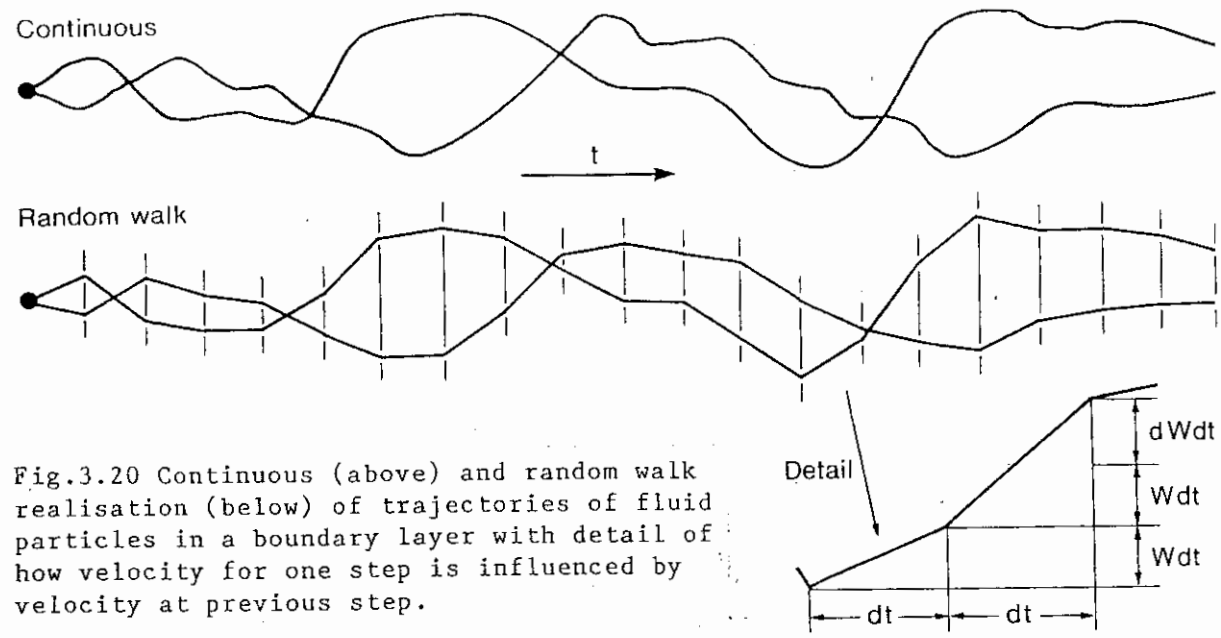

Fig.3.20 Continuous (above) and random walk realisation (below) of trajectories of fluid particles in a boundary layer with detail of how velocity for one step is influenced by velocity at previous step.

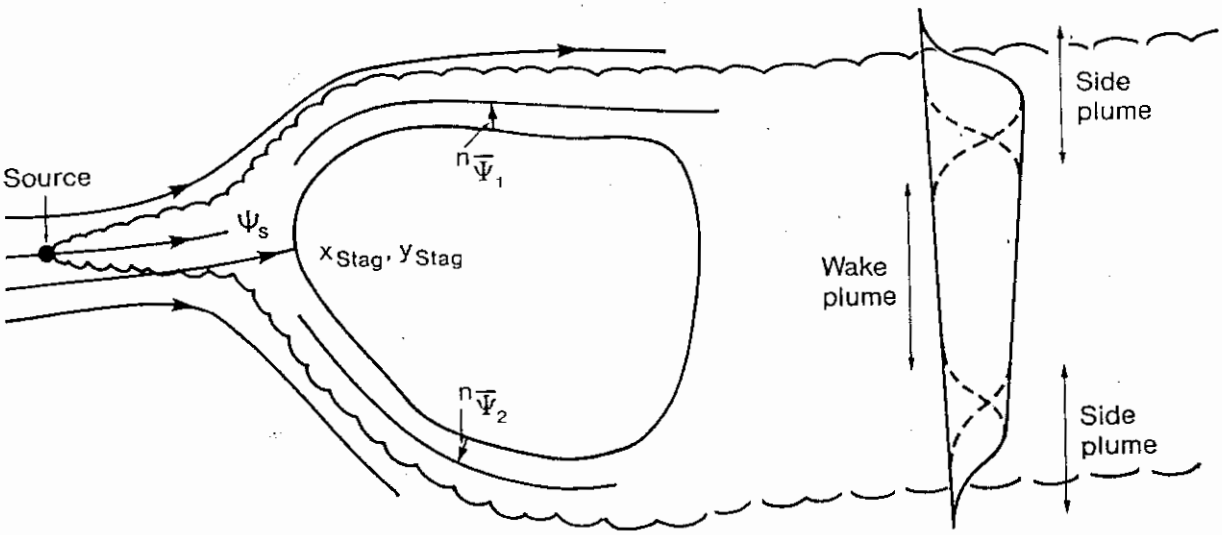

Fig.3.21a Two-way split of a plume from a source located below the dividing streamline in a stable boundary layer and upwind of a three-dimensional hill. The contributions to the downwind plume from the two parts of the divided plume and the plume from the wake are indicated.

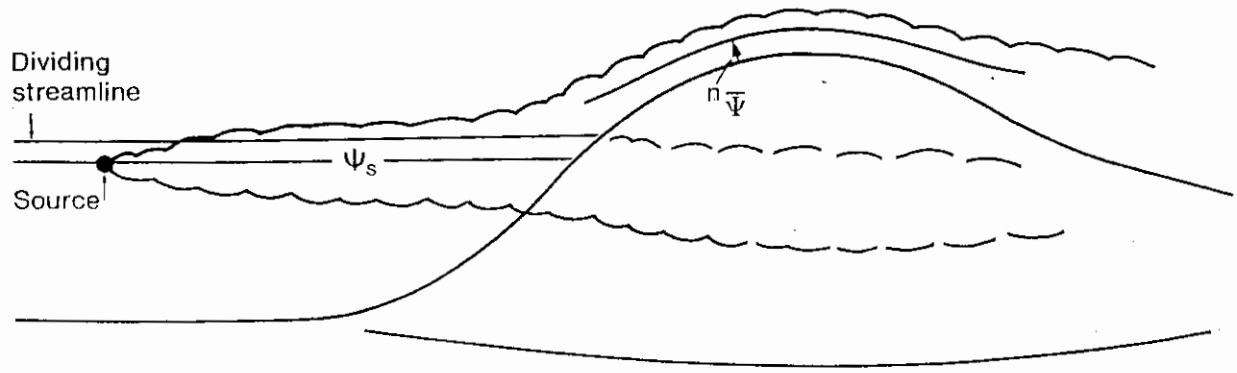

Fig.3.21b Three-way split of a plume from a source located near the level of the dividing streamline in a stable boundary layer and upwind of a three-dimensional hill.

4. CONCLTJSIONS ABOUT BENEFITS AND COSTS OF MORE COMPLEX MODELS

4.1 Improvements in boundary-layer description

A better boundary-layer 'definition' based on the parameter h/L_{MO} could be implemented. This is described in §2.1. The advantages would then be that:

(i) it would be based on recent and authoritative research and an unusual degree of consensus among researchers. **As** the review of Kretzschmar & Mertens (1984) makes very clear, the current U.K. classification is not a world-wide or even a European standard. There would be a great advantage in moving to a world standard and in ensuring that the U.K. was participating fully in the change;

(ii) it would allow better use to be made of local measurements of the boundary-layer depth h, and, perhaps, encourage such measurements to be made (in France they are standard at nuclear power stations);

(iii) it would provide a basis for specifying dispersion parameters as a function of the height of the source;

(iv) it is essential for matching boundary-layer models to models for air flow and dispersion over complex terrain which incorporate variations with time of the boundary layer (of great importance for long-range transport) and the effects of precipitation (which are both included in models being developed by groups at Imperial College and the U.K. Meteorological Office);

(v) the computational cost would be much the same as for the model based on the Pasquill-Smith approach;

(v) it would put in a standard scientific form the advanced methods (especially (ii) and (iii)) introduced by D.J. Moore (Moore & Lee **1982)** for dispersion from CEGB fossil fuel power stations.

4.2 Improvements in air flow modelling

In §§2.2–2.5 it was shown that it is possible to develop general and practical air-flow models over many kinds of complex surface, such as hills, roughness and temperature changes. **A** number of different models are currently available and others are being developed. We summarised the reasons for developing these for dispersion modelling in §§2.3–2.5, The principal points of those sections are:

(i) complex terrain often gives rise to the largest surface concentrations of pollution, or the most anomalous dispersion. Even quite simple models can account for many particular effects as recent field studies in the U.S.A. and U.K. have shown;

(ii) complex terrain effects within 30km of sources also need to be considered in probabilistic risk assessment models. In these models, many situations and cases need to be considered, and simple and fast wind-flow and dispersion models capable of covering most of the likely cases are needed;

(iii) simple and user-friendly schemes for small computer systems are becoming available to model most of the common air-flow situations, to indicate the situations where the models are inadequate, and to model in an *ad-hoc* fashion particular critical situations.

The only disadvantages of using air-flow and dispersion models incorporating real terrain effects is that they are more complex and lengthy to program and operate.

The disadvantage of using simple models is that they may not account for all the effects included in large-scale more computer-intensive models, such as the U.K. Meteorological Office Mesoscale model. However, this model in particular is not suitable for the application considered here because it does not permit a sufficiently detailed description of the terrain over length scales less than 15km, which are of interest in site specific studies. It should be noted that most simple models can be 'flagged' to indicate where their use is uncertain.

4.3 Improvements in dispersion modelling

With better models for the airflow in the atmospheric boundary layer over complex terrain, the evidence is that the present methods of R91, when used for the prediction of dispersion and surface concentrations, can be improved even when Gaussian plume modelling of the dispersion process is used.

For air flow over flat uniform terrain, the main improvements would be in modelling the extreme conditions of strongly stable and unstable flows, and the changes caused by elevated sources (see §§3.2, 3.3). It would be possible to give some indication of the considerable uncertainty in estimating dispersion in strong stable boundary layers.)

For air flow over complex terrain, better air-flow models would enable systematic changes to be estimated of the distribution of ground-level concentration, and deposition, as well as occasional extremely high concentrations on sloping terrain in highly stable conditions.

Sections 3.3 and 3.4 of this review, and that by White et al. (1985), of the more advanced dispersion models currently available suggest that it would be possible to develop significantly improved models for predicting dispersion in the boundary layer and over flat and complex terrain.

More advanced but more scientifically-based air flow models and dispersion models for isolated sources would also help improvements in the modelling of related problems, such as plume rise, dense gas dispersion, dispersion from area sources, and more complex processes in the atmosphere, such as chemical change, washout, deposition, etc.

4.4 Effort and costs of developing a more advanced dispersion model

The main conclusions of this work are that it is indeed possible to develop a more advanced scheme than that described in R91 for predicting the airflow and dispersion up to about 30km from sources in the U.K. and that such a scheme could be implemented on a personal or micro-computer. It should be borne in mind that, to develop such a system, it is necessary to understand and thoroughly appreciate the underlying relevant research work and the attributes and limitations of existing models. Progress could best be made by means of collaboration between the NRPB and other relevant expert groups and by making use of current developments in the U.S.A. and other European countries.

We suggest that it would be both possible and desirable to incorporate as submodels in this scheme processes such as air flow, dispersion, deposition, etc., at present being studied by other U.K. expert groups.

5. ACKNOWLEDGEMENTS

The writing of this report has benefitted from helpful discussions with many other research workers studying various aspects of pollutant dispersion, but especially Drs. J.A. Jones, P.J. Mason, F.B. Smith, H.M. ApSimon, M.L. Williams, B.Y. Underwood, and
W.H. Snyder and colleagues at the U.S. EPA.

The typing and preparation were done by Naomi Coyle and Margaret Downing.

REFERENCES

ADMWG(87)P1. (1987) Proposal for a complex dispersion model.

ApSimon, H.M., Goddard, A.J.H. & Wrigley, J. (1985) Long range atmospheric dispersion of radio isotopes – I. The MESOS model. Atmos. Env. 19, 99-111.

ApSimon, H.M., Kitson, K., Fawcett, M. & Goddard, A.J.H. (1984) Development of a prototype mesoscale computer model incorporating treatment of topography. Commission of the European Communities, Report EUR 9503 EN.

Apsley, D.D., Hunt, J.C.R. & Robins, A.G. (1989) (In preparation.)

Arya, S.P.S. (1984) Parametric relations for the atmospheric boundary layer. Boundary Layer Met. 30, 57-73. / Proc. 29th Oholo Biol. Conf. on Boundary Layer Structure – Modeling and Application to Air Pollution and Wind Energy. Zichron Ya'Acov, Israel. eds. H. Kaplan, N. Dinar. Reidel.

Arya, S.P.S. & Shipman, M.S. (1981) An experimental investigation of flow and diffusion in the disturbed boundary layer over a ridge. Part I. Mean flow and turbulence structure. Atmos. Env. 15, 1173-1184.

Atkinson, B.W. (1981) Mesoscale Atmospheric Circulations. Academic Press.

Betts, P.L.& Haroutunian, V. (1988) Finite element calculations of transient dense gas dispersion. pp.349-384 Inst. of Mathematics and Its Applications Conf. on Stably Stratified Flow and Dense Gas Dispersion, ed. J.S. Puttock. Clarendon Press.

Blumen, W. (1983) Monthly Weather Rev. 111, 1052-

Bouwmeester, R.J.B. (1978) Wind characteristics over ridges. Ph.D. Dissertation, Dept. Civil Eng., Colorado State University, Fort Collins (also as Rep. CER77-78 RJB RNM VAS51).

Bradley, E.F. (1983) The influence of thermal stability and angle of incidence on the acceleration of wind up a slope. J. Wind Eng. Ind. Aero. 15, 231-242.

Briggs, G.A. (1982) Similarity forms for ground-surface surface-layer diffusion. Boundary Layer Met. 23, 489-502.

Briggs, G.A. (1984) Plume rise and buoyancy effects. pp.327-366 (Chap.8), Atmospheric Science and Power Production, ed. D. Randerson. Rep. DOE/TIC-27601, Tech. Info. Center, office of Sci. & Tech Info., US Dept. of Energy.

Briggs, G.A. (1985) Analytical parameterizations of diffusion: the convective boundary layer. J. Clim. Appl. Met. 14, 1167-1186.

Britter, R.E., Hunt, J.C.R. & Richards, K.J. (1981) Air flow over a two-dimensional hill: studies of velocity speed up, roughness effects and turbulence. Q.J. Roy. Met. Soc. 107, 91-110.

Britter, R.E. & McQuaid, J. (1988) Workbook on the dispersion of dense gases. Health & Safety Executive Report.

Brost, R.A. & Wyngaard, J.C. (1978) A model study of the stably stratified planetary boundary layer. J. Atmos. Sci. 35, 1427-1440.

Caneill, J.Y. & Buty, D. (1988) Numerical simulation of the planetary boundary layer over complex topography. Paper 4.3 Proc. 8th Symp. on Turbulence and Diffusion, April 1988, San Diego, California. American Met. Soc.

Carruthers, D.J. & Choularton, T.W. (1982) Air flow over hills of moderate slope. Q.J. Roy. Met. Soc. 108, 603-624.

Carruthers, D.J. & Choularton, T.W. (1983) A model of the seeder-feeder mechanism of orographic rain including stratification and wind drift effects. Q.J. Roy. Met. Soc. 109,575-588.

Carruthers, D.J. & Hunt, J.C.R. (1986) Velocity fluctuations near an interface between a turbulent region and a stably stratified layer. J. Fluid Mech. 165, 475-501.

Carruthers, D.J., Hunt, J.C.R. & Holroyd, R.J. (1989) Airflow and dispersion over complex terrain. Proc. 17th NATO-CCMS Int. Tech. Meeting on Air Pollution Modelling and its Applications. Sept. 1988, Cambridge. Plenum.

Carson, D.J. (1973) The development of a dry-inversion-capped convecting unstable boundary layer. Q.J. Roy. Met. Soc. 99,450.

Carson, D.J. & Richards, J.R. (1978) Modelling surface turbulence fluxes in stable conditions. Boundary Layer Met. 14, 67-81.

Castro, I.P. & Snyder, W.H. (1982) A wind-tunnel study of dispersion from sources downwind of three-dimensional hills. Atmos. Env. 16, 1869-1887.

Caughey, S.J. & Palmer, S.G. (1979) Some aspects of turbulence structure through the depth of the convective boundary layer. Q.J. Roy. Met. Soc. 105, 811-827.

Caughey, S.J., Wyngaard, J.C. & Kaimal, J.C. (1979) Turbulence in the evolving stable boundary layer. J. Atmos. Sci. 6, 1041-1052.

Chatwin, P.C. (1968) The dispersion of a puff of passive contaminant in the constant stress region. Q.J. Roy. Met. Soc. 94, 350-360.

Clarke, R.H. (1979) A model for short and medium range dispersion of radionuclides released to the atmosphere. (First report of a working group on atmospheric dispersion.) National Radiological Protection Board Report NRPB-R91.

Coelho, S.L.V. & Hunt, J.C.R. (1989) On the initial deformation of strong jets in cross flows. J. Fluid Mech. (in press).

Counihan, J. (1972) Flow over concatenated sinusoidal hills. CERL Report RD /L/N57/74.

Counihan, J., Hunt, J.C.R. & Jackson, P.S. (1974) Wakes behind two dimensional surface obstacles in turbulent boundary layers. J. Fluid Mech. 64, 529-563.

Courtney, L.Y. & Arya, S.P.S. (1980) Boundary layer flow and diffusion over a two-dimensional low hill. pp.551-558, 2nd Joint Conf. Appl. Air Pollution Met., New Orleans, American Met. Soc., Boston.

Cox, R.A. (1977) Field studies of local weather and its effects on air pollution at a proposed industrial site. Weather 32, 42-

Csanady, G.T. (1964) Turbulent diffusion in a stratified fluid. J. Atmos. Sci. 21, 439-447.

Deardorff, J.W. (1972) Investigation of neutral and unstable planetary boundary layers. J. Atmos. Sci. 29, 91-115.

Deardorff, J.W. (1985) Laboratory experiments on diffusion: the use of convective mixed layer scaling. J. Clim. Appl. Met. 24, 1143-1151.

Deardorff, J.W. & Willis, G.E. (1975) A parameterization of diffusion into the mixed layer. J. Appl. Met. 14, 1451-1458.

Deaves, D.M. (1976) Wind over hills: a numerical approach. J. Ind. Aero. 1, 371-391.

De Baas, A.F., van Dop, H. & Nieuwstadt, F.T.M. (1986) An application of the Langevin equation for inhomogeneous conditions to dispersion in a convective boundary layer. Q.J. Roy. Met. Soc. 112, 165-180.

Derbyshire, S. (1988) Modelling Nocturnal Boundary Layers. Ph.D. Dissertation, University of Cambridge.

Doran, J.C., Horst, T. & Nickola, P. (1978) Experimental observation of the dependence of lateral and vertical characteristics on source height. Atmos. Env. 12, 2259-2263.

Draxler, R.R. (1976) Determination of atmospheric diffusion parameters. Atmos. Env. 10, 99-105.

Durbin, P.A. & Hunt, J.C.R. (1980) Dispersion from an elevated source in turbulent boundary layers. J. de Mécanique 19, 679-695.

Egan, B.A. (1984) Transport and diffusion in complex terrain. Boundary Layer Met. 30, 3-28/ Proc. 29th Oholo Biol. Conf. on Boundary Layer Structure – Modeling and Application to Air Pollution and Wind Energy. Zichron Ya'Acov, Israel. eds. H. Kaplan, N. Dinar. Reidel.

El Tahry, S., Gosman, A.D. & Launder, B.E. (1981) The two- and three-dimensional dispersion of a passive scalar in a turbulent boundary layer. Int. J. Heat & Mass Trans. 24, 35-46.

Elise(y)ev, V.S. (1977) Trajectories of smoke jets from industrial sources. NERC Li-

brary, U.S. EPA Translation TR77-235 (from Trudy Glav. Geofiz. Obsev. 373, Leningrad).

Fackrell, J.E. & Robins, A.G. (1979) Preliminary report on the wind tunnel valley experiment CEGB (Marchwood). Report MM/MECH/TF 145.

Fackrell, J.E. & Robins, A.G. (1982) Concentration fluctuations and fluxes in plumes from point sources in a turbulent boundary layer. J. Fluid Mech. 117, 1-26.

Frenkiel, J. (1962) Wind profiles over hills in relation to wind power utilization. Q.J. Roy. Met. Soc. 88, 156-169.

Frost, S. (1981) Temperature Dispersion in Turbulent Pipe Flow. Ph.D. Dissertation, *University of Cambridge*.

Fung, J.C.H. & Perkins, R.J. (1988) Particle trajectories in turbulent flow generated by time varying random Fourier modes. Proc. 2nd European Turbulence Conf., Aug. 1988, Technische Universität Berlin, eds. H.H. Fernholz, H.E. Fiedler.

Garratt, J.R. (1982) Observations in the nocturnal boundary layer. Boundary Layer Met. 22, 21-48.

Geiger, R. (1965) The Climate Near The Ground. Harvard Univ. Press.

Godler, D.G. (1972) Relations among stability parameters in the surface layer. Boundary Layer Met. 3, 47-58.

Golding, B.W. (1987) The U.K. Meteorological Office mesoscale model. Boundary Layer Met. 41, 97-107.

Gryning, S.E., Holtslag, A.M.M., Irwin, J., Sivertsen, B. (1987) Applied dispersion modelling based on meteorological scaling parameters. Atmos. Env. 21, 79-89.

Gryning, S.E., Lyck, E. & Hedegaard, K. (1978) Short-range diffusion experiments in unstable conditions over inhomogeneous terrain. Tellus 30, 392-403.

Gryning, S.E. Van Ulden, A.P., Larsen, S.E. (1983) Dispersion from a continuous ground level source investigation by a K-model. Q.J. Roy. Met. Soc. *109*, 355-364.

Hanna, S.R. (1980) Measured σ_y and σ_θ in complex terrain near the TVA Widows Creek Alabama steam plant. Atmos. Env. 14, 401-407.

Hanna, S.R. (1986) Spectra of concentration fluctuations: the two time scales of a meandering plume. Atmos. Env. 20, 1131-1137.

Hilst, G.R. & Simpson, C.I. (1958) Observations of vertical diffusion rates in stable atmospheres. J. Met. 15, 125-126.

Holtslag, A.M.M. & Nieuwstadt, F.T.M. (1986) Scaling the atmospheric boundary layer. Boundary Layer Met. 36, 201-209.

Hunt, A. & Castro, I.P. (1984) Scalar dispersion in model building wakes. J. Wind. Eng. Ind. Aero. 17, 89-115.

Hunt, J.C.R. (1981) Turbulent stratified flow over hills. Paper I1, Proc. Conf. Construire avec le Vent, Centre Sci. TEchn. du Bat., Nantes, France.

Hunt, J.C.R. (1982a) Diffusion in the stable boundary layer. pp.231-274 (Chap.6), Atmospheric Turbulence and Air Pollution Modelling, ed. F.T.M. Nieuwstadt & H. van Dop. Reidel.

Hunt, J.C.R. (1982b) Mechanism for dispersion of pollution around buildings and vehicles. pp.235-266, BMFT/TÜV Coll. on Exhaust Gas Air Pollution caused by Motor Vehicle Emissions. TÜV, Köln.

Hunt, J.C.R. (1984) Turbulence structure in thermal convection and shear free boundary layers. J. Fluid Mech. 138, 161-184.

Hunt, J.C.R. (1985a) Turbulent diffusion from sources in complex flows. Ann. Rev. Fluid Mech. 17, 447-485.

Hunt, J.C.R. (1985b) Diffusion in the stably stratified atmospheric boundary layer. J. Clim. Appl. Met. 24, 1187-1195.

Hunt, J.C.R. (1987a) Modifications to Gaussian plume models to allow for changes in wind speed and direction and mixing height. Atmospheric Dispersion Modelling Working Group note ADMWG/P70.

Hunt, J.C.R. (1987b) Atmospheric diffusion from a steady source in a turbulent air flow: low mean wind speeds. Atmospheric Dispersion Modelling Working Group note ADMWG/P71.

Hunt, J.C.R., Britter, R.E. & Puttock, J.S. (1979) Mathematical models of dispersion of air pollution around buildings and hills. pp.145-200, Proc. Conf. Math. Modelling of Turbulent Diffusion in the Environment, Sept. 1978, ed. C.J. Harris. Academic Press.

Hunt, J.C.R., Kaimal, J.C. & Gaynor, E. (1985) Some observations of turbulence structure in stable layers. Q.J. Roy. Met. Soc. 111, 793-815.

Hunt, J.C.R., Kaimal, J.C. & Gaynor, E. (1988) Eddy structure in the convective boundary layer – new measurements and new concepts. Q.J. Roy. Met. Soc. 114, 827-858.

Hunt, J.C.R., Lalas, D.P., & Asimakopoulos, D.N. (1984) Air flow and dispersion in rough terrain: a report on Euromech 173. J. Fluid Mech. 142, 201-216.

Hunt, J.C.R., Leibovich, S. & Lumley, J.L. (1983) Prediction methods for the dispersion of atmospheric pollutants in complex terrain. Flow analysis Associates (Ithaca, New York), report to State of Maryland Dept. of Natural Resources Power Plant Siting Prog., contract no.P85-81-04.

Hunt, J.C.R., Leibovich, J. & Richards, K.J. (1988) Turbulent shear flow over hills. Q.J. Roy. Met. Soc. 114,

Hunt, J.C.R. & Mulhearn, P.J. (1973) Turbulent dispersion from sources near two-dimensional obstacles. J. Fluid Mech. 61, 245-274.

Hunt, J.C.R., Newley, T.M.J. & Weng, W.-S. (1988) Analysis and computation of turbulent boundary layers with varying pressure gradients. Joint IMA-SMAI Conf. on Computational Methods in Aeronautical Fluid Dynamics, Univ. of Reading, April 1977. ed. P. Stow. Oxford Univ. Press.

Hunt, J.C.R., Puttock, J.C. & Snyder, W.H. (1979) Turbulent diffusion from a point source in stratified and neutral flows around a three-dimensional hill. Part I. Diffusion equation analysis. Atmos. Env. 13, 1227-1239.

Hunt, J.C.R. & Richards, K.J. (1980) (Jan.) Unpublished report in Health and Safety Executive, UKAEA.

Hunt, J.C.R. & Richards, K.J. (1984) Stratified air flow over one or two hills. Boundary Layer Met. 30, 223-259 / Proc. 29th Oholo Biol. Conf. on Boundary Layer Structure – Modeling and Application to Air Pollution and Wind Energy. Zichron Ya'Acov, Israel. eds. H. Kaplan, N. Dinar. Reidel.

Hunt, J.C.R., Richards, K.J. & Brighton, P.W.M. (1988) Stably stratified flow over low hills. Q.J. Roy. Met. Soc. 114, 859-886.

Hunt, J.C.R. & Simpson, J.E. (1982) Atmospheric boundary layers over non-homogeneous terrain. pp.269-318 (Chap.7), Engineering Meteorology. ed. E.J. Plate. Elsevier.

Hunt, J.C.R. & Snyder, W.H. (1980) Effects of stratification on the flow structure and turbulent diffusion around a three-dimensional hill. J. Fluid Mech. 96, 671-704.

Hunt, J.C.R. & Weber, A.H. (1979) A Lagrangian statistical analysis of diffusion from a ground level source in a turbulent boundary layer. Q.J. Roy. Met. Soc. 105, 423-443.

Hunt, J.C.R., Weng, W.-S., & Carruthers, D.J. (1988) Modelling deposition fluxes on hills. pp.623-640. Proc. 16th NATO-CCMS Int. Tech. Meeting on Air Pollution Modelling and its Applications. Lindau (F.R.G.). Plenum.

Irwin, J.S. (1978) Dispersion estimate suggestion no. 6. Unpublished Note, US EPA.

Jackson, P.S.& Hunt, J.C.R. (1975) Turbulent wind flow over a low hill. Q.J. Roy. Met. Soc. 101, 929-955.

Jensen, N.O. & Peterson, R.W. (1978) On the escarpment wind profile. Q.J. Roy. Met. 104, 719-728.

Jones, J.A. (1983) Models to allow for the effects of coastal sites, plume rise and buildings on dispersion of radionuclides and guidance on the value of deposition velocity and washout coefficients. (Fifth Report of a working group on atmospheric dispersion.) National Radiological Protection Board Report NRPB-R157.

Jones, J.A. (1986) The uncertainty in dispersion estimates obtained from the working group models. (Seventh report of a working group on atmospheric dispersion.) National Radiological Protection Board Report NRPB-R199.

Kaimal, J.C., Eberhard, W.L., Moninger, W.R., Gaynor, J.E., Troxel, S.W., Uttal, T., Briggs, G.A. & Stort, G.E.(1986) Project Condors – convective diffusion observed by remote sensors. U.S. Dept. of Commerce, NOAA, Environmental Res. Labs., Boulder, Colo.

Kaimal, J.C., Wyngaard, J.C., Haugen, D.A., Coté, O.R., Izumi, Y., Caughey, S.J., Readings, C.J. (1976) Turbulence structure in the convective boundary layer. J. Atmos. Sci. 33, 2152-2169.

Kretzschmar, J.G. & Mertens, I. (1984) Influence of the turbulent typing scheme upon the cumulative frequency distribution of the calculated relative concentrations for different averaging times. Atmos. Env. 18, 2377-2393.

Khurshudyan, L.H., Snyder, W.H. & Nekrasov, I.V. (1981) Flow and dispersion of pollutants over two dimensional hills. U.S. EPA report, EPA-600/4-81-067.

Lalas, D.P., Asimakopoulos, D.N., Deligiorgi, D.G. & Helmis, C.G. (1983) Sea breeze circulation and photochemical pollution in Athens. Atmos. Env. 17, 1621-1632.

Lamb, R.G. (1979) The effect of release height on material dispersion in the convective planetary boundary layer. Proc. 4th Symp. on Turbulence, Diffusion and Air Pollution, Reno. American Met. Soc.

Lamb, R.G. (1982) Diffusion in the convective boundary layer. pp.159-229 of Atmospheric Turbulence and Air Pollution Modelling. eds. F.T.H. Nieuwstadt & H. van Dop. Reidel.

Lange, R. (1978) ADPIC - a three dimensional transport diffusion model for the dispersal of atmospheric pollutants and its validation against regional tracer studies. J. Appl. Met. 17, 320-329.

Larsen, S.E., Olesen, H.R., Højstrup, J. (1985) Parameterization of the low frequency part of spectra of horizontal velocity components in the stable surface boundary layer. pp.181-204, Inst. of Mathematics and its Applications Conf. on Turbulence and Diffusion in Stable Environments, ed. J.C.R. Hunt. Clarendon Press.

Lavery, T.F.,Bass, A., Strimaitis, D.G., Venkatram, A., Greene, B.R., Drivas, P.J. & Egan, B.A. (1982) EPA complex terrain modeling program: 1st milestone

report (1981). Rep. No. EPA-600/3-82-036.

Lenschow, D.H. (19700 Airplane measurements of planetary boundary layer structure. J. Appl. Met. 9, 874-884.

Lenschow, D.H. & Stephens, P.L. (1980) The role of thermals in the convective boundary layer. Boundary Layer Met. 19, 509-532.

Lenschow, D.H., Wyngaard, J.C. & Pennell, W.T. (1980) Mean field and second moment budgets in a baroclinic convective boundary layer. J. Atmos. Sci. 37, 1313-1326.

Lewellen, W.S., Sykes, R.I. & Oliver, D. (1982) The evaluation of MATHEW/ ADPIC as a real time dispersion model. Aeronautical Res. Assocs. of Princeton Inc., Rep. No. 442 for Div. Health, Safety and Waste Management, Office of Nuclear Regulatory Res., U.S. Nuclear Regulatory Commission.

Ley, A.J. & Thomson, D.J. (1983) A random walk model of dispersion in the diabatic surface layer. Q.J. Roy. Met. Soc. 109, 867-880.

Mahrer, Y. & Pielke, R.A. (1977) The effects of topography on the sea and land breezes in a two dimensional numerical model. Monthly Weather Rev. 105, 1151-1162.

Manins, P.C. & Sawford, B.L. (1979) Katabatic winds: a field case study. Q.J. Roy. Met. Soc. 105, 1011-1025.

Maryon, R.H., Whitlock, J.B.G. & Jenkins, G.J. (1986) An analysis of short-range dispersion experiments on the windward slope of an isolated hill. Atmos. Env. 20, 2157-2173.

Mason, P.J. & King, J.C. (1984) Atmospheric flow over a succession of nearly two-dimensional ridges and valleys. Q.J. Roy. Met. Soc. 110, 821-845.

Mason, P.J. & King, J.C. (1985) Measurements and predictions of flow and turbulence over an isolated hill of moderate slope. Q.J. Roy. Met. Soc. 111, 617-640.

Mason, P.J., MacVean, M.K. & Laffey, A.T. (1988) Large eddy simulation of lateral dispersion. Unpublished lecture given at the 17th NATO-CCMS Int. Tech. Meeting on Air Pollution Modelling and its Applications. Sept. 1988, Cambridge.

Mason, P.J. & Sykes, R.I. (1979) Flow over an isolated hill of moderate slope. Q.J. Roy. Met. Soc. 205, 385-395.

Mason, P.J. & Sykes, R.I. (1980) A two dimensional numerical study of horizontal roll vortices in the neutral atmospheric boundary layer. Q.J. Roy. Met. Soc. 106, 351-366.

Mason, P.J. & Sykes, R.I. (1981) On the influence of topography on plume dispersal.

Boundary Layer Met. 21, 137-157.

Mason, P.J. & Thomson, D.J. (1987) Large eddy simulations of the neutral-static-stability planetary boundary layer. Q.J. Roy. Met. Soc. 113, 413-443.

Mickle, R.R., Cook, N.J., Hoff, A.M., Jensen, N.O., Salmon, J.R., Taylor, P.A., Tetzlaff, G. & Tennissen, H.W. (1988) The Askervein Hill project: vertical profiles of wind and turbulence. Boundary Layer Met. 43, 143-169.

Mikkelson, T., Larsen, S. & Thykier-Nielsen, S. (1984) Description of the Risø puff diffusion model. Nuclear Tech. 67, 56-65.

Misra, P.K. (1982) Dispersion of non-buoyant particles inside a convective boundary layer. Atmos. Eng. 16, 239-243.

Moin, P. & Kim, J. (1982) Numerical investigations of turbulent channel flow. J. Fluid Mech. 118, 341-377.

Moore, D.J. (1975) A simple boundary layer model for predicting time mean ground level concentrations of material emitted from tall chimneys. Proc. Inst. Mech. Eng. 189, 33-43.

Moore, D.J. & Lee, B.Y. (1982) An asymmetric Gaussian plume model. CERL Report RD/L/2225 N/81.

Moussiopoulos, N. & Flassak, T. (1986) Two vectorized algorithms for the effective calculation of mass consistent flow field. J. Clim. Appl. Met. 25, 847-857.

Mylne, K.R. (1989) Experimental measurements of concentration fluctuations. Proc. 17th NATO-CCMS Int. Tech. Meeting on Air Pollution Modelling and its Applications. Sept. 1988, Cambridge. Plenum.

Neff, W.D. & King, C.W. (1988) Observations of complex terrain flows using acoustic sensors: drainage flow structure and evolution. Boundary Layer Met. 43, 15-41.

Nieuwstadt, F.T.M. (1984) The turbulent structure of the stable nocturnal boundary layer. J. Atmos. Sci. 41, 2202-2216.

Nieuwstadt, F.T.M. (1985) A model for the stationary, stable boundary layer. pp.149-179, Inst. of Mathematics and its Applications Conf. on Turbulence and Diffusion in Stable Environments, ed. J.C.R. Hunt. Clarendon Press.

Nieuwstadt, F.T.M. & van Ulden, A.P. (1978) A numerical study on the vertical dispersion of passive contaminants from a continuous source in the atmospheric surface layer. Atmos. Env. 12, 2119-2123.

Paine, R.J., Strimaitis, D.J., Dennis, M.G., Yamartino, R.J., Mills, M.T. & Insley, E.M. (1987) User's guide to the Complex Terrain Dispersion Model. Vol. 1. Model description and user instructions. Atmos. Sci. Res. Lab., Office of Res. & Development, U.S. EPA.

Panofsky, H.A. (1974) The atmospheric boundary layer below 150m. Ann. Rev. Fluid. Mech. 6, 147-177.

Panofsky, H.A. & Dutton, J.A. (1984) Atmospheric Turbulence. Wiley.

Panofsky, H.A., Tennekes, H., Lenschow, D.H., Wyngaard, J.C. (1977) The characteristics of turbulent velocity components in the surface layer under convective conditions. Boundary Layer Met. 11, 355-361.

Pasquill, F. (1961) The estimation of the dispersion of windborne material. Met. Mag. 90, 33-49.

Pasquill, F. (1971) Atmospheric dispersion of pollution. Q.J. Roy. Met. Soc. 97, 369-395.

Pasquill, F. (1974) Atmospheric Diffusion (2nd Edition). Ellis Horwood.

Pasquill, F. & Smith, F.B. (1983) Atmospheric Diffusion (3rd Edition). Ellis Horwood.

Pearson, H.J., Puttock, J.S. & Hunt, J.C.R. (1983) A statistical model of fluid element motions and vertical diffusion in a homogeneous stratified turbulent flow. J. Fluid Mech. 129, 219-249.

Pedgley, D.E. (1971) Some weather patterns in Snowdonia. Weather 29, 284-

Pendergrass, W. & Arya, S.P.S. (1984) Dispersion in neutral boundary layer over a step change in roughness. II. Concentration profiles and dispersion parameters. Atmos. Env. 18, 1281-1296.

Pielke, R.A. (1984) Mesoscale Meteorological Modeling. Academic Press.

Plate, E.J. (1971) Aerodynamic characteristics of atmospheric boundary layers. U.S. Atomic Energy Commission, Office of Information Services.

Plate, E.J. (ed) (1982) Engineering Meteorology. Elsevier.

Poreh, M. & Cermak, J.E. (1984) Wind tunnel simulation of diffusion in a convective boundary layer. Boundary Layer Met. 30, 431-455.

Puttock, J.S. (1978) Modelling the effects of wakes behind hills and buildings on pollutant dispersion. Proc. 9th NATO-CCMS Int. Tech. Meeting on Air Pollution Modelling and its Applications. Toronto, Canada.

R91 – See Clarke (1979)

R157 – See Jones (1983)

R199 – See Jones (1986)

Raithby, G.D., Stubley, G.D. & Taylor, P.A. (1987) The Askervein Hill project: a finite control volume prediction of three-dimensional flows over the hill. Boundary Layer Met. 39, 247-267.

Raynor, G.J., Michael, P., Brown, R.M. & SethuRaman, S. (1975) Studies of atmospheric diffusion from a nearshore oceanic site. J. Appl. Met. 14, 1080-

Restrepo, L.F. (1987) Study plan for the sensitivity analysis of the terrain responsive atmospheric code (TRAC). Report RFP-4066, Rockwell Int. N. American Space Op., Rocky Flats Plant, Golden, Colorado.

Richards, K.J. & Taylor, P.A. (1980) A numerical model of flow over sand waves in water of finite depth. Geophys. J. Roy. Astro. Soc.

Rottman, J.W., Simpson, J.E. & Stansby, P.K. (1987) The motions of a cylinder of fluid released from rest in a cross flow. J. Fluid Mech. 177, 307-337.

Rottman, J.W. & Smith, R.B. (1987) Tow tank simulations of the severe downslope wind. Proc. 3rd Int. Symp. on Stratified Flows, California Inst. of Tech., Pasadena.

Schiermeier, F.A. (1978) Large power plant effluent study. U.S. EPA Rep. APTD-1143.

Schmidt, H. & Schumann, U. (1989) Coherent structures of the convective boundary layer derived from large-scale eddy simulations. J. Fluid Mech. (in press).

Schumann, U., Hauf, T., Höller, H., Schmidt, H. & Volkert, H. (1978) A mesoscale model for the simulation of turbulence, clouds and flow over mountains: formulation and validation examples. Beitr. Phys. Atmos. 60, 413-446.

Scorer, R.S. (1955) Theory of air flow over mountains. Part IV. Separation of flows from the surface. Q.J. Roy. Met. Soc., 81, 340-350.

Scorer, R.S. (1968) Air Pollution. Pergamon.

Scriven, R.A. (1969) Variability and upper bounds for ground level concentration. Phil. Trans. Roy. Soc. 265A, 209-220.

Sheppard, P.A. (1956) Air flow over mountains. Q.J. Roy. Met. Soc. 82, 528-529.

Sherman, C.A. (1978) A mass consistent model for wind fields over complex terrain. J. Appl. Met. 17, 312-319.

Smith, F.B. (1973) A scheme for estimating the vertical dispersion of a plume from a source near ground level. Proc. 3rd meeting of an expert panel on air pollution modelling. Oct.1972, Paris; Brussels, NATO-CCMS report 14.

Smith, F.B. (1989) Short range diffusion in convective zero mean wind conditions. Proc. 17th NATO-CCMS Int. Tech. Meeting. on Air Pollution Modelling and its Applications. Sept. 1988, Cambridge. Plenum.

Smith, F.B. & Blackall, R.M. (1979) The application of field experiment data to the parameterisation of the dispersion of plumes from ground level and elevated sources. pp.201-238, Proc. Conf. Math. Modelling of Turbulent Diffusion in the Environment, Sept. 1978, ed. C.J. Harris. Academic Press.

Smith, F.B. & Carson, D.J. (1977) Some thoughts on the specification of the boundary layer relevant to numerical modelling. Boundary Layer Met. 12, 307-

Smith, R.B. (1980) Linear theory of stratified hydrostatic flow past an isolated mountain. Tellus 32, 348-364.

Snyder, W.H. (1981) Guideline for fluid modelling of atmospheric dispersion. U.S. EPA Report EPA-600/8 81-009.

Snyder, W.H. (1985) Fluid modelling of pollutant transport and diffusion in stably stratified flows over complex terrain. Ann. Rev. Fluid Mech. 17, 239-266.

Snyder, W.H. & Hunt, J.C.R. (1984) turbulent diffusion from a point source in stratified and neutral flows around a three-dimensional hill. Part II. Laboratory measurements of surface concentration. Atmos. Env. 18, 1969-2002.

Snyder, W.H. & Lumley, J.L. (1971) Some measurements of particle velocity autocorrelation functions in a turbulent flow. J. Fluid Mech. 48, 41-71.

Snyder, W.H., Thompson, R.S., Eskridge, R.E., Lawson, R.E., Castro, I.P., Lee, J.T., Hunt, J.C.R. & Ogawa, Y. (1985) The structure of strongly stratified flow over hills: dividing streamline concept. J. Fluid Mech. 152, 249-288.

Squire, K. (1989) Ph.D. Dissertation, Mech. Eng. Dept., Stanford University.

Stapountzis, H. & Britter, R.E. (1987) Turbulent diffusion behind a heated line source in a nearly homogeneous turbulent shear flow. Paper 9.2, 6th Symp. on Turbulent Shear Flows, Toulouse, eds F.J. Durst, B.E. Launder, F.W. Schmidt, J.H. Whitelaw.

Stapountzis, H., Sawford, B.L, Hunt, J.C.R. & Britter, R.E. (1986) Structure of the temperature field downwind of a line source in grid turbulence. J. Fluid Mech. 165, 401-424.

Stretch, D.D., Britter, R.E. & Hunt, J.C.R. (1983) The dispersion of slightly dense contaminants. pp.333-346, Proc. IUTAM Symp. on Atmospheric Dispersion of Heavy Gases and Sand Particles, Delft. eds. G. Ooms & H. Tennekes. Springer Verlag.

Strimaitis, D.G., DiChristofaro, D.C., Greene, B.R., Yamartino, R.J., Venkatram, A., Godden, D.A., Karamchandani, P., Lavery, T.F. & Egan, B.A. (1986) EPA Complex terrain model development: 5th milestone report (1985).

Strimaitis, D.G., Lavery, T.F., Venkatram, A. DiChristofaro, D.C., Greene, B.R. & Egan, B.A. (1985) EPA complex terrain model development: 4th milestone report (1984) Rep. No. EPA-600/3-84-110.

Sykes, R.I. (1978) Stratification effects in boundary layer flow over hills. Proc. Roy. Soc. 361A, 225-243.

Tamura, T. & Kuwahara, K. (1988) Numerical study of aerodynamic behaviour of a

square cylinder. Proc. Coll. on Bluff Body Aerodynamics, Kyoto University, Japan, Oct. 1988.

Taylor, G.I. (1921) Diffusion by continuous movements. Proc. London Math. Soc. 20 (Series 2), 196-202.

Tennekes, H. & Lumley, J.L. (1972) A First Course in Turbulence. M.I.T. Press.

Thompson, R.S. & Snyder, W.H. (1985) Dispersion from a source upwind of a three-dimensional hill of moderate slope. Appendix B., pp.269-286 of Strimaitis et al. 1985.

Thomson, D.J. (1984) Random walk modelling of diffusion in inhomogeneous turbulence. Q.J. Roy. Met. Soc. 120, 1107-1120.

Thomson, D.J. (1986) A random walk model of dispersion in turbulent flows and its application to dispersion in a valley. Q.J. Roy. Met. Soc. 112, 511-530.

Thomson, D.J. (1988) Turbulent diffusion. Proc. 2nd European Turbulence Conf., Aug. 1988, Technische Universität Berlin, eds. H.H. Fernholz, H.E. Fiedler.

Turfus, C. (1986) Diffusion from a continuous source near a surface in steady reversing flow. J. Fluid Mech. 172, 183-209.

Turfus, C. (1988) Calculating mean concentrations for steady sources in recirculating wakes by a particle trajectory method. Atmos. Env. 22, 1271-1290.

Turfus, C. & Hunt, J.C.R. (1987) A stochastic analysis of the displacements of fluid elements in inhomogeneous turbulence using Kraichnan's method of random modes. pp.191-203, Advances in Turbulence, Proc. 1st European Turbulence Conf., July 1986, Lyon, eds. G. Comte-Bellot & J. Mathieu. Springer Verlag.

Turner, D.B. (1964) A diffusion model for an urban area. J.Appl. Met. 3, 83-91.

van Dop, H., Nieuwstadt, F.T.M. & Hunt, J.C.R. (1985) Random walk models for particle displacements in inhomogeneous unsteady turbulent flow. Phys. Fluids 28, 1639-1653.

van Dop, H., Steenkist, R. & Nieuwstadt, F.T.M. (1979) Revised estimates for continuous shore line fumigation. J. Appl. Met. 18, 133-

van Ulden, A.P. &, Holtslag, A.M.M. (1985) Estimation of atmospheric boundary layer parameters for diffusion applications. J. Clim. Appl. Met. 24, 1196-1207.

Venkatram, A. (1989) An examination of the performance of models for dispersion in the convective boundary layer. Proc. 17th NATO-CCMS Int. Tech. Meeting. on Air Pollution Modelling and its Applications. Sept. 1988, Cambridge. Plenum.

Venkatram, A. & Paine, R.J. (1985) A model to estimate dispersion of elevated releases into a shear dominated boundary layer. Atmos. Env. 19, 1797-1895.

Venkatram, A., Strimaitis, D.G.& DiChristofaro, D. (1984) A semi-empirical model to estimate vertical dispersion of elevated releases in the stable boundary layer. Atmos. Env. 18, 923-928.

Walmsley, J.C., Salmon, J.R. & Taylor, P.A. (1982) On the application of a model of boundary layer flow over low hills to real terrain. Boundary Layer Met. 23, 17-46.

Walmsley, J.C., Taylor, P.A. & Keith, T. (1986) A simple model of neutrally stratified boundary layer flow over complex terrain with surface roughness modulations (MS3 DJH/3R). Boundary Layer Met. 36, 157-186.

Weil, J.C. (1985) Updating applied diffusion models. J. Clim. Appl. Met. 24, 1111-1130.

Weil, J.C. (1989) Langevin modelling of dispersion in the convective boundary layer. Proc. 17th NATO-CCMS Int. Tech. Meeting on Air Pollution Modelling and its Applications. Sept. 1988, Cambridge. Plenum.

Weil, J.C. & Brower, R.P. (1982) The Maryland PPSP dispersion model for tall stacks. Rep. PPSP-Mp-36, Maryland Power Plant Siting Prog., Martin Marietta Corp., Baltimore.

Weng, W.-S., Richards, K.J. & Carruthers, D.J. (1988) Some numerical studies of turbulent wakes over hills. Proc. 2nd European Turbulence Conf., Aug. 1988, Technische Universität Berlin, eds. H.H. Fernholz, H.E. Fiedler.

White, F.B. (ed.), Ching, J.K.J., Dennis, R.L. & Snyder, W.H. (1985) Summary of complex terrain model evaluation. Atmos. Sci. Res. Lab., Office or Res. & Development, U.S. EPA.

Wyngaard, J.C. (1985) Structure of the planetary boundary layer and implications for its modelling. J. Clim. Appl. Met. 24, 1131-1142.

Wyngaard, J.C. (1989) Developments in dispersion parameterization and modeling. Proc. 17th NATO-CCMS Int. Tech. Meeting. on Air Pollution Modelling and its Applications. Sept. 1988, Cambridge. Plenum.

Xu, D.-P. & Hunt, J.C.R. (1988) The response of the turbulent boundary layer to arbitrary distributed surface roughness. Q.J. Roy. Met. Soc.

Zeman, O. & Jensen, N.O. (1987) Modification of turbulence characteristics in flow over hills. Q. J. Roy. Met. Soc. 113, 55-80.